A covariant 4D formalism to establish constitutive models : from thermodynamics to numerical applications

Mingchuan Wang

Thèse
de doctorat
de l'UTT

Mingchuan WANG

A Covariant 4D Formalism to Establish Constitutive Models: from Thermodynamics to Numerical Applications

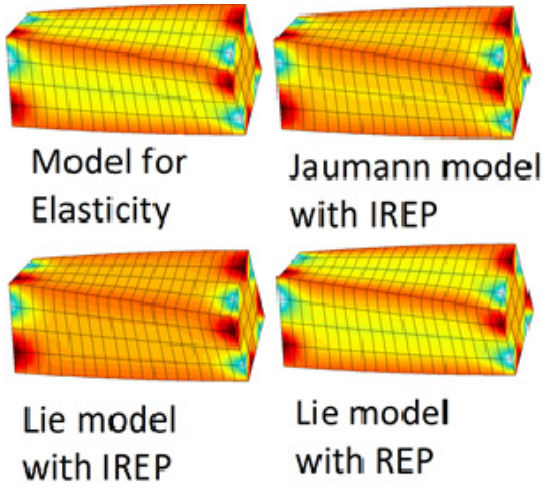

Spécialité :
Matériaux, Mécanique, Optique et Nanotechnologie

2016TROY0025 **Année 2016**

utt
université de technologie
Troyes

THESE

pour l'obtention du grade de

DOCTEUR de l'UNIVERSITE DE TECHNOLOGIE DE TROYES

Spécialité : MATERIAUX, MECANIQUE, OPTIQUE ET NANOTECHNOLOGIE

présentée et soutenue par

Mingchuan WANG

le 21 septembre 2016

A covariant 4D Formalism to Establish Constitutive Models: from Thermodynamics to Numerical Applications

JURY

M. G. DE SAXCÉ	PROFESSEUR DES UNIVERSITES	Président
M. J. CRESSON	PROFESSEUR DES UNIVERSITES	Rapporteur
M. Z. FIALA	RESEARCH DIRECTOR	Examinateur
M. S. FOREST	DIRECTEUR DE RECHERCHE CNRS	Examinateur
M. A. HAMDOUNI	PROFESSEUR DES UNIVERSITES	Examinateur
M. F. JOURDAN	PROFESSEUR DES UNIVERSITES	Rapporteur
M. B. PANICAUD	PROFESSEUR DES UNIVERSITES	Directeur de thèse
Mme E. ROUHAUD	MAITRE DE CONFERENCES - HDR	Directrice de thèse

Personnalité invitée

M. R. KERNER	PROFESSEUR DES UNIVERSITES

Acknowledgements

I express my sincere gratitude at first to Prof. Emmanuell ROUHAUD and Prof. Benoît PANICAUD, my advisors, for their support of my PhD study and for their guide of related research, for their motivation, patience, kindness, knowledge and experiences. It is delightful and memorable to spend more than three years to study and work with them.

Besides my advisors, I would like to thank the rest of my thesis committee: Prof. Jacky CRESSON, Prof. Géry DE SAXCÉ, Prof. Zdeněk FIALA, Prof. Samuel FOREST, Prof. Franck JOURDAN and Prof. Richard KERNER as well as Prof. Aziz HAMDOUNI, for ther encouragement and insightful commnets.

I also give my thanks to Prof. Richard KERNER again, to Prof. Arjen ROOS, Prof. François SIDOROFF, Dr. Guillaume ALTMEYER and Dr. Olivier AMELINE. It is a great pleasure to cooperate with them in this study.

I thank my colleagues in the laboratory of LASMIS ICD UTT and my friends in UTT. Their experiences, opinions and advises are valuable for me to fulfill the tasks of research. I thank also the graduate school of UTT, for their excellent work of organization of my defense and their help during my years of pursuing PhD.

I thank the financial support from UTT in this project and also my personal support from CSC. It is my fortune to have the opportunity to do my study in France with the help of CSC.

Last but not the least, I would like to thank my parents for supporting me spiritually throughout writing the thesis and living my life.

many thanks to my computer

Contents

Abstract

Abstract in English

The objective of this work is to establish mechanical constitutive models for materials undergoing large deformations. Instead of the classical 3D approaches in which the notion of objectivity is ambiguous and different objective transports may be arbitrarily used, the four-dimensional formalism derived from the theories of Relativity is applied. Within a 4D formalism, the two aspects of the notion of objectivity: frame-indifference (or covariance) and indifference to the superposition of rigid body motions can now be distinguished. Besides, the use of this 4D formalism ensures the covariance of the models. For rate-type models, the Lie derivative is chosen as a total time derivative, which is also covariant and indifferent to the superposition of rigid body motions.

Within the 4D formalism, we also propose a framework using 4D thermodynamic to develop 4D constitutive models for hyperelasticity, anisotropic elasticity, hypoelasticity and elastoplasticity. Then, 3D models are derived from 4D models and studied by applying them in numerical simulations with finite element methods using the software Zset.

Résumé en Français

L'objectif de ce travail est d'établir des modèles de comportement mécaniques pour les matériaux, en grandes déformations. Au lieu des approches classiques en 3D dans lesquelles la notion d'objectivité est ambigüe et pour lesquelles différentes dérivées objectives sont utilisées arbitrairement, le formalisme quadridimensionnel dérivé des théories de la Relativité est appliqué. En 4D, les deux aspects de la notion d'objectivité, l'indépendance au référentiel (ou covariance) et l'invariance à la superposition des mouvements de corps rigide, peuvent désormais être distingués. En outre, l'utilisation du formalisme 4D assure la covariance des modèles. Pour les modèles incrémentaux, la dérivée de Lie est choisie, permettant une variation totale par rapport au temps, tout en étant à la fois covariante et invariante à la superposition des mouvements de corps rigide.

Dans ce formalisme 4D, nous proposons également un cadre thermodynamique en 4D pour développer des modèles de comportement en 4D, tels que l'hyperélasticité, l'élasticité anisotrope, l'hypoélasticité et l'élastoplasticité. Ensuite, les projections en 3D sont obtenus à partir de ces modèles en 4D et étudiés en les testant sur des simulations numériques par éléments finis avec le logiciel Zset.

Notations

Operators	
X	Scalar
$\boldsymbol{X}$	Vector, tensor, matrix
$X^{\mu\nu}$, X^{ij}	Contravariant components
$X_{\mu\nu}$, X_{ij}	Covariant components
$(\boldsymbol{X})^S$	Symmetric part of a second-rank tensor
$tr(\boldsymbol{X})$	Trace of a 3D second-rank tensor
$\lvert\boldsymbol{X}\rvert$	Determinant of second-rank tensor or matrix
$\boldsymbol{X}_\mu$, $\boldsymbol{X}_i$	Covariant base vectors
$\boldsymbol{X} \otimes \boldsymbol{X}$	Outer or tensorial product
$\boldsymbol{X} : \boldsymbol{X}$	Inner or scalar product (double contraction)
∇_λ, ∇_i	Gradient operator
$\frac{d}{dt}(.)$	Total derivative to time
$\frac{\partial}{\partial t}(.)$	Partial derivative to time
$u^\lambda \nabla_\lambda(.)$	Covariant rate
$\mathscr{L}_u(.)$	Lie derivative in the velocity field $\boldsymbol{u}$
$\mathscr{T}^J(.)$	Jaumann transport
$\mathscr{T}^{GN}(.)$	Green-Naghdi transport
$\mathscr{T}^C(.)$	Convective transport
$\mathscr{T}^T(.)$	Truesdell transport
Variables	
b	Material parameter for isotropic hardening
$\boldsymbol{b}$	Inverse of the left Cauchy-Green deformation tensor

c	Velocity of light
$\boldsymbol{C}$	Right Cauchy-Green deformation tensor
$\boldsymbol{\mathcal{C}}$	Fourth-rank stiffness tensor
$\boldsymbol{d}$	Rate of deformation tensor
$\boldsymbol{\mathcal{D}}$	Sixth-rank stiffness tensor
e	Internal energy density
$\boldsymbol{e}_\mu$, $\boldsymbol{e}_i$	Base vectors in inertial frame of reference
$\boldsymbol{e}$	Strain tensor
$\boldsymbol{E}$	Material counterpart of the strain tensor
$\mathbf{F}$, $\mathbf{F}'$	Deformation gradient and its inverse
$\mathscr{F}$	Threshold function (yielding limit) for plasticity
$\boldsymbol{g}_\mu$, $\boldsymbol{g}_i$	Base vectors in any frame of reference
$\boldsymbol{I}$	3D identity tensor
J	Density ratio
$\boldsymbol{L}$	Velocity gradient
$\mathcal{L}$	Lagrangian
m_0	Particle mass
n	Particle number density
$\boldsymbol{n}$	Particle current vector
p	Pressure
$\boldsymbol{q}$	Heat flux vector
Q	Material parameter for isotropic hardening
r	Cumulated plastic strain
R	Associated scalar force for r
R_0	Material parameter for isotropic hardening
ds	4D invariant interval
$\boldsymbol{S}$	Deviatoric Cauchy stress tensor
$\mathscr{S}$	Entropy vector
$\boldsymbol{T}$	Momentum-energy tensor
$T^{\mu\nu}_{kin}$, $T^{\mu\nu}_{q}$, $T^{\mu\nu}_{\sigma}$	Respective kinematic, thermo and mechanical

	momentum-energy tensor
$\boldsymbol{u}$	Four-velocity
$\mathcal{U}$	Energy density
$\boldsymbol{v}$	3D velocity
W	the weight of tensor
$\boldsymbol{\beta}$	Left Cauchy-Green deformation tensor
γ	Lorentz factor
$\Gamma^{\mu}_{\kappa\lambda}$	Christoffel's symbol
δ^{Ψ}_{Φ}	Krönecker's symbol
$\boldsymbol{\epsilon_e}$	3D infinitesimal elastic strain tensor
η	Entropy density
$\boldsymbol{\eta}$	Minkowskian tensor
θ	Temperature
κ	Hardening function
λ	Lamé coefficient for elastic materials
Λ	Plastic multiplier
μ	Lamé coefficient for elastic materials
$\boldsymbol{\nu}$	Particle diffusion vector
ρ	Mass density
σ_{eff}	Effective stress
$\boldsymbol{\sigma}$	Cauchy stress tensor
$\boldsymbol{\phi}$	Energy flux vector
Ψ	Helmholtz specific free energy
$\boldsymbol{\omega}$	Spin

Chapter 1

General introduction

Contents

Material modeling and the associated numerical simulations are recognized as a research priority by many industries and research organizations [Ernst&Young, 2006; SAFRAN, 2009; Schuster, 2010]. Combining mathematical models and computer technologies serves two objectives: better understanding and prediction of material behaviors. In a world of constantly renewing technologies, the current need is clearly for a complete multi-physical

approach that describes complex transformations of matter at various scales and possibly under extreme conditions [Vanderheaegen, 2011]. Fig. 1.1 presents examples of such transformations. One of the practical and industrial applications of this modeling activity concerns material processing. Progress in the prediction of the state of the material and the optimization of the entire manufacturing process at lower cost is only possible with the association of complex numerical simulations to advanced experimental work [Belytschko et al., 2000].

Figure 1.1: Examples of large transformations of matter. Clockwise starting with the center: forging process, crash test, rupture of a disk, shot impact, turbulence due to an airplane wing, gas explosion, tensile test of vessel replacement, deformed red blood cells, defects in an extruded metallic part, fatigue test of a tire.

Simulations are now frequently performed in an industrial, academic or research context even if fundamental and applied work is still in progress in many academic and industrial centers to improve these material modelings and the associated numerical simulations. Indeed, the quality of the simulations has yet to be assessed and depends on two limiting factors:

- The computation time limited by the model complexity, the algorithm and the computer efficiency.

- The physical content itself, limited on one hand by the diversity of the occurring phenomena and on the other hand by the resolution scale taken into account.

The validity of the simulations depends on the degree of confidence that is credited to the description of the underlying mechanisms. The convergence and the quality of the solutions may still be improved in several ways:

- Improve the physical consistency of constitutive models.
- Improve the integration scheme.
- Decrease the computation time.
- Assess the physical meaning and results of the converged solution.
- Propose experimental tests to validate the constitutive models and eventually verify the results.

Consider the constitutive models, we recognize it as the mathematical description of the physics of the material behaviors. The correct description of the physics associated to the observed phenomena is essential to capture the specificity of the considered transformations. One of the difficulties encountered to model these complex material behaviors comes from the non-linearities of the phenomena. These non-linearities have different origins and may come, for example, from the material itself, from geometrical effects, from contact between different parts of the structure, from dissipative effects, etc. In most cases, these phenomena occur simultaneously. Some existing approaches to describe the observed non-linearities and to account for rate effects are:

- Associate a phenomenological non-linearity to represent the effects of the kinematics, for a given solicitation.
- Consider lower length scales. For example, the evolution of the anisotropies due to grain rotations in a metallic poly-crystal causes the macroscopic rotation of the representative elementary volume.

- Replace the quantities in the constitutive model with the corresponding infinitesimal rates. It is the incremental tangent approach, dividing the problem into a succession of infinitesimal linear transformations. It is then necessary to adapt the formulation of the constitutive model and propose a proper incremental form.

None of these options offer, so far, a completely satisfactory solution because of the multiplicity of material behaviors. Also, in continuum mechanics, when an incremental formulation is used, "objective" quantities are defined to develop constitutive models and integration schemes. If it is currently recognized as the best approach because it is compatible with the thermodynamic framework [Lemaitre and Chaboche, 1994; Dogui, 1989; Speziale, 1987], this issue is still the object of ongoing debates.

In this chapter, we first recall the classical problems of continuum mechanics that we wish to solve and the associated hypotheses. This enables to pinpoint the open issues still existing in this classical three-dimensional (3D) framework. In the last part, we review how a four-dimensional (4D) description of this same problems can resolve most of the existing open issues.

1.1 Classical problems of continuum mechanics

The objective of this section is to present the existing problems classically proposed in continuum mechanics. Classical could be here interpreted as "standard". The objective is to describe the problems as it is proposed by most reference books on the subject. This section thus constitutes a rapid introduction of the vocabulary and concepts of continuum mechanics as well as an introduction of some of the notations that will be used in this document.

1.1.1 Continuum, material point and position

We wish to model finite transformations of matter with the hypothesis of material continua in mechanics, hence supposing that the material is consisted of continuous mass rather than of discrete elements [Gurtin, 1982; Bonet and Wood, 1997; Salençon, 2012]. A *mate-*

rial point is defined as an elementary volume of this material. This definition, classically found in physics, is equivalent to the definition of a *material point* in fluid mechanics, or with the definition of a *representative elementary volume* in solid mechanics [Belytschko et al., 2000; Bertram, 2012; Besson et al., 2009; Eringen, 1962; Rougée, 1997; Truesdell and Noll, 2003]. Note that the word *particle* refers to elementary particles as defined in physics, such as molecules or atoms. The material point is centered around a point of an Euclidean space and occupies a given position in this three-dimensional space. The position is described by the coordinates z^i $(i = 1, 2, 3)$ of the point within an orthonormal coordinate system ζ^i. A difference in notation is made between the coordinates of the particle (Latin letters) and the coordinate system in which it is expressed (equivalent Greek letters). Einstein's notation and summation convention is used throughout this manuscript. Latin indices vary from one to three for 3D space.

In classical continuum mechanics, the considered coordinate systems are most of the time orthonormal (note that Eringen [Eringen, 1962] has proposed a description of continuum mechanics using general curvilinear coordinate systems). Thus we will limit the 3D coordinate systems to orthonormal ones in this manuscript. In this case, the metric tensor noted $\boldsymbol{I}$ is represented by the 3D identity table and the orthonormal base vectors are noted $\boldsymbol{e}_i$, associated to the coordinate system ζ^i. The metric tensor may be expressed in any curvilinear coordinate systems, but when the notation $\boldsymbol{I}$ is used, it is to stress out the fact that the chosen 3D coordinate system is orthonormal.

1.1.2 3D observers

Within a 3D approach, time is a parameter that is not a coordinate. It is then necessary to associate a chronology measuring the instants of time t to the 3D coordinates. Observers and frames of reference are thus defined to give the possibility to parametrize the 3D spatial coordinate system with time.

First, an inertial (or Galilean, or Standard) observer is defined as it is classically understood in Newtonian Physics. A 3D inertial observer is thus defined as a set of base vectors $\boldsymbol{e}_i$ that do not depend on time. Inertial observers corresponds to sets of base vectors animated with a non accelerated motion with respect to one another. In terms

of notation, an inertial observer is described with the expression $(\boldsymbol{e}_i, \zeta^i, t)$ associating the orthonormal base vectors $\boldsymbol{e}_i$ to the coordinate system ζ^i and the time t.

An Euclidean observer, noted $(\tilde{\boldsymbol{e}}_i, \tilde{\zeta}^i, \tilde{t})$, is then defined such that:

$$\begin{cases} \tilde{\zeta}^i = Q^i{}_j(t)\zeta^j + \lambda^i(t) \\ \tilde{t} = \beta t - \alpha, \end{cases} \tag{1.1}$$

and

$$\tilde{\boldsymbol{e}}_i = Q_i{}^j(t)\boldsymbol{e}_j, \tag{1.2}$$

where $Q^i{}_j$ is an orthogonal matrix, $Q_j{}^i$ is the transpose of $Q^i{}_j$ and λ^i is a vector. These quantities depend only on time. Figure 1.2 illustrates the definition of such observers in a 2D plane. The scalars β and α correspond respectively to a unit change and shift in the chosen origins for the measure of time. It is further supposed, without much loss of generality, that time is equally measured by all observers such that $\tilde{t} = t$. Thus, an Euclidean observer can be generally defined as a set of three base vectors undergoing a rigid body motion with respect to an inertial observer.

Table 1.1 summarizes the notation used for the 3D observers and coordinates.

A frame of reference is next defined as a class of equivalence of observers. For simplicity, in terms of vocabulary, the expressions *observer* and *frame of reference* are considered equivalent in the rest of this manuscript.

Table 1.1: Notations for the observers, coordinate systems and coordinates of a material point. The Euclidean observers are always represented with an $\boldsymbol{e}_i$ for the base vectors. The coordinate systems are represented with a ζ and the coordinates of the material point with a z. When two observers are needed, a tilde is used to differentiate the observers.

Observers	$(\boldsymbol{e}_i, \zeta^i, t)$	$(\tilde{\boldsymbol{e}}_i, \tilde{\zeta}^i, \tilde{t})$
Type	Inertial	Euclidean
Base vectors	$\boldsymbol{e}_i$	$\tilde{\boldsymbol{e}}_i(t) = Q_i{}^j(t)\boldsymbol{e}_j$
Coordinate systems	ζ	$\tilde{\zeta}^i = Q^i{}_j(t)\zeta^j + \lambda^i(t)$
Coordinates of a material point	z^i	$\tilde{z}^i$

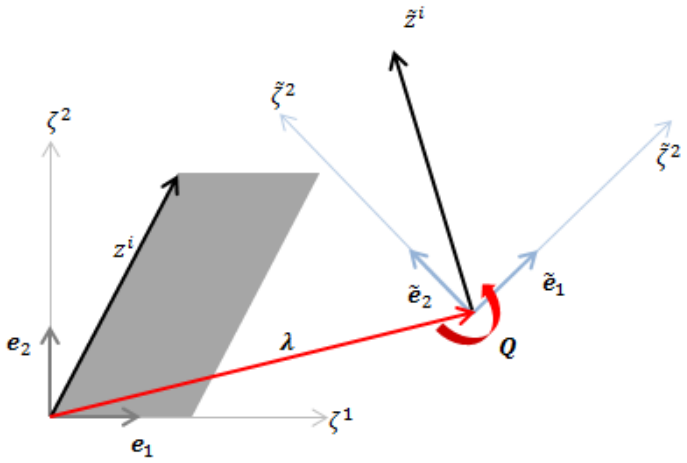

Figure 1.2: Illustration of Euclidean observers in a 2D plane with the coordinate systems, and the coordinates of a material point.

1.1.3 Motion of a material continuum

A material body is identified with a continuous and differentiable 3D manifold. The projection of the ensemble of material points into the three-dimensional space is called a configuration. It offers the complete specification of the positions of the particles of the material body at a given instant, as presented in Fig. 1.3. An instant of reference t_0 is chosen to define the considered volume of matter; at this instant of reference the configuration is Ω_0. The motion of the material body is then described by the configuration Ω_t taken by the body at the time t. The boundary of the body at this instant is denoted $\partial\Omega_t$. The initial configuration, corresponding the configuration taken by the body at the origin of time could be also defined. It is classical to consider that both the reference and the initial configurations are the same for simplicity.

When an observer is given, the positions of each of the particles of the material body can be specified. The coordinates of the particles in the reference configuration are noted Z^i, which defines the material or Lagrangian coordinates. After deformation, the current configuration is defined at the current time t, with the spatial or Eulerian coordinates z^i. Both the material and spatial configurations are usually expressed using the same observer (ζ^i, t).The deformation of the continuum can thus be described with the mapping:

$$z^i = z^i(Z^k, t_0, t). \tag{1.3}$$

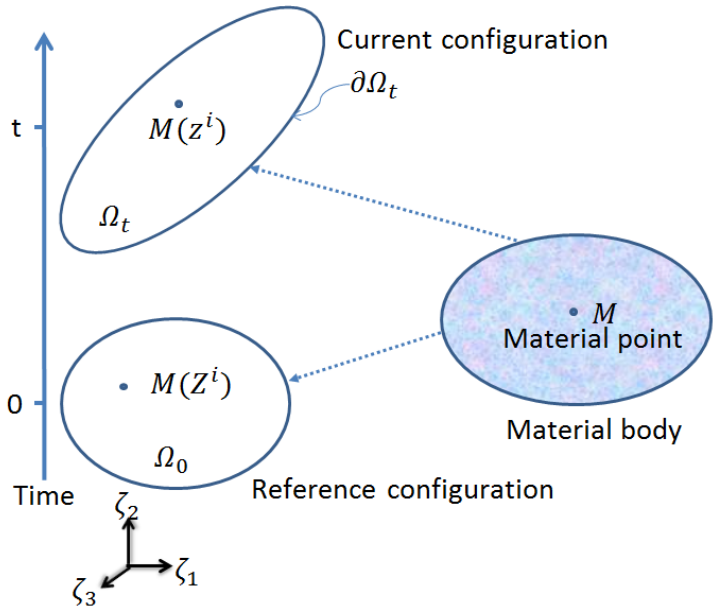

Figure 1.3: Material points, the reference configuration and the current configuration.

It is for example possible to define the specific motion:

$$z^i(t) = Q^i{}_j(t)Z^j + \lambda^i(t). \tag{1.4}$$

Here, the orthogonal matrix $Q^i{}_j$ describes a rigid body rotation and the vector λ^i represents a translation. Within this mapping, the distance between two points in the reference configuration remains constant in the current configuration, according to the definition of rigid body motion [Gurtin, 1982; Garrigues, 2007; De Souza Neto et al., 2011].

The deformation gradient $\boldsymbol{F}$ and its inverse $\boldsymbol{F'}$ are also defined as:

$$F^i{}_j = \frac{\partial z^i}{\partial Z^j} \quad \text{and} \quad F'^i{}_j = \frac{\partial Z^i}{\partial z^j}. \tag{1.5}$$

Several strain tensors may then be defined on the reference or spatial configurations.

We define the 3D left Cauchy-Green or Cauchy's deformation as:

$$\beta^{ij} = F^i{}_a F^j{}_b I^{ab}, \tag{1.6}$$

and its inverse:

$$b_{ij} = F'^a{}_i F'^b{}_j I_{ab}. \tag{1.7}$$

The 3D right Cauchy-Green deformation is:

$$C_{ij} = F^a_{\ i} F^b_{\ j} I_{ab}. \tag{1.8}$$

Two strain tensors are next defined. The Almansi's or Euler strain tensor is:

$$\boldsymbol{e} = e_{ij}\boldsymbol{e}^i \otimes \boldsymbol{e}^j = \frac{1}{2}(I_{ij} - b_{ij})\boldsymbol{e}^i \otimes \boldsymbol{e}^j, \tag{1.9}$$

while the Green's or Lagrange strain tensor is:

$$\boldsymbol{E} = E_{ij}\boldsymbol{e}^i \otimes \boldsymbol{e}^j = \frac{1}{2}(C_{ij} - I_{ij})\boldsymbol{e}^i \otimes \boldsymbol{e}^j. \tag{1.10}$$

To represent variations with respect to time, several quantities are defined. The velocity is

$$v^i = \frac{dz^i}{dt} \tag{1.11}$$

defined in an inertial observer. The velocity gradient is:

$$L^i_{\ j} = \frac{dF^i_{\ a}}{dt} F'^a_{\ j}. \tag{1.12}$$

The rate of deformation and the spin tensor are respectively:

$$d_{ij} = \frac{1}{2}(L_{ij} + L_{ji}) \quad \omega_{ij} = \frac{1}{2}(L_{ij} + L_{ji}), \tag{1.13}$$

corresponding to the symmetric and antisymmetric parts of the velocity gradient. In Eq. 1.12, the operator $\frac{d(.)}{dt}$ corresponds to a total derivative and is also called the material derivative defined as:

$$\frac{d(.)}{dt} = \frac{\partial(.)}{\partial t} + v^i \frac{\partial(.)}{\partial \zeta^i}. \tag{1.14}$$

Note that this operator is an expression of a variation with respect to time and it has to be applied in a inertial frame to be properly used. For a vector $\boldsymbol{w}$, it leads to:

$$\frac{d(\boldsymbol{w})}{dt} = \frac{d(w^i \boldsymbol{e}_i)}{dt} = \frac{d(w^i)}{dt}\boldsymbol{e}_i. \tag{1.15}$$

This can be expressed similarly for tensors of any ranks. In other words, this operator is not frame-indifferent. In 3D mechanics, many objective transports are proposed to fix the non-objectivity of total derivatives. More discussions are proposed in the following sections.

1.1.4 The stress tensor

The forces causing or generated by the deformation of materials can be classified into two categories:

- Surface forces. Forces applied on the surface of the material body. They include the boundary and the internal forces corresponding to interactions between subparts of a body.
- Body forces. Forces applied in the bulk of the material body.

Following Cauchy's principle, in a non-polar material body, the symmetric Cauchy stress tensor $\boldsymbol{\sigma}$ is introduced :

$$\boldsymbol{\sigma} = \sigma^{ij} \boldsymbol{e}_i \otimes \boldsymbol{e}_j \tag{1.16}$$

such that the stress vector $\boldsymbol{t}$, a surface density of force, applied on an elementary surface centered on the position $\boldsymbol{z}$, with the unit normal vector $\boldsymbol{n}$, is:

$$t^i = \sigma^{ij} n_j \tag{1.17}$$

The mechanical pressure p is defined as the opposite of the spherical part of the Cauchy stress tensor:

$$p = -\sigma^{ij} I_{ij} \tag{1.18}$$

and the deviatoric part of this tensor is noted $\boldsymbol{S}$, such that it is always possible to decompose the stress tensor as:

$$\sigma^{ij} = -pI^{ij} + S^{ij} \tag{1.19}$$

1.1.5 Principle of local state

The description of the material continua may be performed in the framework of classical thermodynamics. The system is the considered total volume of matter. Even if irreversible processes may occur in this system, it is supposed that it is locally in a thermodynamic equilibrium and that all thermodynamic state variables and functions of state exist for each particle of the system. The state of the material continua is completely defined by a

given number of local variables defined at each material point and depending only on the material point [Zahalak, 1992; Lemaitre and Chaboche, 1994]. Moreover, the functions of state for the non equilibrium system are the same functions of the local intensive state variables as the corresponding equilibrium thermodynamic quantities. A material continuum is characterized by, at least, the following scalar quantities:

- the density ρ,
- the temperature θ,
- the thermodynamic pressure p (it is further supposed that the thermodynamic pressure is equal to the mechanical pressure defined above),
- the internal energy density e,
- the entropy density η
- the rate of deformation $\boldsymbol{d}$ in the context of the theory of the first gradient [Lemaitre and Chaboche, 1994].

1.1.6 Governing equations

In classical continuum mechanics, the equations governing the deformations of a material are:

- the conservation of mass,
- the principle of linear momentum,
- the principle of angular momentum,
- first and second principles of thermodynamics leading to the Clausius-Duhem inequality,
- and the constitutive model.

The conservation of mass requires that:

$$\frac{d\rho}{dt} + \rho \nabla_i v^i = 0, \tag{1.20}$$

where ∇_i is the operator $\nabla_i = \frac{\partial .}{\partial \zeta^i}$ and v^i is the velocity. Without body forces, the principle of linear momentum requires that:

$$\begin{cases} \nabla_i \sigma^{ij} = \rho \frac{dv^j}{dt} & \text{in } \Omega_t \\ t^i = \sigma^{ij} n_j & \text{on } \partial\Omega_t. \end{cases} \tag{1.21}$$

The principle of angular momentum leads to the fact that the Cauchy stress tensor is symmetric in a non-polar material body [Gurtin, 1982; Lemaitre and Chaboche, 1994; Truesdell and Noll, 2003]:

$$\sigma^{ij} = \sigma^{ji}. \tag{1.22}$$

The combination of the first and second principle of thermodynamics leads to :

$$\sigma^{ij} d_{ij} + \rho \left(\theta \frac{d\eta}{dt} - \frac{de}{dt} \right) - \frac{\phi^i}{\theta} \nabla_i \theta \geq 0, \tag{1.23}$$

where ϕ^i is the energy flux. The Helmholtz specific free energy $\Psi = e - \theta\eta$ is defined leading to the Clausius-Duhem inequality:

$$\sigma^{ij} d_{ij} - \rho \left(\frac{d\Psi}{dt} + \eta \frac{d\theta}{dt} \right) - \frac{\phi^i}{\theta} \nabla_i \theta \geq 0. \tag{1.24}$$

The equations listed above are not sufficient to close the problem. They have to be completed by a relation between the deformation and the stress called a constitutive model, which is also regarded here as one of the governing equations. The study of constitutive relations in continuum mechanics consists in exploring the relation between stress and deformation for a given material [Eringen, 1962; Truesdell, 1966; Truesdell and Noll, 2003; Garrigues, 2007] and is necessarily partly empirical. For example, a constitutive model is represented by non rate-form equations for elastic materials or rate-form equations for hypoelastic, plastic or viscous materials. It is represented here in the general form :

$$\mathscr{T}(\sigma)^{ij} = \mathcal{F}^{ij}(I_{mn}, K_{(i)}, d_{kl}, \sigma_{pq}), \tag{1.25}$$

where $\mathscr{T}(.)$ denotes a transport operator and $\mathcal{F}(.)$ denotes the constitutive equation corresponding to a functional that could depend in general on the metric tensor $\boldsymbol{I}$, a

number n of material parameters $K_{(i)}$, the stress tensor $\boldsymbol{\sigma}$ and the rate of deformation $\boldsymbol{d}$; the density and the temperature are not included for simplicity.

The solution of the problem of continuum mechanics corresponds to the solution of the set of governing equations listed in the present section, associated to the prescribed initial and boundary conditions.

1.2 Open issues concerning classical 3D mechanics

1.2.1 Material objectivity

A constitutive model has to verify the principle of material objectivity to ensure its frame-indifference. This has become common wisdom in the area of continuum mechanics. In their work, Hooke and Poisson [Truesdell and Noll, 2003] already emphasized the necessity to define properly the observer. [Cauchy, 1829] discussed the necessity to use variables measured identically by all observers. [Zaremba, 1937] and [Noll, 1955] gave the first detailed mathematical statements of the notion of objectivity. A historical review and a detailed description can be found for instance in [Eringen, 1962; Nemat-Nasser, 2004; Marsden and Hughes, 1994; Truesdell and Noll, 2003; Speziale, 1987]. [Truesdell and Noll, 2003] define the principle of objectivity as: *"it is a fundamental principle of classical physics that material properties are indifferent, i.e., independent of the frame of reference or observer"*. [Nemat-Nasser, 2004] defines it as: *"Constitutive relations must remain invariant under any rigid-body rotation of the reference coordinate system. This is called objectivity or the material frame indifference."* There are indeed two physical notions:

- On one hand, the indifference with respect to the superposition of rigid body motions. For instance, when an unstrained body is animated with a rigid body motion, no stress is generated in the material. This is related to the material and the observed mechanical quantities. It concerns most materials and mechanical phenomena [Frewer, 2009].

- On the other hand, the independence with respect to the change of observers. For

instance, when an observer moves around an unstrained material, no stress is generated in the material. The phenomena do not depend on the observation. This is a fundamental principle of classical physics.

As stated by [Liu, 2004] indeed, *"the principle of material frame indifference plays an important role in the development of continuum mechanics, by delivering restrictions on the formulation of the constitutive functions of material bodies. It is embedded in the idea that material properties should be independent of observations made by different observers. Since different observers are related by a time-dependent rigid transformation, known as a Euclidean transformation, material frame-indifference is sometimes interpreted as invariance under superposed rigid body motions"*.

Consider two Euclidean observers $(\boldsymbol{e}_i, \zeta^i, t)$ and $(\tilde{\boldsymbol{e}}_i, \tilde{\zeta^i}, \tilde{t})$ such that:

$$\tilde{\zeta}^i = Q^i{}_j(t)\zeta^j + \lambda^i(t). \tag{1.26}$$

A second rank tensor $\boldsymbol{\tau}$ observed by these two observers, such that:

$$\boldsymbol{\tau} = \tau^{ij}\boldsymbol{e}_i \otimes \boldsymbol{e}_j = \tilde{\tau}^{ij}\tilde{\boldsymbol{e}}_i \otimes \tilde{\boldsymbol{e}}_j \tag{1.27}$$

is said to be frame-indifferent, if it verifies the relation:

$$\tilde{\tau}^{ij} = Q^i{}_m(t)Q^j{}_n(t)\tau^{mn}. \tag{1.28}$$

Similarly, a constitutive model (see Eq. 1.25) takes the respective form :

$$\begin{cases} \mathscr{T}(\sigma)^{ij} = \mathcal{F}^{ij}(I_{mn}, K_{(i)}, d_{kl}, \sigma_{pq}) \\ \tilde{\mathscr{T}}(\tilde{\sigma})^{ij} = \tilde{\mathcal{F}}^{ij}(I_{mn}, K_{(i)}, \tilde{d}_{kl}, \tilde{\sigma}_{pq}) \end{cases} \tag{1.29}$$

as observed by these two observers. The model is said to be frame-indifferent, if it verifies:

$$\tilde{\mathscr{T}}(\tilde{\sigma})^{ij} = Q^i{}_k Q^j{}_l \mathscr{T}(\sigma)^{kl}. \tag{1.30}$$

1.2.2 Discussion on the notion of material objectivity

The classical definition of frame-indifference refers to the indifference to the change of Euclidean observers. It does not concern curvilinear changes of observers. This constitutes

a strong limitation of this principle, because it does not insure a complete indifference with respect to changes of any observers. Indeed, the indifference with respect to changes of observers should provide a restriction that is verified for any changes of observers, concerning all kinds of observers. In particular, it is important that the deforming material "sees" the same constitutive model as the other observers. A deforming observer can be associated to the deforming material. It corresponds to the convective frame of reference [Sidoroff, 1982a]. Frame-indifference should thus insure that the constitutive model is indifferent to changes of observers from an Euclidean observer to the convective frame. This is further discussed in Section 1.2.5.

Frame-indifference is not verified by all 3D tensors for example, the velocity vector, the acceleration vector, the deformation gradient, the spin tensor are not frame-indifferent. Thus the principle of linear momentum is not in general frame-indifferent. Frame-indifference is imposed on the quantities representing force and stress due to experimental observations that validate the fact that this quantities are frame-indifferent. Similarly, frame-indifference is imposed on constitutive models because the behavior of materials is experimentally observed to be indifferent with respect to rigid body superposition. The 3D definition of frame-indifference implies the indifference with respect to the superposition of rigid body motions. The difficulty is that, within a three-dimensional formalism, both properties result in the same mathematical condition such that the term "objective" represents, ambiguously, both frame-indifference and the indifference with respect to the superposition of rigid body motions [Truesdell and Noll, 2003; Murdoch, 2003; Murdoch, 2005; Liu, 2005; Muschik and Restuccia, 2008]. The mechanical properties of most known solid materials are indeed indifferent with respect to the superposition of rigid body motions. However, it could be conceived, at least theoretically, that a given material property could depend on the superposition of rigid body motions [Murdoch, 1983; Svendsen and Bertram, 1999; Muschik and Restuccia, 2008; Frewer, 2009]. Such considerations have indeed been formulated concerning specific phenomena or extreme conditions, for example, for liquid crystal behavior [Muschik and Restuccia, 2008] and also for gas behavior and heat conductivity [Barbera and Müller, 2006; Biscari and Cercignani, 1997; Biscari et al., 2000; De Socio and Marino, 2002; Moller, 1972; Muschik and

Restuccia, 2008; Muschik, 2012; Svendsen and Bertram, 1999].

Physical considerations lead to the conclusion that the equations describing these phenomena should nevertheless be indifferent with respect to changes of observers. Thus it could be useful to impose frame-indifference to a quantity that is not indifferent to the superposition of rigid body motions.

In the end, the validity of such an "objective" approach, and the restriction that it imposes on the constitutive models are often questioned and reconsidered; see for example [Dienes, 1979; Murdoch, 1983; Simo and Ortiz, 1985; Kojić and Bathe, 1987; Voyiadjis and Kattan, 1989; Duszek and Perzyna, 1991; Rougée, 1992; Schieck and Stumpf, 1993; Prost-Domasky et al., 1997; Stumpf and Hoppe, 1997; Svendsen and Bertram, 1999; Meyers et al., 2000; Murdoch, 2003; Valanis, 2003; Fiala, 2004; Garrigues, 2007; Muschik and Restuccia, 2008; Besson et al., 2009; Muschik, 2012].

1.2.3 Objective transports

An important issue concerns the definition of material objective time derivatives to represent, objectively, the variations of a tensor with respect to time. These derivatives appear in the rate-forms of constitutive models when the indifference with respect to the superposition of rigid body motions is indeed observed. The difficulty occurs because the total time derivative of an objective tensor is in general not objective. To work out this problem, 3D objective transport operators are generally defined.

This point has been first discussed by [Zaremba, 1903; Jaumann, 1911] who introduced an objective stress transport in constitutive models. The Jaumann transport of a tensor $\boldsymbol{\sigma}$ in an inertial frame is expressed as:

$$\mathscr{T}^J(\sigma)^{ij} = \frac{d\sigma^{ij}}{dt} - \omega^j{}_k\sigma^{ik} - \omega^i{}_k\sigma^{kj}, \tag{1.31}$$

where $\boldsymbol{\omega}$ is the spin tensor and $\frac{d}{dt}$ is the total time derivative. Other objective transports have been introduced. The polar rate or Green-Naghdi transport [Green and Naghdi, 1965] is expressed in an inertial frame as:

$$\mathscr{T}^{GN}(\sigma)^{ij} = \frac{d\sigma^{ij}}{dt} - \frac{dR^i_b}{dt}R^b_k\,\sigma^{kj} - \frac{dR^j_b}{dt}R^b_k\,\sigma^{ik}. \tag{1.32}$$

$\boldsymbol{R}$ is calculated from the polar decomposition of the deformation gradient:

$$F^i{}_j = R^i{}_k U^k{}_j \tag{1.33}$$

with $\boldsymbol{R}$ an orthogonal tensor and $\boldsymbol{U}$ a symmetric positive tensor. These transports suppose the existence of an intermediate rotated configuration. Other types of intermediate configurations can be defined to construct other objective transports [Dogui, 1989; Badreddine et al., 2010]. Among the many other objective transports, there are the various convective transports sometimes also referred as "Oldroyd transports" or "Maxwell transports" [Marsden and Hughes, 1994; Oldroyd, 1950]:

$$\mathscr{T}^{C1}(\sigma)^{ij} = \frac{d\sigma^{ij}}{dt} - \sigma^{ik} L^j{}_k - \sigma^{kj} L^i{}_k \tag{1.34}$$

$$\mathscr{T}^{C2}(\sigma)^i{}_j = \frac{d\sigma^i{}_j}{dt} + \sigma^i{}_k L^k{}_j - \sigma^k{}_j L^i{}_k, \tag{1.35}$$

where $\boldsymbol{L}$ is the velocity gradient. Convective transports, also includes Truesdell's transport [Truesdell, 1955]:

$$\mathscr{T}^{T}(\sigma)^{ij} = \frac{d\sigma^{ij}}{dt} - \sigma^{ik} L^j{}_k - \sigma^{kj} L^i{}_k + \sigma^{ij} L^k{}_k. \tag{1.36}$$

These objective transports are defined for an inertial observer (see Section 1.1). Besides, all these objective transports are constructed on a similar basis: the material derivative of the tensor is corrected with terms that ensure the objectivity of the transport operator. An infinite number of corrections and combinations of these corrections can be performed [Truesdell and Noll, 2003; Besson et al., 2009; Marsden and Hughes, 1994; Eringen, 1962; Nemat-Nasser, 2004; Stumpf and Badur, 1990].

Objective transport operators are applied in particular to the Cauchy stress tensor. The result of each of these transports is proven to be indifferent with respect to the superposition of rigid body motions [Nemat-Nasser, 2004; Marsden and Hughes, 1994; Truesdell and Noll, 2003]. These objective transports are then used to construct constitutive models for complex solid or fluid materials, such as polymers, for plastic and visco-plastic effects in solids and visco-elastic effects in fluids [Besson et al., 2009; Eringen, 1962; Nemat-Nasser, 2004; Sidoroff, 1982a; Stumpf and Badur, 1990; Truesdell and Noll, 2003; Dafalias and Younis, 2007; Dafalias and Younis, 2009; Thiffeault, 2001; Venturi, 2009].

1.2.4 Discussion over the notion of objective transports

As discussed in Section 1.2.3 it is usually verified that the transports are indifferent with respect to rigid body superposition, but it is not verified that it is indifferent with respect to changes of any type of observers.

As presented in Section 1.2.3 above, there are "infinitely many possible objective time fluxes that may be used" [Truesdell and Noll, 2003]. Although Truesdell and Noll postulate that *"the properties of a material are independent of the choice of flux, which, like the choice of a measure of strain, is absolutely immaterial"*, it is admitted that the transport operator is a constitutive choice [Besson et al., 2009; Stumpf and Hoppe, 1997]. If it is commonly admitted that the choice of the objective transport should be adapted to the kinematics of the modeled material, there is no specific mathematical or physical rule to guide this choice. Often the choice of the transport is guided by trial and error methods and corresponds to the one that exhibits the most "reasonable" behavior. However, the solution may indeed exhibit non-physical behaviors [Dienes, 1979; Kojić and Bathe, 1987; Meyers et al., 2000; Schieck and Stumpf, 1993; Stumpf and Hoppe, 1997; Voyiadjis and Kattan, 1989]. This is the case for example, with hypo-elastic models that may be non-reversible. In other cases, a stress might be generated within a material at rest when the observer rotates around the system [Besson et al., 2009]. When Jaumann's transport is used, it is well known that the solution may exhibit stress oscillations when submitted to constantly increasing shearing solicitations [Besson et al., 2009], which are physically senseless.

Numerical formulations using objective transports have been proposed and discussed by several authors; see for example [Dogui, 1989; Crisfield and Jelenić, 1999; Sidoroff and Dogui, 2001; Nemat-Nasser, 2004; Dafalias and Younis, 2009]. Jaumann and Green-Naghdi transports are classically used in commercial finite-element (FE) softwares to solve non-linear problems [Hibbitt et al., 1997; Hallquist et al., 2007]. Objective stress transports have been interchangeably used for comparison [Badreddine et al., 2010; Saanouni and Lestriez, 2009; Besson et al., 2009; Duszek and Perzyna, 1991; Meyers et al., 2000; Prost-Domasky et al., 1997]. In this case, the different mechanical quantities are

evaluated for each of the intermediate rotated configurations corresponding to the specific objective transport. This is very time consuming and the computations might not converge [Badreddine et al., 2010]. Even if a reasonable and numerically converged solution is obtained, it may lead to non-physical results in other conditions. It is further difficult to propose experimental schemes to evaluate or verify the choice of the transport itself. The parameters of the constitutive models are thus often established from simple considerations (for example fitting on stress strain curves), in contrast with the complexity of the considered behavior.

The last consideration concerns the definition of a transport itself. The objective transports are also referred as "objective rates" or "invariant time fluxes". They are commonly called “rates” and indeed used as the variation of a quantity with respect to time. They are discretized and integrated as such in numerical simulations. Nevertheless, most of the transports do not correspond to rates. In other words, they do not correspond to the total variation of a tensor with respect to time. Thus extreme caution should be taken for their discretization and integration.

1.2.5 Eulerian versus Lagrangian descriptions

A important question raises when constructing constitutive models in the framework of finite deformations: how to choose between an Eulerian and a Lagrangian description? The choice of the Eulerian versus the Lagrangian descriptions is not arbitrary, and seems to be constitutive. Moreover, anisotropic behaviors in a thermodynamic framework are difficult to describe in an Eulerian description. Nevertheless, a correspondence can be established with the convected coordinates between the components of some Eulerian and Lagrangian tensors [Sidoroff, 1982a]. This means that a deeper link exists between the two descriptions [Garrigues, 2007]. Moreover, the problem of material objectivity is prominent when dealing with the Eulerian and Lagrangian descriptions. The tensors defined within Lagrangian description are often considered to be objective by construction [Nemat-Nasser, 2004]. However, this is not always the case within an Eulerian description. The difference between these two descriptions seems to contradict the fact that Eulerian and Lagrangian descriptions are equivalent [Sidoroff, 1982a; Dogui, 1989]. Material ob-

jectivity in a Lagrangian description is defined with a rotation matrix expressed at the initial time. For example, a Lagrangian tensor transforms from $\boldsymbol{T}$ to $\tilde{\boldsymbol{T}}$:

$$\tilde{T}^{ij} = Q^i_{0m} Q^j_{0n} T^{mn}. \tag{1.37}$$

According to [Garrigues, 2007], this expression of material objectivity is senseless, because $\boldsymbol{Q}_0$ is not a function of time.

1.2.6 Propositions for a consistent description of continuum mechanics

The different issues raised in this Section lead to the conclusion that continuum mechanics under the hypotheses listed in Section 1.1 should be described within a completely frame-indifferent framework. Any physical phenomena and principle should be described in a frame-indifferent manner. This should be further insured with respect to any changes of observers, not only Euclidean observers. Further, it should be possible to make a distinction between frame-indifference and indifference with respect to rigid body superposition. Indeed, most material properties exhibit a behavior that is indifferent to rigid body superposition.

1.3 The interest of a 4D formalism to describe the finite transformations of materials

1.3.1 Advantages of a 4D formulation for finite deformations

As written by Eringen (1962): *Attempts to secure the invariance of the physical relations of motion from the observer have produced one of the great triumphs of twentieth-century physics. Attempts to free the principles of classical mechanics from the motion of an observer were resolved by Einstein in his general theory of relativity.*

Physical observations lead to the conclusion that the presence, nature and number of the observers do not change the physical phenomena undergone by the matter. Observers

should thus agree on the evaluation of these physical phenomena. This corresponds to the principle of general covariance, first formulated by A. Einstein ([Havas, 1964]). [Landau and Lifshitz, 1975] formulate the covariance principle of General Relativity as: *the laws of nature must be written in the general theory of relativity in a form which is appropriate to any four-dimensional system of coordinates (or, as one says, in a covariant form).* In other words, a model must be expressed using an adapted mathematical form that is strictly the same for each observer. The model should be independent of any arbitrary change of observers. This is possible with a 4D covariant description of physics. 4D tensor densities are all independent of 4D coordinate transformations. Within this 4D context, because the fourth coordinate represents time, the observers are completely defined once the 4D coordinate system is chosen and 4D coordinate transformations describe changes of observers. The 4D formulation provides a clear distinction between the properties of indifference to the superposition of rigid body motions and independence of changes of observers. Within this formalism, all tensors are by construction independent of arbitrary changes of (possibly accelerated and/or deformed) observers. The 4D description also encompasses both the Eulerian and Lagrangean descriptions of material transformations. The Lagrangian case corresponds to a specific observer linked to the material (i.e. to the convective frame of reference). It is further possible to define time derivative operators that are 4D tensors, and acceleration, velocity and spin tensors become independent of the observer. We thus propose to describe the finite transformations of materials with a 4D covariant approach using the formalism of differential geometry.

Differential geometry also known as Ricci-calculus, [Levi-Civita2005, Schouten1954] offers indeed a convenient framework to model the physical quantities describing the finite transformations of a material continuum. Tensor density fields of the considered manifold represent these physical quantities. It is recognized as a formalism of choice to describe the straining motion of material continua within a classical three-dimensional (3D) context; see, for example, [Eringen, 1962; Malvern, 1969; Truesdell and Noll, 2003; Duszek and Perzyna, 1991; Marsden and Hughes, 1994; Simo and Ortiz, 1985; Stumpf and Hoppe, 1997; Thiffeault, 2001; Venturi, 2009; Yavari and Ozakin, 2008]. Within its four-dimensional (4D) context, differential geometry has found a major and essential

application in physics with the theory of General Relativity, which has shown its ability to deal properly with space-time transformations.

1.3.2 Outlines of the thesis

Thanks to the advantages of a 4D formulation, we propose to build a fully covariant four-dimensional description of the finite transformations of a material, considering the classical hypotheses of Newtonian physics and using the mathematical framework of differential geometry. The mechanics of material continua hence described, and the associated constitutive models, will be then necessarily independent of the observer. A 4D thermodynamic framework will be proposed to validate the approach and to construct conservation laws considering possible dissipative effects. The choice of the transport becomes then a constitutive choice based only on physical considerations. Covariant 4D generalization of the existing constitutive models will be written, possibly in an incremental form, in particular for hypo-elastic and plastic behaviors. It will be then possible to project the model into a 3D space to implement the result in existing Finite Element Analysis (FEA) codes. Then, computations will be performed using the existing integration scheme. All these aspects will be detailed in the following chapters.

In Chapter 2, a brief introduction of the four-dimensional formalism is performed. Two total time derivatives, the covariant transport and the Lie derivative, are presented. The Lie derivative, which is the only derivative both covariant and indifferent to the superposition of rigid body motions, will be used in developing rate-form models in the following chapters. A detailed comparison between the two notions related to the principle of objectivity is performed. Last, the motion of materials is described with 4D kinematics. 4D strain tensors and rate of strain tensors are then defined.

In Chapter 3, a general method using 4D thermodynamics and considering dissipative effects is applied to constitute models. The thermodynamics starts with a proposition for the construction of the momentum-energy tensor. Then conservation laws and entropy principle are taken into consideration. They are derived using the proposed momentum-energy tensor. A 4D inequality corresponding to a generalization of Clausius-Duhem inequality is also derived. Last, this inequality is used to develop constitutive models

with specific choices of the Helmholtz specific free energy and considering the principle of maximum dissipation.

In Chapter 4, we mainly discuss the 4D elastic models including hyperelastic models, anisotropic elastic models and hypoelastic models. We obtain a reversible 4D hypoelastic model by using the Lie derivative, which offers an interesting tool for the construction of the elastoplastic model developed in the next chapter.

In Chapter 5, 4D models for plasticity and elastoplasticty are constructed. First, the kinematic way of coupling elasticity and plasticity is discussed. Then, the plastic model derived from thermodynamics is specified. With the chosen additive decomposition, a final model for elastoplasticity is constructed within the 4D formalism, and compared to equivalent 3D existing models.

In the last chapter, the 4D models developed in this work are used to perform Finite Element Analysis (FEA) on structures. Because there is no mature 4D finite element codes, the models have been projected into 3D to be adapted to the existing simulation softwares. The models have been implemented in the Zset© software to perform several simulations.

Chapter 2

The four-dimensional formalism and its application to 4D kinematics

Contents

2.1 Introduction

In this chapter, a general four-dimensional description of the deformation of a continuum is first introduced using the formalism of differential geometry. The vocabulary and notations that are used in the manuscript are first introduced with the 4D description of space-time. The hypotheses of this work are then discussed in view of the 4D framework. Then, a comparison between frame-indifference and indifference with respect to the superposition of rigid body motions is proposed to distinguish them clearly within this 4D formalism. In order to construct 4D rate-form models, the 4D covariant rate and the Lie derivative are introduced. Last, a complete 4D kinematics for a deforming continuum is proposed with in particular the definition of 4D strain tensors and the rate of deformation tensor.

2.2 4D space-time framework

Differential geometry proposes a general mathematical context for the description of tensors and the associated algebras. Classical notions of differential geometry [Levi-Civita et al., 2005; Schouten, 1954; Choquet-Bruhat, 1968; Lee, 2003; Gostiaux, 2005; Spivak, 1999; Kerner, 2014] and 4D physics are reviewed in order to introduce the vocabulary and notations. Further details concerning these subjects are proposed for example in [Misner et al., 1973; Boratav and Kerner, 1991], where the general concepts are given, while the theory of General Relativity applied to physical fields is presented by Landau and Lifshits [Landau and Lifshitz, 1975] and Weinberg [Weinberg, 1972].

2.2.1 4D coordinate systems and frames of reference

In the General Relativity theory, space-time is described with a four-dimensional differentiable manifold ([Boratav and Kerner, 1991]). A set of four coordinates denoted:

$$\xi^\mu = (\xi^1, \xi^2, \xi^3, \xi^4) = (\xi^i, ct) \tag{2.1}$$

is used to parameterize a point of the 4D manifold and this set constitutes an event. The index notation is used and Greek indices (μ, ν ... running from 1 to 4) label the 4D space-time entities, while the Roman indices (i, j ... running from 1 to 3) label the spatial part of the quantity. The coordinate ξ^4 represents the time t multiplied by the constant speed of light in vacuum c such that ξ^4 has dimension of length. Other sets of coordinates could be indifferently chosen to parameterize the points of the manifold. Consider two possible sets of coordinates noted ξ^μ and $\widetilde{\xi}^\mu$. The transformation of the coordinates is given by:

$$d\widetilde{\xi}^\mu = \frac{\partial \widetilde{\xi}^\mu}{\partial \xi^\nu} d\xi^\nu, \tag{2.2}$$

where $\frac{\partial \widetilde{\xi}^\mu}{\partial \xi^\nu}$ is the Jacobian matrix of the coordinate transformation. The determinant of this Jacobian matrix is denoted $\left|\frac{\partial \widetilde{\xi}^\mu}{\partial \xi^\nu}\right|$.

An interval ds is defined as a generalized length element, such that:

$$\begin{aligned} ds^2 &= -(d\zeta^1)^2 - (d\zeta^2)^2 - (d\zeta^3)^2 + (d\zeta^4)^2 \\ &= \eta_{\mu\nu} d\zeta^\mu d\zeta^\nu, \end{aligned} \tag{2.3}$$

where the coordinates ζ^μ represent the 4D coordinates of an event in a 4D Cartesian coordinate system ζ^μ. This particular coordinate system is also said to be standard, Minkowskian, Galilean or inertial and the components of the metric tensor are in this case [Landau and Lifshitz, 1975]:

$$\eta_{\mu\nu} = \begin{pmatrix} -1 & 0 & 0 & 0 \\ 0 & -1 & 0 & 0 \\ 0 & 0 & -1 & 0 \\ 0 & 0 & 0 & +1 \end{pmatrix}. \tag{2.4}$$

It is supposed that such a set of coordinates exists for every point of the manifold. As a 4-scalar, the interval ds is constant under any change of 4D coordinate systems. Using Eqs. 2.2 and 2.3, the covariant components $g_{\mu\nu}$ of the metric tensor take the form:

$$g_{\mu\nu} = \frac{\partial\zeta^{\lambda}}{\partial\xi^{\mu}}\frac{\partial\zeta^{\kappa}}{\partial\xi^{\nu}}\eta_{\lambda\kappa}, \tag{2.5}$$

in any coordinate system ξ^{μ}.

In this thesis, gravitational fields are not taken into account and the components of the metric tensor depend only on the choice of the coordinates. As a consequence, the Riemann 4D curvature tensor of this particular 4D space is equal to zero, such that the considered space-time is Euclidean.

The covariant and contravariant components of the metric tensor are such that:

$$g_{\mu\lambda}g^{\lambda\nu} = g_{\mu}{}^{\nu} = \delta_{\mu}{}^{\nu}, \tag{2.6}$$

where $\delta_{\mu}{}^{\nu}$ is the Krönecker's symbol.

A set of four base vectors $\boldsymbol{g}_{\mu}(\xi^{\kappa})$ (covariant) or $\boldsymbol{g}^{\mu}(\xi^{\kappa})$ (contravariant) is further defined associated to the 4D coordinate system ξ^{κ}. Any set of four vectors representing the local base vectors, can be changed from the set of orthonormal base vectors $\boldsymbol{e}_{\mu}$ or $\boldsymbol{e}^{\mu}$ associated to the 4D inertial coordinate system ζ^{κ} with the relations:

$$\boldsymbol{g}_{\nu} = \frac{\partial\zeta^{\mu}}{\partial\xi^{\nu}}\boldsymbol{e}_{\mu}, \tag{2.7a}$$

$$\boldsymbol{g}^{\nu} = \frac{\partial\xi^{\nu}}{\partial\zeta^{\mu}}\boldsymbol{e}^{\mu}. \tag{2.7b}$$

In the 4D manifold, the coordinates of an event contain the information of both position and time, such that an observer may be defined as a set of four base vectors associated to the chosen coordinate system. It can then be concluded that *the choice of a 4D coordinate system is equivalent to the choice of a frame of reference and 4D coordinate transformations describe changes of observers.* In the rest of this manuscript, the expressions *4D coordinate system* and *frame of reference* are thus used equivalently.

2.2.2 4D tensors

Consider the tangent vector space $\mathscr{V}$ attached to a point of the four-dimensional differential manifold and its dual vector space $\mathscr{V}^{*}$. A type (p, q) tensor $\boldsymbol{\tau}$ said to be p-contravariant

and q-covariant is defined as:

$$\boldsymbol{\tau} = \underbrace{\mathscr{V} \otimes ... \otimes \mathscr{V}}_{p} \otimes \underbrace{\mathscr{V}^* \otimes ... \otimes \mathscr{V}^*}_{q}, \tag{2.8}$$

where "$\otimes$" denotes the tensor product. A 4D second-rank tensor $\boldsymbol{\tau}$ can be expanded in different 4D coordinate systems as:

$$\begin{aligned} \boldsymbol{\tau} &= \tau^{\mu\nu}\boldsymbol{g}_\mu \otimes \boldsymbol{g}_\nu = \tau_{\mu\nu}\boldsymbol{g}^\mu \otimes \boldsymbol{g}^\nu = \tau^\mu{}_\nu \boldsymbol{g}_\mu \otimes \boldsymbol{g}^\nu = \tau_\mu{}^\nu \boldsymbol{g}^\mu \otimes \boldsymbol{g}_\nu \\ &= \widetilde{\tau}^{\mu\nu}\widetilde{\boldsymbol{g}}_\mu \otimes \widetilde{\boldsymbol{g}}_\nu = \widetilde{\tau}_{\mu\nu}\widetilde{\boldsymbol{g}}^\mu \otimes \widetilde{\boldsymbol{g}}^\nu = \widetilde{\tau}^\mu{}_\nu \widetilde{\boldsymbol{g}}_\mu \otimes \widetilde{\boldsymbol{g}}^\nu = \widetilde{\tau}_\mu{}^\nu \widetilde{\boldsymbol{g}}^\mu \otimes \widetilde{\boldsymbol{g}}_\nu, \end{aligned} \tag{2.9}$$

in a Euclidean space, where $\tau^{\mu\nu}$ and $\widetilde{\tau}^{\mu\nu}$ are the contravariant components of this tensor density, $\tau_{\mu\nu}$ and $\widetilde{\tau}_{\mu\nu}$ its covariant components, and $\tau^\mu{}_\nu$, $\tau_\mu{}^\nu$ $\widetilde{\tau}^\mu{}_\nu$ or $\widetilde{\tau}_\mu{}^\nu$ its mixed components. The components of the tensor may be transformed between their covariant and contravariant states with the relations

$$\tau_{\mu\nu} = g_{\mu\alpha}g_{\nu\beta}\tau^{\alpha\beta}, \tag{2.10a}$$

$$\tau^{\mu\nu} = g^{\mu\alpha}g^{\nu\beta}\tau_{\alpha\beta}. \tag{2.10b}$$

Similar relations may be established for tensors of other ranks.

2.2.3 Four-velocity

Let x^μ denote the coordinates of a given event in a given curvilinear coordinate system ξ^μ. If the events are described in a Minkowskian (inertial) 4D coordinate system, the coordinates of the material point are noted z^μ in the coordinate system ζ^μ. The four-velocity of a material point, which is of great importance for kinematics, is now introduced. The definition of the four-velocity denoted $\boldsymbol{u}$ is:

$$u^\mu = \frac{dx^\mu}{d\tau}. \tag{2.11}$$

The interval $d\tau$ taken along the motion of the material point is:

$$\begin{aligned} d\tau^2 &= -(dz^1)^2 - (dz^2)^2 - (dz^3)^2 + (cdt)^2 \\ &= \eta_{\mu\nu}dz^\mu dz^\nu \\ &= g_{\mu\nu}dx^\mu dx^\nu. \end{aligned} \tag{2.12}$$

This interval has the same value in any 4D coordinate system as defined in Eqs. 2.3 and 2.5. This can further be expressed as:

$$d\tau^2 = (cdt)^2 \left(1 - \frac{v^2}{c^2}\right), \tag{2.13}$$

where $v = \|v^i\|$ with $v^i = dz^i/dt$ is the norm of the 3D velocity with respect to the inertial frame. Substituting Eq. 2.13 into Eq. 2.11 leads to:

$$u^\mu = \frac{\frac{dx^\mu}{dt}}{c\sqrt{1 - \frac{v^2}{c^2}}}. \tag{2.14}$$

The parameter γ called the Lorentz factor or Gamma factor is introduced such that:

$$\gamma = \frac{1}{\sqrt{1 - \frac{v^2}{c^2}}}. \tag{2.15}$$

Note that the four-velocity $\boldsymbol{u}$ is a dimensionless quantity. Using Eqs. 2.10 and 2.12, it can be proven that the four-velocity is a unitary vector:

$$u^\mu u_\mu = g_{\mu\nu} u^\mu u^\nu = 1. \tag{2.16}$$

The proper frame of reference corresponds to a frame that is moving with the material point. In this proper frame, the velocity of any material point is $(0, 0, 0, 1)$ by construction.

2.2.4 The principle of covariance

The principle of covariance of General Relativity, due historically to Einstein, states that nature's laws must be expressed using a form that is covariant in any 4D coordinate system $\widetilde{\xi}^\mu$, ξ^μ or ζ^μ, where:

$$\widetilde{\xi}^\mu = \widetilde{\xi}^\mu(\xi^\nu) = \widetilde{\xi}^\mu(\zeta^\nu) \tag{2.17}$$

is a diffeomorphism of space-time onto itself [Synge, 1960; Weinberg, 1972; Boratav and Kerner, 1991; Landau and Lifshitz, 1975]. The indifference to 4D coordinate transformations has to be verified by any 4D tensors, equations or operators. Thus, a scalar a or the

components of the second-rank 4D tensor density $\boldsymbol{\tau}$ verify the relations:

$$\widetilde{a} = \left|\frac{\partial \xi^{\alpha}}{\partial \widetilde{\xi}^{\beta}}\right|^{W} a \tag{2.18a}$$

$$\widetilde{\tau}^{\mu\nu} = \left|\frac{\partial \xi^{\alpha}}{\partial \widetilde{\xi}^{\beta}}\right|^{W} \frac{\partial \widetilde{\xi}^{\mu}}{\partial \xi^{\lambda}} \frac{\partial \widetilde{\xi}^{\nu}}{\partial \xi^{\kappa}} \tau^{\lambda\kappa} \tag{2.18b}$$

$$\widetilde{\tau}_{\mu\nu} = \left|\frac{\partial \xi^{\alpha}}{\partial \widetilde{\xi}^{\beta}}\right|^{W} \frac{\partial \xi^{\lambda}}{\partial \widetilde{\xi}^{\mu}} \frac{\partial \xi^{\kappa}}{\partial \widetilde{\xi}^{\nu}} \tau_{\lambda\kappa}, \tag{2.18c}$$

when the coordinate system is changed from ξ^{α} to $\widetilde{\xi}^{\alpha}$. Equivalent equations may be established for tensor densities of other ranks.

The principle of covariance corresponds to an indifference with respect to the action of the full group of diffeomorphisms. Because the mapping of the events with the 4D coordinate system includes time, there is no mathematical difference between a change of 4D coordinate system and a change of frame of reference, as opposed to the 3D approach. *The principle of covariance thus necessarily ensures the frame-indifference of any 4D tensors, equations and operators.* In other words, a 4D tensor is by construction frame-indifferent and the notions of:

- indifference with respect to transformations of 4D coordinates
- frame-indifference

correspond to the same property within a 4D approach. In contrast, the classical definition of 3D frame-indifference refers to an invariance under Euclidean transformations. The 3D frame-indifference is not verified by all 3D tensors, e.g. the velocity and the acceleration. When a 4D tensor is known in one 4D coordinate system, its components may be computed in any other 4D coordinates systems, i.e. in any frame of reference due to the covariance principle. The covariance (that is the frame-indifference) of rate quantities is thus ensured in 4D. In particular, the four-velocity is covariant as detailed in Appendix A.1.2 and it is possible to define and the acceleration as a 4D vector.
This is the fundamental reason why we propose to construct constitutive models within a 4D formalism.

For clarity, from now on, the expression "frame-indifference" is dedicated to the 3D indifference with respect to Euclidean transformations, whereas "covariance" corresponds to the indifference with respect to the action of the full group of diffeomorphisms within a 4D context.

2.3 Newtonian motions and observers

The goal of this work is to describe the finite deformations of a material body as it is traditionally studied in continuum mechanics. An observer evaluates physical quantities characterizing the state of the material for each instant of time and point of space. These observed transformations could be schematically described as ranging from slow infinitesimal elastic perturbations undergone by a solid material, to, at the other extreme, a gas explosion in a rocket. In other words, in all these transformations, the velocity of the material points are such that the hypotheses of Newton are verified. Indeed, within the range of Newtonian hypotheses, $\frac{v}{c} \ll 1$ for any material point and for any event of any motion. We now define a Newtonian motion. It corresponds to a motion for which the velocity of any material points is very small compared to the velocity of light. In other words, $\gamma \approx 1$ for any of the material points that are considered.

Eq. 2.13 implies that the definition of time can vary. Within a relativistic formulation, time is thus said to be *absolute* when expressed in the inertial frame and *proper* when expressed in the proper frame of reference moving with the material point. The proper time t' is such that $\tau = ct'$. It is not the purpose of this work to evaluate the proper time of a material point. Then, with Eq. 2.13, $d\tau/c = dt' \approx dt$ for Newtonian motions. In other word, the proper time, in these circumstances, is infinitely close to the absolute time. Consequently, in this thesis, t always refers to the absolute time.

Within a Newtonian motion, the four velocity takes the approximate form:

$$u^\mu = \left(\frac{\frac{dx^i}{dt}}{c\sqrt{1-\frac{v^2}{c^2}}}, \frac{1}{\sqrt{1-\frac{v^2}{c^2}}} \right) \approx \left(\frac{\frac{dx^i}{dt}}{c}, 1 \right). \tag{2.19}$$

This could be rewritten:

$$c\, u^{\mu} \approx \left(\frac{dx^i}{dt}, c \right). \tag{2.20}$$

Thus the four-velocity corresponds to the relative velocity within a 3D formalism. It is the velocity as computed in the chosen frame of reference. Also note that the constant c plays the role of a dimensional parameter for the velocity and any time like quantity.

Among the possible 4D coordinates system that could be chosen to describe the motion, For simplicity, we choose to restrict the description of the motions of the material within the hypotheses of classical continuum mechanics. These practical coordinate systems will define the 4D Newtonian observers, whose absolute velocity is comparatively small to that of light. A 4D Newtonian observer is thus defined as a set of base vectors $\boldsymbol{g}_{\mu}$,calculated in Eq. 2.7, for which the measure of time is absolute such that:

$$\xi^4 = \zeta^4 = ct. \tag{2.21}$$

Further, these observers may be accelerated or rotated with respect to the inertial observers, but their velocity has to remain small with respect to that of light such that:

$$ds \approx cdt. \tag{2.22}$$

So, we will consider motions for which the velocity of every material point is small with respect to that of light associated to observers whose velocity is small with respect to the that of light. The description of this motion constitutes what is referred as the Newtonian hypotheses in this work.

2.4 The notion of objectivity under the light of the principle of covariance

In this section, the notion of material objectivity is described within the 4D formalism. Then, a clear distinction is proposed between the principle of covariance and that the property of indifference with respect to superposition of rigid body motions. The two notions are elaborated with two equivalent motions in different frames of reference in 4D, to illustrate that the two are equivalent in 3D but distinguishable in 4D.

2.4.1 Equivalent motions

Consider now a given motion of a material described with the events z^μ in an inertial coordinate system ζ^μ. This inertial observer is represented by the base vectors $\boldsymbol{e}_\mu$. Suppose next that this motion is compose with a rigid body motion, such that (see Fig. 2.1):

$$\begin{cases} z^{*i} = Q^i{}_j(t) z^j + \lambda^i(t) \\ z^{*4} = z^4 = ct, \end{cases} \tag{2.23}$$

where $Q^i{}_j$ is an orthogonal matrix describing the rigid body rotation and λ^i is a vector describing a rigid body translation. They both depend on time only. The motions z^μ and $z^{*\mu}$ are described in the same inertial coordinate system ζ^μ.

Next, we construct the 4D curvilinear coordinate system $\tilde{\xi}^\mu$ attached to the body undergoing the rigid body motion is such that:

$$\begin{cases} \zeta^i = Q^i{}_j \tilde{\xi}^j + \lambda^i \\ \zeta^4 = \tilde{\xi}^4 = ct. \end{cases} \tag{2.24}$$

This coordinate system corresponds to the rotating coordinates associated with the rigid body motion $z^{*\mu}$. This 4D coordinate system is curvilinear because Q and λ depend on t. This observer is represented by the base vectors $\tilde{\boldsymbol{g}}_\mu$. It corresponds to the 4D definition of an Euclidean observer. Note that, to verify the Newtonian hypotheses, Q, λ and $\tilde{\xi}^\mu$ have to be chosen such that the velocity of any point is small compared with the velocity of light.

The material points undergoing the composed motion have the coordinates $\tilde{x}^{*\mu}$ within the coordinate system $\tilde{\xi}^\mu$ and:

$$\begin{cases} \tilde{x}^{*i} = z^i \\ \tilde{x}^{*4} = z^4 = ct. \end{cases} \tag{2.25}$$

In other words, the inertial observer observing the first motion, and the rotating observer observing the motion composed with the rigid body motion see the same motion respectively. The motions z^μ and $z^{*\mu}$ are classically said to be *equivalent motions*.

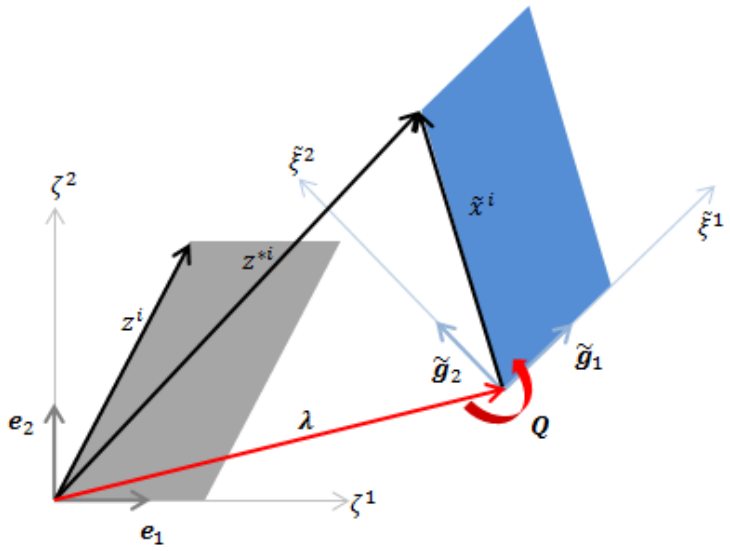

Figure 2.1: Two-dimensional scheme to illustrate the definitions of the inertial and rotating coordinate systems and the associated base vectors. The motion $z^i = \tilde{x}^{*i}$ and its composition with a rigid body motion $z^{*i} = Q^i{}_j(t)z^j + \lambda^i(t)$ are also illustrated.

2.4.2 The principle of covariance applied to Euclidean transformations

The notion of objectivity defined in Section 1.2 is now discussed under the light of the principle of covariance. Consider the 4D coordinate systems ζ^μ and $\tilde{\xi}^\mu$ defined in the previous section:

$$\begin{cases} \zeta^i = Q^i{}_j \tilde{\xi}^j + \lambda^i \\ \zeta^4 = \tilde{\xi}^4 = ct. \end{cases} \tag{2.26}$$

This represents an Euclidean transformation within a 4D formalism. The Jacobian matrix of this change of coordinates is:

$$\frac{\partial \zeta^\mu}{\partial \tilde{\xi}^\nu} = \begin{pmatrix} Q^i{}_j & \dfrac{1}{c}\left[\dfrac{dQ^i{}_j}{dt}\tilde{\xi}^j + \dfrac{d\lambda^i}{dt}\right] \\ 0,0,0 & 1 \end{pmatrix} \text{ and } \left|\frac{\partial \zeta^\mu}{\partial \tilde{\xi}^\nu}\right| = \left|Q^i{}_j\right| = 1, \tag{2.27}$$

where i represents the three first lines and j the three first columns in this 4x4 matrix. Note that:

$$\frac{d\zeta^i}{dt} = c\frac{\partial \zeta^i}{\partial \tilde{\xi}^4} = \frac{dQ^i{}_j}{dt}\tilde{\xi}^j + \frac{d\lambda^i}{dt} \tag{2.28}$$

is the velocity of one of the frames with respect to the other.

As an illustration, to discuss the relation between objectivity and the principle of covariance we consider the second-rank tensor $\boldsymbol{\tau}$. The principle of covariance for this second-rank tensor leads to:

$$\boldsymbol{\tau} = \tau^{\mu\nu}\boldsymbol{e}_\mu \otimes \boldsymbol{e}_\nu = \tilde{\tau}^{\mu\nu}\tilde{\boldsymbol{g}}_\mu \otimes \tilde{\boldsymbol{g}}_\nu, \tag{2.29}$$

where $\tau^{\mu\nu}$ and $\tilde{\tau}^{\mu\nu}$ are the components of the tensor expressed in the coordinate system ζ^μ and $\tilde{\xi}^\mu$ respectively. One has also (Eq. 2.18):

$$\tau^{\mu\nu} = \frac{\partial\zeta^\mu}{\partial\tilde{\xi}^\alpha}\frac{\partial\zeta^\nu}{\partial\tilde{\xi}^\beta}\tilde{\tau}^{\alpha\beta}. \tag{2.30}$$

For the spatial components this leads to:

$$\tau^{ij} = \frac{\partial\zeta^i}{\partial\tilde{\xi}^m}\frac{\partial\zeta^j}{\partial\tilde{\xi}^n}\tilde{\tau}^{mn} + \frac{\partial\zeta^i}{\partial\tilde{\xi}^m}\frac{\partial\zeta^j}{\partial\tilde{\xi}^4}\tilde{\tau}^{m4} + \frac{\partial\zeta^i}{\partial\tilde{\xi}^4}\frac{\partial\zeta^j}{\partial\tilde{\xi}^n}\tilde{\tau}^{4n} + \frac{\partial\zeta^i}{\partial\tilde{\xi}^4}\frac{\partial\zeta^j}{\partial\tilde{\xi}^4}\tilde{\tau}^{44}. \tag{2.31}$$

For the Euclidean transformation defined by Eq. 2.24 and if the tensor is symmetric, one has then:

$$\begin{aligned}\tau^{ij} =& Q^i{}_m Q^j{}_n \tilde{\tau}^{mn} \\ &+\frac{2}{c}\left(\frac{d\lambda^j}{dt} + \frac{dQ^j{}_k}{dt}\tilde{\xi}^k\right)Q^i{}_m\tilde{\tau}^{m4} + \frac{1}{c^2}\left(\frac{d\lambda^i}{dt} + \frac{dQ^i{}_l}{dt}\tilde{\xi}^l\right)\left(\frac{d\lambda^j}{dt} + \frac{dQ^j{}_k}{dt}\tilde{\xi}^k\right)\tilde{\tau}^{44}.\end{aligned} \tag{2.32}$$

In the equation above the spatial components $\tilde{\tau}^{mn}$ of the tensor have been separated from the other components. In this equation, if the terms in red are omitted, this equation corresponds exactly to the 3D definition of objectivity for a second-rank tensor (see Eq. 1.28). These red terms come from the 4D description: they are proportional to $\frac{\tilde{\tau}^{m4}}{c}$ and $\frac{\tilde{\tau}^{44}}{c^2}$ respectively. The tensor is thus objective, if, within a Newtonian motion, $\frac{\tilde{\tau}^{m4}}{c} << \tilde{\tau}^{mn}$ and $\frac{\tilde{\tau}^{44}}{c^2} << \tilde{\tau}^{mn}$ for all (m,n). But, if this is not verified, the covariance of the tensor is still ensured thanks to the terms in red. This is illustrated with the four-velocity in Appendix A.1.

2.4.3 Indifference with respect to the superposition of rigid body motions

The physical quantity represented by the second-rank tensor $\boldsymbol{\tau}$ is now evaluated for both of the equivalent motions defined in Section 2.4.1. Consider thus the inertial observer

observing the physical quantity represented by the tensor $\boldsymbol{\tau}(z^\mu)$ associated with the motion z^μ. Consider also the motion $z^{*\mu}$ and the associated physical quantity $\boldsymbol{\tau}^*(z^{*\mu})$ observed by the rotating observer moving with this rigid body motion. *A priori* these two tensors are different because they are associated to different motions. The principle of indifference with respect to superposition of the rigid body motions can be stated as a specific property of many mechanical phenomena. As interpreted logically from its name, this principle states that the observer $\tilde{\boldsymbol{g}}_\mu(\tilde{\xi}^\mu)$ observing the motion $z^{*\mu}$ observes the same physical phenomena as what is seen by the inertial observer observing the motion z^μ (see Fig. 2.1) because to motions are equivalent. Thus, if the observed quantity is indifferent with respect to the superposition of rigid body motions, the components of the two tensors $\boldsymbol{\tau}(z^\mu)$ and $\boldsymbol{\tau}^*(z^\mu)$ should respect the following relation:

$$\tau^{ij} = \tilde{\tau}^{*ij}. \tag{2.33}$$

In other words, the observers are not able to decide whether they are undergoing a rigid body motion when observing the components of a quantity that is indifferent with respect to the superposition of rigid body motions. Within a 4D formalism, this is true for the spatial components of the tensors and for a Newtonian motion but it does not imply that Eq. 2.29 is verified.

2.4.4 The principle of covariance versus objectivity and constitutive models

It can be concluded that the 4D formalism offers the possibility to distinguish the properties of frame-indifference and indifference to the superposition of rigid body motions. Indeed, all 4D tensors are by construction covariant (in other words frame-indifferent within a 3D vocabulary). It is thus possible to define 4D tensor, by construction covariant, but that does depend on the superposition of rigid body motions. Within a 4D context, indifference to the superposition of rigid body motions is a possible characteristic of a tensor as defined in Section 2.4.3.

The 4D formalism constitues thus an opportunity to construct constitutive models consistently. In this context, it is possible to impose both:

- the covariance because it is a principle of physics and only 4D tensors must be chosen to construct the model,
- the indifference with respect to the superposition of rigid body motions when necessary.

2.5 4D derivative operators

When constructing a material constitutive model in an incremental form, an instantaneous variation of the tensor over a time increment is needed. In the 3D context, the derivative with respect to time is not frame-indifferent. Numerous 3D Objective operators have thus been proposed to solve this difficulty. However, they are not the true derivatives with respect to time. The 4D description is a natural formalism to express derivatives in physics including all the time effects and for all 4D coordinate systems. In this section, 4D derivative operators are defined, whose results are 4D tensors and thus necessarily covariant. Those notions of differential geometry can be found in [Schouten, 1954; Levi-Civita et al., 2005; Choquet-Bruhat, 1968; Lee, 2003; Gostiaux, 2005; Spivak, 1999; Kerner, 2014].

2.5.1 Covariant derivatives

The gradient of the components of a tensor within a 4D curvilinear coordinate system ξ^μ is given by the partial derivatives:

$$\frac{\partial \tau^{\mu\nu}}{\partial \xi^\lambda}. \tag{2.34}$$

This quantity depends on the choice of the 4D coordinate system. To construct a covariant operator, the covariant derivative is defined. The components of the covariant derivative operator of a second-rank tensor $\boldsymbol{\tau}$ take the form:

$$\nabla_\lambda \tau^{\mu\nu} = \frac{\partial \tau^{\mu\nu}}{\partial \xi^\lambda} + \Gamma^\mu_{\kappa\lambda}\tau^{\kappa\nu} + \Gamma^\nu_{\kappa\lambda}\tau^{\mu\kappa} - W\Gamma^\kappa_{\kappa\lambda}\tau^{\mu\nu}. \tag{2.35}$$

The coefficients of the connection can be identified with the Christoffel's symbols [Talpaert, 2000] because the space is Euclidean (see details in [Weinberg, 1972]). W is the weight of tensor density. For example, the weight of Cauchy's stress tensor is equal to one ($W = 1$), while the weight of a deformation tensor is equal to zero ($W = 0$) [Oldroyd, 1950; Schouten, 1954]. The Christoffel's symbols are given by:

$$\Gamma^{\alpha}_{\beta\gamma} = \frac{1}{2} g^{\alpha\delta} \left(\frac{\partial g_{\delta\gamma}}{\partial \xi^{\beta}} + \frac{\partial g_{\delta\beta}}{\partial \xi^{\gamma}} - \frac{\partial g_{\beta\gamma}}{\partial \xi^{\delta}} \right). \tag{2.36}$$

Note that, for every point of space-time, there exists a set of coordinates with a Mankowskian metric in which all the Christoffel's symbols vanish.

2.5.2 Rates

In 3D, the derivatives with respect to time depends on the choice of the frame of reference, whereas, in 4D, it is possible to define covariant rates. This section is dedicated to the definition of a rate. Consider the motion of a material body and a 4D tensor field $\boldsymbol{\tau}$. The coordinates of the material points are x^{μ} in the coordinate system ξ^{μ}. For a small increment of the interval ds, the coordinates of the particle go from x^{μ} to $x'^{\mu} = x^{\mu} + u^{\mu} ds$ with the four-velocity u^{μ}. The value of the tensor density goes then from $\boldsymbol{\tau}(x^{\mu})$ to $\boldsymbol{\tau}(x'^{\mu})$. An illustration of the trajectory of the points in space-time is given in Fig 2.2. The

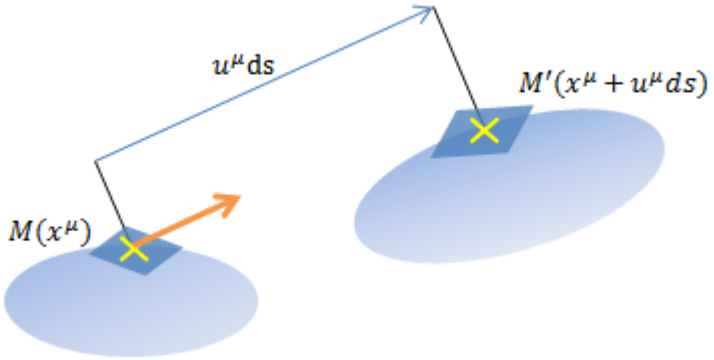

Figure 2.2: Illustration of the space-time description, the flow and the tangent spaces at each time

variation of the tensor is then over the interval ds is thus:

$$\lim_{ds \to 0} \frac{\boldsymbol{\tau}(x'^{\mu}) - \boldsymbol{\tau}(x^{\mu})}{ds} = \lim_{ds \to 0} \frac{\boldsymbol{\tau}(x^{\mu} + u^{\mu} ds) - \boldsymbol{\tau}(x^{\mu})}{ds}. \tag{2.37}$$

This is only possible definition for the variation of a tensor with respect to the time along a trajectory and corresponds to a 4D generalization of a material derivative. For a second-rank tensor, this can be written as:

$$\lim_{ds\to 0} \frac{\tau^{\mu\nu}(x'^{\mu})\boldsymbol{g}_{\mu}(x'^{\mu}) \otimes \boldsymbol{g}_{\nu}(x'^{\mu}) - \tau^{\mu\nu}(x^{\mu})\boldsymbol{g}_{\mu}(x^{\mu}) \otimes \boldsymbol{g}_{\nu}(x^{\mu})}{ds}, \tag{2.38}$$

concerning its contravariant components. Depending on the choice that is made for the variation of the base vectors, two types of time derivatives may be defined. First, if the base vectors are considered constant, a covariant rate is defined. Second, if the base vectors are transformed by the motion to represent the variation as seen by the moving point, the Lie derivative in the velocity field is defined. Both rates will be presented in the following sections.

2.5.3 Covariant rate

A covariant transport corresponding to the operator $u^{\lambda}\nabla_{\lambda}(.)$ is defined. When applied respectively to a scalar a and to a second-rank tensor $\boldsymbol{\tau}$, it becomes:

$$u^{\lambda}\nabla_{\lambda}a = \frac{da}{ds} - Wu^{\lambda}\Gamma^{\kappa}_{\kappa\lambda}a \tag{2.39}$$

$$u^{\lambda}\nabla_{\lambda}\tau^{\mu\nu} \;=\; \frac{d\tau^{\mu\nu}}{ds} + u^{\lambda}\left(\Gamma^{\mu}_{\kappa\lambda}\tau^{\kappa\nu} + \Gamma^{\nu}_{\kappa\lambda}\tau^{\mu\kappa} - W\Gamma^{\kappa}_{\kappa\lambda}\tau^{\mu\nu}\right), \tag{2.40}$$

where the operator $\frac{d(.)}{ds}$ corresponds to, respectively:

$$\frac{da}{ds} = u^{\lambda}\frac{\partial a}{\partial \xi^{\lambda}} \tag{2.41}$$

$$\frac{d\tau^{\mu\nu}}{ds} = u^{\lambda}\frac{\partial \tau^{\mu\nu}}{\partial \xi^{\lambda}}. \tag{2.42}$$

Note that the result of this last operator is not a four-tensor. When the velocity of the material point is small with respect to the velocity of light, by remembering that, in this case, $x^4 = ct$ and $ds/c \approx dt$, the covariant rate becomes:

$$cu^{\lambda}\nabla_{\lambda}\tau^{\mu\nu} = \frac{dx^{\lambda}}{dt}\nabla_{\lambda}\tau^{\mu\nu} = \frac{d\tau^{\mu\nu}}{dt} + \frac{dx^{\lambda}}{dt}\left(\,\Gamma^{\mu}_{\kappa\lambda}\tau^{\kappa\nu} + \Gamma^{\nu}_{\kappa\lambda}\tau^{\mu\kappa} - W\Gamma^{\kappa}_{\kappa\lambda}\tau^{\mu\nu}\right). \tag{2.43}$$

Similar operators may be defined for tensor densities of other ranks. The covariant rate of a tensor density (Eq. 2.43) within a Newtonian context is further decomposed to interpret the meaning of each term such that:

$$cu^{\lambda}\nabla_{\lambda}\tau^{\mu\nu} \approx \left[\left[\frac{\partial\tau^{\mu\nu}}{\partial t}\right]\right] + \left[\frac{dx^{i}}{dt}\frac{\partial\tau^{\mu\nu}}{\partial x^{i}}\right] + \frac{dx^{\lambda}}{dt}\left(\Gamma^{\mu}_{\kappa\lambda}\tau^{\kappa\nu} + \Gamma^{\nu}_{\kappa\lambda}\tau^{\mu\kappa} - W\Gamma^{\kappa}_{\kappa\lambda}\tau^{\mu\nu}\right), \qquad (2.44)$$

where the indices i varies from 1 to 3. The different terms of Eq. 2.44 could then be interpreted as:

- Term between double brackets: the partial time derivative of the tensor density.
- Term between brackets: the time derivative of the tensor density due to the fact that the particle could have a 3D-velocity with respect to the observer.
- The terms with Christoffel's symbols correspond to the increment of the tensor that is due to the fact that the chosen coordinates could possibly depend on the event (for curvilinear frames).

This decomposition shows that the operator is constructed with the total time differential of the tensor within the coordinate system (the operator $\frac{d}{dt}$ in Eq. 2.43), corrected by terms that give the variation of the tensor due to the possible variations of the coordinates with respect to time. It could be interpreted as the 4D generalization of the 3D material derivative. This operator can be shifted by the metric tensor to pass from contravariant to covariant components. The last terms of the decomposition of Eq. 2.44 prove that this rate is indeed covariant, but depend on the superposition of a rigid body motion.

2.5.4 The Lie derivative

Definition

The possibility to define a 4D rate operator whose result is both covariant and indifferent with respect to superposition of rigid body motions is now discussed. We wish to establish the value of the local instantaneous total time derivative of $\boldsymbol{\tau}$ *as seen by the moving particle*. The Lie derivative of $\boldsymbol{\tau}$ along the velocity field $\boldsymbol{u}$ is noted $\mathscr{L}_{u}(\boldsymbol{\tau})$ as demonstrated, for example, in [Schouten, 1954]. This operator could be interpreted as a Lagrangean

entity (as seen by the material point), computed within an Eulerian formalism (it is defined at a given event of space-time). The explicit forms of the Lie derivative for, respectively, a 4-scalar density a, the covariant components and the contravariant components of a second-rank tensor density $\boldsymbol{\tau}$ ([Schouten, 1954]) are:

$$\mathscr{L}_u(a) = u^\lambda \frac{\partial a}{\partial \xi^\lambda} + Wa\frac{\partial u^\lambda}{\partial \xi^\lambda} \tag{2.45a}$$

$$\mathscr{L}_u(\tau)_{\mu\nu} = u^\lambda \frac{\partial \tau_{\mu\nu}}{\partial \xi^\lambda} + \tau_{\lambda\nu}\frac{\partial u^\lambda}{\partial \xi^\mu} + \tau_{\mu\lambda}\frac{\partial u^\lambda}{\partial \xi^\nu} + W\tau_{\mu\nu}\frac{\partial u^\lambda}{\partial \xi^\lambda} \tag{2.45b}$$

$$\mathscr{L}_u(\tau)^{\mu\nu} = u^\lambda \frac{\partial \tau^{\mu\nu}}{\partial \xi^\lambda} - \tau^{\lambda\nu}\frac{\partial u^\mu}{\partial \xi^\lambda} - \tau^{\mu\lambda}\frac{\partial u^\nu}{\partial \xi^\lambda} + W\tau^{\mu\nu}\frac{\partial u^\lambda}{\partial \xi^\lambda}. \tag{2.45c}$$

The Lie derivative is an operator that acts on two tensors: the velocity and the tensor itself. It acts on the whole tensor and not only on its components.

Properties

The Lie derivative is a covariant rate that is covariant by construction. It verifies Leibnitz' rule and the chain rule, in other words:

$$\mathscr{L}_u(T(v,w,...)) = \frac{\partial T}{\partial v}\mathscr{L}_u(v) + \frac{\partial T}{\partial w}\mathscr{L}_u(w) + ... \tag{2.46}$$

The Lie derivative further verifies that [Marsden and Hughes, 1994]:

$$\mathscr{L}_{(a_1u_1+a_2u_2)}(\tau)^{\mu\nu} = a_1\mathscr{L}_{u_1}(\tau)^{\mu\nu} + a_2\mathscr{L}_{u_2}(\tau)^{\mu\nu}. \tag{2.47}$$

The expressions of the Lie derivative include a change in the sign of the corrective terms depending on the variance of the tensor components. This leads to the fact that, the Lie derivatives of contravariant and covariant components are not equal, even when they are expressed within an Cartesian set of base vectors. This is due to the fact that the Lie derivative of the metric tensor is not equal to zero. To illustrate this point, we calculate the Lie derivative of the following relation:

$$\begin{aligned}\mathscr{L}_u(\tau)^{\mu\nu} &= \mathscr{L}_u(g^{\mu\kappa}g^{\nu\lambda}\tau_{\kappa\lambda}) \\ &= \mathscr{L}_u(g^{\mu\kappa})g^{\nu\lambda}\tau_{\kappa\lambda} + g^{\mu\kappa}\mathscr{L}_u(g^{\nu\lambda})\tau_{\kappa\lambda} + g^{\mu\kappa}g^{\nu\lambda}\mathscr{L}_u(\tau_{\kappa\lambda}).\end{aligned} \tag{2.48}$$

In conclusion, it is necessary to be cautious when passing from the contravariant components to the covariant components when the Lie derivative is used.

As an example, consider a tensor expressed in a way:

$$\sigma^{\mu\nu} = Mg^{\mu\nu}, \tag{2.49}$$

where $\boldsymbol{\sigma}$ is a stress-like tensor, M is a scalar with a weight that is different from zero and $\boldsymbol{g}$ is the metric tensor, useful to model the transformations of solids. Applying the chain's rule for the Lie derivative to Eq. 2.49 [Marsden and Hughes, 1994], it leads to:

$$\mathscr{L}_u(\sigma)^{\mu\nu} = \mathscr{L}_u(M)g^{\mu\nu} + M\mathscr{L}_u(g)^{\mu\nu}. \tag{2.50}$$

It is worth noting that in general, the Lie derivative of a scalar with a non-zero weight is not zero.

It can be proven that the Lie derivative is also indifferent with respect to the superposition of rigid body motions. It is possible to decompose the velocity field in an isometry part u_ξ and a non-isometry part u^*. The isometry fields correspond to rigid body motions that keep the body undeformed. Indeed, stress is not produced by such a motion, for the considered materials. These fields are the Killing vectors of the metric, for which the Lie derivative is zeroby definition [Schouten, 1954]. Applying the relation of Eq. 2.47 for the decomposition of the velocity field in Eq. 2.50, it leads to:

$$\begin{aligned}\mathscr{L}_u(\sigma)^{\mu\nu} &= \mathscr{L}_u(M)g^{\mu\nu} + M\mathscr{L}_{a_1u_\xi+u^*}(g)^{\mu\nu} \\ &= \mathscr{L}_u(M)g^{\mu\nu} + a_1M\mathscr{L}_{u_\xi}(g)^{\mu\nu} + M\mathscr{L}_{u^*}(g)^{\mu\nu} \\ &= \mathscr{L}_u(M)g^{\mu\nu} + M\mathscr{L}_{u^*}(g)^{\mu\nu}. \end{aligned} \tag{2.51}$$

For pure isometry for which $u^* = 0$, the considered behavior model is simply equal to $\mathscr{L}_{u_\xi}(\sigma)^{\mu\nu} = \mathscr{L}_{u_\xi}(M)g^{\mu\nu}$. Indeed, the Lie derivative is indifferent with respect to the superposition to rigid body motions. Other derivatives add terms that depend on rigid body motion.

2.6 Covariant description of the motion of a continuum within Newtonian hypotheses

The description of a deformable continuum within a four-dimensional and relativistic context has been proposed by many authors; see for example [Bressan, 1963; Capurro,

1983; Edelen, 1967; Epstein et al., 2006; Ferrarese and Bini, 2008; Grot and Eringen, 1966; Kienzler and Herrmann, 2003; Kijowski and Magli, 1997; Lamoureux-Brousse, 1989; Maugin, 1971b; Maugin, 1971a; Valanis, 2003; Williams, 1989]. Their work has been essentially developed to describe relativistic phenomena. It is devoted to conservation relations, to 4D definitions for a stress tensor and to the kinematics with the definition for deformation tensors. Some of this work is restricted to special relativity [Grot and Eringen, 1966; Williams, 1989; Kienzler and Herrmann, 2003]. It therefore excludes the use of 4D curvilinear coordinates that could be interesting for a convective description of the problem or for the description of non-inertial transformations. Four-dimensional formulations of constitutive models have been developed for elastic materials [Lamoureux-Brousse, 1989] or for neutron stars as well as detectors and emitters of gravitational waves. 4D constitutive models for non-viscous fluids and some propositions for viscous dissipation have also been proposed [Landau and Lifshitz, 1987; Öttinger, 1998b; Öttinger, 1998a]. Many models concern astrophysics. These studies are useful for the development of the present proposition because we can rely on these formulations for the construction of non-relativistic 4D strain tensors [Frewer, 2009] and [Matolcsi and Ván, 2007] have shown that a space-time formulation offers many possibilities to properly describe the finite transformations of material continua within the context of Newtonian hypotheses. [Matolcsi and Ván, 2006; Matolcsi and Ván, 2007] have demonstrated the interest of the 4D time derivative for continuum mechanics. None of these authors have applied these propositions to construct material constitutive models or numerical methods to solve continuum mechanics problems.

2.6.1 Material transformations

Consider the finite transformations of a material continuum (Fig. 2.3). This transformation of matter, presented with a classical 3D approach in Section 1.1, is now described within a four-dimensional covariant formalism. The volume of matter is considered with a varying time and is identified with a 4D differentiable manifold. A material point is defined as an elementary 3D volume of matter. The motion of the material continuum is described by the specification of the events undergone by the material points within this

4D manifold. This motion is identified with a set of worldlines (trajectories) that spans a connected open domain of the manifold.

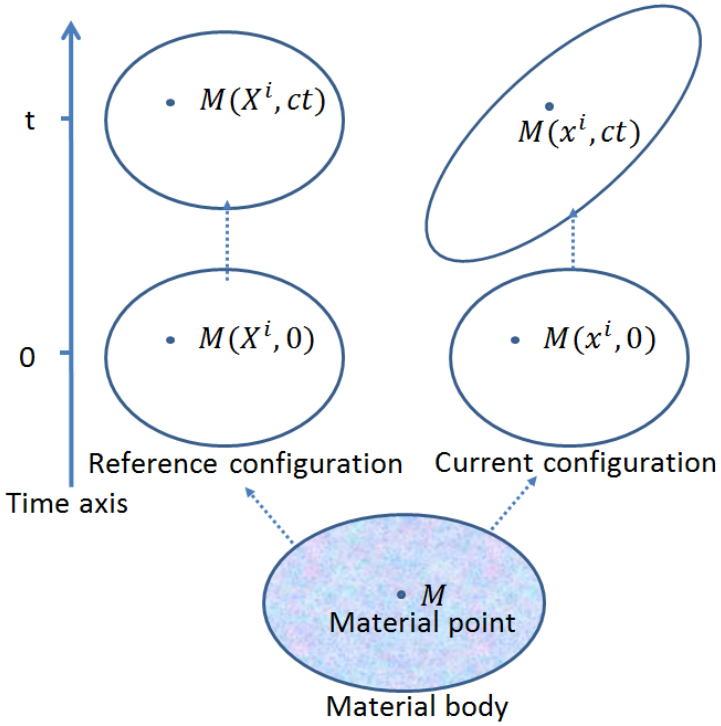

Figure 2.3: The material transformations in 4D. The material point, the 4D reference configuration and the 4D current configuration

.

Configurations are defined corresponding to the state of the 4D manifold at a given instant (see Section 2.2.3 for the definition of time). Among all the events undergone by the material body, two subsets are of specific interest (se Fig. 2.3):

- The reference events identified with the reference configuration.
- The current events identified with the current configuration.

The reference events correspond to a set of events chosen to define the material body at a given instant of reference. It is identified with the initial and neutral configuration of the body for simplicity. The coordinates of these events are noted X^μ in the curvilinear coordinate system ξ^μ (or Z^μ within a Galilean/Minkowskian or inertial coordinate system ζ^μ).

The current events corresponds to the events that are observed at a chosen instant, upon motion and deformation of the body. It is the current configuration which is generalized from the 3D "spatial" or Eulerian state. Note that the fourth coordinate of the reference events is the time multiplied by a constant. The coordinate X^4 or Z^4 is proposed to corresponds to the instant of reference, which is not the initial instant. The reference events thus describe the reference 3D material configuration at the current instant of time. The reference configuration is classically chosen to be the initial configuration, and the origin of time of all coordinate systems is then naturally chosen to be the same as the one defined for the reference state,

$$x^4 = X^4 = z^4 = Z^4 = ct. \tag{2.52}$$

Under this hypothesis, the spatial components of X^μ or Z^μ correspond to the initial positions of the material points in 3D manifold. The motion of the material can then be described by the coordinate of the events undergone by the material points through the specification of the bijective, continuous and differentiable functions x^μ such that:

$$x^\mu = x^\mu(X^\nu) = \begin{cases} x^i = x^i(X^k, x^4) \\ x^4 = X^4 = ct. \end{cases} \tag{2.53}$$

2.6.2 Two coordinate systems

We here specify two coordinate systems often used to describe the motions. The first coordinate system is the inertial 4D coordinate system which has been already introduced in Section 2.2.1. It is noted ζ^μ with coordinates z^μ, base vectors $\boldsymbol{e}_\mu(\zeta^\mu)$ and contravariant components of metric tensor $\eta^{\mu\nu}$. z^μ corresponds to the current states, while Z^μ corresponds to the reference states within the inertial coordinate system. Eq. 2.53 can be then written as:

$$z^\mu = z^\mu(Z^\nu) = \begin{cases} z^i = z^i(Z^k, ct) \\ z^4 = Z^4 = ct. \end{cases} \tag{2.54}$$

The second coordinate system $\hat{\xi}^\mu$ with coordinates $\hat{x}^\mu$, base vectors $\hat{\boldsymbol{g}}_\mu(\hat{\xi}^\mu)$ and contravariant components of metric tensor $\hat{g}^{\mu\nu}$ is a 4D generalization of the 3D convective coordinate

system; see examples in [Malvern, 1969; Belytschko et al., 2000; Murdoch, 2006]. It is defined such that any motion can always be written as:

$$\begin{cases} \hat{x}^k = \hat{X}^k = X^k \\ \hat{x}^4 = ct. \end{cases} \tag{2.55}$$

For simplicity, we suppose that the metric used to describe the reference configuration is Minkowskian $\eta^{\mu\nu}$ or $\eta_{\mu\nu}$. Using Eqs. 2.18, the metric in the convective coordinate system is:

$$\hat{g}^{\mu\nu} = \frac{\partial \hat{x}^\mu}{\partial z^\alpha}\frac{\partial \hat{x}^\nu}{\partial z^\beta}\eta^{\alpha\beta} \tag{2.56a}$$

$$\hat{g}_{\mu\nu} = \frac{\partial z^\alpha}{\partial \hat{x}^\mu}\frac{\partial z^\beta}{\partial \hat{x}^\nu}\eta_{\alpha\beta}. \tag{2.56b}$$

2.6.3 4D deformation gradient

General definitions for 4D deformation and strain tensors have been proposed by Lamoureux-Brousse [Lamoureux-Brousse, 1989] for General Relativity applications. They are applied here to the 4D non-relativistic limit. Two different motions $x^\mu(X^\nu)$ and $x'^\mu(X^\nu)$ of the same material body are compared. These two motions are described within two different coordinate systems, respectively, ξ^μ and ξ'^μ, associated with the two respective covariant components of the metric tensor $g_{\mu\nu}$ and $g'_{\mu\nu}$, linked to the material body. The reference configuration is described indifferently by X^μ or X'^μ ($X^\mu = X'^\mu$), within each respective coordinate system. Each coordinate system is chosen here to have the same origin for time. To compare two motions of a given material body, a 4D generalization of the deformation gradients $F'^\mu{}_\nu$ and its inverse $F'^\mu{}_\nu$ are defined such that:

$$F^\mu{}_\nu = \frac{\partial x^\mu}{\partial x'^\nu} \tag{2.57a}$$

$$F'^\mu{}_\nu = \frac{\partial x'^\mu}{\partial x^\nu}. \tag{2.57b}$$

Such quantities defined by Eqs. 2.57 do not transform since they are not tensors, but coordinate transformations. In 4D, such quantities are simply Jacobian matrix. We now choose to compare a given motion x^μ to the neutral motion such that:

$$\begin{cases} x'^i = \hat{x}'^i = X'^i = X^i \\ x'^4 = \hat{x}'^4 = ct, \end{cases} \tag{2.58}$$

which also corresponds to no motion within a 3D context. It is regarded as the comparison between the current state of the motion and its reference state. The metric tensor associated to this no motion is noted $\boldsymbol{G}$ instead of $\boldsymbol{g}'$. Then the deformation gradient can also be written as:

$$F^{\mu}_{\ \nu} = \frac{\partial x^{\mu}}{\partial X^{\nu}} = \frac{\partial x^{\mu}}{\partial \hat{x}^{\nu}} \tag{2.59a}$$

$$F'^{\mu}_{\ \nu} = \frac{\partial X^{\mu}}{\partial x^{\nu}} = \frac{\partial \hat{x}^{\mu}}{\partial x^{\nu}}. \tag{2.59b}$$

In the respective inertial and convective coordinate systems, and using Eqs. 2.56 and 2.59, we have the relations for the metric components:

$$\hat{g}^{\mu\nu} = F'^{\mu}_{\ \alpha} F'^{\nu}_{\ \beta} \eta^{\alpha\beta} \tag{2.60a}$$

$$\hat{g}_{\mu\nu} = F^{\alpha}_{\ \mu} F^{\beta}_{\ \nu} \eta_{\alpha\beta} \tag{2.60b}$$

2.6.4 Definitions of 4D strain and deformation tensors

It is now possible to define the 4D strain tensor $\boldsymbol{e}$, following Lamoureux-Brousse [Lamoureux-Brousse, 1989], as:

$$e_{\mu\nu} = \frac{1}{2}(g_{\mu\nu} - b_{\mu\nu}) \tag{2.61}$$

where $\boldsymbol{b}$ is the 4D generalization of the inverse of the left Cauchy-Green or Cauchy's deformation tensor, constructed from the inverse of the material transformation gradient $F'^{\mu}_{\ \nu}$, as:

$$b_{\mu\nu} = F'^{\alpha}_{\ \mu} F'^{\beta}_{\ \nu} G_{\alpha\beta} \tag{2.62}$$

The tensors above have been chosen because they offer a correct description of finite deformations similar to the ones used for the 3D Eulerian description, for modelling fluids and metal forming processes [Sidoroff and Dogui, 2001; Labergère et al., 2009]. We also define the 4D equivalent of the "material" counterparts of the above strain tensors as:

$$E_{\mu\nu} = \frac{1}{2}(C_{\mu\nu} - G_{\mu\nu}) \tag{2.63}$$

where $C_{\mu\nu}$ is the 4D generalization of the right Cauchy-Green or Green's deformation tensor, defined from the material transformation gradient $F^{\mu}_{\ \nu}$, as:

$$C_{\mu\nu} = F^{\alpha}_{\ \mu} F^{\beta}_{\ \nu} g_{\alpha\beta}. \tag{2.64}$$

Then, we have:

$$E_{\mu\nu} = F^{\alpha}_{\ \mu} F^{\beta}_{\ \nu} e_{\alpha\beta}. \tag{2.65}$$

2.6.5 Examples of strain tensors

To illustrate the definitions of strain tensors, the components of the deformation gradient and strain tensors are detailed in the inertial 4D coordinate system ζ^{μ}, where z^{μ} and Z^{μ} represent the current and reference events. At first, the deformation gradient is calculated:

$$F^{\mu}_{\ \nu} = \frac{\partial z^{\mu}}{\partial Z^{\nu}} = \begin{pmatrix} F^{i}_{\ j} & \frac{v^i}{c} \\ 0,0,0 & 1 \end{pmatrix} \quad \text{and} \quad F'^{\mu}_{\ \nu} = \frac{\partial Z^{\mu}}{\partial z^{\nu}} = \begin{pmatrix} F'^{i}_{\ j} & \frac{V^i}{c} \\ 0,0,0 & 1 \end{pmatrix} \tag{2.66}$$

where $v^i = \frac{\partial z^i}{\partial t}$ is the 3D velocity in the Cartesian space and $V^i = \frac{\partial Z^i}{\partial t}$. The covariant components of 4D Eulerian strain tensor $e_{\mu\nu}$ become:

$$e_{\mu\nu} = \frac{1}{2}(\eta_{\mu\nu} - b_{\mu\nu}) = \frac{1}{2}(\eta_{\mu\nu} - F'^{\alpha}_{\ \mu} F'^{\beta}_{\ \nu} \eta_{\alpha\beta}) = \begin{pmatrix} -e^{3D}_{ij} & -\frac{F'^{k}_{\ i} V^l \delta_{kl}}{2c} \\ -\frac{F'^{l}_{\ j} V^k \delta_{kl}}{2c} & \frac{V^2}{2c^2} \end{pmatrix}. \tag{2.67}$$

When the velocity is comparatively small to that of light, Eq. 2.67 can be approximated to:

$$e_{\mu\nu} \approx \begin{pmatrix} -e^{3D}_{ij} & 0 \\ 0 & 0 \end{pmatrix}. \tag{2.68}$$

Then a simple shearing transformation is now considered within the inertial coordinate system:

$$\begin{cases} z^1 = Z^1 + \gamma Z^2 \\ z^2 = Z^2 \\ z^3 = Z^3 \\ z^4 = Z^4 = ct, \end{cases} \tag{2.69}$$

where γ is any function of z^4. To respect the hypothesis of this work, the geometry and shearing velocity of the considered motion are such that the velocities for all the events

are negligible compared to that of light. The deformation gradient $\boldsymbol{F}$ can be expressed in term of matrix:

$$F^{\mu}_{\ \nu} = \begin{pmatrix} 1 & \gamma & 0 & \frac{z^2}{c}\frac{\gamma}{dt} \\ 0 & 1 & 0 & 0 \\ 0 & 0 & 1 & 0 \\ 0 & 0 & 0 & 1 \end{pmatrix}, \tag{2.70}$$

The covariant components of the tensor $\boldsymbol{e}$ are:

$$e_{\mu\nu} = \frac{1}{2}\begin{pmatrix} 0 & -\gamma & 0 & -\frac{z^2}{c}\frac{d\gamma}{dt} \\ -\gamma & \gamma^2 & 0 & \frac{\gamma z^2}{c}\frac{d\gamma}{dt} \\ 0 & 0 & 0 & 0 \\ -\frac{z^2}{c}\frac{d\gamma}{dt} & \frac{\gamma z^2}{c}\frac{d\gamma}{dt} & 0 & \frac{(z^2)^2}{c^2}\left(\frac{d\gamma}{dt}\right)^2 \end{pmatrix} \approx \frac{1}{2}\begin{pmatrix} 0 & -\gamma & 0 & 0 \\ -\gamma & \gamma^2 & 0 & 0 \\ 0 & 0 & 0 & 0 \\ 0 & 0 & 0 & 0 \end{pmatrix}. \tag{2.71}$$

The same hypothesis and example can be applied to a pure traction that:

$$\begin{cases} z^1 = (1+\lambda)Z^1 \\ z^2 = Z^2 \\ z^3 = Z^3 \\ z^4 = Z^4 = ct, \end{cases} \tag{2.72}$$

The covariant components of the tensor $\boldsymbol{e}$ are:

$$e_{\mu\nu} = \frac{1}{2}\begin{pmatrix} \frac{1}{(1+\lambda^2)} - 1 & 0 & 0 & -\frac{z^1}{c(1+\lambda)^3}\frac{d\gamma}{dt} \\ 0 & 0 & 0 & 0 \\ 0 & 0 & 0 & 0 \\ -\frac{z^1}{c(1+\lambda)^3}\frac{d\gamma}{dt} & 0 & 0 & \frac{(z^1)^2}{c^2(1+\lambda)^4}\left(\frac{d\gamma}{dt}\right)^2 \end{pmatrix} \approx \frac{1}{2}\begin{pmatrix} \frac{1}{(1+\lambda^2)} - 1 & 0 & 0 & 0 \\ 0 & 0 & 0 & 0 \\ 0 & 0 & 0 & 0 \\ 0 & 0 & 0 & 0 \end{pmatrix}. \tag{2.73}$$

2.6.6 Rate of deformation and spin tensors

In addition, the definition of the variation of strain is important in modelling rate-form constitutive models. The velocity gradient denoted $\boldsymbol{L}$ is defined:

$$L^{\mu}_{\ \nu} = \nabla_\nu u^\mu = \frac{\partial u^\mu}{\partial \xi^\nu} + \Gamma^{\mu}_{\kappa\nu} u^\kappa, \tag{2.74}$$

The symmetric and antisymmetric parts of the velocity gradient correspond respectively to the rate of deformation $\boldsymbol{d}$ and spin $\boldsymbol{\omega}$ defined by:

$$d^{\mu}{}_{\nu} = \frac{1}{2}(\nabla_{\nu}u^{\mu} + \nabla_{\mu}u^{\nu}) \tag{2.75a}$$

$$\omega^{\mu}{}_{\nu} = \frac{1}{2}(\nabla_{\nu}u^{\mu} - \nabla_{\mu}u^{\nu}). \tag{2.75b}$$

2.6.7 Relations with the Lie derivative

Considering the fact that a metric connection has been defined, the expressions of the Lie derivatives may be rewritten with the velocity gradient:

$$\mathscr{L}_u(a) = u^{\lambda}\nabla_{\lambda}(a) + Wad^{\lambda}{}_{\lambda} \tag{2.76a}$$

$$\mathscr{L}_u(\tau)_{\mu\nu} = u^{\lambda}\nabla_{\lambda}(\tau_{\mu\nu}) + \tau_{\lambda\nu}L^{\lambda}{}_{\mu} + \tau_{\mu\lambda}L^{\lambda}{}_{\nu} + W\tau_{\mu\nu}d^{\lambda}{}_{\lambda} \tag{2.76b}$$

$$\mathscr{L}_u(\tau)^{\mu\nu} = u^{\lambda}\nabla_{\lambda}(T^{\mu\nu}) - \tau^{\lambda\nu}L^{\mu}{}_{\lambda} - \tau^{\mu\lambda}L^{\nu}{}_{\lambda} + W\tau^{\mu\nu}d^{\lambda}{}_{\lambda}. \tag{2.76c}$$

Given the definition of the Lie derivative and of the rate of deformation, it can be derived that:

$$\mathscr{L}_u(g)_{\mu\nu} = 2d_{\mu\nu} \tag{2.77}$$

$$\mathscr{L}_u(g)^{\mu\nu} = -2d^{\mu\nu}. \tag{2.78}$$

Given the definition of the deformation tensor $\boldsymbol{b}$ in Eq. 2.62, the covariant components of its Lie derivative equal to zero:

$$\mathscr{L}_u(b)_{\mu\nu} = 0. \tag{2.79}$$

Then, with the definition of the strain tensor $\boldsymbol{e}$ (Eq. 2.61), it is possible to verify that the rate of deformation represents the variation of the strain in the sense of the Lie derivative, such that:

$$\mathscr{L}_u(e)_{\mu\nu} = \frac{1}{2}\mathscr{L}_u(g)_{\mu\nu} \tag{2.80}$$

$$= d_{\mu\nu}. \tag{2.81}$$

Note that the Eqs. 2.79 and 2.81 are not valid for the contravariant components:

$$\mathscr{L}_u(b)^{\mu\nu} \neq 0 \quad \mathscr{L}_u(e)^{\mu\nu} \neq d^{\mu\nu}. \tag{2.82}$$

2.7 Conclusions

This chapter introduces the four-dimensional formalism used in this manuscript. It enables to highlight that objectivity can be seen as a particular case of the principle of covariance used in General Relativity. Within the 4D formalism, indeed, a change of frame of reference is described by a change of 4D coordinates. Thus, if a quantity is a 4D tensor, then it is necessarily covariant. It has been further shown that within the 4D formalism, the principle of covariance is not equivalent to indifference with respect to the superposition of rigid body motions. The 4D formalism, indeed, offers the possibility to construct a covariant tensor that can depend on the superposition of rigid body motions. This leads to the conclusion that constitutive models for materials should be written using 4D tensors to benefit from the full potentials of the 4D formalism.

In addition, the 4D formalism offers a consistent framework to define meaningful time derivatives. Thus the covariant rate and the Lie derivative have been introduced. They should thus be used within constitutive models. The Lie derivative of any tensor is chosen as the only frame-indifferent time derivative operator that is also indifferent with respect to superposition of rigid body motions. It will be used to construct rate-form models, e.g. models for hypoelasticity and plasticity in 4D formalism.

Chapter 3

Four-dimensional thermodynamics

Contents

3.1 Introduction

The previous chapter discussed the kinematic fields in the 4D formalism applied to motions of materials. Further on, 4D kinematic tensors should be applied in constitutive models. These models can be found by experimental methods [Chaboche, 2008; Osakada, 2010]. However, general frameworks in physics have been developed and applied, so that

universal principles of thermodynamics may be considered to obtain those constitutive models [Landau and Lifshitz, 1976; Lemaitre and Chaboche, 1994; Khan and Huang, 1995; Lubarda, 2002; Nemat-Nasser, 2004; Salençon, 2012]. The chosen physical degrees of freedom, such as the stress and the strain tensors, are coupled in balance equations and inequalities. Then, the variational method is applied to find the constitutive models in 3D formalism [Salençon, 2012], especially for elasticity [Nemat-Nasser, 1972; Nemat-Nasser, 1974] or for plasticity [Nemat-Nasser, 2004].

The method of thermodynamics can be prolonged into 4D formalism. A serious and significant work has been performed by Tolman [Tolman, 1930], Möller [Moller, 1972], Lichnerowicz [Lichnerowicz, 2013] and Tsallis [Tsallis et al., 1995] and other physicians in the relativistic thermodynamics. However, from the classical scope of the early work of Eckart [Eckart, 1940] and Landau and Lifshitz [Landau and Lifshitz, 1987], there are still some debates [Israel and Stewart, 1979a; Israel and Stewart, 1979b; Hiscock and Lindblom, 1983; Hiscock and Lindblom, 1985; Hiscock and Lindblom, 1987; Jou et al., 1988; Andersson and Comer, 2007] in defining dissipation terms. The disagreements arise when discussing the problem of causality and dealing with non-equilibrium state in relativity. In my thesis, interests are focused on the non-relativistic material motions. In that case, it is enough to study the dissipations from the basic assumptions of the work of [Landau and Lifshitz, 1987], [Eckart, 1940] and [Grot and Eringen, 1966], which will be detailed later in this chapter.

In this chapter, following the systematic work of [Eckart, 1940] and that of [Grot and Eringen, 1966], we give the definitions and proper decompositions of the momentum-energy tensor $\boldsymbol{T}$, the particle current vector $\boldsymbol{n}$ and the entropy vector $\mathscr{S}$. They are used in the conservation equations and inequality in order to couple the 4D stress tensor and the strain tensor and/or rate of strain tensor using a thermodynamics framework. With specific choice of Helmholtz specific free energy and Newtonian hypothesis, 4D constitutive models for non-dissipative or dissipative material motions can be deduced.

3.2 Principles considered in 4D thermodynamics

At first, let us examine the mathematical choices used in the 4D construction of models from thermodynamics. The fundamental principles for a thermo-mechanical constitutive models have been postulated by [Truesdell and Noll, 2003]:

- Determination for stress. It says that the past history of the motion of the material continua determines the state of stress in that body;
- Local action. It says that only the local motion of a particle can determine the state of stress, regardless of the motion outside any arbitrarily small region around it;
- Material frame-indifference. As discussed in Section 2.2.4, this principle corresponds to the principle of covariance in a 4D formalism,

There are also several universal principles that govern the arbitrary motion of material continua. In 4D formalism, they can be derived from invariance properties and fundamental thermodynamic principles:

- Causality. The superluminal propagation of signals is not allowed, which limits the definition of the entropy vector [Grot and Eringen, 1966; Anderson and Kimn, 2007].
- Conservation of particles [Eckart, 1940; Grot and Eringen, 1966; Landau and Lifshitz, 1975; Boratav and Kerner, 1991]. No creation or annihilation of molecules is considered when describing motion of material continua.
- Invariance to the space rotation. Through the Noether's theorem, this leads to the conservation of angular momentum.
- Invariance to the space translation. Through the Noether's theorem, this leads to the conservation of momentum.
- Conservation of energy. In the relativity theories, the mass is energy. Thus this principle means the mass-energy is conserved. It corresponds to the first thermodynamic principle.

- Principle of the maximum entropy. It is the second thermodynamic principle. This principle can turn to be the 4D Clausius-Duhem inequality.

- Gibbs fundamental principle. This governs the relation between Helmholtz free energy, internal energy and the entropy [Eckart, 1940; Grot and Eringen, 1966; Muschik and von Borzeszkowski, 2015].

- Least action principle. It says that the motion corresponds to a minimum value for the existing action functional of the system. This principle helps to derive the Lagrangian equations of motion in the relativity theories.

All the principles mentioned above are considered to obtain constitutive models from 4D thermodynamics.

3.3 Momentum-energy tensor

The study of momentum-energy tensor $T^{\mu\nu}$ is important in relativistic as well as in non-relativistic field theories [Synge, 1960; Weinberg, 1972; Landau and Lifshitz, 1975; Boratav and Kerner, 1991; Edelen, 1967; Takahashi, 1986; Williams, 1989; Maugin, 1992; Erdmenger and Osborn, 1997]. It can be deduced from the action functional defined with a Lagrangian and used in the least action principle of the motion of the mechanical system [Landau and Lifshitz, 1975]. This tensor merges the density and flux of energy and momentum in the 4D fields. The momentum-energy tensor can be related to 4D Cauchy stress by proper decompositions, as it will be explained in Section 3.3.3. Thus, it is possible to develop constitutive models by dealing with this tensor to couple with strain tensors and/or rate of strain tensors.

3.3.1 General form of the momentum-energy tensor

With the projection operator $(\delta^{\mu}_{\ \nu} - u^{\mu}u_{\nu})$ defined with the Krönecker's symbol and the four velocity in Eq. 2.11, the momentum-energy tensor can be decomposed into a scalar, a vector and a second rank tensor [Eckart, 1940; Grot and Eringen, 1966; Schellstede et al.,

2014]. They are:

$$\mathcal{U} = T^{\mu\nu}u_\mu u_\nu \tag{3.1a}$$

$$q^\mu = (\delta^\mu_{\ \alpha} - u^\mu u_\alpha)T^{\alpha\beta}u_\beta \tag{3.1b}$$

$$T^{\mu\nu}_\sigma = (\delta^\mu_{\ \alpha} - u^\mu u_\alpha)(\delta^\nu_{\ \beta} - u^\nu u_\beta)T^{\alpha\beta}. \tag{3.1c}$$

Note that the nD Krönecker's symbol $\delta^\Phi_{\ \Psi}$ ($\Phi = 2, 3, 4...n$, $\Psi = 2, 3, 4...n$) is calculated as:

$$\delta^\Phi_{\ \Psi} = \begin{cases} 1 & \text{if } \Phi = \Psi \\ 0 & \text{if } \Phi \neq \Psi. \end{cases}$$

We can rewrite the momentum-energy tensor as:

$$\begin{aligned} T^{\mu\nu} &= T^{\mu\nu} + \left(T^{\alpha\beta}u_\alpha u_\beta u^\mu u^\nu - T^{\alpha\beta}u_\alpha u_\beta u^\mu u^\nu\right) + \left(T^{\alpha\beta}u_\alpha u_\beta u^\mu u^\nu - T^{\alpha\beta}u_\alpha u_\beta u^\mu u^\nu\right) \\ &+ \left(T^{\mu\alpha}u_\alpha u^\nu - T^{\mu\alpha}u_\alpha u^\nu\right) + \left(T^{\nu\beta}u_\beta u^\mu - T^{\nu\beta}u_\beta u^\mu\right) \qquad (3.2) \\ &= T^{\alpha\beta}u_\alpha u_\beta u^\mu u^\nu + \left(T^{\mu\alpha} - T^{\alpha\beta}u_\beta u^\mu\right)u_\alpha u^\nu + \left(T^{\nu\beta} - T^{\alpha\beta}u_\alpha u^\nu\right)u_\beta u^\mu \\ &+ \left(T^{\mu\nu} - T^{\mu\alpha}u_\alpha u^\nu - T^{\nu\beta}u_\beta u^\mu + T^{\alpha\beta}u_\alpha u_\beta u^\mu u^\nu\right). \qquad (3.3) \end{aligned}$$

Substituting the definitions in Eqs. 3.1 into Eq. 3.3, the decomposition is calculated as:

$$T^{\mu\nu} = \mathcal{U}u^\mu u^\nu + q^\mu u^\nu + q^\nu u^\mu + T^{\mu\nu}_\sigma. \tag{3.4}$$

We can specify each term in Eq. 3.4 to interpret their physical meanings. Suppose that the motion is in the proper frame of reference where the four velocity $u^\mu = (0, 0, 0, 1)$. In that case, the table of components of the scalar $\mathcal{U}$, the vector q^μ and the tensor $T^{\mu\nu}_\sigma$ can be obtained, such as:

$$\mathcal{U} = T^{44} \quad ; \quad q^\mu = \begin{pmatrix} T^{14} \\ T^{24} \\ T^{34} \\ 0 \end{pmatrix} \quad ; \quad T^{\mu\nu}_\sigma = \begin{pmatrix} T^{11} & T^{12} & T^{13} & 0 \\ T^{21} & T^{22} & T^{23} & 0 \\ T^{31} & T^{32} & T^{33} & 0 \\ 0 & 0 & 0 & 0 \end{pmatrix} \tag{3.5}$$

According to Landau [Landau and Lifshitz, 1975], the momentum-energy tensor can be deduced from least action principle, expressed in a table form in the proper frame of

reference:

$$T^{\mu\nu} = \begin{pmatrix} \sigma^{11} & \sigma^{12} & \sigma^{13} & \phi^1/c \\ \sigma^{21} & \sigma^{22} & \sigma^{23} & \phi^2/c \\ \sigma^{31} & \sigma^{32} & \sigma^{33} & \phi^3/c \\ \phi^1/c & \phi^2/c & \phi^3/c & \mathcal{U} \end{pmatrix} \tag{3.6}$$

Its spatial component is a three-dimensional tensor of momentum flux density (and can be later interpreted to be the opposite of 3D Cauchy tensor), denoted as σ^{ij}. The vector ϕ^i is the energy flux density, presenting the amount of field energy passing through a unit area of the surface in a unit time. $\mathcal{U}$ is the energy density, the energy per unit volume. In a non-polar medium, the momentum-energy tensor is symmetric which can be proved with the balance law of angular momentum [Landau and Lifshitz, 1975; Eckart, 1940; Grot and Eringen, 1966; Schellstede et al., 2014], such as:

$$T^{\mu\nu} = T^{\nu\mu} \quad \Longrightarrow \quad \sigma^{ij} = \sigma^{ji}. \tag{3.7}$$

Comparing Eq. 3.6 and Eq. 3.5, we can interpret each term in Eq. 3.4.

- The term $\mathcal{U}u^\mu u^\nu$ can be interpreted as the kinetic momentum-energy tensor. Because the Einstein mass-energy formula tells that the mass is equivalent to the energy in the relativistic theories [Synge, 1960; Boratav and Kerner, 1991], we can also write:

  $$\mathcal{U} = \rho_r c^2, \tag{3.8}$$

  where ρ_r represents the relativistic total mass density (relativistic mass per unit of volume). Then the kinetic momentum-energy tensor $T^{\mu\nu}_{kin}$, can be defined such that:

  $$T^{\mu\nu}_{kin} = \mathcal{U}u^\mu u^\nu = \rho_r c^2 u^\mu u^\nu. \tag{3.9}$$

- The term $(q^\mu u^\nu + q^\nu u^\mu)$ can be interpreted as the thermal momentum-energy tensor, noted $T^{\mu\nu}_q$. The vector q^μ is the heat flux vector. We have:

  $$T^{\mu\nu}_q = q^\mu u^\nu + q^\nu u^\mu \quad \text{with} \quad q^i = \frac{\phi^i}{c}. \tag{3.10}$$

- The term $T_\sigma^{\mu\nu}$ can be interpreted as the mechanical momentum-energy tensor. From Eqs. 3.5 and 3.6, we can see correspondence of the spatial components of the mechanical momentum-energy tensor T_σ^{ij} to the momentum flux density σ^{ij} in the proper frame of reference:

$$T_\sigma^{ij} = \sigma^{ij}. \tag{3.11}$$

With the definitions in Eqs. 3.9 and 3.10, the decomposition of momentum-energy tensor in Eq. 3.4 can be rewritten as:

$$T^{\mu\nu} = \rho_r c^2 u^\mu u^\nu + q^\mu u^\nu + q^\nu u^\mu + T_\sigma^{\mu\nu} \tag{3.12}$$

$$= T_{kin}^{\mu\nu} + T_q^{\mu\nu} + T_\sigma^{\mu\nu}. \tag{3.13}$$

3.3.2 Choice of the velocity field: Landau versus Eckart

When talking about the choice of velocity field in the decomposition of the momentum-energy tensor, there is another field variable needed to be considered, the particle current vector $\boldsymbol{n}$, which is generally defined [Andersson and Comer, 2007]:

$$n^\mu = n_r u^\mu + \nu^\mu, \tag{3.14}$$

where the scalar n_r is the relativistic particle number density (per unit of volume) and the vector ν^μ represents the particle diffusion vector. Together with the momentum-energy tensor, these two field variables are combined:

$$\begin{cases} T^{\mu\nu} = \rho_r c^2 u^\mu u^\nu + q^\mu u^\nu + q^\nu u^\mu + T_\sigma^{\mu\nu} \\ n^\mu \quad = n_r u^\mu + \nu^\mu. \end{cases} \tag{3.15}$$

The heat flux vector q^μ and particle diffusion vector ν^μ are the dissipative terms corresponding to the heat and particle current respectively.

The decomposition of momentum-energy tensor and particle current are quite general. Either of the dissipative terms q^μ and ν^μ can be zero with a specific choice of the four-velocity $\boldsymbol{u}$, especially in relativistic fluid mechanics [Andersson and Comer, 2007]. There are two choices of the four-velocity commonly used in the fluid mechanics, the formulation due to Eckart [Eckart, 1940] and that of Landau and Lifshitz [Landau and Lifshitz, 1987].

In fact, these two choices are special limits of the general decomposition of the momentum-energy tensor and that of the particle current in Eq. 3.15. Other decompositions can possibly be chosen between Eckart and Landau, even though they might not have practical interest.

Landau description The four velocity $\mathbf{u}_L$ (subscript "L" denotes the objects in the description of Landau and Lifshitz) is defined so that no conductive energy flux can be observed, $q^\mu = 0$. If we multiply Eq. 3.15 by the four-velocity $u_{L\mu}$, the following equation can be obtained using Eq. 3.8 (more details are shown in Appendix B.1), seeing Fig.3.1:

$$T^{\mu\nu}u_{L\nu} = \rho_L c^2 u_L^{\ \mu} \quad \text{with} \quad q^\mu = 0, \tag{3.16}$$

where ρ_L is the relativistic total mass density in the description of Landau and Lifshitz.

However, there is a conductive particle diffusion current vector ν^μ in the formulation of the particle current:

$$n^\mu = n_L u_L^{\ \mu} + \nu^\mu, \tag{3.17}$$

where n_L is the relativistic particle number density in the description of Landau and Lifshitz. In the description of Landau and Lifshiz, we have:

$$\begin{cases} T^{\mu\nu} = \rho_L c^2 u_L^\mu u_L^\nu + T_\sigma^{\mu\nu} \\ n^\mu \ \ = n_L u_L^\mu + \nu^\mu. \end{cases} \tag{3.18}$$

Eckart The four velocity $\mathbf{u}_E$ is defined so that its direction is parallel to that of the particle current (subscript "E" notes the objects in the theory of Eckart), seeing Fig.3.1:

$$n^\mu = n_E u_E^{\ \mu} \quad \text{with} \quad \nu^\mu = 0, \tag{3.19}$$

where n_E is the relativistic particle number density in the description of Eckart.

There is no extra term corresponding to particle diffusions in the formulation of the particle current, but a dissipation corresponding to the energy flux can be observed as the transmission of heat (seeing details in Appendix B.1):

$$T^{\mu\nu}u_{E\nu} = \rho_E c^2 u_E^{\ \mu} + q^\mu, \tag{3.20}$$

where ρ_E is the relativistic total mass density in the description of Eckart. In the description of Eckart we have:

$$\begin{cases} T^{\mu\nu} = \rho_E c^2 u_E^\mu u_E^\nu + q^\mu u_E^\nu + q^\nu u_E^\mu + T_\sigma^{\mu\nu} \\ n^\mu \quad = n_E u_E^\mu. \end{cases} \tag{3.21}$$

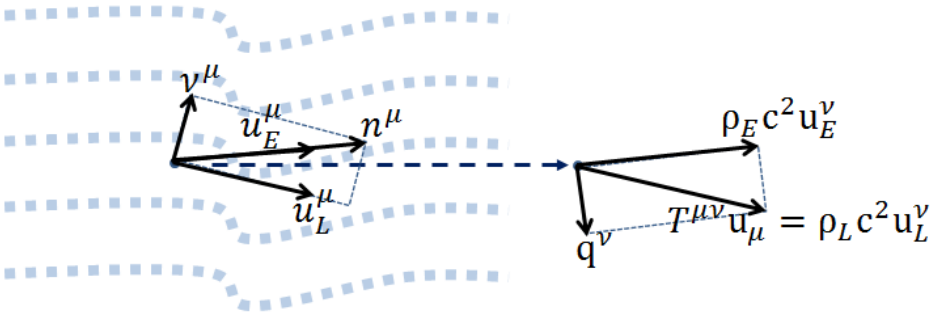

Figure 3.1: Descriptions of the decompositions proposed by Landau and Lifshiz and by Eckart for the four-velocity.

Comparison For these two methods of descriptions, the pairs of objects (ρ_L, ρ_E), (n_L, n_E) are different because of the difference of $\gamma = 1/\sqrt{1 - v^2/c^2}$, and more precisely, because of the different choice of the four-velocity $(\mathbf{u}_L, \mathbf{u}_E)$. In fact, Landau and Eckart describe the same physical phenomenon in different frames of reference, and quantities are covariant. Thanks to the principle of covariance, they can be transformed between each other [Israel, 1989].

Even though the equivalence of these two choices of frame, Schellstede [Schellstede et al., 2014] shows a preference to the choice of Eckart in the reason that it can deduce the first law of thermodynamics more easily at the appropriate order of approximation. For solid materials, the hypothesis of Eckart is more understandable than that of Landau: the four-velocity of particle current is the speed of material points in the motion. Thus, Eckart's definition of four-velocity is chosen in the rest of the text:

$$\begin{cases} T^{\mu\nu} = \rho_r c^2 u^\mu u^\nu + q^\mu u^\nu + q^\nu u^\mu + T_\sigma^{\mu\nu} \\ n^\mu \quad = n_r u^\mu. \end{cases} \tag{3.22}$$

The subscript "E" is thus removed from the Eq. 3.21.

3.3.3 Link with the 4D stress tensor

The momentum-energy tensor and the particle current vector should be used to constitute balance equations. Before that, we have to give its link with the stress tensor. Classically, the mechanical momentum-energy tensor is regarded as the stress tensor in relativistic mechanics [Eckart, 1940; Grot and Eringen, 1966; Andersson and Comer, 2007; Schellstede et al., 2014]. As shown in Section 3.3.1, in the proper frame of reference where the four velocity is $u^\mu = (0, 0, 0, 1)$, Eq. 3.11 gives a link between these two tensors:

$$T_\sigma^{\mu\nu} = \begin{pmatrix} \sigma^{11} & \sigma^{12} & \sigma^{33} & 0 \\ \sigma^{12} & \sigma^{22} & \sigma^{23} & 0 \\ \sigma^{13} & \sigma^{23} & \sigma^{33} & 0 \\ 0 & 0 & 0 & 0 \end{pmatrix} \tag{3.23}$$

However, in any frame of reference, it is not practical to choose this tensor as the stress tensor, for the following reasons. On one hand, consider a 3D isotropic elastic behavior [Lemaitre and Chaboche, 1994; Marsden and Hughes, 1994; Bertram, 2012]:

$$\sigma^{ij} = \lambda tr(\boldsymbol{e}) g^{ij} + 2\mu e^{ij}, \tag{3.24}$$

where $tr(\boldsymbol{e})$ denotes the trace of the strain tensor $\boldsymbol{e}$, $tr(\boldsymbol{e}) = e_{ij}g^{ij}$, and λ, μ are the Lamé coefficients. If the model of Eq. 3.24 is generated in 4D with $T_\sigma^{\mu\nu}$ as the stress tensor, we have:

$$T_\sigma^{\mu\nu} \stackrel{?}{=} \lambda(e_{\alpha\beta}g^{\alpha\beta})g^{\mu\nu} + 2\mu e^{\mu\nu}. \tag{3.25}$$

In fact, the equality of Eq. 3.25 cannot be valid. For example, in an inertial frame of reference where the components of metric tensor equals to $\eta^{\mu\nu}$, we can calculate the component T_σ^{44} at the non-relativistic limit:

$$T_\sigma^{44} = \lambda(-e_{11} - e_{22} - e_{33} + e_{44}) + 2\mu e_{44} \approx -\lambda(e_{11} + e_{22} + e_{33}), \tag{3.26}$$

which contradicts the table of components in Eq. 3.23 where $T_\sigma^{44} = 0$.

On the other hand, if the table of components in Eq. 3.23 is respected, the 3D model should be generated in 4D as:

$$T_\sigma^{\mu\nu} = \lambda \left(e_{\alpha\beta}(g^{\alpha\beta} - u^\alpha u^\beta)\right)(g^{\mu\nu} - u^\mu u^\nu) + 2\mu e^{\mu\nu} \tag{3.27}$$

However, the tensor $(g^{\mu\nu} - u^\mu u^\nu)$ is not a metric tensor.

Therefore, we propose to use the 4D generalized Cauchy stress tensor $\sigma^{\mu\nu}$ in the following procedure for constituting models, which will be presented in Chapters 4 and 5. This tensor can be related to the mechanical momentum-energy tensor, such as:

$$T_\sigma^{\mu\nu} = \sigma^{\mu\nu} - \sigma^{\mu\alpha}u_\alpha u^\nu - \sigma^{\nu\beta}u_\beta u^\mu + \sigma^{\alpha\beta}u_\alpha u_\beta u^\mu u^\nu. \tag{3.28}$$

Now the decomposition of momentum-energy tensor and particle current vector used in the balance equations are summarized as below:

$$\begin{cases} T^{\mu\nu} = \rho_r c^2 u^\mu u^\nu + q^\mu u^\nu + q^\nu u^\mu \\ \qquad +\sigma^{\mu\nu} - \sigma^{\mu\alpha}u_\alpha u^\nu - \sigma^{\nu\beta}u_\beta u^\mu + \sigma^{\alpha\beta}u_\alpha u_\beta u^\mu u^\nu \\ n^\mu \quad = n_r u^\mu \end{cases} \tag{3.29}$$

Another example can be found to highlight the choice of Eqs. 3.28. Considering a system submitted to a spherical tensor (hydrostatic pressure p):

$$p = -\frac{1}{4}\sigma^{\mu\nu}g_{\mu\nu}, \tag{3.30}$$

whose 4D Cauchy stress tensor is:

$$\sigma^{\mu\nu} = -pg^{\mu\nu}. \tag{3.31}$$

If there is no transmission of the heat, we obtain:

$$\begin{aligned} T^{\mu\nu} &= T_{kin}^{\mu\nu} + T_\sigma^{\mu\nu} && (3.32)\\ &= \rho_r c^2 u^\mu u^\nu - pg^{\mu\nu} + pg^{\mu\alpha}u_\alpha u^\nu + pg^{\nu\alpha}u_\alpha u^\mu - pg^{\alpha\beta}u_\alpha u_\beta u^\mu u^\nu && (3.33)\\ &= (\rho_r c^2 + p)u^\mu u^\nu - pg^{\mu\nu}, && (3.34) \end{aligned}$$

which corresponds strictly to the momentum-energy tensor for 4D perfect fluid given in Landau's book of Fluid Mechanics [Landau and Lifshitz, 1987; Fukuma and Sakatani, 2011; Andersson and Comer, 2007].

3.4 Conservation equations for 4D thermodynamics

After a discussion of the decomposition of momentum-energy tensor and particle current vector, now it is convenient to apply them in the conservation equations. In this

section, the conservation of particle numbers, energy and momentum are investigated in order to construct balance equations. The phenomenon of dissipation is also taken into consideration so that the Clausius-Duhem inequality (a version of the second law of thermodynamics in continuum mechanics) is also studied to obtain the constitutive models. Despite of its importance for symmetry of momentum-energy tensor, we will not discuss the conservation of angular momentum in my thesis. We just use the result of $T^{\mu\nu} = T^{\nu\mu}$ in the hypothesis of non-polar media [Grot and Eringen, 1966; Landau and Lifshitz, 1987; Andersson and Comer, 2007].

3.4.1 Conservation of the particle current

In 3D Newtonian mechanics, we talk about the conservation of mass, but this is not directly the case in 4D relativistic mechanics. Therefore, the first conservation under consideration in this thesis is the conservation of particles. It is assumed that the particles are not created or annihilated, in the considered assumptions. In 4D, this conservation can be expressed through the divergence of the particle current, which is zero:

$$\nabla_\mu n^\mu = 0 \tag{3.35}$$

Here we use the notation ∇_μ to denote the divergence. With the chosen definition for the particle current in this thesis, from Eq. 3.29, we have:

$$\nabla_\mu (n_r u^\mu) = 0 \tag{3.36}$$

The conservation of mass and the conservation of particles are not equivalent in relativistic mechanics, even for a single particle. It is well known that the relativistic mass m_{0r} may vary with the velocity [Landau and Lifshitz, 1975]. The subscript "0" denotes that the mass is only for one particle and "r" is for relativistic quantities. There is inherit hypothesis that all the particles have the same mass. If not, m_{0r} represents the average relativistic mass of a particle $\bar{m}_{0r}$. The conservation of mass may be deduced from the conservation of particles if m_{0r} is constant. However, this is not the case in relativistic mechanics.

$$\nabla_\mu (m_{0r} n_r u^\mu) \not\Rightarrow \nabla_\mu (n_r u^\mu) = 0, \tag{3.37}$$

which contradicts the analysis of [Schellstede et al., 2014]. These two conservations are equivalent in non-relativistic mechanics, which will be shown later in Section 3.5.1.

3.4.2 Conservation of the momentum and energy

In addition to the conservation of particles and angular momentum, there are two other important conserved quantities (mentioned in Section 3.2), the energy and the momentum. Thus, we need two balance equations to describe them. However, the momentum-energy tensor $T^{\mu\nu}$ in 4D deals with both the energy density and the momentum density, including dissipation effect (heat flux). Thus, in 4D only one balance equation is enough to describe the conservation of energy and momentum [Landau and Lifshitz, 1975; Landau and Lifshitz, 1987; Eckart, 1940; Grot and Eringen, 1966]. Locally, the 4D conservation is such that the four-divergence of the momentum-energy tensor is zero [Grot and Eringen, 1966; Andersson and Comer, 2007; Schellstede et al., 2014]:

$$\nabla_\nu T^{\mu\nu} = 0. \tag{3.38}$$

If we apply the Eq. 3.38 along the the four velocity u_μ, we can get:

$$u_\mu \nabla_\nu T^{\mu\nu} = 0. \tag{3.39}$$

According to the product rule, Eq. 3.39 turns to be:

$$u_\mu \nabla_\nu T^{\mu\nu} = \nabla_\nu \left(T^{\mu\nu} u_\mu\right) - T^{\mu\nu} \nabla_\nu u_\mu = 0. \tag{3.40}$$

Now we calculate the two terms $\nabla_\nu \left(T^{\mu\nu} u_\mu\right)$ and $T^{\mu\nu} \nabla_\nu u_\mu$ separately. At first, substituting Eq. 3.20 into $\nabla_\nu \left(T^{\mu\nu} u_\mu\right)$, it can be obtained the expansion of this term, such as:

$$\nabla_\nu \left(T^{\mu\nu} u_\mu\right) = \nabla_\nu (\rho_r c^2 u^\nu) + \nabla_\nu (q^\nu). \tag{3.41}$$

For the other term $T^{\mu\nu} \nabla_\nu u_\mu$, with the definition of the gradient of velocity in Eq. 2.74 and rate of deformation in Eq. 2.75, it can be obtained that (with more details in Appendix B.2):

$$T^{\mu\nu} \nabla_\nu u_\mu = q^\mu (u^\nu \nabla_\nu u_\mu) + (\sigma^{\mu\nu} - \sigma^{\mu\alpha} u_\alpha u^\nu - \sigma^{\nu\beta} u_\beta u^\mu + \sigma^{\alpha\beta} u_\alpha u_\beta u^\mu u^\nu) d_{\mu\nu}. \tag{3.42}$$

The combination of Eq. 3.40, Eq. 3.41 and Eq. 3.42 leads to:

$$u_\mu \nabla_\nu T^{\mu\nu} = \nabla_\nu(\rho_r c^2 u^\nu) + \nabla_\nu q^\nu - q^\mu(u^\nu \nabla_\nu u_\mu) \\ - (\sigma^{\mu\nu} - \sigma^{\mu\alpha} u_\alpha u^\nu - \sigma^{\nu\beta} u_\beta u^\mu + \sigma^{\alpha\beta} u_\alpha u_\beta u^\mu u^\nu) d_{\mu\nu} = 0. \tag{3.43}$$

Finally, we can get the expression of conservation of momentum-energy in 4D:

$$\nabla_\nu(\rho_r c^2 u^\nu) + \nabla_\nu q^\nu = q^\mu(u^\nu \nabla_\nu u_\mu) + (\sigma^{\mu\nu} - \sigma^{\mu\alpha} u_\alpha u^\nu - \sigma^{\nu\beta} u_\beta u^\mu + \sigma^{\alpha\beta} u_\alpha u_\beta u^\mu u^\nu) d_{\mu\nu}. \tag{3.44}$$

The conservation of momentum-energy is not applied in constitutive models, however, it serves as the 4D local expression of the strong form in term of finite element methods. The same as 3D finite element methods, Eqs. 3.44 along with 3.36 governs the global forces and boundary conditions by their integrations in the material body. It is possible to obtain its passage to the weak form by the principle of virtual work. The information of 3D strong form and weak form can be found in the books concerning finite element methods [Belytschko et al., 2000; De Souza Neto et al., 2011]. However, finite element methods within 4D formalism are not yet developed in this thesis.

In Eqs.3.42 and 3.44, the gradient of deformation $L_{\mu\nu}$ is replaced by the rate of deformation $d_{\mu\nu}$, because: 1) the momentum-energy is symmetric in non-polar media, and 2) the double dot product of a symmetric tensor with an arbitrary tensor equals to the symmetric tensor "times" the symmetric part of the second tensor:

$$T^{\mu\nu} L_{\mu\nu} = T^{\mu\nu} L^S_{\mu\nu} = T^{\mu\nu} d_{\mu\nu}, \tag{3.45}$$

where the superscript S denotes the symmetric part.

The conservation of momentum and energy in Eq. 3.38 can be projected into 3D in Newtonian hypothesis. The first three equations of the equation set Eq. 3.38 turn to be the conservation of the momentum in 3D (presented in Eq. 1.21).

The last equation of the equation set Eq. 3.38 turns to be the conservation of energy in 3D. More details can be seen in Appendix B.3.

3.4.3 4D inequality of Clausius-Duhem

In the theory of irreversible processes, the direction of the energy transformation is also an important criterion to be considered for physically meaningful models. In 3D, this

criterion is based on the second law of thermodynamics or the principle of the maximum entropy, which can also be constructed in 4D. To model the phenomenon of irreversibility during the energy transformation, the entropy vector $\mathscr{S}^\mu$ should be defined at first in 4D, following Eckart [Eckart, 1940] and Grot and Eringen [Grot and Eringen, 1966]:

$$\mathscr{S}^\mu = \rho_r \eta_r u^\mu + \frac{T_q^{\mu\nu} u_\nu}{\theta}. \tag{3.46}$$

Here, the scalar η_r denotes the relativistic specific entropy density (per mass) and θ denotes the temperature. The principle of entropy can be expressed in a local form:

$$\theta \nabla_\mu \mathscr{S}^\mu = \theta \nabla_\mu (\rho_r \eta_r u^\mu) + \nabla_\mu q^\mu - \frac{q^\mu}{\theta} \nabla_\mu \theta \geq 0. \tag{3.47}$$

In the scope of mechanics of continuum, the second law of thermodynamics is specified in the form of an inequality called the Clausius-Duhem inequality. In 4D, this inequality can be expressed as following, by adding the zero term from the conservation of momentum-energy:

$$\theta \nabla_\mu \mathscr{S}^\mu - u_\mu \nabla_\nu T^{\mu\nu} \geq 0. \tag{3.48}$$

When the process is reversible, the inequality turns to be a balance equation that represents the conservation of entropy. Otherwise, the value of the left side of inequality is greater than zero. As the second term in the left side of inequality in Eq. 3.48 is calculated in Eq. 3.43, the Clausius-Duhem inequality in 4D can be expressed as:

$$\begin{aligned} &\theta \nabla_\mu (\rho_r \eta_r u^\mu) - \frac{q^\mu}{\theta} \nabla_\mu \theta - \nabla_\mu (\rho_r c^2 u^\mu) + q^\mu (u^\nu \nabla_\nu u_\mu) \\ &+ (\sigma^{\mu\nu} - \sigma^{\mu\alpha} u_\alpha u^\nu - \sigma^{\nu\beta} u_\beta u^\mu + \sigma^{\alpha\beta} u_\alpha u_\beta u^\mu u^\nu) d_{\mu\nu} \geq 0, \end{aligned} \tag{3.49}$$

or equivalently,

$$\theta \nabla_\mu (\rho_r \eta_r u^\mu) - \frac{q^\mu}{\theta} \nabla_\mu \theta - \nabla_\mu (\rho_r c^2 u^\mu) + q^\mu (u^\nu \nabla_\nu u_\mu) + T_\sigma^{\mu\nu} d_{\mu\nu} \geq 0, \tag{3.50}$$

which are expressions of the second law of thermodynamics within the relativity theories. This inequality can be used in deducing constitutive models for relativistic materials. However, it is assumed that materials under transformations do not undergo motions in a large velocity compared to that of light. Further on, covariant relations can still be obtained within 4D formalism without relativistic effects. Thus, an simplified form of

the 4D inequality according to Newtonian hypothesis will be developed to construct the constitutive models for materials studied in the thesis. More details are presented in the next section.

The scalar 4D Clausius-Duhem inequality of Eq. 3.49 can be related to the 3D version (presented in Eqs. 1.23) within the Newtonian hypothesis. More details can be seen in Appendix B.4.2.

3.5 Newtonian approximation for 4D conservation equations and inequality

3.5.1 Particle conservation and mass conservation in Newtonian mechanics

At first, let us examine the conservation of particles in Newtonian mechanics. In Newtonian hypothesis, we have the following densities:

- n, the particle number density
- ρ, the mass density

We can assume that all the particles have the same mass for one particle m_0 in Newtonian hypothesis. Otherwise, m_0 can represent the average mass for a particle $\bar{m}_0$. Then, we can relate the two densities above:

$$\rho = m_0 n. \tag{3.51}$$

With the assumption that the 4D velocity of the particle is small comparing to that of light $v \ll c$, the relativistic particle number density n_r is approximated to n.

$$n_r \approx n, \tag{3.52}$$

Thus, the relativistic conservation of particle current Eq. 3.36 (multiplied by c) turns to be

$$\nabla_\nu (ncu^\nu) \approx 0. \tag{3.53}$$

We multiply the above equation with a constant m_0. Another conservation is obtained as:

$$\nabla_\nu(m_0 ncu^\nu) = \nabla_\nu(\rho cu^\nu) = 0. \tag{3.54}$$

In fact, the term ρcu^μ is the mass current, so that it can be concluded that the conservation of particles leads to the conservation of mass in Newtonian mechanics. In other words, these two balance equations are equivalent in classical mechanics.

3.5.2 Clausius-Duhem inequality in Newtonian mechanics

The Clausius-Duhem inequality can also be rewritten in Newtonian mechanics from its 4D expression. Before studying this inequality, let us check out the mass density and its Newtonian approximation at first. From the famous Einstein mass-energy equation, we have:

$$\mathcal{U} = \rho_r c^2 = \gamma\rho c^2 + \gamma\rho e, \tag{3.55}$$

where $\mathcal{U}$ denotes the total energy density (per volume) and e denotes the specific internal energy density (per mass) in Newtonian hypothesis. In Einstein equation, the relativistic mass contributes to the total energy. The total energy contains two contributions, the one due to mass, and the one due to internal energy. With the approximations:

$$\gamma \approx 1 + \frac{v^2}{2c^2} \approx 1,$$

we have

$$\mathcal{U} = \rho_r c^2 \approx \rho c^2 + \rho e. \tag{3.56}$$

In addition, if we define η as the specific entropy density (per mass) in Newtonian hypothesis, it is easy to approximate the entropy density per volume to its Newtonian limit:

$$\rho_r \eta_r = \gamma\rho\eta \approx \rho\eta. \tag{3.57}$$

Then each term of the Clausius-Duhem inequality of Eq. 3.49 can be approximated. Details of the approximation are shown in Appendix B.4.1. In the process of approximation, $(\sigma^{\mu\nu} - \sigma^{\mu\alpha}u_\alpha u^\nu - \sigma^{\nu\beta}u_\beta u^\mu + \sigma^{\alpha\beta}u_\alpha u_\beta u^\mu u^\nu)d_{\mu\nu} \approx \sigma^{\mu\nu}d_{\mu\nu}$, we have used an important assumption for the fourth components of the Cauchy stress tensor that $\sigma^{4\mu}d_{4\mu}$ can be

negligible comparing to the other components $\sigma^{ij}d_{ij}$ in Newtonian hypothesis. This approximation can be derived from the approximation of the strain tensor in Eq. 2.68 and the relation of the Lie derivative of the strain and the rate of deformation in Eq. 2.81. At last, we can obtain Newtonian limit of the 4D Clausius-Duhem inequality:

$$\theta\rho u^{\mu}\nabla_{\mu}\eta - \frac{q^{\mu}}{\theta}\nabla_{\mu}\theta - \rho u^{\mu}\nabla_{\mu}e + \sigma^{\mu\nu}d_{\mu\nu} \geq 0. \tag{3.58}$$

The Helmholtz specific free energy can be defined from the Gibbs fundamental principle [Eckart, 1940; Grot and Eringen, 1966; Muschik and von Borzeszkowski, 2015]. It is defined as:

$$\Psi = e - \theta\eta. \tag{3.59}$$

Then the covariant rate of the Eq. 3.59 can be calculated as:

$$u^{\mu}\nabla_{\mu}\Psi = u^{\mu}\nabla_{\mu}e - \theta u^{\mu}\nabla_{\mu}\eta - \eta u^{\mu}\nabla_{\mu}\theta. \tag{3.60}$$

Substituting Eq. 3.60 into Clausius-Duhem inequality in Eq. 3.58, we will get:

$$-\rho\left(u^{\lambda}\nabla_{\lambda}\Psi - \eta u^{\lambda}\nabla_{\lambda}\theta\right) - \frac{q^{\mu}}{\theta}\nabla_{\mu}\theta + \sigma^{\mu\nu}d_{\mu\nu} \geq 0, \tag{3.61}$$

the 4D Clausius-Duhem inequality in Newtonian hypothesis. Eq. 3.61 will be used to constitute elastic and elastoplastic behaviors in Newtonian hypothesis, with proper choices of the Helmholtz specific free energy. If the relativistic effects are taken into consideration, the Clausius-Duhem inequality in Eq. 3.58 has to be used instead of Eq. 3.61. It is possible to develop constitutive models from Eq. 3.58 in relativistic mechanics, then approximate the model into the scope of Newtonian mechanics. However, the extra terms in Eq. 3.58 comparing to its Newtonian form Eq. 3.61, make the procedure of developing models much more complicated, unless using $T^{\mu\nu}_{\sigma}$ directly, which is out of the scope of this thesis. Prospective works could be done in applying the relativistic Clausius-Duhem inequality of Eq. 3.58 directly.

Note that Eq. 3.61 is a scalar equation. All the tensors and operators constituting Eq. 3.61 are covariant. It is valid in any frame of reference in Newtonian hypothesis, thanks to the principle of covariance, which is the benefit of applying 4D approach. The

weight of the scalar density of Helmholtz specific free energy W_Ψ and of temperature W_θ are zero, because the Helmholtz specific free energy is united by mass and thus strain-like:

$$W_\Psi = 0 \quad ; \quad W_\theta = 0 \tag{3.62}$$

We have thus:

$$\mathscr{L}_u(\Psi) = u^\lambda \nabla_\lambda(\Psi) + \Psi W_\Psi d^\mu_\mu = u^\lambda \nabla_\lambda(\Psi) \tag{3.63}$$

$$\mathscr{L}_u(\theta) = u^\lambda \nabla_\lambda(\theta) + \theta W_\theta d^\mu_\mu = u^\lambda \nabla_\lambda(\theta). \tag{3.64}$$

Then the Clausius-Duhem inequality in Newtonian hypothesis. Eq. 3.61 can be written as:

$$-\rho\left(\mathscr{L}_u(\Psi) - \eta \mathscr{L}_u(\theta)\right) - \frac{q^\mu}{\theta}\nabla_\mu\theta + \sigma^{\mu\nu} d_{\mu\nu} \geq 0. \tag{3.65}$$

3.6 Conclusions

In this chapter, a systematic method is sketched for 4D thermodynamics. Following the framework of Eckart [Eckart, 1940] and Grot and Eringen [Grot and Eringen, 1966], three field variables, the momentum-energy tensor $T^{\mu\nu}$, the particle current n^μ and the entropy vector $\mathscr{S}^\mu$, have been chosen to construct balance equations and inequality, with respect to general physical principles of the relativity theories. At last, the 4D conservation of particles, momentum-energy and Clausius-Duhem inequality are obtained to link different variables. This systematic work can be applied to deduce the constitutive equations for material motions and thermal conduction considering relativistic effects.

Assumptions for the 4D Cauchy stress tensor is performed. The decompositions of momentum-energy tensor corresponding to this choice is done. At last but not least, constitutive models developed with the chosen 4D Cauchy stress tensor will be coherent with the classical 3D continuum mechanics.

To develop the models for elastoplasticity in non-relativistic limit, approximations of the 4D balance equations and inequality within Newtonian mechanics are performed. A covariant 4D Clausius-Duhem inequality within Newtonian mechanics is obtained. With proper choice of the Helmholtz specific free energy and its decomposition, the chosen

degrees of freedom, such as the Cauchy stress tensor, the strain tensor (or rate of deformation), the material parameters etc. can be coupled to ensure the validity of the 4D Clausius-Duhem inequality. As a consequence, constitutive models for hyperelastic and plastic materials can now be obtained in a 4D formalism. Thus, we can conclude that this attempt is successful in adapting 4D thermodynamics for continuum mechanics. In the following chapters, the model for hyperelasticiy in (Chapter 4) and that for plasticity in (Chapter 5) will serve as examples to illustrate the possibility of obtaining constitute models for materials from 4D thermodynamics.

Chapter 4

Constitutive models for elasticity with the four-dimensional formalism

Contents

4.1 Introduction

In this chapter, constitutive models for hyperelasticity, anisotropic elasticity and hypoelasticity are investigated. From the developed framework of thermodynamics in Chapter 3, 4D hyperelastic model can be obtained with a chosen Helmholtz specific free energy. Moreover, other 4D models for elasticity can be also obtained by copying the 3D approach coupling phenomenologically the stress and the strain. With these methods, 4D

models for elasticity can be obtained. Then, with the method of the representation theory generalized in 4D, anisotropic elastic models and hypoelastic models are investigated.

4.2 4D constitutive models for hyperelasticity

One constitutive model derived from a Helmholtz specific free energy for elastic material is by definition a hyperelastic model under the isothermal or adiabatic conditions as well as the isotropic transformation [Bertram, 2012].

Consider a material without temperature gradient ($\nabla_\mu \theta = 0$ and $\mathscr{L}_u(\theta) = 0$) or without transmission of heat ($q^\mu = 0$), meaning that the transformation is respectively isothermal or adiabatic. In addition, consider that the transformation is isentropic. The Eq. 3.65 turns to be a balance equation without dissipation terms and is thus reversible:

$$-\rho \mathscr{L}_u(\Psi) + \sigma^{\mu\nu} d_{\mu\nu} = 0. \tag{4.1}$$

At this step, it is necessary to define the Helmholtz specific free energy. It can be chosen as a function of different mechanical elastic variables [Boehler, 1978]:

$$\Psi = \Psi_{elasticity}(\lambda/\rho, \mu/\rho, e_{\mu\nu}, g^{\mu\nu}) \tag{4.2}$$

$$= \frac{\lambda}{2\rho}(e_{\mu\nu} g^{\mu\nu})^2 + \frac{\mu}{\rho}(e_{\mu\nu} g^{\mu\alpha} g^{\nu\beta} e_{\alpha\beta}) \tag{4.3}$$

$$= \frac{\lambda}{2\rho}(e_{\mu\nu} g^{\mu\nu})^2 + \frac{\mu}{\rho}(e_{\mu\nu} e^{\mu\nu}), \tag{4.4}$$

In Eq. 4.2, λ and μ are Lamé coefficients for elastic materials. $e_{\mu\nu}$ is the strain tensor. $g^{\mu\nu}$ is the metric. With the calculation of the Lie derivative in Eq. 2.45 and the chain rule in Eq. 2.47, the Lie derivative of the Helmholtz specific free energy for elasticity can be calculated, with special relations seeing Eqs. 2.77 , 2.78 and 2.81:

$$\mathscr{L}_u(\Psi) = \frac{\partial \Psi}{\partial(\lambda/\rho)} \mathscr{L}_u(\lambda/\rho) + \frac{\partial \Psi}{\partial(\mu/\rho)} \mathscr{L}_u(\mu/\rho) + \frac{\partial \Psi}{\partial e_{\mu\nu}} \mathscr{L}_u(e_{\mu\nu}) + \frac{\partial \Psi}{\partial g^{\mu\nu}} \mathscr{L}_u(g^{\mu\nu}) \tag{4.5}$$

$$= \frac{\lambda}{\rho}(g^{\mu\nu} d_{\mu\nu}) \frac{\partial \Psi}{\partial(\lambda/\rho)} + \frac{\mu}{\rho}(g^{\mu\nu} d_{\mu\nu}) \frac{\partial \Psi}{\partial(\mu/\rho)} + d_{\mu\nu} \frac{\partial \Psi}{\partial e_{\mu\nu}} - 2 d^{\mu\nu} \frac{\partial \Psi}{\partial g^{\mu\nu}}. \tag{4.6}$$

In Eq. 4.6, attention should be paid in the calculation of the Lie derivative of the coefficients λ/ρ and μ/ρ, for example, λ/ρ is a strain-like scalar:

$$\mathscr{L}_u(\lambda/\rho) = u^\lambda \nabla_\lambda(\lambda/\rho) = -\frac{\lambda}{\rho^2} u^\lambda \nabla_\lambda(\rho) = -\frac{\lambda}{\rho^2}\left(-\rho(d_{\mu\nu} g^{\mu\nu})\right) = \frac{\lambda}{\rho}(d_{\mu\nu} g^{\mu\nu}). \tag{4.7}$$

Further calculations lead to the following result with Eq. 4.1:

$$(-\lambda g^{\mu\nu}\frac{\partial\Psi}{\partial(\lambda/\rho)} - \mu g^{\mu\nu}\frac{\partial\Psi}{\partial(\mu/\rho)} - \rho\frac{\partial\Psi}{\partial e_{\mu\nu}} + 2\rho\frac{\partial\Psi}{\partial g^{\alpha\beta}}g^{\alpha\mu}g^{\beta\nu} + \sigma^{\mu\nu})d_{\mu\nu} = 0. \tag{4.8}$$

Because the rate of deformation tensor is not necessarily zero, the terms in the parenthesis have to be equal to zero, leading to:

$$\sigma^{\mu\nu} = \lambda g^{\mu\nu}\frac{\partial\Psi}{\partial(\lambda/\rho)} + \mu g^{\mu\nu}\frac{\partial\Psi}{\partial(\mu/\rho)} + \rho\frac{\partial\Psi}{\partial e_{\mu\nu}} - 2\rho\frac{\partial\Psi}{\partial g^{\alpha\beta}}g^{\alpha\mu}g^{\beta\nu}. \tag{4.9}$$

Then using the chosen Helmholtz specific free energy of Eq. 4.3, we can calculate that

$$\frac{\partial\Psi}{\partial(\lambda/\rho)} = \frac{1}{2}(e_{\mu\nu}g^{\mu\nu})^2 \tag{4.10a}$$

$$\frac{\partial\Psi}{\partial(\mu/\rho)} = e_{\mu\nu}e^{\mu\nu} \tag{4.10b}$$

$$\frac{\partial\Psi}{\partial e_{\mu\nu}} = \frac{\lambda}{\rho}(e_{\alpha\beta}g^{\alpha\beta})g^{\mu\nu} + \frac{2\mu}{\rho}e_{\mu\nu} \tag{4.10c}$$

$$\frac{\partial\Psi}{\partial g^{\alpha\beta}} = \frac{\lambda}{\rho}(e_{\kappa\lambda}g^{\kappa\lambda})e_{\alpha\beta} + \frac{2\mu}{\rho}e_{\kappa\alpha}e^{\kappa}{}_{\beta}. \tag{4.10d}$$

After substituting Eqs. 4.10 into Eq. 4.9, we have the constitutive equation for hyperelasticity.

$$\begin{aligned}\sigma^{\mu\nu} = {} & \lambda(e_{\alpha\beta}g^{\alpha\beta})g^{\mu\nu} + 2\mu e^{\mu\nu} + 0.5\lambda(e_{\alpha\beta}g^{\alpha\beta})^2 g^{\mu\nu} + \mu(e_{\alpha\beta}e^{\alpha\beta})g^{\mu\nu} \\ & - 2\lambda(e_{\alpha\beta}g^{\alpha\beta})e^{\mu\nu} - 4\mu(e^{\mu\delta}e^{\nu}{}_{\delta}).\end{aligned} \tag{4.11}$$

This model will be called <u>model 1</u>. Note that with different choices of the Helmholtz specific free energy different hyperelastic models can be obtained. The model is non-linear because the stress is a function of the second-order of the strain. when the strain is approximated to zero, the terms of second-order trend to zero more quickly than the terms of first-order:

$$\lim_{\boldsymbol{e}\to 0}\boldsymbol{\sigma} = f(\boldsymbol{e}) + O(\boldsymbol{e}^2). \tag{4.12}$$

A simpler model can be obtained when the second-order infinitesimal terms are neglected:

$$\begin{aligned}\lim_{\boldsymbol{e}\to 0}\boldsymbol{\sigma} &\approx f(\boldsymbol{e}) \\ \lim_{\boldsymbol{e}\to 0}\sigma^{\mu\nu} &\approx \lambda(e_{\alpha\beta}g^{\alpha\beta})g^{\mu\nu} + 2\mu e^{\mu\nu}.\end{aligned} \tag{4.13}$$

4.3 4D constitutive models for elasticity

Besides 4D thermodynamics, there is another efficient approach to develop 4D constitutive models for elasticity. It is based on specific definition of 4D stiffness applied here for linear elastic behavior. When considering the more general linear coupling between a second-order stress tensor and second-order elastic strain tensor, it is possible to give a specific relation for the 4D stiffness tensor [Sidoroff, 1982a]. This approach is investigated mainly in Section 4.3.2 in comparison to classical 4D generalization of elasticity developed in Section 4.3.1.

4.3.1 4D constitutive models for isotropic elasticity

At first, let us consider a model corresponding to a linear 3D isotropic behavior [Lemaitre and Chaboche, 1994; Marsden and Hughes, 1994; Bertram, 2012]. A 4D model in analogy to this 3D model can be obtained:

$$\sigma^{\mu\nu} = \lambda(g^{\alpha\beta}e_{\alpha\beta})g^{\mu\nu} + 2\mu e^{\mu\nu}. \tag{4.14}$$

This model is a Hookean-like behavior generalized in the 4D framework. Eqs. 4.14 will be called model 2. It is in the same expression as Eq. 4.13. This model can be expressed in the inertial coordinate system, where the components of the metric tensor are those of Minkovskian tensor $\eta_{\mu\nu}$. Linear relationships between the components of stress and strain can be obtained, for example:

$$\begin{cases} \sigma^{11} = (\lambda + 2\mu)e^{11} + \lambda(e^{22} + e^{33} - e^{44}) \\ \sigma^{12} = 2\mu e^{12} \\ \sigma^{44} = (\lambda + 2\mu)e^{44} - \mu(e^{11} - e^{22} - e^{33}) \end{cases} \tag{4.15}$$

Besides model 2, there are also two possibilities of isotropic behavior. Following the way to name model 2, they are called model 3 and 4 respectively. The model 3 is:

$$\sigma^{\mu\nu}J = \lambda(b^{\alpha\beta}e_{\alpha\beta})b^{\mu\nu} + 2\mu e_{\alpha\beta}b^{\mu\alpha}b^{\nu\beta}, \tag{4.16}$$

with $\boldsymbol{b}$ the deformation tensor as defined in Eq. 2.62 and J the mass density ratio:

$$J = |F|\,. \tag{4.17}$$

The model 4 is:

$$\sigma^{\mu\nu} J = \lambda(\beta^{\alpha\beta} e_{\alpha\beta})\beta^{\mu\nu} + 2\mu e_{\alpha\beta}\beta^{\mu\alpha}\beta^{\nu\beta}, \tag{4.18}$$

where $\boldsymbol{\beta} = \boldsymbol{b}^{-1}$, the 4D generalized left Cauchy-Green deformation tensor. Definitely, model 3 and 4 cannot give linear relationships between the components of stress and strain in the inertial coordinate system. However, linear relationships can be respected in convective coordinate system.

Components in convective coordinate system

We now derive the expressions of the quantities within the convective coordinate system defined in Eq. 2.55 in Chapter 2. The change of coordinate can be expressed as:

$$\hat{\tau}^{\mu\nu} = J^W F'^{\mu}_{\ \alpha} F'^{\nu}_{\ \beta} \tau^{\alpha\beta} \quad ; \quad \hat{\tau}_{\mu\nu} = J^W F^{\alpha}_{\ \mu} F^{\beta}_{\ \nu} \tau_{\alpha\beta}, \tag{4.19}$$

for a second-rank tensor $\boldsymbol{\tau}$ of weight W. For the stress tensor, we have:

$$\hat{\sigma}^{\mu\nu} = J F'^{\mu}_{\ \alpha} F'^{\nu}_{\ \beta} \sigma^{\alpha\beta} \quad ; \quad \hat{\sigma}_{\mu\nu} = J F^{\alpha}_{\ \mu} F^{\beta}_{\ \nu} \sigma_{\alpha\beta}. \tag{4.20}$$

For the strain tensor, we have:

$$\hat{e}^{\mu\nu} = F'^{\mu}_{\ \alpha} F'^{\nu}_{\ \beta} e^{\alpha\beta} = E^{\mu\nu} \quad ; \quad \hat{e}_{\mu\nu} = F^{\alpha}_{\ \mu} F^{\beta}_{\ \nu} e_{\alpha\beta} = E_{\mu\nu}. \tag{4.21}$$

In addition, the deformation gradient is (using Eqs. 2.59 and 2.55):

$$\hat{F}^{\mu}_{\ \nu} = \frac{\partial \hat{x}^{\mu}}{\partial \hat{x}^{\nu}} = \hat{F}'^{\mu}_{\ \nu} = \delta^{\mu}_{\ \nu}, \tag{4.22}$$

where $\delta^{\mu}_{\ \nu}$ is the 4D Krönecker's symbol. The covariant components of deformation tensor $\boldsymbol{b}$ in convective coordinate system $\hat{b}_{\mu\nu}$ can be further shown to be (with Eqs. 2.62 and 4.22):

$$\hat{b}_{\mu\nu} = \hat{F}'^{\alpha}_{\ \mu} \hat{F}'^{\beta}_{\ \nu} \hat{G}_{\alpha\beta} = \hat{G}_{\mu\nu} = G_{\mu\nu} = \eta_{\mu\nu}, \tag{4.23}$$

because the coordinate system of the reference configuration is orthonormal by hypothesis (see Section 2.6.2). Then, the contravariant components of deformation tensor $\boldsymbol{\beta}$ in convetive coordinate system $\hat{\beta}^{\mu\nu}$ can be calculated as:

$$\hat{\beta}^{\mu\alpha}\hat{b}_{\alpha\nu} = \hat{b}^{-1\mu\alpha}\hat{b}_{\alpha\nu} = \delta^{\mu}_{\ \nu} \implies \hat{\beta}^{\mu\nu} = \eta^{\mu\nu} \tag{4.24}$$

If we express model 3 (Eq. 4.16) with covariant components of stress and model 4 (Eq. 4.18) with contravariant components of stress in convective coordinate system, we get (with Eqs. 4.20 and 4.21):

$$\hat{\sigma}_{\mu\nu} = \lambda(E^{\alpha\beta}\hat{b}_{\alpha\beta})\hat{b}_{\mu\nu} + 2\mu E^{\alpha\beta}\hat{b}_{\mu\alpha}\hat{b}_{\nu\beta} \tag{4.25}$$

$$\hat{\sigma}^{\mu\nu} = \lambda(E_{\alpha\beta}\hat{\beta}^{\alpha\beta})\hat{\beta}^{\mu\nu} + 2\mu E_{\alpha\beta}\hat{\beta}^{\mu\alpha}\hat{\beta}^{\nu\beta}. \tag{4.26}$$

Then substituting the values of components of deformation tensors $\boldsymbol{b}$ and $\boldsymbol{\beta}$ in convective coordinate system calculated in Eqs. 4.23 and 4.24, we can get linear relationships, for example:

$$\begin{cases} \hat{\sigma}_{11} = (\lambda + 2\mu)E^{11} + \lambda(E^{22} + E^{33} - E^{44}) \\ \hat{\sigma}_{12} = 2\mu E^{12} \qquad \text{from model 3,} \\ \hat{\sigma}_{44} = (\lambda + 2\mu)E^{44} - \mu(E^{11} - E^{22} - E^{33}) \end{cases} \tag{4.27}$$

and

$$\begin{cases} \hat{\sigma}^{11} = (\lambda + 2\mu)E_{11} + \lambda(E_{22} + E_{33} - E_{44}) \\ \hat{\sigma}^{12} = 2\mu E_{12} \qquad \text{from model 4.} \\ \hat{\sigma}^{44} = (\lambda + 2\mu)E_{44} - \mu(E_{11} - E_{22} - E_{33}) \end{cases} \tag{4.28}$$

Models 3 and 4 are found by the method which is based on the linear combination between stress and strain tensors defined in different frames of reference. A more systematic procedure [Truesdell and Noll, 2003] ought to be used, but the present method is sufficient to find the class of investigated elastic relations. The tensor variance (co or contravariant) is of primary importance to find the elastic models in the present method. Indeed, the coupling between different variances is the way to obtain the different possible relations. From a mathematical point of view, it is always possible to find an equation to relate covariant or contravariant stress tensor to a specific covariant or contravariant strain tensor. Thus, more models than models 2, 3 and 4 can be found considering linearity in other frames of reference, because the 4D formalism enables the covariance of the constitutive models.

Table 4.1: Comparison between the four models for isotropic elasticity

Prototype	$\sigma^{\mu\nu} = \mathcal{C}^{\mu\nu\alpha\beta} e_{\alpha\beta} + \mathcal{D}^{\mu\nu\alpha\beta\gamma\delta} e_{\alpha\beta} e_{\gamma\delta}$
model 1	$\mathcal{C}^{\mu\nu\alpha\beta} = \lambda g^{\alpha\beta} g^{\mu\nu} + \mu g^{\mu\alpha} g^{\nu\beta} + \mu g^{\mu\beta} g^{\nu\alpha}$ $\mathcal{D}^{\mu\nu\alpha\beta\gamma\delta} = 0.5\lambda g^{\alpha\beta} g^{\gamma\delta} g^{\mu\nu} + \mu g^{\alpha\gamma} g^{\beta\delta} g^{\mu\nu} - 2\lambda g^{\gamma\delta} g^{\alpha\mu} g^{\beta\nu} - 4\mu g^{\alpha\gamma} g^{\beta\mu} g^{\delta\nu}$
model 2	$\mathcal{C}^{\mu\nu\alpha\beta} = \lambda g^{\alpha\beta} g^{\mu\nu} + \mu g^{\mu\alpha} g^{\nu\beta} + \mu g^{\mu\beta} g^{\nu\alpha} \quad \mathcal{D}^{\mu\nu\alpha\beta\gamma\delta} = 0$
model 3	$\mathcal{C}^{\mu\nu\alpha\beta} = \lambda b^{\alpha\beta} b^{\mu\nu} + \mu b^{\mu\alpha} b^{\nu\beta} + \mu b^{\mu\beta} b^{\nu\alpha} \quad \mathcal{D}^{\mu\nu\alpha\beta\gamma\delta} = 0$
model 4	$\mathcal{C}^{\mu\nu\alpha\beta} = \lambda \beta^{\alpha\beta} \beta^{\mu\nu} + \mu \beta^{\mu\alpha} \beta^{\nu\beta} + \mu \beta^{\mu\beta} \beta^{\nu\alpha} \quad \mathcal{D}^{\mu\nu\alpha\beta\gamma\delta} = 0$

4.3.2 4D constitutive models for anisotropic elasticity

Prototype relation using a fourth-rank stiffness tensor

It is interesting and useful to extend the 4D elastic behaviours to anisotropic materials. The linear coupling between two second-rank tensors is performed through a fourth-rank stiffness tensor $\mathcal{C}$ in 4 dimensions. The coupling between a second-rank tensor and an outer product of two second-rank tenors is performed through a sixth-rank stiffness tensor $\mathcal{D}$ in 4 dimensions. A prototype relation can be written as:

$$stress^{\mu\nu} = \mathcal{C}^{\mu\nu\alpha\beta} strain_{\alpha\beta} + \mathcal{D}^{\mu\nu\alpha\beta\gamma\delta} strain_{\alpha\beta} strain_{\gamma\delta}. \tag{4.29}$$

It is obvious that this prototype is suitable for Model 1, but much complex for models 2, 3 and 4. A summary of these four isotropic elastic models is shown in Tab. 4.1. All those relations will be used as a basis for further generalization to anisotropic elastic behavior. For the latter three models, the prototype can be simplified by removing the second term in the right of Eq. 4.29, such as:

$$stress^{\mu\nu} = \mathcal{C}^{\mu\nu\alpha\beta} strain_{\alpha\beta}. \tag{4.30}$$

In this thesis, only the expression of stiffness tensors $\mathcal{C}$ for anisotropic elasticity is studied. It merely aims to illustrate the possibility of developing models for anisotropic elasticity using the 4D formalism.

Symmetries of the four-rank stiffness tensor

Generally in 4D, there are now $4^4 = 256$ components for the fourth-rank stiffness tensor $\mathcal{C}$. The number of the components can be reduced by the properties of symmetry. According to the definitions of the four-dimensional strain tensors introduced in the present work (Eq. 2.61 and Eq. 2.62), these tensors are symmetric because the metric tensor is symmetric. It corresponds to the conditions:

$$strain_{\alpha\beta} = strain_{\beta\alpha}. \tag{4.31}$$

Concerning the stress tensor, the symmetry of the stress tensor is assumed, based on the conservation of angular momentum [Landau and Lifshitz, 1975; Eckart, 1940; Grot and Eringen, 1966; Schellstede et al., 2014]. It corresponds to the conditions:

$$stress^{\alpha\beta} = stress^{\beta\alpha}. \tag{4.32}$$

Consequently, the components of the stiffness tensor have the following properties:

$$\mathcal{C}^{\alpha\beta\gamma\delta} = \mathcal{C}^{\beta\alpha\gamma\delta} = \mathcal{C}^{\alpha\beta\delta\gamma} = \mathcal{C}^{\beta\alpha\delta\gamma}. \tag{4.33}$$

Because of these relations, there are now only 100 independent components for the stiffness tensor. Using the analogy with the 3D case, we extrapolate the 4D Voigt notation (see Tab. 4.2) representing a 4D nth-rank tensor to a 10D $(n/2)$th-rank matrix. Now, the stress and strain can be treated as 10-vectors and the stiffness as a 10×10 matrix $\mathcal{C}^{\Lambda\Theta}$ (Greek capital letters are used to distinguish from the original 4D space-time). The elastic model can be expressed as:

$$stress^{\Lambda} = \mathcal{C}^{\Lambda\Theta} strain_{\Theta}. \tag{4.34}$$

Now, it is possible to explore whether $\mathcal{C}^{\Lambda\Theta}$ is symmetric? At first, let us suppose that it is not symmetric, so it can be decomposed into two parts, symmetric part and antisymmetric part:

$$\mathcal{C}^{\Lambda\Theta} = (\mathcal{C}^{\Lambda\Theta})^{sym} + (\mathcal{C}^{\Lambda\Theta})^{asym}. \tag{4.35}$$

Table 4.2: 4D Voigt notation and some examples of passage from the 4D tensor components to its matrix counterpart in Voigt notation.

passage				examples
Λ	$\mu\nu$	Λ	$\mu\nu$	$\sigma^1 = \sigma^{11}$
1	11	6	24 or 42	$\sigma^5 = \sigma^{34} = \sigma^{43}$
2	22	7	14 or 41	$e^2 = e^{22}$
3	33	8	13 or 31	$e^6 = 2e^{24} = 2e^{42}$
4	44	9	12 or 21	$\mathcal{C}^{34} = \mathcal{C}^{3344}$
5	34 or 43	X	23 or 32	$\mathcal{C}^{1X} = \mathcal{C}^{1123} = \mathcal{C}^{1132}$

A Helmholtz specific free energy may be written in the Voigt formalism with this decomposition:

$$\rho\Psi_{elasticity} = \frac{1}{2}\mathcal{C}^{\Lambda\Theta} strain_\Lambda strain_\Theta \tag{4.36}$$

$$= \frac{1}{2}\left((\mathcal{C}^{\Lambda\Theta})^{sym} + (\mathcal{C}^{\Lambda\Theta})^{asym}\right) strain_\Lambda strain_\Theta \tag{4.37}$$

$$= \frac{1}{2}(\mathcal{C}^{\Lambda\Theta})^{sym} strain_\Lambda strain_\Theta. \tag{4.38}$$

The antisymmetric term vanishes because the term $strain_\Lambda strain_\Theta$ corresponds to a symmetric matrix. As a consequence, only the symmetric part of the stiffness tensor can take part in the elastic behavior of non-polar media, and thus will be considered:

$$\mathcal{C}^{\Lambda\Theta} = \mathcal{C}^{\Theta\Lambda} \Longleftrightarrow \mathcal{C}^{\alpha\beta\gamma\delta} = \mathcal{C}^{\gamma\delta\alpha\beta}. \tag{4.39}$$

Generalizations of anisotropic behavior for models 3 and 4

To generalize the third and fourth models, two approaches can be developed. For isotropic behaviour, models 3 and 4 correspond to a stiffness expressed in the convective frame as a function of the inertial metric tensor, because the expression is build as a linear relation in the convective frame. First, by considering the general anisotropic expression given by

Eq. 4.30 for a convective frame, a relation can be suggested:

$$\hat{\sigma}^{\mu\nu} = \hat{\mathcal{C}}^{\mu\nu\alpha\beta}\hat{e}_{\alpha\beta}. \tag{4.40}$$

For any observer, Eq. 4.40 now becomes:

$$\sigma^{\mu\nu} = J^{-1}F^{\mu}_{\ \kappa}F^{\nu}_{\ \lambda}F^{\alpha}_{\ \theta}F^{\beta}_{\ \gamma}\hat{\mathcal{C}}^{\kappa\lambda\theta\gamma}e_{\alpha\beta}. \tag{4.41}$$

This equation represent the generalization of model 4. For an isotropic behaviour, it is possible to obtain Eq. 4.18. This approach depends strongly on the particular expression of the stiffness tensor given for a specific observer (i.e. the convective frame). This means that the considered methodology is not fully covariant. However, it is based on a simple and linear relation (Eq. 4.40).

Another approach can be used to obtain a generalization for anisotropic behavior. We look for a relation depending on $\boldsymbol{\beta}$ that is non-linear for a general observer (except the convective frame). Consequently, a non-linear coupling with tensor $\boldsymbol{\beta}$ has to be built. For any observer, the following relation can be suggested based on Eq. 4.18:

$$\sigma^{\mu\nu} = \mathcal{C}^{\mu\gamma\delta\kappa}\beta^{\lambda}_{\ \kappa}e_{\lambda\delta}\beta^{\nu}_{\ \gamma}. \tag{4.42}$$

For isotropic behaviour, it is possible to obtain Eq. 4.18. This means that both Eqs. 4.41 and 4.42 degenerate to the same isotropic expression. However, the second method is fully covariant. But its expression does not necessarily verify the form given by Eq. 4.30.

For model 3, the same two approaches can be performed with the same conclusions. For example, the possible models for anisotropic behavior are:

$$\hat{\sigma}_{\mu\nu} = \hat{\mathcal{C}}_{\mu\nu\alpha\beta}\hat{e}^{\alpha\beta} \tag{4.43}$$

$$\iff \sigma_{\mu\nu} = J^{-1}F'^{\kappa}_{\ \mu}F'^{\lambda}_{\ \nu}F'^{\theta}_{\ \alpha}F'^{\gamma}_{\ \beta}\hat{\mathcal{C}}_{\kappa\lambda\theta\gamma}e^{\alpha\beta}, \tag{4.44}$$

or for a fully covariant approach:

$$\sigma^{\mu\nu} = \mathcal{C}^{\mu\gamma\delta\kappa}b^{\lambda}_{\ \kappa}e_{\lambda\delta}b^{\nu}_{\ \gamma}. \tag{4.45}$$

These models are specific and lead to two possible anisotropic generalizations for which one is linear but not covariant due to the particular definition of the stiffness tensor, and the other is non-linear and fully covariant, but does not correspond to the expected coupling as defined by Eq. 4.30.

Generalization of anisotropic behavior for model 2

For the model 2, in which the definition of the stiffness tensor is given or measured for the same observer, only one generalization is possible. The proposed expression is simply:

$$\sigma^{\mu\nu} = \mathcal{C}^{\mu\nu\alpha\beta} e_{\alpha\beta}. \tag{4.46}$$

This expression is linear and fully covariant. It corresponds to the expected coupling as defined in Eq. 4.30. For isotropic behaviour, model 2 corresponds to the expression of stiffness expressed in any frame as a function of the corresponding metric.

The isotropic stiffness tensor (as any isotropic fourth-rank tensor) can be expressed in a general coordinate system as a function of the metric tensor [Landau and Lifshitz, 1975], such as:

$$\mathcal{C}^{\alpha\beta\gamma\delta} = \lambda g^{\alpha\beta} g^{\gamma\delta} + \mu(g^{\alpha\gamma} g^{\beta\delta} + g^{\beta\gamma} g^{\alpha\delta}). \tag{4.47}$$

This expression has only two independent components. It can be questioned whether the same methodology of reduction as in 3D can be used to simplify or eliminate some of the components of the general anisotropic stiffness tensor. This step can be performed a priori considering the possible material symmetries compatible with different passive transformations. This means that the changes between two observers are considered for a given and undeformed material. Because of the covariance principle, the 4D stiffness tensor is covariant. Specific transformations are investigated which lead to the same material before and after the coordinate transformation matrix Ω. Both conditions can be summarized in the following equations:

$$\mathcal{C}^{\alpha\beta\gamma\delta} = \tilde{\mathcal{C}}^{\alpha\beta\gamma\delta} = |\Omega|^{-1} \Omega^{\alpha}_{\kappa} \Omega^{\beta}_{\lambda} \Omega^{\gamma}_{\mu} \Omega^{\delta}_{\nu} \mathcal{C}^{\kappa\lambda\mu\nu}. \tag{4.48}$$

Some of the symmetries can be directly copied on the 3D case. To verify the symmetry, Mathematica© software has been used. For instance, we considered some reflection symmetry with respect to each space plane and to time. The last one corresponds to the reversibility of time. The matrix of coordinate transformations and that of the stiffness tensor in Voigt notation are then shown in Appendix C. At last, the stiffness matrix for

isotropic elasticity (model 2) in Voigt notation is:

$$\mathcal{C}^{\Lambda\Theta} = \begin{pmatrix} \mathcal{C}^{**} & \mathcal{C}^{12} & \mathcal{C}^{12} & -\mathcal{C}^{12} & 0 & 0 & 0 & 0 & 0 & 0 \\ \mathcal{C}^{12} & \mathcal{C}^{**} & \mathcal{C}^{12} & -\mathcal{C}^{12} & 0 & 0 & 0 & 0 & 0 & 0 \\ \mathcal{C}^{12} & \mathcal{C}^{12} & \mathcal{C}^{**} & -\mathcal{C}^{12} & 0 & 0 & 0 & 0 & 0 & 0 \\ -\mathcal{C}^{12} & -\mathcal{C}^{12} & -\mathcal{C}^{12} & \mathcal{C}^{**} & 0 & 0 & 0 & 0 & 0 & 0 \\ 0 & 0 & 0 & 0 & -\mathcal{C}^{88} & 0 & 0 & 0 & 0 & 0 \\ 0 & 0 & 0 & 0 & 0 & -\mathcal{C}^{88} & 0 & 0 & 0 & 0 \\ 0 & 0 & 0 & 0 & 0 & 0 & -\mathcal{C}^{88} & 0 & 0 & 0 \\ 0 & 0 & 0 & 0 & 0 & 0 & 0 & \mathcal{C}^{88} & 0 & 0 \\ 0 & 0 & 0 & 0 & 0 & 0 & 0 & 0 & \mathcal{C}^{88} & 0 \\ 0 & 0 & 0 & 0 & 0 & 0 & 0 & 0 & 0 & \mathcal{C}^{88} \end{pmatrix}, \tag{4.49}$$

with $\mathcal{C}^{**} = \mathcal{C}^{12} + 2\mathcal{C}^{88}$. $\mathcal{C}^{12}$ and $\mathcal{C}^{88}$ are two material parameters. As expected, the matrix depends only on these two parameters. It is possible to find the relations between these two material parameters and the Lamé coefficients:

$$\mathcal{C}^{12} = \lambda \;\; ; \;\; \mathcal{C}^{88} = \mu. \tag{4.50}$$

4.4 4D constitutive model for hypoelasticity

After a discussion on the 4D constitutive models for elasticity, it is now possible to develop models for hypoelasticity using the representation theory (between strain and stress tensors) in 4D. Hypoelastic models in the form proposed by [Eringen, 1962] in 3D can be generalized in 4D:

$$\mathscr{T}^{4D}(\sigma)^{\mu\nu} = \mathcal{H}^{\mu\nu\alpha\beta} d_{\alpha\beta}, \tag{4.51}$$

where $\mathscr{T}^{4D}$ is a stress transport and $\mathcal{H}$ is a symmetric fourth-rank tensor that may depend on the stress tensor $\boldsymbol{\sigma}$. $\boldsymbol{d}$ is the rate of deformation. A reversible hypoelastic model using the Lie derivative is developed in this section, as well as irreversible hypoelastic models using the Lie derivative and the Jaumann transport.

4.4.1 Reversible models for hypoelasticity

At first, a reversible hypoelastic model is derived from the elastic model chosen in the previous section (for example the model 2 for elasticity in Eq. 4.14) to illustrate the methodology. Computing the Lie derivative on both sides of Eq. 4.14 eventually leads to:

$$\mathscr{L}_u(\sigma)^{\mu\nu} = \mathcal{H}_R^{\mu\nu\alpha\beta} d_{\alpha\beta}, \tag{4.52}$$

where

$$\begin{aligned} \mathcal{H}_R^{\mu\nu\alpha\beta} &= \left(1 + \frac{\lambda(g_{\gamma\delta}\sigma^{\gamma\delta})}{\mu(4\lambda+2\mu)}\right)\left(\lambda g^{\mu\nu}g^{\alpha\beta} + 2\mu g^{\mu\alpha}g^{\nu\beta}\right) \\ &+ \sigma^{\mu\nu}g^{\alpha\beta} - \frac{\lambda}{\mu}g^{\mu\nu}\sigma^{\alpha\beta} - 2(g^{\mu\alpha}\sigma^{\beta\nu} + g^{\nu\alpha}\sigma^{\beta\mu}). \end{aligned} \tag{4.53}$$

The following equation:

$$e_{\mu\nu} = \frac{1}{2\mu}\sigma_{\mu\nu} - \frac{\lambda}{2\mu(4\lambda+2\mu)}(\sigma^{\alpha\beta}g_{\alpha\beta})g_{\mu\nu}, \tag{4.54}$$

has been used in the derivation to establish the form of $\mathcal{H}_R$ as a function of the stress. Eq. 4.54 can be calculated from Eq. 4.14 in two steps:

- Multiply Eq. 4.14 by $g_{\mu\nu}$ to calculate $(e_{\mu\nu}g^{\mu\nu})$
- Substitute the expression of $(\sigma^{\mu\nu}g_{\mu\nu})$ into Eq. 4.54 to calculate $e_{\mu\nu}$

Finally, Eq. 4.53 is obtained.

Eq. 4.52 can also be rewritten:

$$\begin{aligned} \mathscr{L}_u(\sigma)^{\mu\nu} &= \left(1 + \frac{\lambda(g_{\gamma\delta}\sigma^{\gamma\delta})}{\mu(4\lambda+2\mu)}\right)\left(\lambda(d_{\alpha\beta}g^{\alpha\beta})g^{\mu\nu} + 2\mu d^{\mu\nu}\right) \\ &+ \sigma^{\mu\nu}(d_{\alpha\beta}g^{\alpha\beta}) - \frac{\lambda}{\mu}g^{\mu\nu}\sigma^{\alpha\beta}d_{\alpha\beta} \\ &- 2g^{\mu\alpha}\sigma^{\beta\nu}d_{\alpha\beta} - 2g^{\nu\alpha}\sigma^{\beta\mu}d_{\alpha\beta}. \end{aligned} \tag{4.55}$$

This hypoelastic model when integrated will reproduce exactly the model corresponding to Eq. 4.14. It is hence reversible and the fourth-rank tensor $\mathcal{H}$ corresponds to a reversible model. That is why it is noted $\mathcal{H}_R$. This is possible, because the kinematic relation between the strain and the rate of deformation (Eq. 2.81) is taken into account

in the derivation. This methodology could be applied to any of the hyperelastic models mentioned in Section 4.3. Another 4D objective transport could also be used to derive this hypoelastic model from the hyperelastic one, as long as the correct relation between the strain and the rate of deformation (Eq. 2.81) is used. This would change the form of $\mathcal{H}_R$, but the hypoelastic model obtained in this case would be strictly equivalent to the initial hyperelastic model, provided that the methodology used for derivation is similar to the present one. The above model will be compared with two other hypoelastic models in Chapter 6.

4.4.2 Irreversible models for hypoelasticity

Another method can be applied to obtain hypoelastic models. Models can be constructed by replacing, in Eq. 4.14, the strain tensor by the rate of deformation $\boldsymbol{d}$ and the stress tensor by an objective transport of this stress. There is a lot of choices of objective transport. We can use the Lie derivative or any other 4D generalized transports such as the Jaumann transport, the Green-Naghdi transport, the Truesdell convective transports etc., which are mentioned in Section 1.2.3 of Chapter 1. The Lie derivative is chosen because it is the only transport that is both covariant and indifferent to the superposition of rigid body motions. The use of the Jaumann transport for example will be also considered for illustration. We will later compare (see Chapter 6) the reversible hypoelastic model of Eq. 4.51 with the two following hypoelastic models:

$$\mathscr{L}_u(\sigma)^{\mu\nu} = 2\mu d^{\ \mu\nu} + \lambda(d_{\alpha\beta}g^{\alpha\beta})g^{\mu\nu} \tag{4.56}$$

$$\mathscr{T}^{4D}(\sigma)^{\mu\nu} = 2\mu d^{\mu\nu} + \lambda(d_{\alpha\beta}g^{\alpha\beta})g^{\mu\nu}, \tag{4.57}$$

where $\mathscr{T}^{4D}(\boldsymbol{\sigma})$ is a 4D generalization transport of the stress $\boldsymbol{\sigma}$. There are different choices for this operator. We use the 4D generalization of the 3D Jaumann transport [Jaumann, 1911], as one of the corotational transport [Xiao et al., 2000b; Bertram, 2012; Shutov and Ihlemann, 2014] for illustration

$$\mathscr{T}^{J}(\sigma)^{\mu\nu} = u^{\lambda}\nabla_{\lambda}(\sigma^{\mu\nu}) - \omega^{\mu}_{\ \alpha}\sigma^{\alpha\nu} + \sigma^{\mu\alpha}\omega_{\alpha}^{\ \nu}. \tag{4.58}$$

Note that the four tensor $\mathscr{T}^{4D}(\boldsymbol{\sigma})$ is covariant because it is a 4D tensor, but is not a time derivative and can be proven to depend on the superposition of rigid body motions due to the definition of the covariant derivative and of the spin tensor ([Rouhaud et al., 2013]). The metric $\boldsymbol{g}$ depends on the choice of the frame of reference. Eqs. 4.56 and 4.57 may be rewritten:

$$\mathscr{L}_u(\sigma)^{\mu\nu} = \mathcal{H}^{\mu\nu\alpha\beta} d_{e\alpha\beta} \tag{4.59}$$

$$\mathscr{T}^{4D}(\sigma)^{\mu\nu} = \mathcal{H}^{\mu\nu\alpha\beta} d_{e\alpha\beta} \tag{4.60}$$

$$\text{where } \mathcal{H}^{\mu\nu\alpha\beta} = \lambda g^{\mu\nu} g^{\alpha\beta} + \mu(g^{\mu\alpha} g^{\nu\beta} + g^{\nu\alpha} g^{\mu\beta}). \tag{4.61}$$

Note that the metric $\boldsymbol{g}$ is not specifically associated to a frame of reference. Also note that in this case $\mathcal{H}$ is a constant tensor as opposed to $\mathcal{H}_R$, because it does not depend on the stress. Indeed, the two last hypoelastic models are linear whereas the hypoelastic model derived from the hyperelastic model is non-linear. The non-linear terms correspond to a necessary correction for the model to be reversible. The choice of the transport is not constitutive for the reversible model; indeed it is strictly equivalent to the hyperelastic model. The other hypoelastic models depend on the choice of the transport. It has been proven that these latter models (Eqs. 4.59 and 4.60) are *not* reversible. Consequently, these hypoelastic models are not equivalent to any given hyperelastic model.

4.5 3D projection of elastic models

The 4D constitutive models developed in this chapter can be projected into 3D, in order to apply them in engineering simulations where the Newtonian hypothesis is considered.

Hookean-like elasticity Within the Newtonian approximation and in the inertial coordinate system, we have the 3D Hookean-like elastic model (derived from the 4D version in Eq. 4.14) :

$$\sigma^{ij} = \lambda tr(e) g^{ij} + 2\mu e^{ij}, \tag{4.62}$$

where $\boldsymbol{g}$ is the 3D metric tensor and $tr(.)$ denotes the trace of a 3D tensor:

$$tr(\boldsymbol{e}) = e_{ij} g^{ij}. \tag{4.63}$$

Its inverted form is:

$$e^{ij} = \frac{1}{2\mu}\sigma^{ij} - \frac{\lambda}{2\mu(3\lambda + 2\mu)} tr(\boldsymbol{\sigma}) g^{ij}. \tag{4.64}$$

Comparing with the 4D form, given by Eq. 4.54, we can see that the coefficients of the second term in the right side of the equation are not the same. This is because the trace of a 3D stress tensor is in general not equal to the trace of a 4D stress tensor. Indeed, unlike the 4D strain tensor, the component σ^{44} of the 4D stress tensor does not tend towards zero at the non-relativistic limit. If Eq. 4.14 is multiplied by $g_{\mu\nu}$, we have:

$$\sigma^{\mu\nu} g_{\mu\nu} = (4\lambda + 2\mu)(e_{\mu\nu} g^{\mu\nu}). \tag{4.65}$$

If Eq. 4.62 is multiplied by g_{ij}, we have:

$$tr(\boldsymbol{\sigma}) = \sigma^{ij} g_{ij} = (3\lambda + 2\mu) tr(\boldsymbol{e}). \tag{4.66}$$

From the approximation in Eq. 2.68, the following relation is obtained:

$$e_{\mu\nu} g^{\mu\nu} = e_{ij} g^{ij} = tr(\boldsymbol{e}), \tag{4.67}$$

which leads to the relation:

$$\frac{\eta_{\mu\nu}\sigma^{\mu\nu}}{tr(\boldsymbol{\sigma})} = \frac{4\lambda + 2\mu}{3\lambda + 2\mu}. \tag{4.68}$$

Anisotropic elasticity In addition, the 3D version of the model for anisotropic elasticity taking model 2 as reference (Eq. 4.46) is:

$$\sigma^{ij} = \mathcal{C}^{ijab} e_{ab}. \tag{4.69}$$

where $\mathcal{C}^{ijab}$ is the 3D fourth-rank stiffness tensor. It can be expressed in Voigt notation, with a 6×6 matrix $\mathcal{C}^{AB}$, where A and B vary from 1 to 6. As an example, the stiffness matrix for 3D isotropic elasticity (model 2) in Voigt notation can be obtained by taking the 3D equations from the 4D models. Consider only the case that $\mu = i$ and $\nu = j$ in Eq. 4.46:

$$\sigma^{ij} = \mathcal{C}^{ij\alpha\beta} e_{\alpha\beta} \tag{4.70}$$

We can express the equation above in Voigt notation, using the 4D stiffness matrix for isotropic elasticity in Eq. 4.49 and the passage reference in Tab. 4.2:

$$\begin{cases} \sigma^1 = \mathcal{C}^{**}e_1 + \mathcal{C}^{12}e_2 + \mathcal{C}^{12}e_3 - \mathcal{C}^{12}e_4 \\ \sigma^2 = \mathcal{C}^{12}e_1 + \mathcal{C}^{**}e_2 + \mathcal{C}^{12}e_3 - \mathcal{C}^{12}e_4 \\ \sigma^3 = \mathcal{C}^{12}e_1 + \mathcal{C}^{12}e_2 + \mathcal{C}^{**}e_3 - \mathcal{C}^{12}e_4 \\ \sigma^8 = \mathcal{C}^{88}e_8 \\ \sigma^9 = \mathcal{C}^{88}e_9 \\ \sigma^X = \mathcal{C}^{88}e_X \end{cases} \tag{4.71}$$

with $\mathcal{C}^{**} = \lambda + 2\mu$, $\mathcal{C}^{12} = \lambda$ and $\mathcal{C}^{88} = \mu$. Within the Newtonian approximation, the fourth components of strain tensor are approximated to zero, $e_4 \approx 0$. Thus, the 3D Voigt notation of the stiffness matrix is:

$$\mathcal{C}^{AB} = \begin{pmatrix} \lambda+2\mu & \lambda & \lambda & 0 & 0 & 0 \\ \lambda & \lambda+2\mu & \lambda & 0 & 0 & 0 \\ \lambda & \lambda & \lambda+2\mu & 0 & 0 & 0 \\ 0 & 0 & 0 & \mu & 0 & 0 \\ 0 & 0 & 0 & 0 & \mu & 0 \\ 0 & 0 & 0 & 0 & 0 & \mu \end{pmatrix} \tag{4.72}$$

This projection from 4D to 3D is performed by taking parts of the equations from the equation set of the 4D constitutive models. The taken equations only concern about the spatial components of the stress tensor. Normally speaking, the spatial components of the stress tensor generally depend on the fourth components of the strain tensor (for example, e_4 in Eq. 4.71), which can be approximated to zero within the Newtonian hypothesis.

Hypoelasticity Using the same technique as illustrated for 3D anisotropic elastic models, the 4D hypoelastic models can be projected into 3D with the approximation $d_{i4} \approx 0$. The reversible hypoelastic model (Eq.4.51) has the 3D form:

$$\mathscr{L}_v(\sigma)^{ij} = \mathcal{H}_R^{ijab} d_{ab}, \tag{4.73}$$

where

$$\begin{aligned}\mathcal{H}_R^{ijab} &= \left(\lambda + \frac{\lambda^2\, tr(\sigma)}{\mu(3\lambda+2\mu)}\right) g^{ij}g^{ab} + \left(2\mu + \frac{2\lambda\, tr(\sigma)}{3\lambda+2\mu}\right) g^{ia}g^{jb} \\ &+ \sigma^{ij}g^{ab} - \frac{\lambda}{\mu}g^{ij}\sigma^{ab} - 2(g^{ia}\sigma^{bj} + g^{ja}\sigma^{bi}),\end{aligned}$$

in terms of components. The irreversible hypoelastic models (Eqs. 4.59 and 4.60) have the 3D form in terms of components:

$$\mathscr{L}_v(\sigma)^{ij} = \mathcal{H}^{ijab}d_{ab} \tag{4.74}$$

$$\mathscr{T}^{4D}(\sigma)^{ij} = \mathcal{H}^{ijab}d_{ab} \tag{4.75}$$

$$\text{where}\quad \mathcal{H}^{ijkl} = \lambda g^{ij}g^{ab} + \mu(g^{ia}g^{jb} + g^{ja}g^{ib})$$

The 3D expression of the Lie derivative and the Jaumann transport (as examples of 3D objective transports) are:

$$\mathscr{L}_v(\sigma)^{ij} = \frac{d\sigma^{ij}}{dt} - \sigma^{lj}L^i_l - \sigma^{il}L^j_l + \sigma^{ij}d^l{}_l. \tag{4.76}$$

$$\mathscr{T}^J(\sigma)^{ij} = \frac{d\sigma^{ij}}{dt} - \omega^i{}_l\sigma^{lj} + \sigma^{il}\omega_l{}^j. \tag{4.77}$$

Note that the 3D projected models are only part of the equations for the 4D models, which are expressed in the inertial frame of reference within the Newtonian hypothesis. The 3D models are only used in the numerical simulation and mathematical deductions have to be done with the 4D formalism. In this sense, there is no necessary in discussing the objectivity of the 3D models. In other words, the covariance and the indifference to the the superposition of the rigid body motions only make sense in 4D. That is one important reason that the constitutive models has to be established in 4D. Even though their 3D projections (such as Eqs. 4.72 and 4.75) can also be obtained in the approaches of classical 3D mechanics, the 4D formalism is capable to deal with the general cases, for example, relativistic, dependent to the superposition of rigid body motions, or rigorous to the effect of time variation etc.

4.6 Conclusions

In this chapter, constitutive models for hyperelasticity, anisotropic elasticity and hypoelasticity have been investigated and established.

When considering finite transformations of elastic materials, it is important to properly choose the correct quantity as well as the correct relation. It is possible to extend an elastic behavior to finite deformations by using at least three different kind of modeling. First, it is possible to consider a thermodynamical approach which is based on a non-dissipative condition that leads to the partial derivative of thermodynamic potentials with respect to physical variables. Second, it is possible to directly replace the quantity by adapted ones copying the existing relation. Third, it is possible to consider variations of quantities. A non-linear 4D constitutive model for hyperelasticity is obtained by the first method, such that the stress equals to a combination of the first order and second order of strain. By the other two methods, different 4D constitutive models for isotropic elasticity are also obtained.

4D anisotropic elastic models have been also investigated, such that the stress equals to the inner product of a fourth-order stiffness tensor and the strain. The Voigt notation of this stiffness for anisotropic elastic materials can be deduced by using material symmetries (including the isotropic one as the more symmetrical case) from a general anisotropic stiffness tensor. This stiffness has to be the same as the one obtained from a purely mathematical point of view, which gives directly a fourth-rank isotropic tensor as a function of the second-rank metric tensor. However, this is possible if and only if more symmetries are considered. In 3D, only spatial reflections and spatial rotations are taken into account. In 4D, it is also necessary to consider time reflection (which, as turns out, has no particular influence) and space-time rotation linked to the Lorentz transformation, which leads to specific conditions on the stiffness components. Space reflection, space rotation for a given or for an arbitrary angle are time-independent symmetries, whereas time reflection, space-time rotation (Lorentz transformation) are time-dependent symmetries. The latter are slightly different because they act on the movement of the system. Therefore, the time-dependent transformations can no more be seen as simple geometrical

transformations and should be used in a different way.

At last, 4D hypoelastic models are investigated. It is possible to express the hypoelastic behaviors by two ways. The first one is to replace the strain tensor by the rate of deformation and the stress tensor by an objective transport of this stress in the elastic model. The second one is to calculate the derivative or evaluate the objective transport of each side of the equation of the corresponding elastic model. Only the second method leads to an equivalent hypoelastic model to the reference one. Because the hypoelastic model is rate-form, an objective transport should be chosen to construct the behavior. There is a priori a lot of possible choices of objective transport: the Lie derivative, the 4D Jaumann transport, 4D Truesdell convective transport ... The Lie derivative is proposed to construct the integrable hypoelastic behavior, ensuring simultaneously that:

- The transport operator corresponds to a time derivative.
- The transport operator includes naturally the effect of time variation, through the 4D formalism.
- The stress transport is indifferent to the superposition of rigid body motions.
- The stress transport is covariant because of the 4D formalism.

Chapter 5

Constitutive models for plasticity with the four-dimensional formalism

Contents

5.1 Introduction

After the development of 4D elastic models, this chapter deals with the 4D elastoplastic models. A basic assumption is made that the elastoplastic deformation is decomposed into an elastic part and a plastic part. On one hand, the constitutive models for elastic part can be obtained with the results of the Chapter 4. On the other hand, according to the experimental observations [Chaboche, 2008; Osakada, 2010], the modeling of plastic

part should respect that: 1) Plastic deformations cause an energy dissipation, 2) Plastic deformations depend on the history of deformation, thus rate-form models have to be developed [Khan and Huang, 1995]. The rate-form constitutive model for plastic part should be obtained with the method of 4D thermodynamics considering energy dissipations

In this chapter, we first discuss the choice of decomposition of deformation. After that, 4D plastic model is obtained from the framework of 4D thermodynamic developed in Chapter 3 considering the energy dissipations. Then, the rate-form elastic model, i.e. hypoelastic model for the elastic part, and the rate-form plastic model are combined according to the chosen decomposition. As a consequence, the 4D constitutive model for elastoplasticity can be obtained.

5.2 Kinematic decompositions for elastoplasticity

When a material undergoes an elastoplastic deformation, two mechanisms have to be considered to establish the elastoplastic model in the general framework of standard material models [Lubarda, 2002; Nemat-Nasser, 2004; Bertram, 2012]. It is then necessary to specify a composition for these two mechanisms. A classical hypothesis considers that the elastic and plastic strains evolve differently, whereas both mechanisms see the same stress and the same stress variation. Within this hypothesis, the kinematic quantities cannot be uniquely decomposed. In this section, different ways of decomposition of kinematics are reviewed. The classical composition of 3D kinematic quantities will be generalized in the 4D formalism.

Multiplicative decomposition of deformation gradient

Consider the first case. A material undergoes an elastoplastic deformation from its initial configuration to its current configuration. Imagine that the material is unloaded purely elastically until a stress-free state, which is interpreted as a local intermediate configuration. In this intermediate configuration, only plastic deformation remains. A multiplicative decomposition [Lee, 1969; Khan and Huang, 1995; Lubarda, 2002; Bertram, 2012] of

deformation gradient $F^{\mu}_{\ \nu}$ can be chosen to describe the deformation described above:

$$F^{\mu}_{\ \nu} = F^{\mu}_{e\kappa} F^{\kappa}_{p\nu} \tag{5.1}$$

where $F^{\mu}_{e\kappa}$ and $F^{\kappa}_{p\nu}$ are respectively the elastic and plastic deformation gradients. Similar as the definition of velocity $\boldsymbol{L}$, the rate of deformation $\boldsymbol{d}$ and the spin $\boldsymbol{\omega}$ in Eqs. 2.74 and 2.75, their elastic and plastic parts can be calculated:

$$L^{\mu}_{e\nu(1)} = (u^{\lambda}\nabla_{\lambda}F^{\mu}_{e\kappa})F'^{\kappa}_{\ e\ \nu} \qquad L^{\mu}_{p\nu(1)} = (u^{\lambda}\nabla_{\lambda}F^{\mu}_{p\kappa})F'^{\kappa}_{\ p\ \nu} \tag{5.2}$$

$$d^{\mu}_{e\nu(1)} = \frac{1}{2}\left(L^{\mu}_{e\nu(1)} + L^{\nu}_{e\mu(1)}\right) \qquad d^{\mu}_{p\nu(1)} = \frac{1}{2}\left(L^{\mu}_{p\nu(1)} + L^{\nu}_{p\mu(1)}\right) \tag{5.3}$$

$$\omega^{\mu}_{e\nu(1)} = \frac{1}{2}\left(L^{\mu}_{e\nu(1)} - L^{\nu}_{e\mu(1)}\right) \qquad \omega^{\mu}_{p\nu(1)} = \frac{1}{2}\left(L^{\mu}_{p\nu(1)} - L^{\nu}_{p\mu(1)}\right). \tag{5.4}$$

In Eqs. 5.2, 5.3 and 5.4, the subscript "(1)" denotes that the elastic and plastic rates of deformation correspond to the definition of this first case. In addition, we can find a relation between the rate of deformation $\boldsymbol{d}$ and its elastic and plastic parts $\boldsymbol{d}_e$ and $\boldsymbol{d}_p$, using Eqs 5.1, 5.2 and 5.3:

$$d_{\mu\nu} = g_{\mu\alpha}d^{\alpha}_{\ \nu} \tag{5.5}$$

$$= g_{\mu\alpha}\left((u^{\lambda}\nabla_{\lambda}F^{\alpha}_{\ \kappa})F'^{\kappa}_{\ \nu}\right)^{S} \tag{5.6}$$

$$= g_{\mu\alpha}\left(\left(F^{\alpha}_{e\gamma}u^{\lambda}\nabla_{\lambda}F^{\gamma}_{p\kappa} + (u^{\lambda}\nabla_{\lambda}F^{\alpha}_{e\gamma})F^{\gamma}_{p\kappa}\right)F'^{\kappa}_{\ p\ \delta}F'^{\delta}_{\ e\ \nu}\right)^{S} \tag{5.7}$$

$$= g_{\mu\alpha}\left((u^{\lambda}\nabla_{\lambda}F^{\alpha}_{e\delta})F'^{\delta}_{\ e\ \nu} + F^{\alpha}_{e\gamma}(u^{\lambda}\nabla_{\lambda}F^{\gamma}_{p\kappa})F'^{\kappa}_{\ p\ \delta}F'^{\delta}_{\ p\ \nu}\right)^{S} \tag{5.8}$$

$$= d_{e\mu\nu(1)} + g_{\mu\alpha}\left(F^{\alpha}_{e\gamma}L^{\gamma}_{p\delta(1)}F'^{\delta}_{\ p\ \nu}\right)^{S}. \tag{5.9}$$

In fact, we wish to decompose the rate of deformation in the Clausius-Duhem inequality Eq. 3.65, reminding that

$$-\rho\left(\mathscr{L}_u(\Psi) - \eta\mathscr{L}_u(\theta)\right) - \frac{q^{\mu}}{\theta}\nabla_{\mu}\theta + \sigma^{\mu\nu}d_{\mu\nu} \geq 0.$$

The decomposition should completely separate the term $\sigma^{\mu\nu}d_{\mu\nu}$ into one term corresponding to the elastic deformation and an other term corresponding to the plastic deformation. The first term goes with the derivation of the elastic Helmholtz specific free energy to constitute an elastic model, whereas the second term along with the derivation of the plastic Helmholtz specific free energy is used to model the plastic contribution. The multiplicative decomposition of the deformation gradient in the first case can not be strictly derived

into the additive decomposition of the rate of deformation, such as $\boldsymbol{d} = \boldsymbol{d}_e + \boldsymbol{d}_p$. Without any approximation, the plastic part of the term $\sigma^{\mu\nu} d_{\mu\nu}$ will be $\sigma^{\mu\nu} g_{\mu\alpha} \left(F^{\alpha}_{e\gamma} L^{\gamma}_{p\delta(1)} F'^{\delta}_{p\ \nu} \right)^S$. With the hypothesis that the representation of elasticity is $\boldsymbol{F}_e$ and plasticity is $\boldsymbol{F}_p$ in the decomposition in Eq. 5.1, the term $\sigma^{\mu\nu} g_{\mu\alpha} \left(F^{\alpha}_{e\gamma} L^{\gamma}_{p\delta(1)} F'^{\delta}_{p\ \nu} \right)^S$ is definitely not purely plasticity. Therefore, an additive composition of the rate of deformation is also investigated.

Additive decomposition of convective strain

Consider the second case. The 4D equivalent of the material components $E_{\mu\nu}$ of the 4D strain tensor $\boldsymbol{e}$ defined in Eq. 2.63 is decomposed into its elastic and plastic parts:

$$E_{\mu\nu} = E_{e\mu\nu} + E_{p\mu\nu}, \tag{5.10}$$

similar to the 3D decomposition of elastic and plastic Green strain tensor [Hill, 1959; Nemat-Nasser, 1982; Mandel, 1983; Bertram, 2012]. In a general frame of reference, only the Lie derivative is the total time derivative. As a special form of Lie derivative in the convective frame of reference, the covariant rate can be regarded as a time derivative in this frame. Calculating the covariant rate of each term in Eq. 5.10 leads to:

$$u^{\lambda} \nabla_{\lambda} E_{\mu\nu} = u^{\lambda} \nabla_{\lambda} E_{e\mu\nu} + u^{\lambda} \nabla_{\lambda} E_{p\mu\nu}. \tag{5.11}$$

The transformation from the components of strain tensor $e_{\mu\nu}$ to its material components $E_{\mu\nu}$ in the convective frame can be performed by the change of 4D coordinate system, seeing Eq. 2.65. Because of the covariance of the Lie derivative, the same transformation suits for the passage from the Lie derivative of the components of strain tensor $\mathscr{L}_u(e)_{\mu\nu}$ to the covariant rate of the material components $u^{\lambda} \nabla_{\lambda} E_{\alpha\beta}$:

$$\mathscr{L}_u(e)_{\mu\nu} = F'^{\alpha}_{\ \ \mu} F'^{\beta}_{\ \ \nu} (u^{\lambda} \nabla_{\lambda} E_{\alpha\beta}). \tag{5.12}$$

Using Eqs. 2.81 and substituting Eq. 5.11 in Eq. 5.12, we have:

$$d_{\mu\nu} = \mathscr{L}_u(e)_{\mu\nu} = F'^{\alpha}_{\ \ \mu} F'^{\beta}_{\ \ \nu} (u^{\lambda} \nabla_{\lambda} E_{e\alpha\beta}) + F'^{\alpha}_{\ \ \mu} F'^{\beta}_{\ \ \nu} (u^{\lambda} \nabla_{\lambda} E_{p\alpha\beta}). \tag{5.13}$$

We can define the elastic and plastic rate of deformation from Eq. 5.13:

$$d_{\mu\nu} = d_{e\mu\nu(2)} + d_{p\mu\nu(2)} \tag{5.14}$$

$$\text{with } d_{e\mu\nu(2)} = F'^{\alpha}{}_{\mu} F'^{\beta}{}_{\nu} (u^{\lambda} \nabla_{\lambda} E_{e\alpha\beta}) \tag{5.15}$$

$$\text{and } d_{p\mu\nu(2)} = F'^{\alpha}{}_{\mu} F'^{\beta}{}_{\nu} (u^{\lambda} \nabla_{\lambda} E_{p\alpha\beta}), \tag{5.16}$$

where the subscript "(2)" denotes that the elastic and plastic rates of deformation correspond to the definition of this second case. From this definition, it infers that there exists elastic and plastic stain tensors, $\boldsymbol{e}_e$ and $\boldsymbol{e}_p$ respectively,

$$d_{e\mu\nu(2)} = \mathscr{L}_u(e_e)_{\mu\nu} \tag{5.17}$$

$$d_{p\mu\nu(2)} = \mathscr{L}_u(e_p)_{\mu\nu}, \tag{5.18}$$

and they can be transformed from the covariant rates of the material components:

$$\mathscr{L}_u(e_e)_{\mu\nu} = F'^{\alpha}{}_{\mu} F'^{\beta}{}_{\nu} (u^{\lambda} \nabla_{\lambda} E_{e\alpha\beta}) \tag{5.19}$$

$$\mathscr{L}_u(e_p)_{\mu\nu} = F'^{\alpha}{}_{\mu} F'^{\beta}{}_{\nu} (u^{\lambda} \nabla_{\lambda} E_{p\alpha\beta}). \tag{5.20}$$

Note that, in Eqs. 5.17-5.20 the velocity field in which the Lie derivative is calculated, is the total velocity $\boldsymbol{u}$. Comparing with additive decomposition of the rate of deformation derived from the first case, Eq. 5.9, then the following relation is obtained:

$$\begin{cases} d_{e\mu\nu(2)} = d_{e\mu\nu(1)} \\ d_{p\mu\nu(2)} = g_{\mu\alpha} \left(F^{\alpha}_{e\gamma} L^{\gamma}_{p\delta(1)} F'^{\delta}_{p\ \nu} \right)^{S} . \end{cases} \tag{5.21}$$

Thus, these two cases can be related. The second case offers the possibility to decompose the rate of deformation additively, but not correctly. We can interpret from Eqs. 5.19 and 5.20 that both elastic and plastic strains defined in this case contain simultaneously the information of the elastic and plastic deformation, meaning that the decomposition is not covariant according to Eq. 5.21. This contradiction lies in the choice of the velocity field in the calculation of the Lie derivative. Besides, the additive decomposition of the rate of deformation corresponding to the additive decomposition of the material components of the strain tensor is only valid in a special frame of reference (components $E_{\mu\nu}$ in convective frame of reference). To solve these problems, another additive decomposition is proposed.

Additive decomposition of rate of deformation

Consider the third case. The idea is to assume a decomposition of the rate of deformation directly from the Clausius-Duhem inequality Eq. 3.58. An additive decomposition of the rate of deformation is here assumed for the kinematic decomposition:

$$d_{\mu\nu} = d_{e\mu\nu(3)} + d_{p\mu\nu(3)}, \tag{5.22}$$

where the subscript "(3)" denotes that the elastic and plastic rates of deformation correspond to the definition of this third case. We define the quantities $\boldsymbol{u}_e$ and $\boldsymbol{u}_p$ homogeneous in dimension with a four-velocity that could be interpreted as the four-velocities of the elastic ($\boldsymbol{u}_e$) and plastic ($\boldsymbol{u}_p$) mechanisms inside the elementary volume of reference. Note that in general $\boldsymbol{u} \neq \boldsymbol{u}_e + \boldsymbol{u}_p$. Also note that the plastic strain is not used in the plastic part of the model derived from the Clausius-Duhem inequality Eq. 3.58. More specifically, as the plastic model is rate-form, the variable representing the deformation of plasticity is the plastic rate of deformation $\boldsymbol{d}_p$. The accumulated plastic strain is used and constructed with the plastic rate of deformation, in stead of the plastic strain. Thus, there is no need to define or calculate the plastic strain as in the first and second cases. The elastic strain is defined following the elastic rate of deformation, so that:

$$\mathscr{L}_{u_e}(e_e)_{\mu\nu} = d_{e\mu\nu(3)}. \tag{5.23}$$

It is further considered that the elastic and plastic mechanisms have the same spin as the elementary volume of reference, thus:

$$L^{\mu}_{e\nu(3)} = d^{\mu}_{e\nu(3)} + \omega^{\mu}_{\ \nu(3)} \tag{5.24}$$

$$L^{\mu}_{p\nu(3)} = d^{\mu}_{p\nu(3)} + \omega^{\mu}_{\ \nu(3)}. \tag{5.25}$$

We also suppose that the elastic and plastic mechanisms see the same stress and stress gradient such that respectively:

$$\sigma^{\mu\nu} = \sigma^{\mu\nu}_{e(3)} = \sigma^{\mu\nu}_{p(3)}, \tag{5.26}$$

and

$$u^{\lambda}\nabla_{\lambda}(\sigma^{\mu\nu}) = u^{\lambda}_{e}\nabla_{\lambda}(\sigma^{\mu\nu}_{e(3)}) = u^{\lambda}_{p}\nabla_{\lambda}(\sigma^{\mu\nu}_{p(3)}). \tag{5.27}$$

The Lie derivative of the stress may then be evaluated in the velocity field, but also in the plastic or elastic velocity field, such that:

$$\mathscr{L}_u(\sigma)^{\mu\nu} = u^\lambda \nabla_\lambda(\sigma^{\mu\nu}) - \sigma^{\lambda\nu} L^\mu{}_\lambda - \sigma^{\mu\lambda} L^\nu{}_\lambda + \sigma^{\mu\nu} d^\lambda{}_\lambda \tag{5.28}$$

$$\mathscr{L}_{u_e}(\sigma)^{\mu\nu} = u^\lambda \nabla_\lambda(\sigma^{\mu\nu}) - \sigma^{\lambda\nu} L^\mu_{e\lambda(3)} - \sigma^{\mu\lambda} L^\nu_{e\lambda(3)} + \sigma^{\mu\nu} d^\lambda_{e\lambda(3)} \tag{5.29}$$

$$\mathscr{L}_{u_p}(\sigma)^{\mu\nu} = u^\lambda \nabla_\lambda(\sigma^{\mu\nu}) - \sigma^{\lambda\nu} L^\mu_{p\lambda(3)} - \sigma^{\mu\lambda} L^\nu_{p\lambda(3)} + \sigma^{\mu\nu} d^\lambda_{p\lambda(3)}. \tag{5.30}$$

The consistency of elastoplastic models depends in particular on the consistent definition of the kinematic and kinetic decompositions of the elastic and plastic mechanisms. It is necessary in particular to consistently identify the velocity fields in the different transport operators. In the first case, the plastic velocity field is associated to the term $\eta_{\mu\alpha}\left(F^\alpha_{e\gamma} L^\gamma_{p\delta(1)} F'^\delta_{p\ \nu}\right)^S$ in Eq. 5.9. Comparing with first case, the assumption of the combination of the elastic and plastic rates of deformation is that they are connected in series. Thus the plastic rate of deformation contains no information of elasticity. Comparing with the second case, the elastic strain calculated in Eq. 5.23 can be regarded as linked to a purely elastic kinematic, because the velocity $\boldsymbol{u}_e$ is different from the total velocity $\boldsymbol{u}$. Thus, the third case presents no contradiction with the assumption that the elastic part and the plastic part of the kinematic are totally separated. The additive decomposition in this case is used in the models proposed further. Without special statements, the subscript "(3)" will be omitted in the rest of this text.

5.3 4D constitutive model for plasticity

5.3.1 Flow theory for plasticity from thermodynamics

To constitute plasticity from 4D thermodynamics, an assumption should be first made to define the state variables which correspond to elasticity and plasticity respectively. We suppose a partition of the Helmholtz specific free energy:

$$\Psi = \Psi_{elasticity}(\lambda/\rho, \mu/\rho, e_{e\mu\nu}, g^{\mu\nu}) + \Psi_{plasticity}(r, Q_m), \tag{5.31}$$

where the elastic strain $e_{e\mu\nu}$ and the cumulated plastic strain r are variables for elastic and plastic deformations respectively. $\boldsymbol{e}_e$ is a tensor. r is a scalar, which will be detailed in

Section 5.3.2. λ and μ are the Lamé coefficients for elastic materials. Q_m are m constants of material for isotropic hardening. The rate of deformation is decomposed additively using Eq. 5.22.

With the decomposition of the Helmholtz specific free energy in Eq. 5.31 and that of the rate of deformation in Eq. 5.22, the Clausius-Duhem inequality Eq. 3.58 turns to be:

$$(-\rho u_e^\mu \nabla_\mu \Psi_{elasticity} + \sigma^{\mu\nu} d_{e\mu\nu}) + \left(-\rho u_p^\mu \nabla_\mu \Psi_{plasticity} + \sigma^{\mu\nu} d_{p\mu\nu}\right) \geq 0. \tag{5.32}$$

Again, the transmission of heat is not taken into consideration. As the elastic deformation is reversible, thus no dissipation is generated:

$$\rho u_e^\mu \nabla_\mu \Psi_{elasticity} = \sigma^{\mu\nu} d_{e\mu\nu}. \tag{5.33}$$

The constitutive relation between the stress and the elastic strain can be obtained using the same method as in Section. 4.2:

$$\sigma^{\mu\nu} = \lambda g^{\mu\nu} \frac{\partial \Psi_{elasticity}}{\partial(\lambda/\rho)} + \mu g^{\mu\nu} \frac{\partial \Psi_{elasticity}}{\partial(\mu/\rho)} + \rho \frac{\partial \Psi_{elasticity}}{\partial e_{e\mu\nu}} - 2\rho \frac{\partial \Psi_{elasticity}}{\partial g^{\alpha\beta}} g^{\alpha\mu} g^{\beta\nu}. \tag{5.34}$$

The same constitutive model for elasticity as Eq. 4.14 can be obtained with a choice of the elastic Helmholz specific free energy, such that:

$$\sigma^{\mu\nu} = \lambda (e_{e\alpha\beta} g^{\alpha\beta}) g^{\mu\nu} + 2\mu e_e^{\mu\nu}. \tag{5.35}$$

The only dissipation term in the Clausius-Duhem inequality in Eq. 5.32 is the one concerning plasticity. We can define it as the plastic dissipation:

$$\Phi_{plasticity} = \sigma^{\mu\nu} d_{p\mu\nu} - \rho u^\mu \nabla_\mu \Psi_{plasticity}. \tag{5.36}$$

With the plastic Helmholtz specific free enengy in Eq. 5.31, the dissipation can be derived as:

$$\Phi_{plasticity} = \sigma^{\mu\nu} d_{p\mu\nu} - \rho \frac{\partial \Psi_{plasticity}}{\partial r} u^\mu \nabla_\mu r - \sum \rho \frac{\partial \Psi_{plasticity}}{\partial Q_m} u^\mu \nabla_\mu Q_m. \tag{5.37}$$

Then we can define an associated scalar force for r:

$$R = \rho \frac{\partial \Psi_{plasticity}}{\partial r}. \tag{5.38}$$

With the assumption that the material parameters for plasticity are constant in the space-time, the dissipation can be simplified as:

$$\Phi_{plasticity} = \sigma^{\mu\nu} d_{p\mu\nu} - R u_p^{\mu} \nabla_{\mu} r. \tag{5.39}$$

In addition, plasticity is assumed to begin when the state of stress reaches a certain threshold [Hill, 1983; Khan and Huang, 1995; Lubarda, 2002; Borja, 2013]. This threshold is the yielding limit. This condition is modeled by an inequality:

$$\begin{cases} \mathscr{F} = \mathscr{F}(\sigma^{\mu\nu}) = 0 & \text{if plasticity} \\ \mathscr{F} = \mathscr{F}(\sigma^{\mu\nu}) < 0 & \text{if elasticity.} \end{cases} \tag{5.40}$$

To model the plasticity, there are two rules that has to be respected: 1) The state of stress yields the condition in Eq. 5.40, 2) The dissipation Eq. 5.39 reaches a maximum. In other words, *among all the admissible states ($\sigma^{\mu\nu}$ and R) obeying Eq. 5.40, the solution ($d_{p\mu\nu}$ and $u^{\lambda}\nabla_{\lambda}(r)$) is the one that maximize the plastic dissipation in Eq. 5.39.* Hence, the Lagrange method is used, with a Lagrangian variable $\mathcal{L}$ and a multiplier Λ:

$$\mathcal{L} = -\Phi_{plasticity} + \Lambda \mathscr{F} = -\sigma^{\mu\nu} d_{p\mu\nu} + R u^{\lambda} \nabla_{\lambda}(r) + \Lambda \mathscr{F}. \tag{5.41}$$

To calculate the maximum of the Lagrangian, we have for plastic deformations:

$$\frac{\partial \mathcal{L}}{\partial \sigma^{\mu\nu}} = -d_{p\mu\nu} + \Lambda \frac{\partial \mathscr{F}}{\partial \sigma^{\mu\nu}} = 0 \quad \frac{\partial \mathcal{L}}{\partial R} = u^{\lambda} \nabla_{\lambda} r - \Lambda = 0 \quad \frac{\partial \mathcal{L}}{\partial \Lambda} = \mathscr{F} = 0. \tag{5.42}$$

Thus, a constitutive model for plasticity can be obtained:

$$d_{p\mu\nu} = \Lambda \frac{\partial \mathscr{F}}{\partial \sigma^{\mu\nu}}, \tag{5.43}$$

which is similar to the 3D flow theory for plasticity [Lemaitre and Chaboche, 1994; Khan and Huang, 1995; Chaboche, 2008].

5.3.2 4D plasticity

We wish to establish a relation between the stress and the plastic rate of deformation. We choose to copy the 3D methodology and construct a 4D associated plastic potential theory. The elastoplastic state is determined by a yield surface in the stress space. The

yield threshold scalar density function $\mathscr{F}$ is defined in Eq. 5.44, and used in the plastic flow proposed in Eq. 5.43 to obtain Eq. 5.45:

$$\mathscr{F} = \sigma_{eff} - \kappa = 0 \tag{5.44}$$

$$d_{p\mu\nu} = \Lambda \frac{\partial \sigma_{eff}}{\partial \sigma^{\mu\nu}}, \tag{5.45}$$

where σ_{eff} is the effective stress and κ is a function describing hardening phenomena. To derive the form of the plastic multiplier Λ, the consistency condition is applied by taking the Lie derivative of both sides of Eq. 5.44, evaluated in the plastic velocity field $\boldsymbol{u}_p$:

$$\mathscr{L}_{u_p}(\sigma_{eff}) = \mathscr{L}_{u_p}(\kappa). \tag{5.46}$$

We consider only an isotropic hardening. The evolution of the yield surface κ depends on the cumulated plastic strain r. The rate of cumulated plastic strain can be calculated by:

$$u_p^\lambda \nabla_\lambda(r) = \mathscr{L}_{u_p}(r) = \frac{dr}{ds} \equiv \sqrt{d_p{}^{\alpha\beta} d_{p\alpha\beta}} = \Lambda, \tag{5.47}$$

because r is a scalar quantity (see Eq. 2.76a). The last equality in the equation above may be derived using Eq. 5.42. The scalar function κ is homogeneous to a stress dimension. It depends on r and on the different material parameters Q_m that have the dimension of stress.

$$\kappa = \kappa(r, Q_m). \tag{5.48}$$

The Lie derivative of κ is then, using the chain rule (Eq. 2.46):

$$\mathscr{L}_{u_p}(\kappa) = \frac{\partial \kappa}{\partial r} \mathscr{L}_{u_p}(r) + \sum_m \frac{\partial \kappa}{\partial Q_m} \mathscr{L}_{u_p}(Q_m) = \frac{\partial \kappa}{\partial r} \Lambda + C d_{p\,\lambda}^{\lambda}, \tag{5.49}$$

because the quantities Q_m are scalar densities of weight equal to one, thus $\mathscr{L}_{u_p}(Q_m) = Q_m d_{p\ \lambda}^{\lambda}$ and we define

$$C = \sum_m Q_m \frac{\partial \kappa}{\partial Q_m} \tag{5.50}$$

To further explicit the model, it is necessary to choose a specific form for the effective stress that is here constructed by choosing the Von Mises criterion [Khan and Huang, 1995], whose extension in 4D is:

$$\sigma_{eff} = \sqrt{S^{\alpha\beta} S_{\alpha\beta}} \tag{5.51}$$

where $\boldsymbol{S}$ is the deviatoric part of $\boldsymbol{\sigma}$ such that:

$$S^{\mu\nu} = \sigma^{\mu\nu} - \frac{(\sigma^{\alpha\beta} g_{\alpha\beta})}{4} g^{\mu\nu}.$$

The Lie derivative of the effective stress is, with Eq. 5.27 (the details of the derivation are given in Appendix D.1):

$$\mathscr{L}_{u_p}(\sigma_{eff}) = \frac{S_{\alpha\beta}}{\sigma_{eff}} u^\lambda \nabla_\lambda(\sigma^{\alpha\beta}) + \sigma_{eff}\ d_{p\,\lambda}^{\lambda}. \tag{5.52}$$

Then, combining Eqs. 5.46, 5.49 and 5.52, the plastic multiplier becomes:

$$\Lambda = \frac{\mathscr{L}_{u_p}(\sigma_{eff}) - C d_{p\,\lambda}^{\lambda}}{\frac{\partial \kappa}{\partial r}} \tag{5.53}$$

$$= \frac{1}{\frac{\partial \kappa}{\partial r}} \left[\frac{S_{\alpha\beta}}{\sigma_{eff}} u^\lambda \nabla_\lambda(\sigma^{\alpha\beta}) + d_{p\,\lambda}^{\lambda} \left(\sigma_{eff} - C\right) \right]. \tag{5.54}$$

If the plastic deformation is isochoric, $d_{p\,\lambda}^{\lambda} = 0$ and in this case:

$$\Lambda = \frac{1}{\frac{\partial \kappa}{\partial r}} \frac{S_{\alpha\beta}}{\sigma_{eff}} u^\lambda \nabla_\lambda(\sigma^{\alpha\beta}). \tag{5.55}$$

The plastic rate of deformation (Eq. 5.44) for an isochoric plastic deformation is given by:

$$d_{p_{\mu\nu}} = \Lambda \frac{S_{\mu\nu}}{\sigma_{eff}} = \mathcal{P} S_{\mu\nu}, \tag{5.56}$$

with the scalar

$$\mathcal{P} = \frac{S_{\alpha\beta}\ u^\lambda \nabla_\lambda(\sigma^{\alpha\beta})}{\sigma_{eff}^2 \frac{\partial \kappa}{\partial r}}.$$

The detailed expression of $\mathscr{L}_{u_p}(\sigma_{eff})$ in Eq. 5.52 and $\boldsymbol{d_p}$ in Eq. 5.56 are frame-indifferent by construction and indifferent to the superposition of rigid body motion even though the quantity $u^\lambda \nabla_\lambda(\sigma^{\alpha\beta})$ is not indifferent to the rigid body motion superposition. This is detailed in Appendix D.1 and is due to the fact that σ_{eff} is a scalar quantity. The choice of the transport in the deductions above is not constitutive, because it is applied on a scalar quantity (another objective transport could have been used and would have lead to the same final result). Thus, the expression of the plastic multiplier has been derived without any constitutive hypothesis on the transport operator, but only with consistent kinematic choices.

5.3.3 4D elastoplasticity

We now merge all the equations to construct complete elastoplastic models. Each of the hypoelastic models derived in Section 4.4 (Eq. 4.51, 4.59 or 4.60) are combined with the isochoric plastic rate of deformation given by Eq. 5.56 and the additive decomposition of the rate of deformation (Eq. 5.22). Three 4D elastoplastic models are thus constructed. Following the development of the three hypoelastic models in Section 4.4 of Chapter 4, taking reference of Eq. 5.35, the elastic part is modelled with one of the three models below:

$$\mathscr{L}_{u_e}(\sigma)^{\mu\nu} = \mathcal{H}_R^{\mu\nu\alpha\beta} d_{e\alpha\beta} \tag{5.57}$$

$$\mathscr{L}_{u_e}(\sigma)^{\mu\nu} = \mathcal{H}^{\mu\nu\alpha\beta} d_{e\alpha\beta} \tag{5.58}$$

$$\mathscr{D}^J(\sigma)^{\mu\nu} = \mathcal{H}^{\mu\nu\alpha\beta} d_{e\alpha\beta}, \tag{5.59}$$

with:

$$\mathscr{L}_{u_e}(\sigma)^{\mu\nu} = u^\lambda \nabla_\lambda(\sigma^{\mu\nu}) - \sigma^{\lambda\nu} L^\mu_{e_\lambda} - \sigma^{\mu\lambda} L^\nu_{e_\lambda} + \sigma^{\mu\nu} d^\lambda_\lambda \tag{5.60}$$

$$\mathscr{D}^J(\sigma)^{\mu\nu} = u^\lambda \nabla_\lambda(\sigma^{\mu\nu}) - \omega^\mu_{\ \alpha}\sigma^{\alpha\nu} + \sigma^{\mu\alpha}\omega_\alpha^{\ \nu}. \tag{5.61}$$

The plastic rate of deformation from Eq. 5.56 is:

$$d_{p_{\mu\nu}} = \mathcal{P} S_{\mu\nu} \text{ with } d^\lambda_{p\,\lambda} = 0 \text{ and } \mathcal{P} = \frac{S_{\alpha\beta}\ u^\lambda \nabla_\lambda(\sigma^{\alpha\beta})}{\sigma^2_{eff}\frac{\partial\kappa}{\partial r}}. \tag{5.62}$$

Plastic and elastic mechanisms are combined through the kinematic relations:

$$\begin{aligned} L^\mu_{\ \nu} &= d^\mu_{\ \nu} + \omega^\mu_{\ \nu} \\ d_{\mu\nu} &= d_{e\mu\nu} + d_{p_{\mu\nu}} \\ L^\mu_{e\nu} &= d^\mu_{e\nu} + \omega^\mu_{\ \nu}. \end{aligned} \tag{5.63}$$

The elastic fourth-rank tensor $\mathcal{H}_R$ and the hypoelastic fourth-rank tensor $\mathcal{H}$ are respectively detailed in Eqs. 4.51 and 4.61. The three systems of equations above (one for each case of hypoelastic models) are solved for the plastic rate of deformation d_p. The complete derivation is presented in Appendix D.2.

The final forms of the three 4D elastoplastic models from 4D thermodynamics with the hypotheses of additive decomposition and isotropic hardening (details of calculation are shown in Appendix D.2.1 and D.2.2) are:

- The elastoplastic model with a reversible hypoelastic part is:

$$\mathscr{L}_{u_e}(\sigma)^{\mu\nu} = \mathcal{H}_R^{\mu\nu\alpha\beta}(d_{\alpha\beta} - d^{\mathcal{R}}_{p\alpha\beta}), \tag{5.64}$$

where $\mathcal{H}_R$ is given by Eq. 4.53 and

$$d^{\mathcal{R}}_{p\alpha\beta} = S^{\kappa\lambda}\frac{Ad_{\kappa\lambda} - 2d_{\kappa\theta}\sigma^{\theta}_{\ \lambda}}{\sigma^2_{eff}(\partial\kappa/\partial r + A) - 2S_{\kappa\theta}\sigma^{\theta}_{\ \lambda}S^{\lambda\kappa}}S_{\alpha\beta}, \tag{5.65}$$

with

$$A = 2\mu + \frac{2\lambda(g_{\gamma\delta}\sigma^{\gamma\delta})}{4\lambda + 2\mu}. \tag{5.66}$$

- The elastoplastic model with an irreversible hypoelastic part constructed with a Lie derivative is:

$$\begin{aligned}\mathscr{L}_{u_e}(\sigma)^{\mu\nu} &= \mathcal{H}^{\mu\nu\alpha\beta}(d_{\alpha\beta} - d^{\mathcal{H}}_{p\alpha\beta}) \\ &= 2\mu d^{\mu\nu} + \lambda(d_{\alpha\beta}g^{\alpha\beta})g^{\mu\nu} \\ &- 2\mu\frac{S^{\rho\theta}\left(2\sigma_{\rho}^{\ \lambda}d_{\theta\lambda} + 2\mu\ d_{\rho\theta} - \sigma_{\rho\theta}d^{\lambda}_{\ \lambda}\right)}{\sigma^2_{eff}(\frac{\partial\kappa}{\partial r} + 2\mu) + 2\sigma^{\alpha\lambda}S^{\beta}_{\ \lambda}S_{\alpha\beta}}S^{\mu\nu}.\end{aligned} \tag{5.67}$$

- The elastoplastic model with an irreversible hypoelastic part constructed with a Jaumann transport is:

$$\mathscr{T}^J(\sigma)^{\mu\nu} = 2\mu d^{\mu\nu} + \lambda(d_{\alpha\beta}g^{\alpha\beta})g^{\mu\nu} - \frac{4\mu^2\ S^{\rho\theta}d_{\rho\theta}}{\sigma^2_{eff}(\frac{\partial\kappa}{\partial r} + 2\mu)}S^{\mu\nu}. \tag{5.68}$$

The models above are covariant since they have been constructed within a 4D context. The models constructed with a Lie derivative are also indifferent to the superposition of rigid body motions. Note that Eq. 5.57 represents a model with a non-linear hypoelastic part that can be proved to be reversible; this is not the case for the other two models. Thus, only the model constructed with Eq. 5.57 represents a correct elastoplastic model, which corresponds to the assumption that only the plastic deformation causes dissipations of energy.

5.4 3D projection and comparison with classical elasto-plasic models

5.4.1 Projection of the 4D models in 3D space

To solve the proposed models for engineering applications and to compare the models with existing 3D models, we consider non-relativistic cases. The equations are projected in a 3D coordinate system. This method is discussed in Sections. 4.5. To identify 3D equations, the indices are denoted with Roman letters as opposed to Greek letters for 4D equations.

The reversible hypoelastic model (Eq.4.51) has the 3D form:

$$\mathscr{L}_{v_e}(\sigma)^{ij} = \mathcal{H}_R^{ijab} d_{eab} \tag{5.69}$$

where

$$\begin{aligned} \mathcal{H}_R^{ijab} &= \left(\lambda + \frac{\lambda^2\, tr(\boldsymbol{\sigma})}{\mu(3\lambda+2\mu)}\right) g^{ij}g^{ab} + \left(2\mu + \frac{2\lambda\, tr(\boldsymbol{\sigma})}{3\lambda+2\mu}\right) g^{ia}g^{jb} \\ &+ \sigma^{ij}g^{ab} - \frac{\lambda}{\mu} g^{ij}\sigma^{ab} - 2(g^{ia}\sigma^{bj} + g^{ja}\sigma^{bi}). \end{aligned}$$

The irreversible hypoelastic models (Eqs. 4.59 and 4.60) have the 3D form:

$$\mathscr{L}_{v_e}(\sigma)^{ij} = \mathcal{H}^{ijab} d_{e_{ab}} \tag{5.70}$$

$$\mathscr{T}^J(\sigma)^{ij} = \mathcal{H}^{ijab} d_{e_{ab}} \tag{5.71}$$

$$\text{where } \mathcal{H}^{ijkl} = \lambda g^{ij}g^{ab} + \mu(g^{ia}g^{jb} + g^{ja}g^{ib}).$$

Remind that the 3D expressions of the Lie derivative and Jaumann transports are:

$$\mathscr{L}_{v_e}(\sigma)^{ij} = \frac{d\sigma^{ij}}{dt} - \sigma^{lj}L^i_{e_l} - \sigma^{il}L^j_{e_l} + \sigma^{ij}d^l_{\ l} \tag{5.72}$$

$$\mathscr{T}^J(\sigma)^{ij} = \frac{d\sigma^{ij}}{dt} - \omega^i_{\ l}\sigma^{lj} + \sigma^{il}\omega_l^{\ j}. \tag{5.73}$$

The 3D projection of 4D hypoelastic models is already done in Section 4.5. The difference between the 3D models in this chapter, Eqs. 5.69, 5.70 and 5.71, with those in Chapter 4, Eqs. 4.73, 4.74 and 4.75, is that the velocity field, the strain tensor and the Lie derivative

are considered in the elastic region. In other words, $\boldsymbol{u}$, $\boldsymbol{e}$ and $\boldsymbol{L}$ in Eqs. 4.73, 4.74 and 4.75 turn to be $\boldsymbol{u}_e$, $\boldsymbol{e}_e$ and $\boldsymbol{L}_e$ in Eqs. 5.69, 5.70 and 5.71. The same technique in Section 4.5 can be applied to project the 4D plastic model into 3D. The 3D plastic rate of deformation is given by:

$$d_{p_{ij}} = \mathcal{P} S_{ij} \text{ with } d^l_{p\,l} = 0 \text{ and } \mathcal{P} = \frac{S_{ab}\,\frac{d\sigma^{ab}}{dt}}{\sigma^2_{eff}\frac{\partial \kappa}{\partial r}}. \tag{5.74}$$

The plastic and elastic mechanisms are combined through the kinematic relations:

$$\begin{aligned} L^i_j &= d^i_j + \omega^i_{\ j} \\ d_{ij} &= d_{eij} + d_{p_{ij}} \\ L^i_{ej} &= d^i_{ej} + \omega^i_{\ j}. \end{aligned} \tag{5.75}$$

The 3D projection of the elastoplastic models (Eqs. 5.64, 5.67 and 5.68) finally leads to:

- For the elastoplastic model with a reversible hypoelastic part (denoted REP in the Figures of Section 6.2):

$$\mathscr{L}_{v_e}(\sigma)^{ij} = \mathcal{H}^{ijab}_R (d_{ab} - d^{\mathcal{R}}_{pab}), \tag{5.76}$$

  where $\mathcal{H}_R$ is given by Eq. 5.69 and

$$d^{\mathcal{R}}_{pab} = S^{kl} \frac{A d_{kl} - 2 d_{kt}\sigma^t_{\ l}}{\sigma^2_{eff}(\partial\kappa/\partial r + A) - 2 S_{kt}\sigma^t_{\ l} S^{lk}} S_{ab}, \tag{5.77}$$

  with

$$A = 2\mu + \frac{2\lambda tr(\boldsymbol{\sigma})}{3\lambda + 2\mu}. \tag{5.78}$$

- For the elastoplastic model with an irreversible hypoelastic part, constructed with a Lie derivative (denoted IREP in the Figures of Section 6.2):

$$\begin{aligned} \mathscr{L}_{v_e}(\sigma)^{ij} &= \mathcal{H}^{ijab}(d_{ab} - d^{\mathcal{H}}_{pab}) \\ &= 2\mu d^{ij} + \lambda\, tr(\boldsymbol{d})\eta^{ij} \\ &- 2\mu \frac{S^{rt}\left(2\sigma_r^{\ l} d_{tl} + 2\mu\, d_{rt} - \sigma_{rt}\, tr(\boldsymbol{d})\right)}{\sigma^2_{eff}(\frac{\partial\kappa}{\partial r} + 2\mu) + 2\sigma^{al} S^b_{\ l} S_{ab}} S^{ij}. \end{aligned} \tag{5.79}$$

- For the elastoplastic model with an irreversible hypoelastic part, constructed with a Jaumann transport:

$$\mathscr{T}^J(\sigma)^{ij} \quad = \quad 2\mu d^{ij} + \lambda\, tr(\boldsymbol{d})\eta^{ij} - \frac{4\mu^2\, S^{ab}d_{ab}}{\sigma_{eff}^2(\frac{\partial\kappa}{\partial r} + 2\mu)}S^{ij}. \tag{5.80}$$

Note that the spatial components of the 4D deviatoric stress tensor $S^{\mu\nu}$ are not equal to the components of the 3D deviatoric stress. A counter example is given. In 3D, the trace of the deviatoric stress tensor, which is the summation of the three components in diagonal in the inertial frame of reference, equals to zero due to its definition, $S^{ij}g_{ij} = 0$. However, in 4D, the summation of the three spatial components in diagonal equals the fourth one, $S^{11} + S^{22} + S^{33} = S^{44}$ in the inertial frame of reference, calculated from $S^{\mu\nu}\eta_{\mu\nu} = 0$. As S^{44} is not necessarily zero, the 4D derivatoric stress tensor cannot be projected into 3D directly by simply taking its spatial components to generate a 3D tensor.

The projection performed in this section for the 3D plastic model is done by mimicking the procedure for constituting the 4D plastic model. The model is obtained by using the flow theory, defining the effective stress, applying the condition of consistence and then deducing the models. Considering the plastic model in Eq. 5.62, the plastic rate of deformation equals to a scalar multiplied by the deviatoric stress tensor. The rule of projection from 4D deviatoric tensors to its 3D can be the same for both side of the tensor in Eq. 5.62. Then the 3D plastic model, Eq. 5.74, can still be obtained, as long as the scalar $\mathcal{P}$ is the same in 3D and 4D.

There is another proposal. We can define a tensor $\boldsymbol{S}_{pseudo}$ who serves as the deviatoric stress tensor:

$$S^{\mu\nu}_{pseudo} = T^{\mu\nu}_{\sigma} - \frac{1}{3}T^{\alpha\beta}_{\sigma}(g_{\alpha\beta} - u_\alpha u_\beta)(g^{\mu\nu} - u_\mu u_\nu). \tag{5.81}$$

With this definition, the 3D trace of the spatial components is zero. However, this definition will complicate the procedure of developing models by introducing the four-velocity. Prospective work may be performed in two aspects: 1) elaboration of the projection in 3D of 4D, 2) development of models with the new definition of 4D tensor who serves as the deviatoric stress tensor in Eq. 5.81. The goal is to verify the equivalence of 4D and 3D plastic models.

5.4.2 Classical 3D models

Many elastoplastic models have been proposed in the context of finite deformations ([Lubarda, 2002; Nemat-Nasser, 2004; Bertram, 2012]). We have chosen to compare the models established above with an advanced model presented by Sidoroff [Sidoroff, 1982b], because it is representative of the classical 3D approach [Xiao et al., 2000a; Volokh, 2013; Shutov and Ihlemann, 2014]. This model considers isotropic hardening and use Von Mises criterion. It is constructed with a methodology that is similar to the one presented for the 4D models in Section 5.2. Regarding kinematic choices, to combine the elastic and plastic mechanisms, a multiplicative decomposition of the deformation gradient $\boldsymbol{F}$ is often considered in 3D models. The elastic part $\boldsymbol{F}_e$ and plastic part $\boldsymbol{F}_p$ are defined [Lee, 1969; Nemat-Nasser, 1979] such that:

$$F^i_{\ j} = F^i_{ek} F^k_{pj}, \tag{5.82}$$

which is the same case as the first case discussed in Section 5.2. As it is already mentioned, this multiplicative decomposition causes a difficulty in decomposing the rate of deformation additively. To overcome this difficulty, and define a kinematic expression for the plastic rate of deformation, it is usually supposed that the elastic deformation is small such that [Badreddine et al., 2010]:

$$e_e^{ij} \approx \epsilon_e^{ij} \ll I^{ij}, \tag{5.83}$$

where ϵ_e^{ij} is the infinitesimal strain tensor representing the elastic part of the deformation. This approximation is, for example, valid when the elastoplastic models are dedicated to metallic materials. Within this small elastic deformations approximation, the elastic model can be transformed into a hypoelastic model [Sidoroff, 1982b]:

$$\mathscr{T}^J(\sigma)^{ij} = 2\mu {d_e}^{ij} + \lambda tr(\boldsymbol{d}_e) g^{ij}, \tag{5.84}$$

which *a posteriori* justifies the choice of the hypoelastic model presented by Eq. 4.58. Within the small elastic deformations approximation, it is also possible to obtain an additive decomposition in terms of the plastic rate of deformation and it can be demonstrated that:

$$d_{ij} \approx \mathscr{T}^J(\epsilon_e)_{ij} + d_{pij}. \tag{5.85}$$

This additive decomposition is classically used in 3D models ([Lubarda, 2002; Nemat-Nasser, 2004; Bertram, 2012]). Thus, even if a multiplicative decomposition (Eq. 5.82) is chosen as a starting point to construct the model, an additive decomposition in terms of rates of deformation is necessary and eventually used to derive the elastoplastic model. The elastoplastic model presented by Sidoroff is ([Sidoroff, 1982b]) a typical rate-form elastoplastic model in large deformation with a small elastic strain:

$$\mathscr{T}^J(\sigma)^{ij} = 2\mu d^{ij} + \lambda\, tr(\boldsymbol{d}) g^{ij} - \frac{4\mu^2\, S^{ab} d_{ab}}{\sigma_{eff}^2(\frac{\partial \kappa}{\partial r} + 2\mu)} S^{ij}. \tag{5.86}$$

which corresponds exactly to Eq. 5.80, the 3D projection of the 4D model developed with Jaumann's transport. It is an elastoplastic model constructed with an irreversible hypoelastic model including a Jaumann transport. This model is denoted "Jaumann model with IREP" in the Figures of Section 6.2.

5.5 Conclusions

We have proposed to construct elastoplastic models using a 4D formalism to take advantage of the inherently frame-indifferent context of this approach, corresponding to the use of the covariance principle. The constitutive models hence built, but also all the operators and physical laws are thus frame-indifferent.

The use of Lie derivative is considered throughout the procedure of 4D modelling: it is first used to derive a hypoelastic model from the hyperelastic model chosen to model the elastic part of the material. This hyperelastic model is derived from the frameworks of thermodynamics developed in Chapter 3. It is also used in the derivation of the plastic behavior of the material. The elastic and plastic mechanisms of the model are combined by a simple additive decomposition of the rates of deformation. We have compared this model with two other elastoplastic models constructed with linear hypoelasticity. One is constructed with the Lie derivative and the other with the Jaumann transport. The models constructed in 4D are then projected in 3D to be compared with existing elastoplastic models. It shows differences in the form of relation and will show some differences in the numerical simulations in Chapter 6.

Chapter 6

Applications to numerical simulations

Contents

6.1 Introduction

4D constitutive models for hyperelasticity, anisotropic elasticity, hypoelasticity and elastoplasticity have been developed in Chapters 4 and 5. These 4D models have been also projected into 3D, which is presented in Sections 4.5 and 5.4.1. With the Zset© software, the projected 3D models can now be used in Finite Element Analysis.

In this chapter, different numerical simulations will be performed with the previous developed models for elasticity, hypoelasticity and elastoplasticity. The calculations are done with one cube with one element mesh, as well as with one bar with several elements

mesh. For the cube, tensile and gliding are simulated using the elastic models and elastoplastic models. Thus, different elastic/elastoplastic models are analyzed and compared. For the bar, torsion is simulated to study the hypoelastic models while the bending is used for studying the elastoplastic models. An example of algorithm of local integration for the elastoplastic model is given in Appendix E.1.

6.2 Calculations in one element

Numerical simulations have been performed to compare the elastic/elastoplastic models detailed in the previous sections. For the simulations of elasticity, the parameters have been chosen to correspond to steel. The parameters of Lamé are given in Tab. 6.1. For the simulations of elastoplasticity, the parameters of elastic part are the same as those of pure elasticity. The plastic part is chosen so that the isotropic hardening is non-linear

$$\kappa = R_0 + Q(1 - e^{-br}) \text{ and } \frac{\partial \kappa}{\partial r} = Qbe^{-br}, \tag{6.1}$$

where R_0, Q and b are material constants. The parameters of isotropic hardening are also given in Tab. 6.1.

λ (MPa)	μ (MPa)	R_0 (MPa)	Q (MPa)	b
150000	100000	400	2500	2

Table 6.1: Material parameters (steel 480) [Badreddine, 2006]

6.2.1 Calculations in one element with elastic models

We compare the results given by the different elastic models. They are listed in terms of components.

- 3D projection of nonlinear hyperelastic model (model 1 in Eq. 4.11):

$$\sigma^{ij} = 0.5\lambda(tr(\boldsymbol{e}))^2 I^{ij} + \mu(e^a_c e^c_a)I^{ij} + \lambda tr(\boldsymbol{e})I^{ij} + 2\mu e^{ij} - 2\lambda tr(\boldsymbol{e})e^{ij} - 4\mu e^{ci}e^j_c. \tag{6.2}$$

- 3D projection of linear elastic model, or Hookean-like model (model 2 in Eq. 4.14):

$$\sigma^{ij} = \lambda(I^{ab}e_{ab})I^{ij} + 2\mu e^{ij}. \tag{6.3}$$

- 3D projection of model 3 (in Eq. 4.16):

$$\hat{\sigma}^{mn} = \hat{g}^{mi}\hat{g}^{nj}\hat{\sigma}_{ij} = \hat{g}^{mi}\hat{g}^{nj}\left(\lambda(E^{ab}I_{ab})I^{ij} + 2\mu E^{ab}I_{ia}I_{jb}\right) \tag{6.4}$$

$$\iff \sigma^{ij}J = \lambda(b^{ab}e_{ab})b^{ij} + 2\mu e_{ab}b^{ia}b^{jb}. \tag{6.5}$$

- 3D projection of model 4 (in Eq. 4.18):

$$\hat{\sigma}^{ij} = \lambda(E_{ab}I^{ab})I_{ij} + 2\mu E_{ab}I^{ia}I^{jb} \tag{6.6}$$

$$\iff \sigma^{ij}J = \lambda(\beta^{ab}e_{ab})\beta^{ij} + 2\mu e_{ab}\beta^{ia}\beta^{jb}. \tag{6.7}$$

The comparison between different models is performed with a combination of in-plane gliding and traction applied to a material point as illustrated in Fig. 6.1.

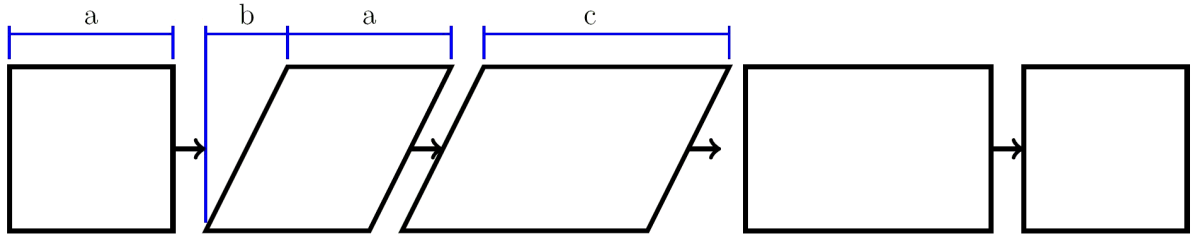

Figure 6.1: The cyclic combination of loading and unloading of traction and gliding applied on a cubic element within the domain of elasticity. a is the reference length of the edge of the cube. b is the final value of the lengths corresponding to the slide and c to the traction.

Several series of loading have been applied to the cube with different values for b and c, defined in Fig. 6.1. Two series of results are presented in 6.2 and 6.3 corresponding respectively to a moderate deformation and a large deformation. These deformations have been chosen to highlight the differences of the elastic models. These models have been tested for large deformations which are not realistic for metals, but quite more realistic for polymers or biomaterials.

The top of the Figs. 6.2 and 6.3 present the varying components of the deformation gradient $\boldsymbol{F}$ that has been imposed and the resulting deformation tensor $\boldsymbol{e}$. The resulting

component σ^{11} of the Cauchy stress tensor $\boldsymbol{\sigma}$ are next presented for the elastic models listed in Section 6.2.1.

As expected, model 2 gives the linear curve representing the relation between the stress $\boldsymbol{\sigma}$ and the strain $\boldsymbol{e}$ in Eulerian description, seeing right middle of Figs. 6.2 and 6.3. The bottom figures of Figs. 6.2 and 6.3 show the linear relations in Lagrangian description for model 3 and model 4: Covariant components of $\hat{\boldsymbol{\sigma}}$ are linear to contravariant components of $\boldsymbol{E}$ in model 3; Contravariant components of $\hat{\boldsymbol{\sigma}}$ are linear to covariant components of $\boldsymbol{E}$ in model 4. Note that the right middle figure of Fig. 6.3 shows different slopes for $\sigma^{11} = f(e_{11})$. We know that $\sigma^{11} = (\lambda + 2\mu)e_{11} + 2\mu(e_{22} + e_{33})$. $(e_{22} + e_{33})$ is also linear to e_{11}. In different phrase of loading, the value of $(e_{22} + e_{33})$ change, which explains the difference of slope in different phrases.

These four models present different results for the same loading. When the deformation is small (see the left middle in Fig. 6.2), model 2 gives the similar result as model 1. Remind that these two models have the same first-order of strain $(\lambda tr(\boldsymbol{e})\boldsymbol{I} + 2\mu\boldsymbol{e})$. However, the model 1 has the terms of second-order of strain but the model 2 does not. The smaller the deformation is, the smaller effect to the result does the second-order of strain have. Thus, model 1 can be approximated by model 2 in small deformation and vice versa. When the deformation is large (see the left middle in Fig. 6.3), the difference between model 1 and model 2 are much smaller than that between any two models. Comparing the expressions between model 1 and model 2, and that between model 2 and model 3 or model 4, we can find that the differences are given by the different combinations of deformation quantities, for example, the strain tensors $\boldsymbol{e}$, $\boldsymbol{b}$ and $\boldsymbol{\beta}$. The model 2 uses only first-order of deformation quantities. The model 1 adds extra terms of second-order of deformation quantities to the model 2, thus it is a combination of first-order and second-order. The model 3 and 4 are totally constructed by the third-order of deformation quantities, for example $(\boldsymbol{b} : \boldsymbol{e})\boldsymbol{b}$. Apparently, the higher orders of the deformation quantities give a larger difference in the result for the loading of large deformation. That the reason why the difference between model 1 and model 2 are small. Definitely, the effect of the high order of the strain in the construction of the models can not be ignored in large deformation.

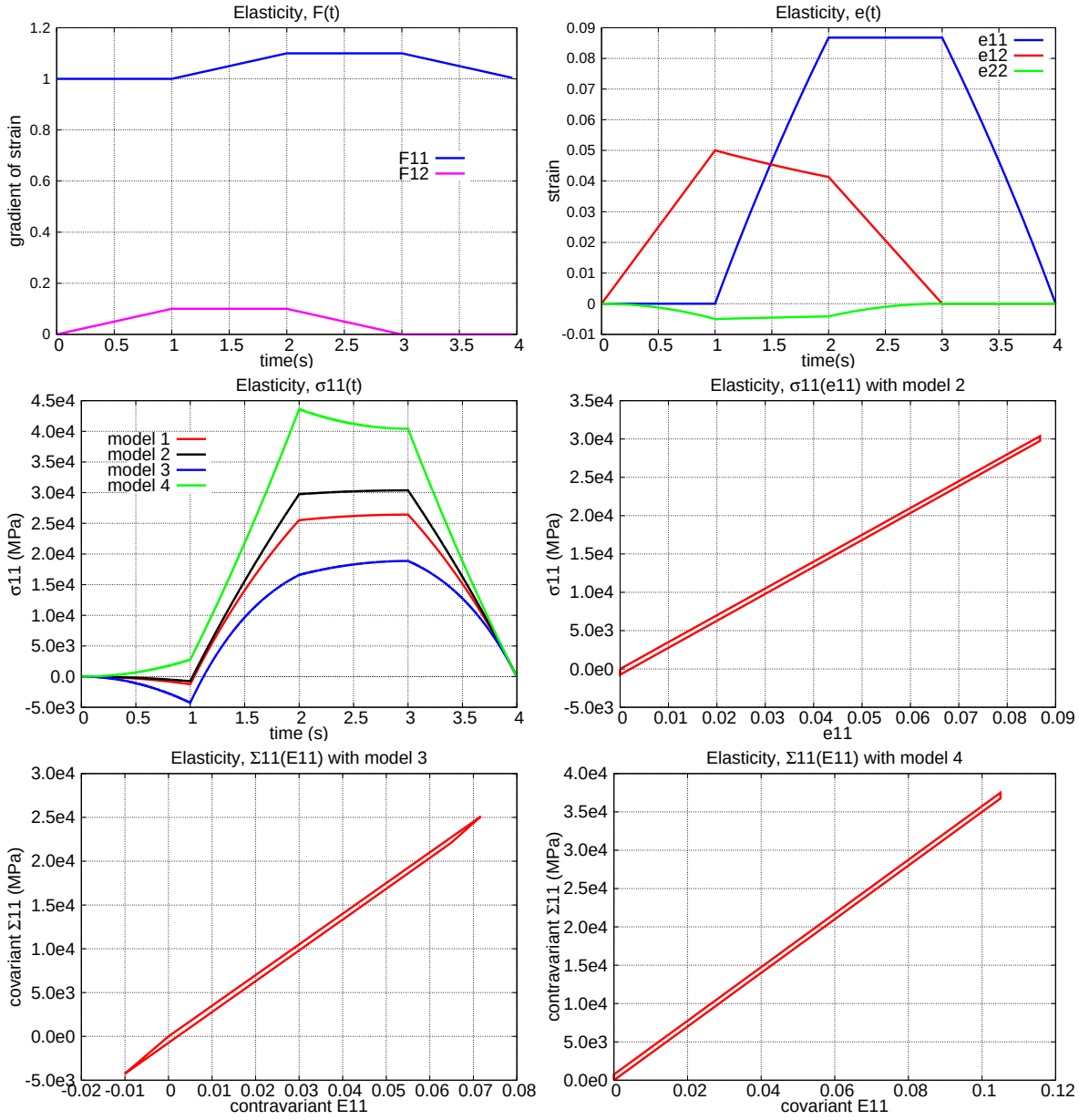

Figure 6.2: Stress as a function of time and strain for a cycle in deformation (represented in Figure 6.1) at moderated deformation (reaching $b/a = 0.1$ and $(c-a)/a = 0.1$). The varying components of the deformation gradient $\boldsymbol{F}$ and strain $\boldsymbol{e}$ are given on the top figures. The varying components of the stress tensor are given in the left middle figure for the elastic models and the elastic models listed in Section 6.2.1. The linear relation between stress and strain for model 2 is given in the right middle figure. The linear relation between covariant components of $\hat{\boldsymbol{\sigma}}$ (noted $\boldsymbol{\Sigma}$ in figures) and contravariant components of $\boldsymbol{e}$ for model 3 is in the left bottom figure while that between contravariant components of $\hat{\boldsymbol{\sigma}}$ (noted $\boldsymbol{\Sigma}$ in figures) and covariant components of $\boldsymbol{e}$ for model 4 is in the right bottom figure.

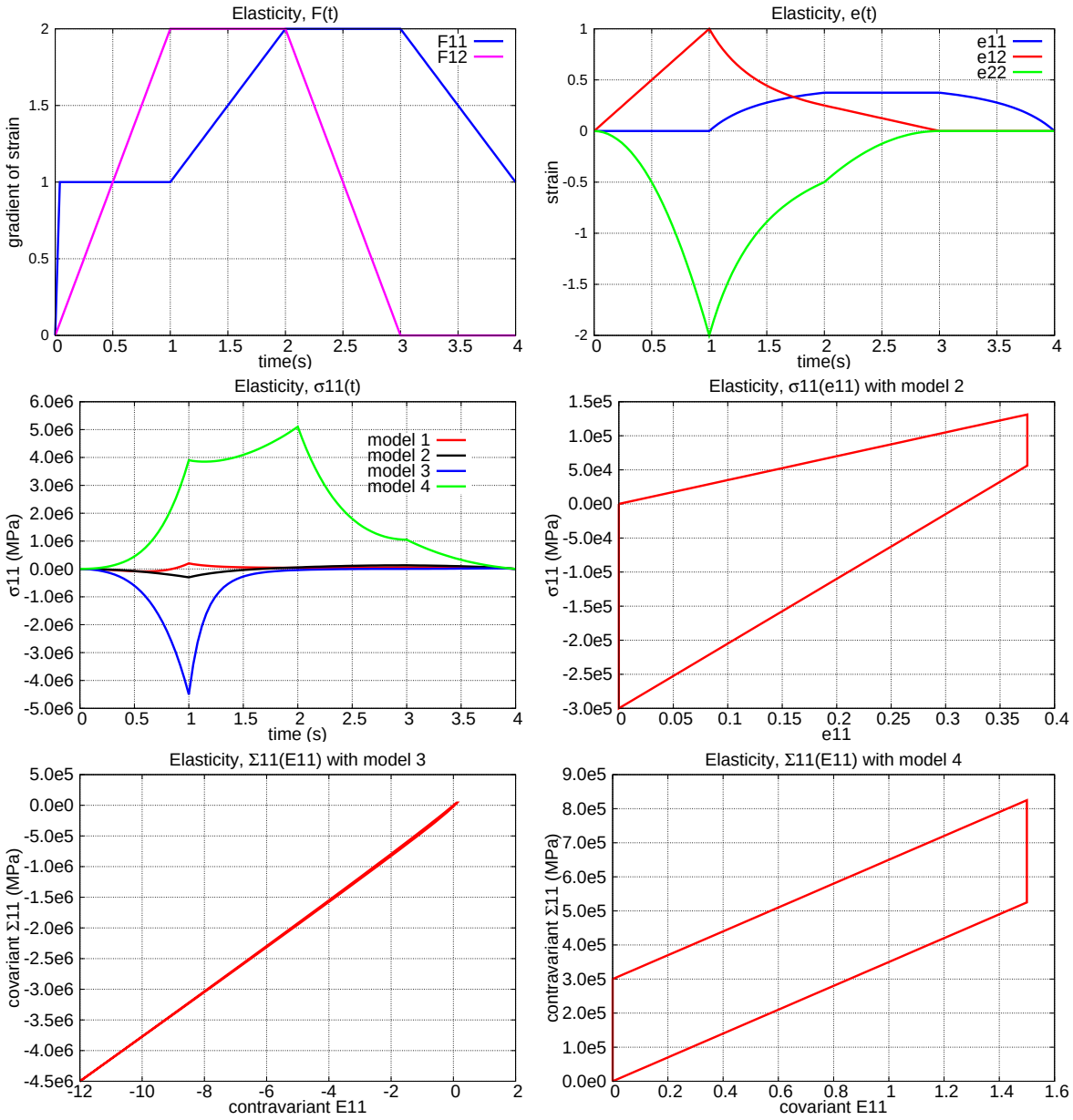

Figure 6.3: Stress as a function of time and strain for a cycle in deformation (represented in Figure 6.1) at large deformation (reaching $b/a = 1$ and $(c-a)/a = 1$). The varying components of the deformation gradient $\boldsymbol{F}$ and strain $\boldsymbol{e}$ are given on the top figures. The varying components of the stress tensor are given in the left middle figure for the elastic models and the elastic models listed in Section 6.2.1. The linear relation between covariant components of $\hat{\boldsymbol{\sigma}}$ (noted $\boldsymbol{\Sigma}$ in figures) and contravariant components of $\boldsymbol{e}$ for model 3 is in the left bottom figure while that between contravariant components of $\hat{\boldsymbol{\sigma}}$ (noted $\boldsymbol{\Sigma}$ in figures) and covariant components of $\boldsymbol{e}$ for model 4 is in the right bottom figure.

6.2.2 Calculations in one element with hypoelastic models

We compare the results given by the different hypoelastic models. The objective transports used here are the Lie derivative and the Jaumann transport. The models are listed below.

- 3D projection of reversible hypoelastic model (Eq. 4.51) with the Lie derivative. This model will be called the Lie model with reversible elastic part (REP) in the figures of results of calculations. Remind the Lie model with REP:

$$\mathscr{L}_v(\sigma)^{ij} = \mathcal{H}_R^{ijab} d_{eab} \tag{6.8}$$

$$\begin{aligned} \text{with} \quad \mathcal{H}_R^{ijab} &= \left(\lambda + \frac{\lambda^2\, tr(\boldsymbol{\sigma})}{\mu(3\lambda+2\mu)}\right) I^{ij} I^{ab} + \left(2\mu + \frac{2\lambda\, tr(\boldsymbol{\sigma})}{3\lambda+2\mu}\right) I^{ia} I^{jb} \\ &+ \sigma^{ij} I^{ab} - \frac{\lambda}{\mu} I^{ij} \sigma^{ab} - 2(I^{ia}\sigma^{bj} + I^{ja}\sigma^{bi}). \end{aligned}$$

- 3D projection of irreversible hypoelastic models (Eq. 4.59) with the Lie derivative. This model will be called the Lie model with irreversible elastic part (IREP) in the figures. Remind the Lie model with IREP:

$$\mathscr{L}_v(\sigma)^{ij} = \mathcal{H}^{ijab} d_{ab}, \tag{6.9}$$

$$\text{with} \quad \mathcal{H}^{ijab} = \lambda I^{ij} I^{ab} + \mu(I^{ia} I^{jb} + I^{ja} I^{ib}).$$

- 3D projection of irreversible hypoelastic models (Eq. 4.60) with the Jaumann transport. This model will be called the Jaumann model with irreversible elastic part (IREP) in the figures. Remind the Jaumann model with IREP:

$$\mathscr{D}^J(\sigma)^{ij} = \mathcal{H}^{ijab} d_{ab}, \tag{6.10}$$

$$\text{with} \quad \mathcal{H}^{ijab} = \lambda I^{ij} I^{ab} + \mu(I^{ia} I^{jb} + I^{ja} I^{ib}).$$

- 3D projection of linear elastic model, or Hookean-like model. As all the three hypoelastic models mentioned above are developed from this elastic model, thus it will serve as a reference. This model will be called model for elasticity in the figures corresponding to the model 2 listed in Eq. 6.3.

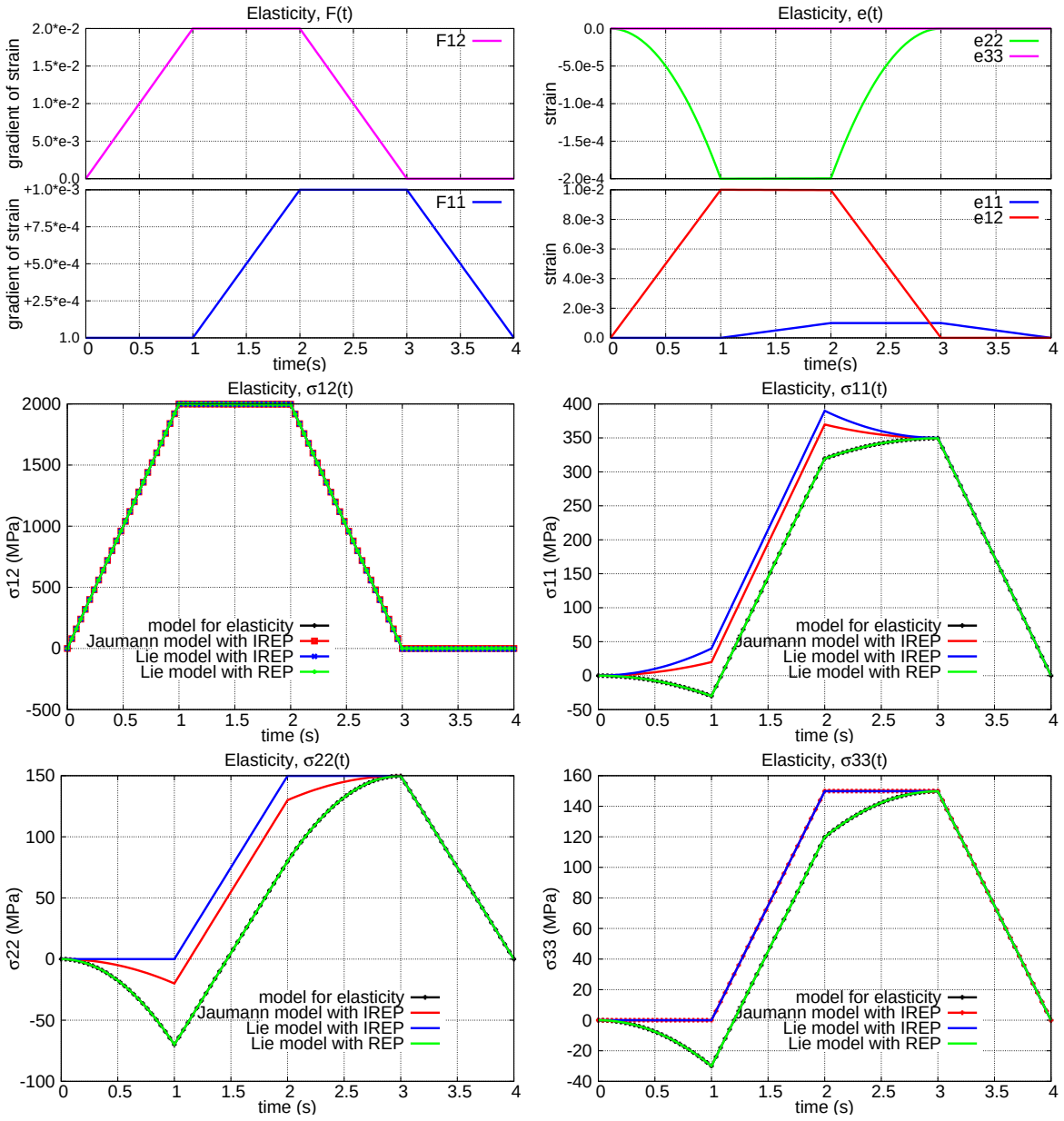

Figure 6.4: Deformation and stress as a function of time for a cycle in deformation (represented in Fig. 6.1) at moderated deformation (reaching $b/a = 0.02$ and $(c-a)/a = 0.001$) and without plasticity. The varying components of the deformation gradient $\boldsymbol{F}$ and strain $\boldsymbol{e}$ are given on the top figures. The varying components of the stress tensor are given in the other figures for the elastic model and the hypoelastic models listed in Section 6.2.2. The hypoelastic models are constructed with the Jaumann transport or with the Lie derivative. They are either reversible (REP) or irreversible (IREP).

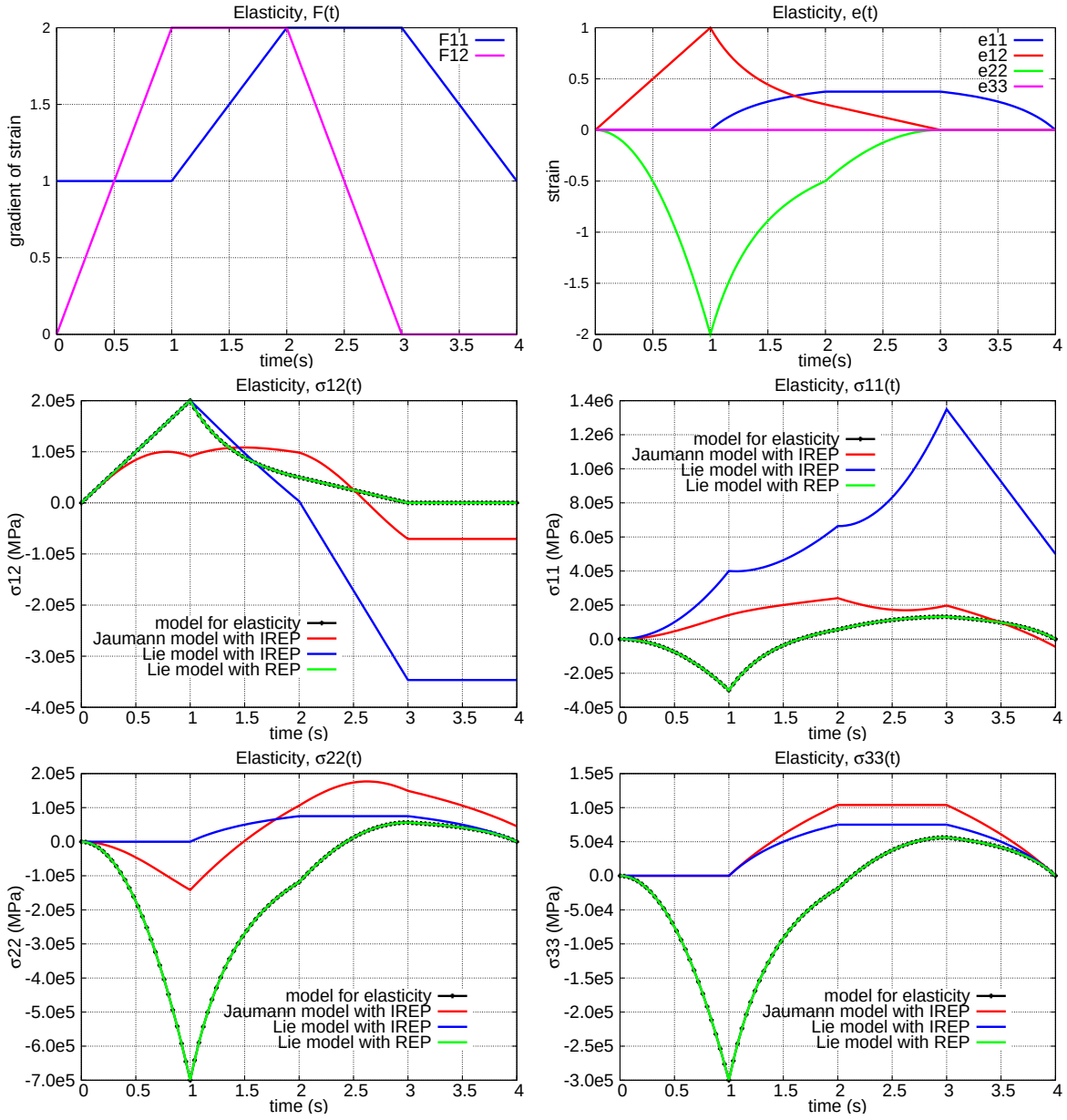

Figure 6.5: Deformation and stress as a function of time for a cycle in deformation (represented in Figure 6.1) with an important deformation (reaching $b/a = 2$ and $(c-a)/a = 1$) and without plasticity. The varying components of the deformation gradient $\boldsymbol{F}$ and strain tensor $\boldsymbol{e}$ are given on the top figures. The varying components of the Cauchy stress tensor $\boldsymbol{\sigma}$ are given in the other figures for the elastic model and the hypoelastic models listed in Section 6.2.2. The hypoelastic models are constructed with the Jaumann transport or the Lie derivative. They are either reversible (REP) or irreversible (IREP).

The comparison is performed with combination of in-plane gliding and traction applied to a material point as illustrated in Fig. 6.1. This type of loading highlights in particular the (ir)reversibility of the models. Several series of loading have been applied to the cube with different values for b and c, defined in Fig. 6.1. Two series of results are presented in Figs. 6.4 and 6.5 corresponding respectively to a moderate deformation and an important deformation. These deformations have been chosen to highlight the differences of the hypoelastic models.

The tops of the Figs. 6.4 and 6.5 present the varying components of the deformation gradient $\boldsymbol{F}$ that have been imposed and the resulting deformation tensor $\boldsymbol{e}$. The resulting components of the Cauchy stress tensor $\boldsymbol{\sigma}$ are next presented for the elastic model and the three hypoelastic models derived in Section 5.4.1. The stress-strain curves are given as the complementary in Annex F. As expected, the reversible hypoelastic model constructed with the Lie derivative gives exactly the same results as the elastic model, illustrating the fact that this hypoelastic model is equivalent to the reference elastic model. For very small deformations, it has been observed that all the hypoelastic models give the same resulting stress as the elastic model.

For moderate deformations, the resulting stress tensors computed with each of the model are rather close to each other, the shearing component σ^{12} being exactly the same for all the models. Small differences appear for the other components of the stress. In particular for σ^{11}, the two hypoelastic irreversible models result in a positive value, while the elastic model and the reversible hypoelastic model result in a negative value. Also, the component σ^{33} remains equal to zero for the irreversible hypoelastic models during gliding (first solicitation of the cycle), while the elastic model predicts a compression in this direction. The reversible hypoelastic model is able to describe volumetric effects accurately and thus predicts the correct evolution of this stress component as well. For important elastic deformations, the differences in the hypoelastic models are major, illustrating, in particular, the irreversibility of the hypoelastic models when they are not derived from reversible elastic models. Thus, hypoelastic models constructed with an objective transport and linear in $\boldsymbol{d}$ have to be used with caution. An hypoelastic model directly derived from the elastic model representing the material has to be preferred to obtain accurate

results.

6.2.3 Calculations in one element with elastoplastic models

We compare the results given by the different elastoplastic models. The objective transports used here are the Lie derivative and the Jaumann transport. The elastic parts of these elastoplastic models correspond to the hypoelastic models discussed in Section 6.2.2. The models are listed below.

- 3D projection of elastoplastic model with the Lie derivative and a reversible hypoelastic part (Eq. 5.64). This model is called Lie model with REP in the figures of results.

$$\begin{aligned}
\mathscr{L}_{v_e}(\sigma)^{ij} &= \mathcal{H}_R^{ijab}(d_{ab} - d_{pab}^{\mathcal{R}}) \qquad (6.11)\\
\text{with} \quad \mathcal{H}_R^{ijab} &= \left(\lambda + \frac{\lambda^2\, tr(\boldsymbol{\sigma})}{\mu(3\lambda+2\mu)}\right) I^{ij} I^{ab} + \left(2\mu + \frac{2\lambda\, tr(\boldsymbol{\sigma})}{3\lambda+2\mu}\right) I^{ia} I^{jb}\\
&+ \sigma^{ij} I^{ab} - \frac{\lambda}{\mu} I^{ij}\sigma^{ab} - 2(I^{ia}\sigma^{bj} + I^{ja}\sigma^{bi})\\
d_{pab}^{\mathcal{R}} &= S^{kl}\frac{A d_{kl} - 2 d_{kt}\sigma^t_{\ l}}{\sigma_{eff}^2(\partial\kappa/\partial r + A) - 2 S_{kt}\sigma^t_{\ l} S^{lk}} S_{ab}\\
A &= 2\mu + \frac{2\lambda tr(\boldsymbol{\sigma})}{3\lambda+2\mu}.
\end{aligned}$$

- 3D projection of elastoplastic model with the Lie derivative and an irreversible hypoelastic part (Eq. 5.67). This model is called Lie model with IREP in the figures of results.

$$\begin{aligned}
\mathscr{L}_{v_e}(\sigma)^{ij} &= 2\mu d^{ij} + \lambda\, tr(\boldsymbol{d}) I^{ij}\\
&- 2\mu \frac{S^{rt}\left(2\sigma_r^{\ l} d_{tl} + 2\mu\, d_{rt} - \sigma_{rt}\, tr(\boldsymbol{d})\right)}{\sigma_{eff}^2(\frac{\partial\kappa}{\partial r} + 2\mu) + 2\sigma^{al} S^b_{\ l} S_{ab}} S^{ij}. \qquad (6.12)
\end{aligned}$$

- 3D projection of elastoplastic model with the Jaumann derivative and an irreversible hypoelastic part (Eq. 5.68). This model is called Jaumann model with IREP in the figures of results.

$$\mathscr{D}^J(\sigma)^{ij} = 2\mu d^{ij} + \lambda\, tr(\boldsymbol{d}) I^{ij} - \frac{4\mu^2\, S^{ab} d_{ab}}{\sigma_{eff}^2(\frac{\partial\kappa}{\partial r} + 2\mu)} S^{ij}. \qquad (6.13)$$

We can compare and analyze these three elastoplastic models through the results given by the calculation performed with these models. The models have been submitted to traction, gliding and to a loading/unloading cycle in gliding.

Fig. 6.6 presents the results obtained for traction for the three models and a maximal elongation of 300% in direction 1. The varying components of the deformation gradient and strain tensor $\boldsymbol{e}$ are presented on the top and middle figures. The stress in the first direction is presented in the bottom figure. In this kind of loading, even for very large deformations, it is not possible to distinguish the models. The difference of the results obtained by these three models is very small as it can be observed in the magnification of the bottom figure. Figs. 6.7 and 6.8 present the results given by the elastoplastic models for gliding with a small and large deformation respectively.Fig. 6.8 presents also a loading/unloading cycle in gliding. For the tangential component σ^{12}, all the models produce the same solution for all the cases. A stress-strain curve for σ^{12} is given in Annex F. It is not the case for the other components, for which significant differences are observed. For the stress component σ^{33}, the value is negative for the hypoelastic model constructed from the reference elastic model, positive for the irreversible model constructed with the Lie derivative and equal to zero for the model constructed with the Jaumann derivative. These differences are amplified for large deformations. The hypoelastic model constructed from the elastic model is the only one able to predict the elastic phase accurately, whatever the components. When unloading is considered, σ^{12} reaches zero and the deformation is prolonged until the material enters plasticity again. Differences appear in the stress components. At the unloaded stage ($\sigma^{12} = 0$), residual stresses exist in the material due to the constraining boundary conditions that are different. This is more important for σ^{33} for which the residual stress is either positive, zero or negative, depending on the models.

The difference in the results is mainly due to the model of the elastic part of the material. Indeed the model for plasticity is the same, but the results in plasticity are affected. Thus using an hypoelastic model that is not equivalent to the elastic model representing the material affects also the general elastoplastic results.

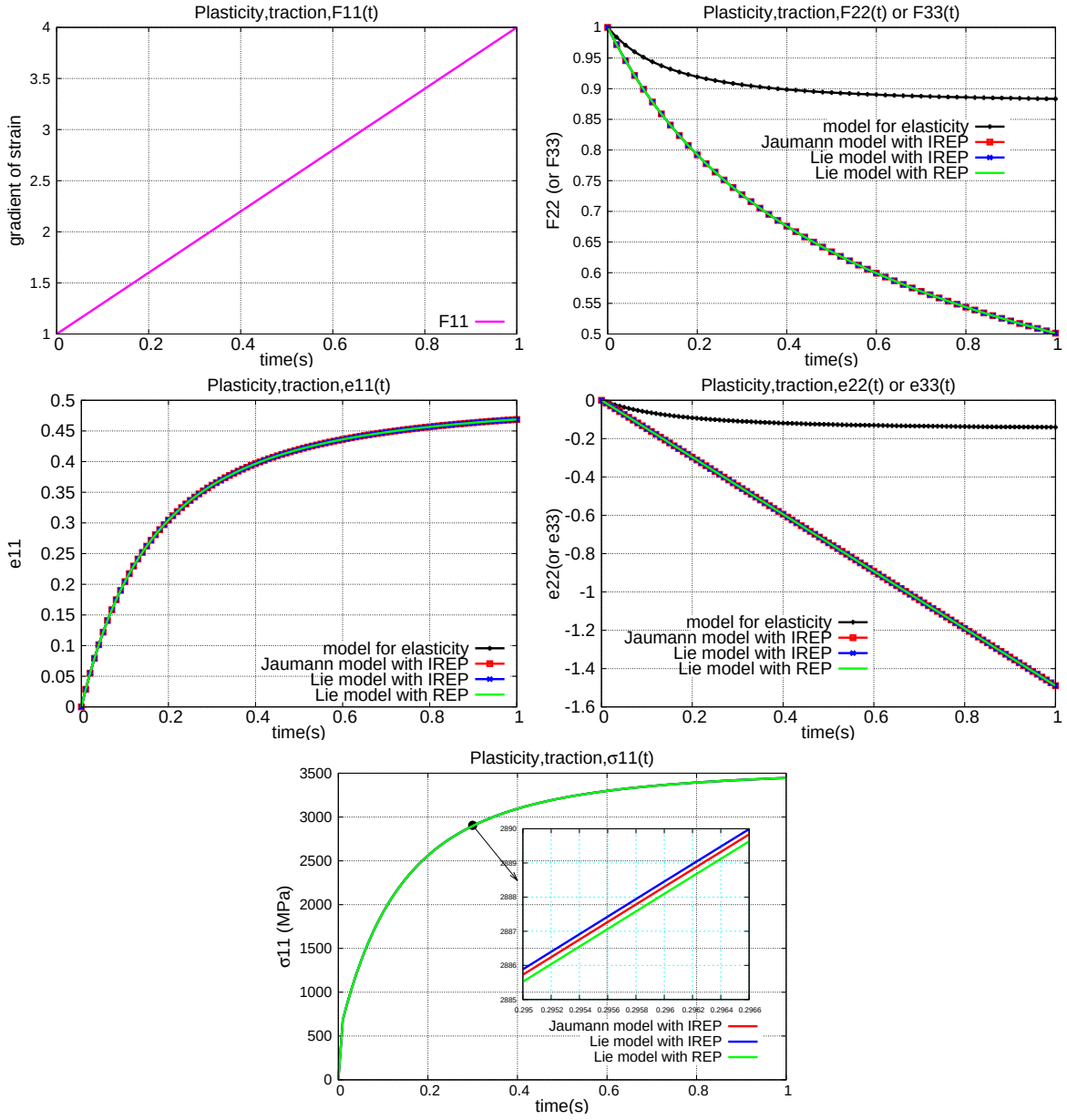

Figure 6.6: Varying components of the deformation gradient $\boldsymbol{F}$, strain tensor $\boldsymbol{e}$ and Cauchy stress tensor $\boldsymbol{\sigma}$ as a function of time for the traction of an elementary volume of reference for the hyperelastic model and the elastoplastic models listed in Section 6.2.3. The maximal elongation of the volume reaches 300% in direction 1.

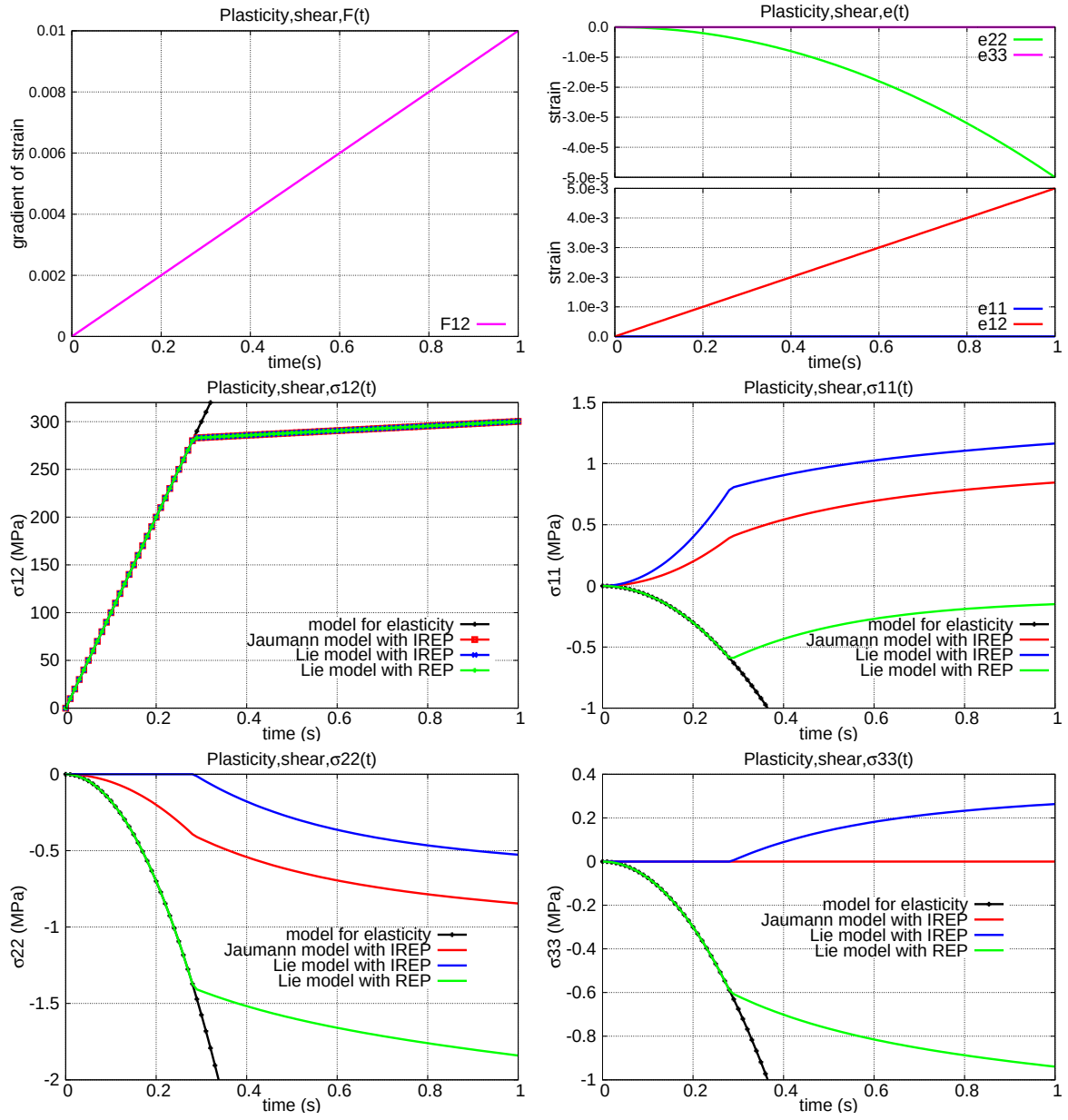

Figure 6.7: Varying components of the deformation gradient $\boldsymbol{F}$, strain tensor $\boldsymbol{e}$ and Cauchy stress tensor $\boldsymbol{\sigma}$ as a function of time for gliding and limited to small deformations reaching $b/a = 0.01$ as defined in Figure 6.1. The deformation is applied on an elementary volume of reference for all the elastoplastic models derived in Section 6.2.3. The solution obtained with the elastic model is also presented for comparison.

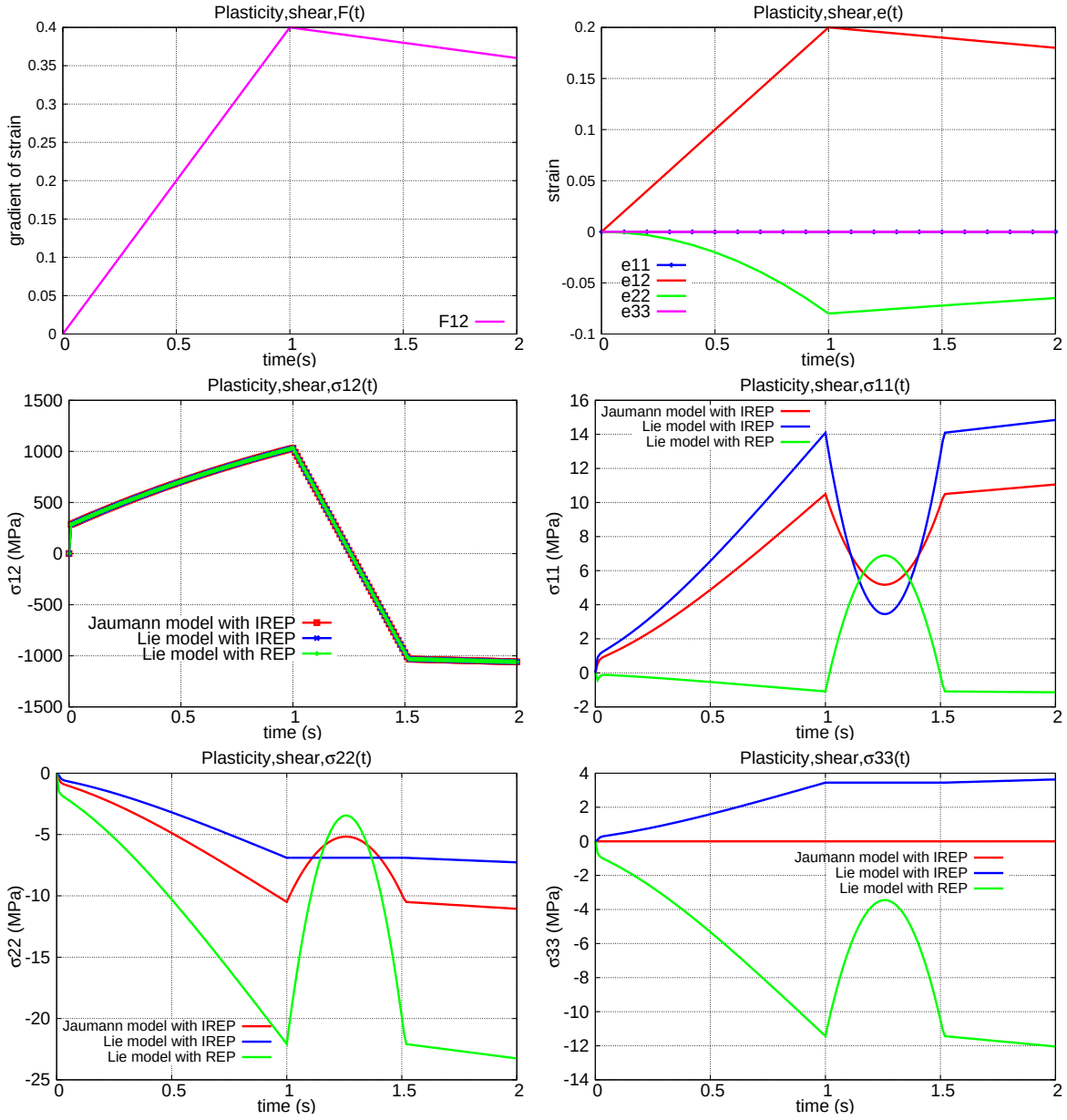

Figure 6.8: Varying components of the deformation gradient $\boldsymbol{F}$, strain tensor $\boldsymbol{e}$ and Cauchy stress tensor $\boldsymbol{\sigma}$ as a function of time for a loading/unloading cycle considering an important total deformation. The maximal value of b/a reaches 0.4 and is next lowered to 0.36 as defined in Figure 6.1.

6.3 Calculations with several elements meshed bar

Calculations of loaded structure with several elements mesh have been performed to compare the hypoelastic models (listed in Section 6.2.2) and elastoplastic models (listed in Section 6.2.3). A short bar that undergoes a torsion and a tensile is considered to study the hypoelastic models. All the calculations are performed at large deformation. After that, A beam that bends is calculated to study the elastoplastic models. The deformation will be small. The phenomenon of isotropic hardening during the deformation will be simulated and compared for the three elastoplastic models. The parameters of materials have been already given in Tab. 6.1 in the last section.

6.3.1 A brief study of element size

We consider a short bar that undergoes complex loadings, seeing Fig. 6.9. The short bar has a length of a and a rectangular transection with dimensions $b \times c$. We have: $a : b : c = 5 : 2 : 2$. The bar is meshed with a number of elements. The element type is 3D

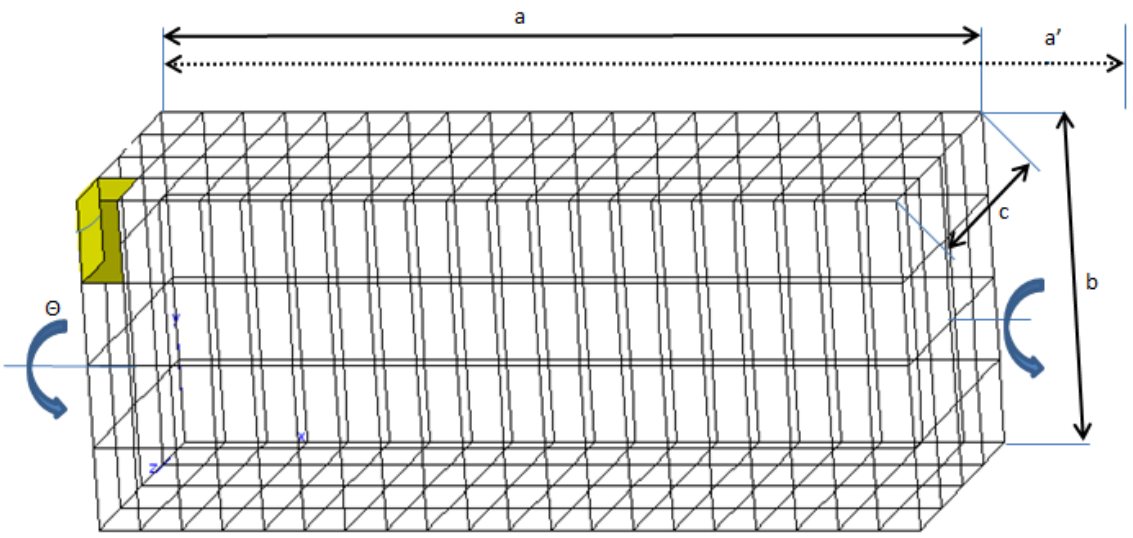

Figure 6.9: The mesh and the dimensions of the short bar used in the calculation combining torsion, tensile and unloadings with different hypoelastic models.

20-noded quadrilateral as often used in infinitesimal elastoplastic analysis [De Souza Neto et al., 2011], which is used with a 8-Gauss point (reduced) numerical integration rule.

The reduced integration is applied to avoid the phenomenon of volumetric "locking" near incompressibility conditions.

Before calculating the combination of the torsion and traction, a study of the size of the element is done. It is studied with the Lie model with REP. Just a torsion of the short bar is considered:

- $0 - 1s$. The bar is twisted of 90 degrees.
- $1 - 2s$. The torsion in the bar is unloaded.

The side along with the axis of rotation is divided into N parts, $N = 10, 20, 40, 80$. The other two sides are divided into 4 parts. The distribution of the component σ^{22} in the bar, when the torsion is unloaded, is showed in Fig. 6.10.

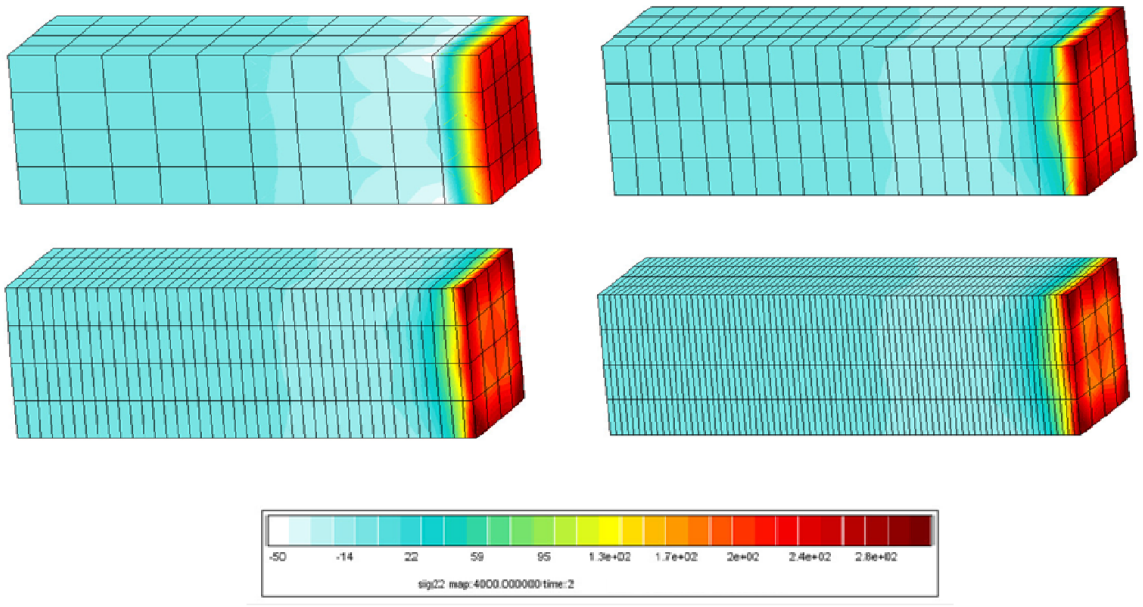

Figure 6.10: The distribution of values of components σ^{22} in the short bar when the the torsion is unloaded (at the moment $2s$). This calculation uses the Lie model with REP. The side along with the axis of rotation is divided into 10, 20, 40, 80 parts.

It is to study the influence of N to the result of simulation. Fig. 6.11 illustrate that with bigger number of N, the value of components σ^{22} converges. However, the time of calculation is proportional to the size of elements. In fact, 20 parts of the side (or 320

elements of the bar) are sufficient to compare the three hypoelastic models. Thus, taking consideration of both the cost and accuracy of the calculation, we use $N = 20$ in the calculation of combination of torsion and traction in the following section.

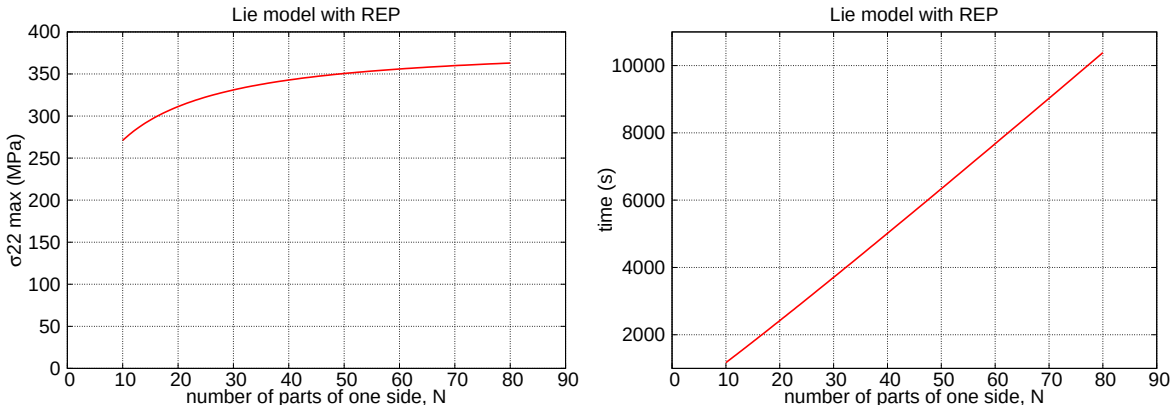

Figure 6.11: The study of convergence of the element size. Figures illustrate the error of one components of stress σ^{22} and the time of calculation in function of the number of parts in one side along with the axis of rotation.

6.3.2 Calculations of bar torsion and traction with hypoelastic models

The combination of complex loadings lasts 4 seconds:

- $0 - 1s$. The bar is twisted of 30 degrees.
- $1 - 2s$. The bar is stretched to a', and $a : a' = 5 : 6$.
- $2 - 3s$. The torsion in the bar is unloaded.
- $3 - 4s$. The tensile in the bar is unloaded.

The deformation of complex loadings is calculated with the three hypoelastic models (listed in Section 6.2.2). The elastic model is also used as the reference. Figs. 6.13, 6.14 and 6.15 present the distribution of the component σ^{11} in the bar. In each of these three figures, the top left presents the result calculated with the reference elastic model (Eq. 6.3). The other three present the results calculated with different hypoelastic models:

the Jaumann model with IREP (Eq. 6.10), the Lie model with IREP (Eq. 6.9) and the Lie model with REP (Eq. 6.8) respectively. These three figures present the results for different times of deformation of the bar: Fig. 6.13 is when the bar is fully twisted; Fig. 6.14 is when the bar is fully stretched, thus fully loaded; Fig. 6.15 is the moment when the deformation imposed in the egde of the bar returns to zero.

At first, we compare the top left and bottom right of each of the Figs. 6.13, 6.14 and 6.15. As expected, the reversible hypoelastic model constructed with the Lie derivative gives the same results as the elastic model. Because this hypoelastic model is derived from the reference elastic model.

Then, we compare all the four parts in each of the Figs. 6.13, 6.14 and 6.15. In Fig. 6.13, the results with irreversible hypoelastic models have already shown a great difference. For example, the maximum value of component σ^{11}, (σ^{11}_{max}), is in the element marked in yellow in Fig. 6.9. For the result of model for elasticity, $\sigma^{11}_{max}|_{model\ for\ elasticity}$ equals to $11500MPa$, while that of the Jaumann model with IREP and the Lie model with IREP have respectively the values $\sigma^{11}_{max}|_{Jaumann\ model\ with\ IREP} = 12880MPa$ and $\sigma^{11}_{max}|_{Lie\ model\ with\ IREP} = 13655MPa$ respectively. The Jaumann model with IREP exceeds 12% of the model for elasticity (or the Lie model with REP) and the Lie model with IREP exceeds 19%.

$$\begin{aligned} \frac{\sigma^{11}_{max}|_{Jaumann\ model\ with\ IREP} - \sigma^{11}_{max}|_{model\ for\ elasticity}}{\sigma^{11}_{max}|_{model\ for\ elasticity}} &= 0.12 \\ \frac{\sigma^{11}_{max}|_{Lie\ model\ with\ IREP} - \sigma^{11}_{max}|_{model\ for\ elasticity}}{\sigma^{11}_{max}|_{model\ for\ elasticity}} &= 0.19 \end{aligned}$$

The Lie model with IREP gives a worse result than the Jaumann model. In Fig. 6.14, the difference between the four models becomes greater. The Jaumann model with IREP exceeds 26% to the model for elasticity (or the Lie model with REP) and the Lie model with IREP exceeds 49%. The Lie model with REP gives a slight residual stress $\sigma^{11}_{residual}|_{Lie\ model\ with\ REP} = 6.7MPa$, which is the accumulated error because of the discretization by finite elements and the integration step [Belytschko et al., 2000]. This error can be reduced by smaller time discretization, seeing Fig. 6.12. Thus, the Lie model with REP can give a reversible result for its elastic part. As for the irreversible hypoelastic models, the Jaumann model with IREP and the Lie model with IREP, the residual stress are

$\sigma^{11}_{residual}|_{Jaumann\ model\ with\ IREP} = 135.2MPa$ and $\sigma^{11}_{residual}|_{Lie\ model\ with\ IREP} = 633.5MPa$ respectively, which can not be diminished much even with smaller time discretization when integrated, seeing Fig. 6.12. To finish the calculation, it needs $1.25 \times 10^5 s$ for Lie model with REP, $1.09 \times 10^5 s$ for Lie model with IREP and $1.09 \times 10^5 s$ for Jaumann model with IREP, when the time discretization is $1/20000s$. To obtain an accurate result, the Lie model with IREP does not scarify much time in calculation comparing the other two models.

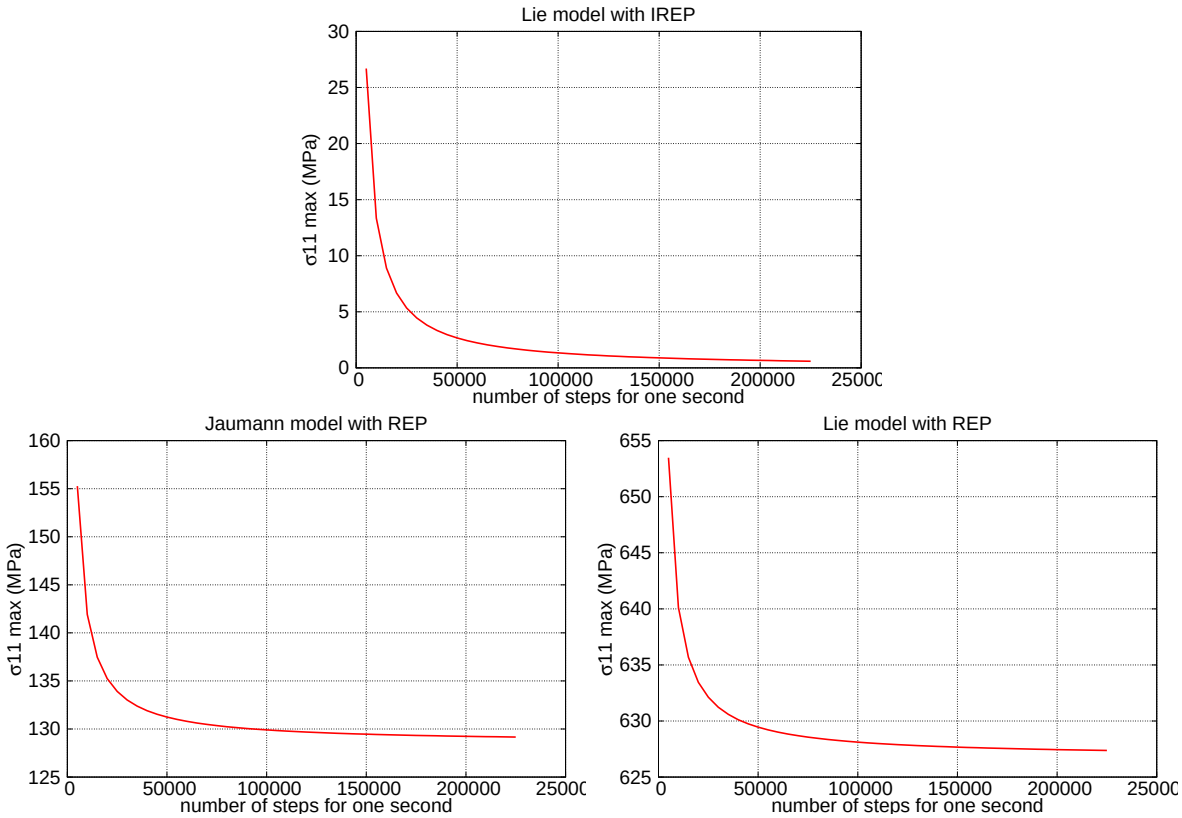

Figure 6.12: The study of convergence of the time discretization of the three elastoplastic models. Figures illustrate the error of one components of residual stress $\sigma^{11}_{residual}$ in function of the number of time steps n. The time discretization can be calculated as $\Delta t = 1/n\ s$

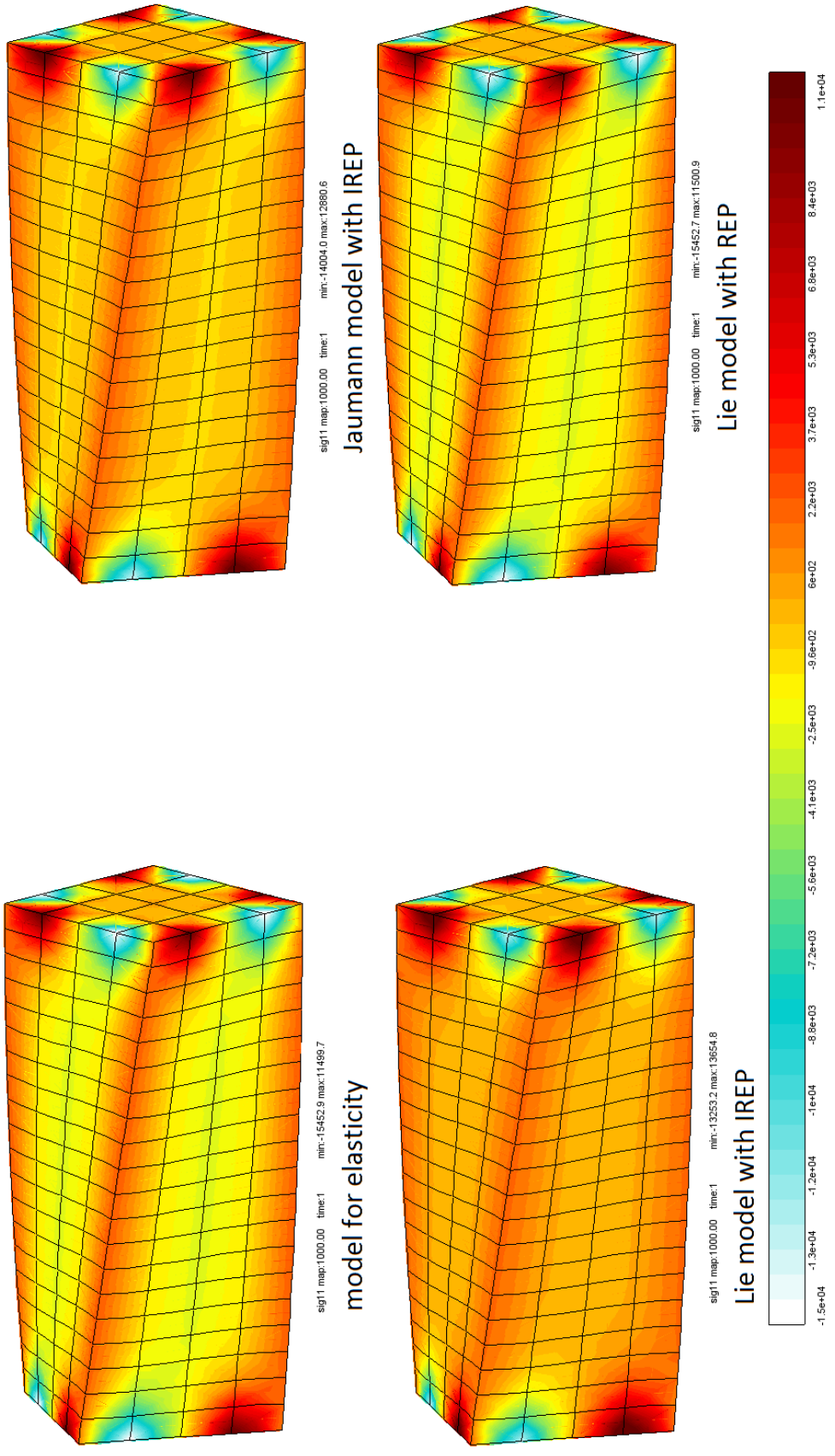

Figure 6.13: The distribution of values of components σ^{11} in the short bar when the torsion is fully loaded (at the moment $1s$). This calculation uses the elastic model as a reference and three hypoelastic models listed in Section 6.2.2.

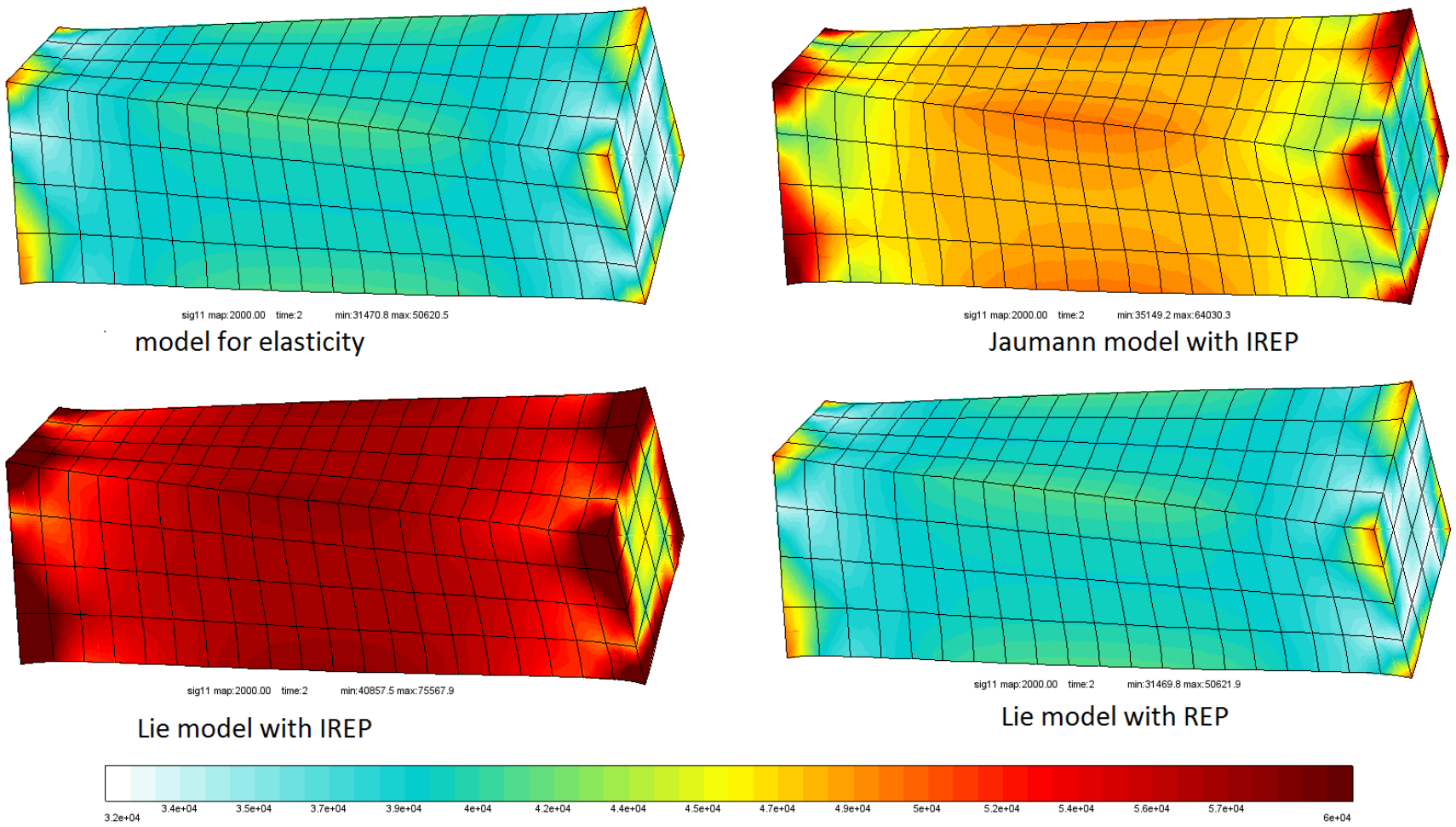

Figure 6.14: The distribution of values of components σ^{11} in the short bar when the the tensile is fully loaded (at the moment $2s$). This calculation uses the elastic model as a reference and three hypoelastic models listed in Section 6.2.2.

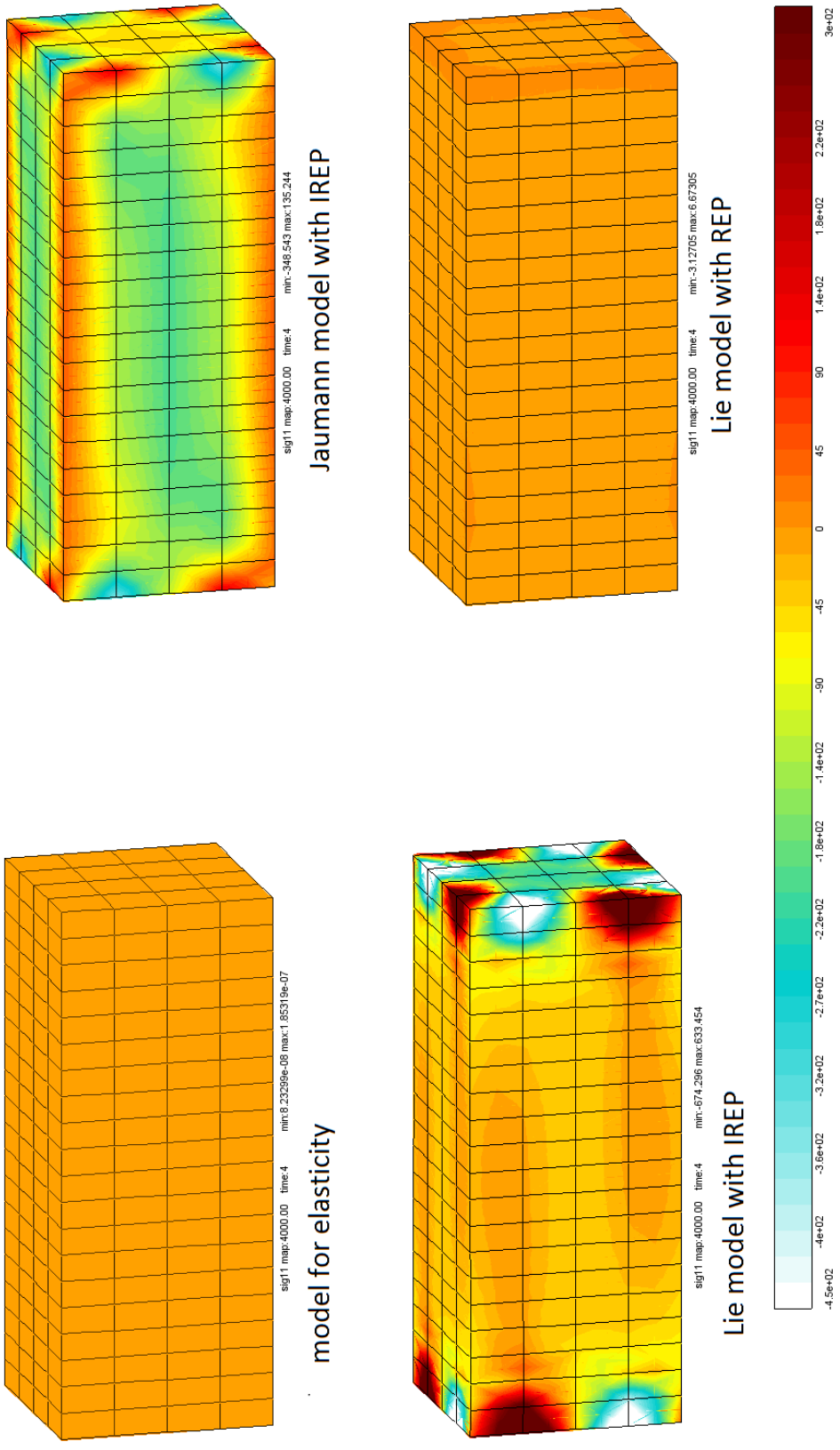

Figure 6.15: The distribution of values of components σ^{11} in the short bar when unloaded (at the moment $4s$). This calculation uses the elastic model as a reference and three hypoelastic models listed in Section 6.2.2.

6.3.3 Calculations of bar bending with elastoplastic models

After the short bar undergoes a torsion and tensile, let us consider a beam (see Fig. 6.16) that bends downwards at first and then bends back upwards. The beam has a length of a and a rectangular section with dimension $b \times c$. We have: $a : b : c = 20 : 1 : 1$. The bar is meshed with 320 20-noded quadrilateral reduced elements.

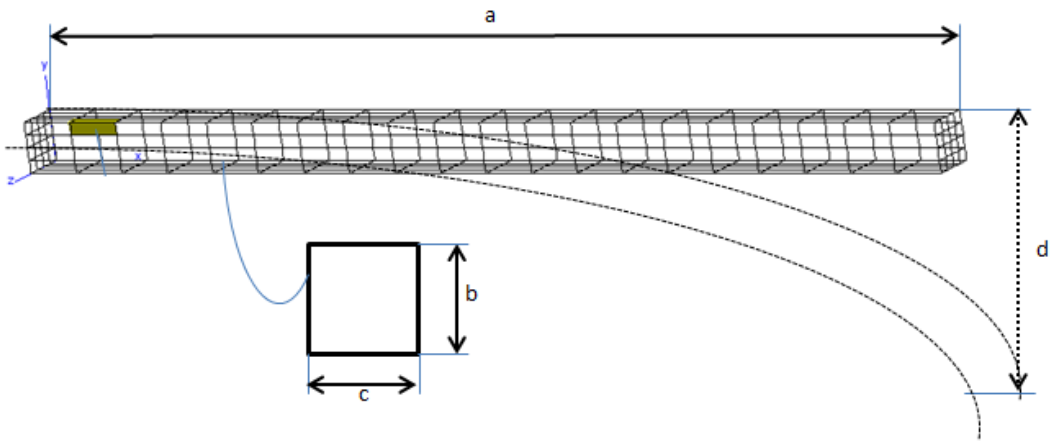

Figure 6.16: The mesh and the dimensions of the beam used in the calculation of bending with different elastoplastic models.

The bending lasts 2 seconds:

- $0 - 1s$. The bar bends downwards so that $d : a = 5 : 10$.
- $1 - 2s$. The bar bends back upwards so that $d : a = 3 : 10$

This calculation is performed with three elastoplastic models, listed in Section 6.2.3. Figs. 6.17, 6.18 and 6.19, presents the distribution of the r value in the bar. The r value is the cumulated plastic strain, which is introduced in Section 5.3.2. This variable enables to study the phenomenon of isotropic hardening. When r equals to zero, or remains constant (unloading) the deformation of the region is elastic. The value of r increases when the isotropic hardening is cumulated.

Fig. 6.17 presents the distribution of the value r in the bar calculated with the Lie model with REP (Eq. 6.11) at different times during the deformation. In the beginning,

the bar is free of deformation (Fig. 6.17(1)). Then, with increments of deformation, the plasticity begins at $0.056s$ (Fig. 6.17(2)) with the maximum value in the bar 3.27×10^{-5} for r value, which can be found in the element marked in yellow in Fig. 6.16. After the plasticity begins, the isotropic hardening continues to increase until the bar bends to its maximum distance in the bottom (Fig. 6.17(3)) at $1s$. The maximum value of r in the bar is 0.095. At the same time, the bar begins to bend upwards, thus the deformation is elastic. At $1.425s$, the plasticity occurs again (Fig. 6.17(4)) with the maximum value in the bar 0.095. At last, the bar finishes its deformation at $2s$ (Fig. 6.17(5)) with the maximum value in the bar 0.106. From the moment of $0.056s$ to $1s$, the isotropic hardening varies from 0 to 0.095. In addition, from the moment of $1.425s$ to $2s$, the isotropic hardening accumulates from 0.095 to 0.106. This result of calculation is consistent with the phenomenon of isotropic hardening. Before the moment of $1s$, the isotropic hardening cumulates. After the moment of $1.425s$, the isotropic hardening cumulates again. As long as the bar reaches the domain of plasticity, it is hardened. In fact, all the calculation with the elastoplastic models simulate well this phenomena.

Fig. 6.18 presents the comparison of the r value in the bar when r firstly turns to non-zero. This moment is used to study the beginning of the plasticity. It is calculated with the different elastoplastic models listed in Section 6.2.3, the Jaumann model with IREP (Eq. 6.13), the Lie model with IREP (Eq. 6.12) and the Lie model with REP (Eq. 6.11). The plasticity begins at the same time, at $0.056s$, for the three models. However, the values r are not exactly the same for these three, 2.98×10^{-5} for the Jaumann model with IREP, 3.12×10^{-5} for the Lie model with IREP and 3.37×10^{-5}. This difference is small. In term of expression, the difference between the three models is only their elastic parts. Therefore, when the elastic deformation is very small, the three models lead to similar results of calculation.

Fig. 6.19 presents the comparison of the value r in the bar in the moment when r begins to increase. This moment is used to study the restart of the plasticity for the three elastoplastic models. The restart moment of plasticity for the three models are not exactly the same, $1.424s$ for the Jaumann model with IREP, $1.423s$ for the Lie model with IREP and 1.425 for the Lie model with REP. The values r are respectively 0.0953

for the Jaumann model with IREP, 0.0953 for the Lie model with IREP, 0.0952 for the Lie model with REP. The difference is still small but bigger than that at the moment 0.056. That's because the elastic deformation increases as well as the yielding limit, during the increase of elastoplastic deformation. The bar needs more elastic deformation to be yielded when bending downwards than it does when bending upwards. From the results of simulation, it is noticeable that the elastic deformation in Fig. 6.19 is larger than that in Fig. 6.18. Comparing Figs. 6.18 and 6.18, we can conclude that with the larger deformation, the difference between these three elastoplastic models becomes larger. However, this difference is not as important as in Fig. 6.8.

The calculation with the elastoplastic models performed so far do not illustrate a great difference. However, elastic part of the three models give an evident difference when the deformation is large enough, seeing the example of torsion and tensile with the hypoelastic models. Further study can be orientated to the case that the elastoplastic deformation has a large elastic part. This kind of simulation can be performed for unrealistic material, elastomer-like or polymer-like materials.

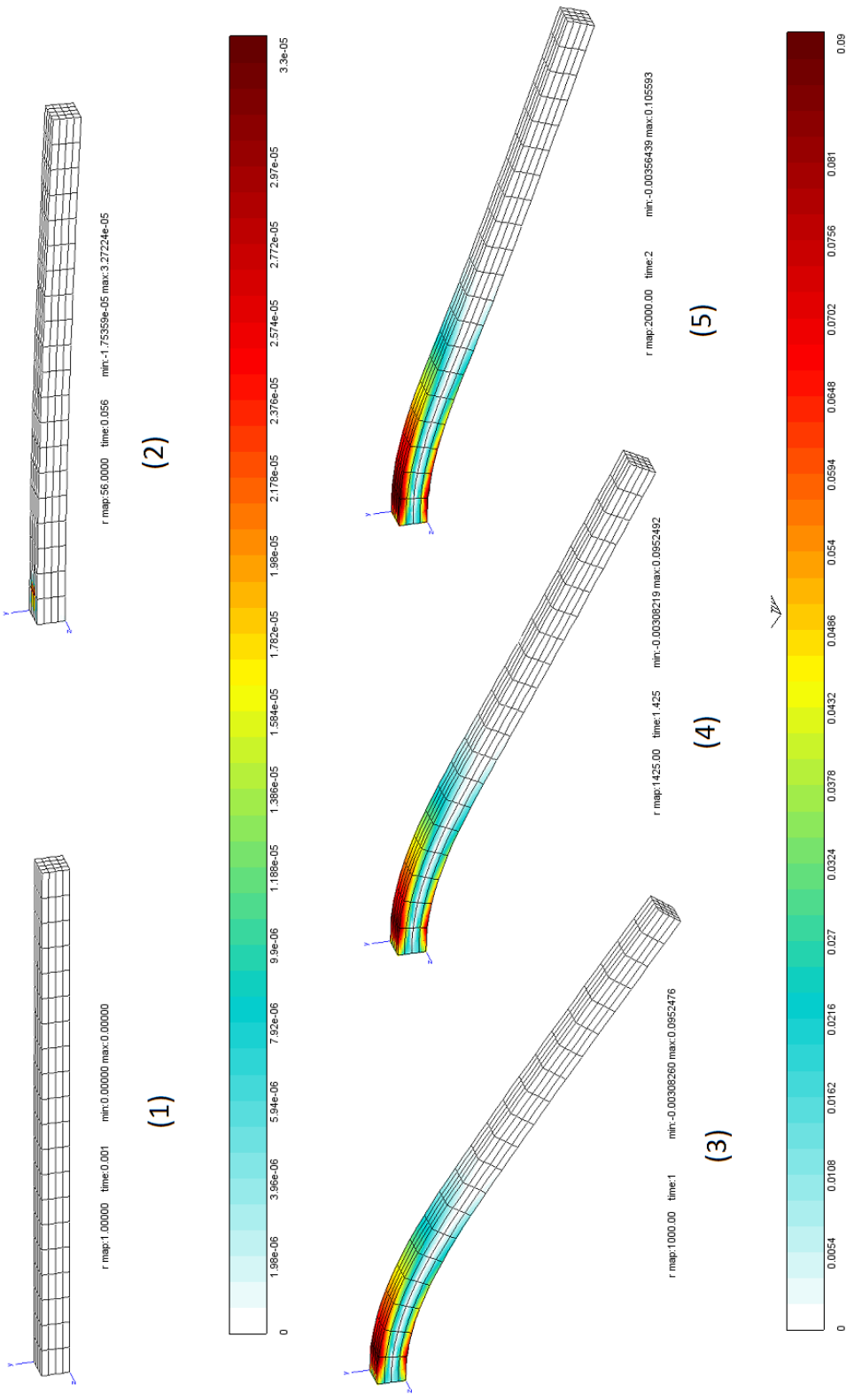

Figure 6.17: The distribution of values of r in the beam in different moments during the deformation. (1) Initial state, (2) beginning of plasticity, (3) end of the bending downwards then start of the bending upwards, (4) restart of plasticity, (5) end of the bending upwards. The elastoplastic model used in this calculation is the Lie model with REP (Eq. 6.11).

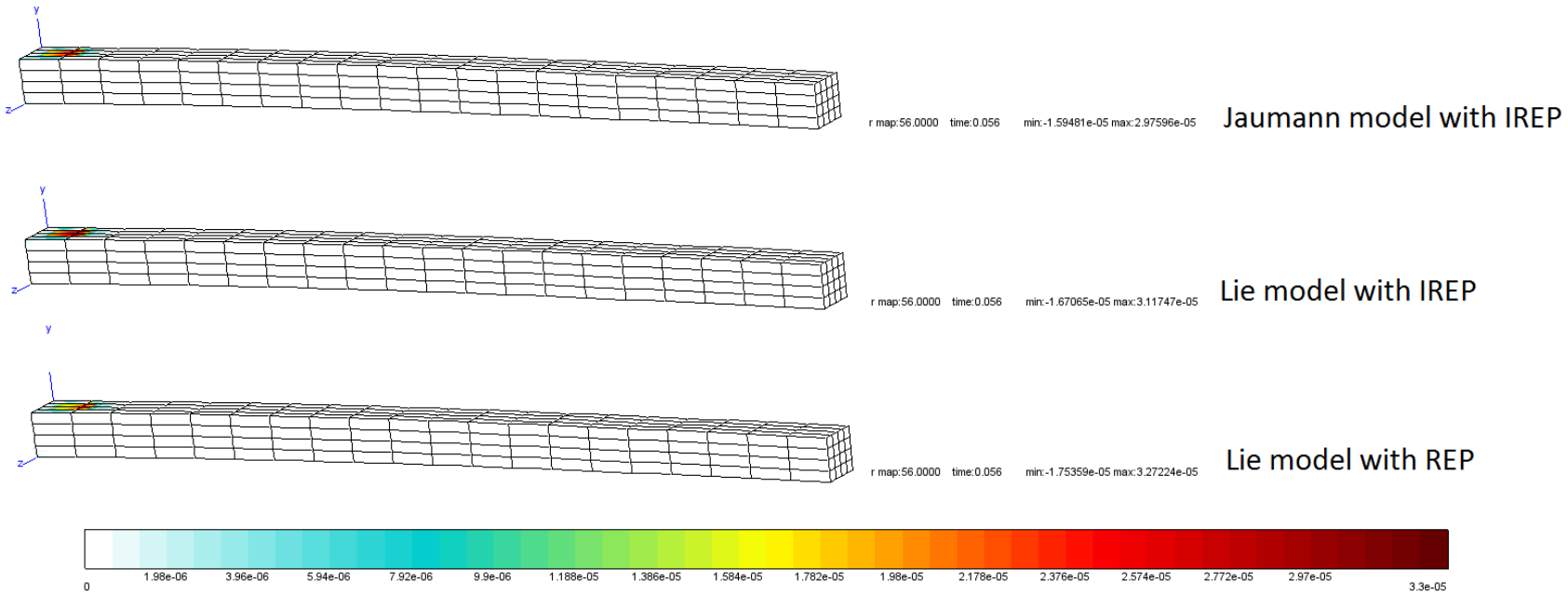

Figure 6.18: The distribution of values of r in the beam in the moment when the plasticity begins during the bending downwards of the bar. It is calculated with the three elastoplastic models listed in Section 6.2.3.

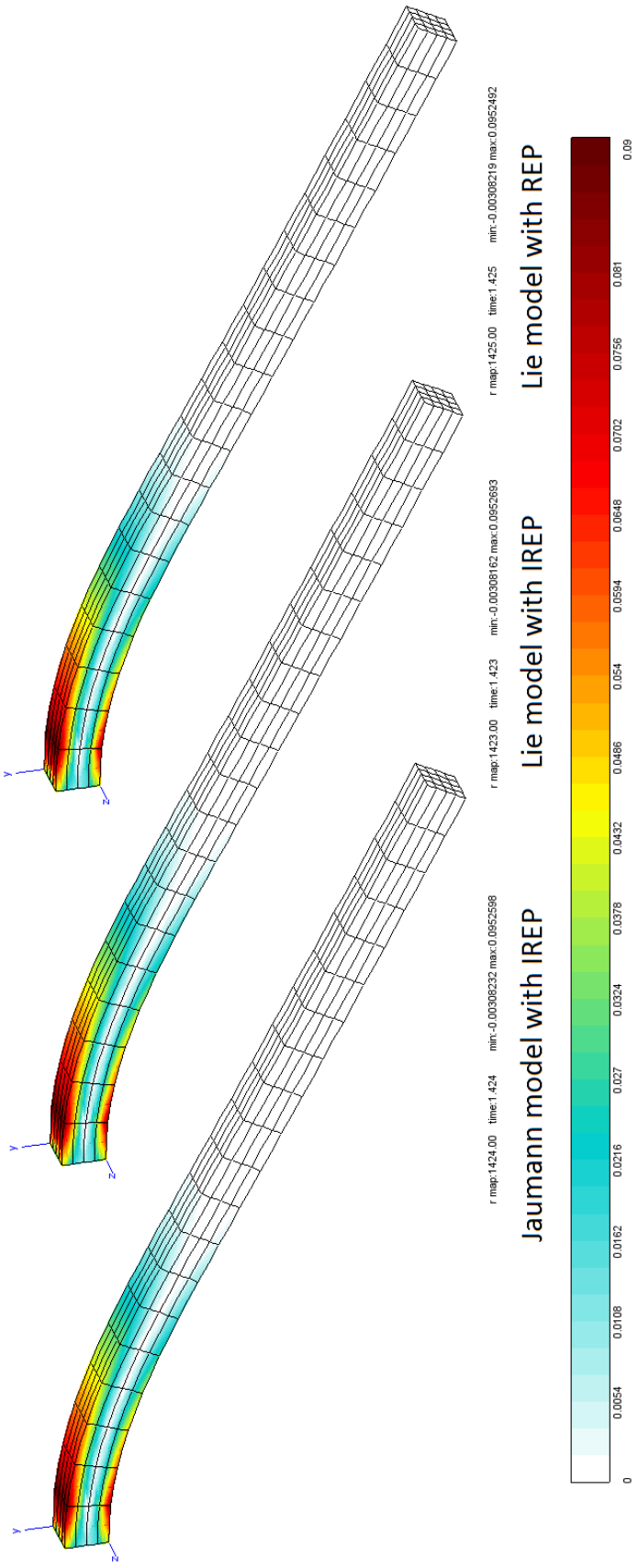

Figure 6.19: The distribution of values of r in the beam in the moment when the plasticity restarts during the bending back upwards of the bar. It is calculated with the three elastoplastic models listed in Section 6.2.3.

6.4 Conclusions

The 3D projection of 4D constitutive models can be applied for the simulation of elastic and elastoplastic deformations. Numerical simulations of one element and fine meshed elements have been carried out with the models for elasticity, hypoelasticity and elastoplasticity.

The linearity of the elastic models has been verified for complex loading paths and deformation scales in one element. The simulation of complex loading paths in one element illustrates the equivalence between the reversible hypoelastic models constructed with the Lie derivative and the Hookean-like elastic model. The irreversibility of the three models are also illustrated by the simulation in one element. When the imposed deformation returns to zero, there should be no stress remaining in the material. Among the three models, only the Lie model with REP succeed in modeling this phenomena. The other hypoelastic models constructed with the Jaumann transport and the Lie derivative leads to differences to the reference elastic model. The larger the deformation is, the larger the difference between the three hypoelastic models are. Therefore, the numerical simulation for metal materials observe a small difference, because the elastic deformation for these kinds of material is comparatively small. However, the difference can be highlighted by the numerical simulations for polymers or biomaterials, whose elastic deformation can reach a large scale. The simulation of gliding in one element is performed to compare the three elastoplastic models. The difference between the three models lies in the their elastic parts. Thus they will show a larger difference in the results of simulation, when elastic deformation gets larger.

The same conclusion can be drawn from the simulation of several elements meshed bar with different hypoelastic and elastoplastic models. The simulation performed with Lie model with REP fits the Hookean-like model while the other two do not. The larger the elastic deformation is, the larger difference between the three models have, both in the simulation of elasticity and plasticity. Besides, the simulation of several elements also illustrates that the reversibility of the Lie model with REP costs amount of time of calculation. To finish the same simulation, the Lie model with REP costs more than 15%

time than the other two. This surmount of time is valuable only when the difference of the models is really large. In other words, the most suitable case where Lie model with REP is applied, is that the elastic deformation is relatively large, e.g. elastomers, biomaterials, high-yielding metals etc. when an accurate result is needed.

Conclusions and perspectives

Conclusions

In this thesis, a fully covariant four-dimensional description of large deformations of materials has been proposed, considering the classical hypotheses of Newtonian physics and using the mathematical framework of differential geometry.

The problems of objectivity, in particular the choice of objective transports, to which the 3D formalism faces, can be solved with the use of a 4D formalism. Within the 4D formalism, the principle of covariance ensures the indifference of all physical quantities, laws and equations with respect to any change of observers. The 3D notion of frame-indifference can be distinguished from the principle of indifference with respect to the superposition of rigid body motions. It also enables to define a derivative with respect to time, the Lie derivative, which is not only covariant, but also indifferent with respect to the superposition of rigid body motions. Thus, it can be used to construct 4D rate-form constitutive models.

Following the framework of Eckart [Eckart, 1940] and Grot and Eringen [Grot and Eringen, 1966], a tentative study of the 4D thermodynamics has been proposed. In this 4D description of thermodynamics, the 4D conservations of particles, momentum-energy and the 4D inequality of Clausius-Duhem have been developed. Then, an original choice of decompositions of momentum-energy tensor enables to couple kinematics and stress to construct constitutive models.

Covariant constitutive models for hyperelasticity, anisotropic elasticity, hypoelasticity and elastoplasticity are developed. A nonlinear second-order hyperelastic model has been also derived with a thermodynamic approach. In analogy with the 3D Hookean elastic

model, 4D linear constitutive models for elasticity have been first developed. Anisotropic elastic models and hypoelastic models have been constructed, taking the 4D Hookean-like elastic model as a reference. For the 4D elastoplastic models, the rate of deformation has been decomposed into an elastic part and an plastic part additively. The models for the elastic part are the hypoelastic models. The model for the plastic part have been derived from the 4D thermodynamics considering dissipations, leading to a 4D flow theory for plasticity.

All the proposed 4D constitutive models are projected into 3D in order to be implemented into a finite element code. The finite element analysis is performed with Zset© software. Simple loadings on one point have been first performed for different elastic models, hypoelastic models and elastoplastic models. The models proposed in this work have been compared to existing 3D models. The results of the calculation illustrate the interest of the Lie derivative and the reversibility of the hypoelastic model developed with this operator.

The 4D formalism is validated in developing covariant constitutive models for large deformations of materials in this thesis. Mathematical modeling and numerical simulations illustrate the possibility of constructing physically meaningful models for hyperelasticity, hypoelasticity and elastoplasticity within the framework of 4D formalism, and thermodynamics.

Perspectives

The 3D projection of the developed 4D constitutive models for hypoelastic and elastoplastic materials can be studied further. As differences occur between these models, the interest of further research will lie in the comparison of the performances of models in complex loadings and geometries and the evaluation of the consistence with the results of experiments. As the reversible model developed with the Lie derivative shows its advantages in large elastic deformation, these models may be used for the simulation of the deformation of polymers and biomaterials.

The systematic method of developing 4D constitutive models in this thesis may be

applied further in developing generalized models for any type of material behaviors. With this 4D approach, new theoretical models, which are covariant and physically meaningful, would be obtained. Using the Lie derivative, 4D rate-dependent models may be developed, such as 4D models for viscoelasticity, viscoplasticity inspired by the work of [Lemaitre and Chaboche, 1994; Wineman, 2009; Marques and Creus, 2012; Bertram, 2012] within a 3D formalism. In developing these rate-dependent models, 4D thermodynamics should be adapted in order to take into account the dissipation terms of viscosity. Also, with the distinction of covariance and indifference with respect to the superposition of rigid body motions, 4D models for phenomena, of which the behavior depends on the superposition of rigid body motions, may be studied in the future.

As for the finite element method, a simultaneous discretization of space and time is possible; this method is called space-time finite-element method (STFEM). Four-dimensional numerical integration schemes have been proposed in a mathematical context and not only for relativistic physics [Oden, 1969b; Oden, 1969a; Tremblay et al., 2003; Collino et al., 2006]. It has been shown that the quality of the results depends strongly on the structure of the space-time elements. Moreover, this STFEM has proven its efficiency and strength for classical mechanics. The results are more accurate and the computing time decreases; the improvement might be significant [Anderson and Kimn, 2007; Adélaïde et al., 2003a; Adélaïde et al., 2003b]. In addition, there are still problems to solve, especially in the context of a four-dimensional formalism applied to mechanical phenomena. Most of these methods use a 4D integration scheme but not a 4D description of the physics (that is, with 4D tensors). It could be interesting to rewrite the integration scheme using the Lie derivative and to develop a fully coupled covariant 4D finite element solver. In a consequence, innovative numerical tools will be developed, so that the numerical simulation of the forming processes will be more efficient and accurate.

Appendix A

Illustration of the principle of covariance in Chapter 2

A.1 Illustration with a rigid body motion

To illustrate the fact that the 4D change of coordinates is equivalent to a change of 3D frame of reference, it is proposed to evaluate the velocity of a point included in a rigid body that undergoes a rigid body motion with respect to an inertial frame of reference. The velocity of the body is evaluated in the inertial coordinate system ζ^μ and in the coordinate system ξ^μ attached to the body, both with the 3D and 4D approaches. The rigid motion has been chosen as an illustrative example because it is, clearly, correlated to 3D changes of frames.

A.1.1 Translation in the 3D approach

When a change of coordinates is defined through a body motion, it is necessary to distinguish, on one hand, the description of the motion itself, a translation here, such that:

$$z^i = Z^i + l^i, \tag{A.1}$$

where z^i is the current position of the body expressed as a function of Z^i the initial position of the body (described here in the same 3D coordinate system). On the other

hand, the 3D change of coordinates is defined as:

$$z^i = x^i + l^i, \tag{A.2}$$

where the same event is described with the coordinates z^i in the inertial frame and x^i in the moving frame. The 3D velocity in the inertial frame is then given by:

$$v^i = \dot{z}^i = \dot{l}^i. \tag{A.3}$$

Within the moving frame, the components of the 3D velocity are strictly speaking not defined, but it is possible to evaluate $\dot{x}^i$, corresponding to the components of the velocity of a point belonging to the rigid body with respect to the moving frame. In the considered case, these are expected to be equal to zero for each material point of the body. This cannot be deduced from a 3D direct and objective change of coordinates. It makes of the 3D velocity a non-objective quantity.

A.1.2 A translation in the 4D approach

The components U^μ of the four-velocity in the inertial frame are (from Eq. 2.14 and A.3):

$$U^\mu = \frac{dz^\mu}{ds} = \left(\frac{\dot{l}^i}{c\sqrt{1-\frac{\dot{l}^2}{c^2}}}, \frac{1}{\sqrt{1-\frac{\dot{l}^2}{c^2}}} \right). \tag{A.4}$$

Because the four-velocity is a 4D vector, it is thus frame-indifferent and it is possible to find its components u^μ in the moving coordinate system with the 4D change of coordinates:

$$\begin{cases} x^i = (z^i - l^i) \\ x^4 = z^4 = ct \end{cases} \tag{A.5}$$

and (from Eq. 2.17):

$$\frac{\partial x^\mu}{\partial z^\nu} = \begin{pmatrix} 1 & 0 & 0 & -\dot{l}^1/c \\ 0 & 1 & 0 & -\dot{l}^2/c \\ 0 & 0 & 1 & -\dot{l}^3/c \\ 0 & 0 & 0 & 1 \end{pmatrix}. \tag{A.6}$$

To find with Eq. 2.10:

$$\begin{cases} u^i = 0 \\ u^4 = U^4 = \frac{1}{\sqrt{1-\frac{\dot{l}^2}{c^2}}} \end{cases} \tag{A.7}$$

A.1.3 General body motion

Now consider a general body motion with a translation $\boldsymbol{l}$ and a rigid rotation $\boldsymbol{Q}$ such that:

$$z^i \;=\; Q^i{}_j Z^j + l^i. \tag{A.8}$$

Following the same definitions and derivation steps as for the translation above, the 3D velocity in the inertial frame is then given by:

$$v^i \;=\; \dot{z}^i = \dot{Q}^i{}_j x^j + Q^i{}_j \dot{x}^j + \dot{l}^i = \dot{Q}^i{}_k Q^k{}_j (z^j - l^j) + \dot{l}^i, \tag{A.9}$$

with $\dot{x}^i = 0$ for any points belonging to the rigid body. The four-velocity in the inertial frame is given by Eq. 2.14 where v^2 is the square of the 3D speed that can be computed from Eq. A.4. The components of the four-velocity in the moving coordinate system become (applying Eqs. 2.14 and 2.10 with Eq. A.9, using the fact that $v^i = \dot{Q}^i{}_j x^j + \dot{l}^i$, $z^i = Q^i{}_j x^j + l^j$ and noting that $Q^i{}_k \dot{Q}^k{}_j = -\dot{Q}^i{}_k Q^k{}_j$:

$$\begin{cases} u^i = \frac{1}{c\sqrt{1-\frac{v^2}{c^2}}} \left(Q^i{}_j v^j + \dot{Q}^i{}_j z^j - \frac{d(Q^i{}_j l^j)}{dt} \right) = 0 \\ u^4 = U^4 \end{cases} \tag{A.10}$$

Thus, applying the change of coordinates of the 4D space-time to the four-velocity (Eq. A.10), it has been demonstrated that the spatial components of the four-velocity are strictly zero in the moving frame. It is also clear from this example that the components of the four-velocity carry the rigid body motion of the frame, even when expressed in that moving frame, through the intervention of the fourth component in the change of coordinates (U^4 in Eq. A.10). This makes of the four-velocity a frame-indifferent quantity in the sense that it can be also expressed in any non-inertial frames of reference through an adapted change of coordinates. It appears from the example of the velocity that 3D non-objective tensors including a time rate become frame-indifferent in 4D. Eqs. A.8 and A.10 also imply that the components of the four-velocity depend on the considered rigid body motion. Thus, although it is frame-indifferent, the four-velocity is not indifferent to the rigid body motion superposition.

Appendix B

Details of calculations corresponding to Chapter 3

B.1 Calculation of $T^{\mu\nu}u_\mu$

We have the result:

$$u^\mu u_\mu = 1, \tag{B.1}$$

and

$$(\delta^\mu{}_\alpha - u^\mu u_\alpha)u_\mu = u_\alpha - u^\mu u_\mu u_\alpha = u_\alpha - u_\alpha = 0. \tag{B.2}$$

Remember that:

$$q^\mu = (\delta^\mu{}_\alpha - u^\mu u_\alpha)T^{\alpha\beta}u_\beta \tag{B.3a}$$

$$T^{\mu\nu}_\sigma = (\delta^\mu{}_\alpha - u^\mu u_\alpha)(\delta^\mu{}_\beta - u^\mu u_\beta)T^{\alpha\beta}, \tag{B.3b}$$

then we can calculate out following results:

$$T^{\mu\nu}_{kin}u_\nu = \rho_r c^2 u^\mu u^\nu u_\nu = \rho_r c^2 u^\mu \tag{B.4a}$$

$$\begin{aligned} T^{\mu\nu}_q u_\nu &= q^\mu u^\nu u_\nu + q^\nu u^\mu u_\nu = q^\mu + \left((\delta^\nu{}_\alpha - u^\nu u_\alpha)T^{\alpha\beta}u_\beta\right)u_\nu \\ &= q^\mu + \left((\delta^\nu{}_\alpha - u^\nu u_\alpha)u_\nu\right)T^{\alpha\beta}u_\beta = q^\mu \end{aligned} \tag{B.4b}$$

$$T^{\mu\nu}_\sigma u_\nu = (\delta^\mu{}_\alpha - u^\mu u_\alpha)\left((\delta^\nu{}_\beta - u^\nu u_\beta)u_\nu\right)T^{\alpha\beta} = 0. \tag{B.4c}$$

Then

$$T^{\mu\nu}u_\nu = T^{\mu\nu}_{kin}u_\nu + T^{\mu\nu}_q u_\nu + T^{\mu\nu}_\sigma u_\nu = \rho_r c^2 u^\mu + q^\mu. \tag{B.5}$$

If $q^\mu = 0$, we have the expression for Landau description:

$$T^{\mu\nu}u_{L\nu} = \rho_L c^2 u_L^{\ \mu}. \tag{B.6}$$

If not, this is the expression for Eckart description:

$$T^{\mu\nu}u_{E\nu} = \rho_E c^2 u_E^{\ \mu} + q^\mu. \tag{B.7}$$

B.2 Calculations for the conservation of momentum energy

We want to obtain the following equation:

$$\nabla_\nu(\rho_r c^2 u^\nu) + \nabla_\nu q^\nu = q^\mu(u^\nu\nabla_\nu u_\mu) + (\sigma^{\mu\nu} - \sigma^{\mu\alpha}u_\alpha u^\nu - \sigma^{\nu\beta}u_\beta u^\mu + \sigma^{\alpha\beta}u_\alpha u_\beta u^\mu u^\nu)d_{\mu\nu}, \tag{B.8}$$

from the conservation of momentum energy along a four velocity:

$$u_\mu\nabla_\nu T^{\mu\nu} = \nabla_\nu\left(T^{\mu\nu}u_\mu\right) - T^{\mu\nu}\nabla_\nu u_\mu = 0. \tag{B.9}$$

From Eq. B.5, I repeat that

$$T^{\mu\nu}u_\nu = \rho_r c^2 u^\mu + q^\mu. \tag{B.10}$$

Thus, we have the expression for one term $\nabla_\nu\left(T^{\mu\nu}u_\mu\right)$:

$$\nabla_\nu\left(T^{\mu\nu}u_\mu\right) = \nabla_\nu(\rho_r c^2 u^\nu) + \nabla_\nu q^\nu. \tag{B.11}$$

For the term $T^{\mu\nu}\nabla_\nu u_\mu$, we should at first consider the fact that

$$u_\mu\nabla_\nu u^\mu + u^\mu\nabla_\nu u_\mu = \nabla_\nu(u^\mu u_\mu) = \nabla_\nu 1 = 0. \tag{B.12}$$

The covariant derivative can be shifted with the metric to change the variance:

$$u_\mu\nabla_\nu u^\mu = u_\mu\nabla_\nu(g^{\mu\alpha}u_\alpha) = u_\mu g^{\mu\alpha}\nabla_\nu u_\alpha = u^\alpha\nabla_\nu u_\alpha. \tag{B.13}$$

From Eqs.B.12 and B.13, we have

$$u_\mu\nabla_\nu u^\mu = u^\mu\nabla_\nu u_\mu = 0. \tag{B.14}$$

We can thus continue to simplify the calculation:

$$T^{\mu\nu}_{kin}\nabla_\nu u_\mu = \rho_r c^2 u^\nu u^\mu \nabla_\nu u_\mu = 0 \tag{B.15a}$$

$$T^{\mu\nu}_{q}\nabla_\nu u_\mu = q^\mu u^\nu \nabla_\nu u_\mu + q^\nu u^\mu \nabla_\nu u_\mu = q^\mu u^\nu \nabla_\nu u_\mu \tag{B.15b}$$

$$\begin{aligned} T^{\mu\nu}_{\sigma}\nabla_\nu u_\mu &= T^{\mu\nu}_{\sigma} L_{\mu\nu} = T^{\mu\nu}_{\sigma} d_{\mu\nu} \\ &= (\sigma^{\mu\nu} - \sigma^{\mu\alpha}u_\alpha u^\nu - \sigma^{\nu\beta}u_\beta u^\mu + \sigma^{\alpha\beta}u_\alpha u_\beta u^\mu u^\nu) d_{\mu\nu} \end{aligned} \tag{B.15c}$$

where the Eq. B.15c uses the result that double dot product of a symmetric tensor with an arbitrary tensor equals to the symmetric tensor "times" the symmetric part of the second tensor:

$$T^{\mu\nu}L_{\mu\nu} = T^{\mu\nu}L^S_{\mu\nu} = T^{\mu\nu}d_{\mu\nu}. \tag{B.16}$$

Thus, we have:

$$T^{\mu\nu}\nabla_\nu u^\mu = q^\mu(u^\nu \nabla_\nu u_\mu) + (\sigma^{\mu\nu} - \sigma^{\mu\alpha}u_\alpha u^\nu - \sigma^{\nu\beta}u_\beta u^\mu + \sigma^{\alpha\beta}u_\alpha u_\beta u^\mu u^\nu) d_{\mu\nu}. \tag{B.17}$$

Substituting Eqs. B.11 and B.17 in Eq. B.9, eventually leads to Eq. B.8.

B.3 Conservation of momentum and that of energy in Newtonian mechanics

Remind that the conservation of momentum energy:

$$\nabla_\nu T^{\mu\nu} = 0 \tag{B.18}$$

will be approximated within Newtonian mechanics in Euclidean space-time.

Conservation of momentum in Newtonian mechanics and 3D projection

At first let $\mu = i$ where $i = 1, 2, 3$ in Eq. B.3, we have

$$\nabla_\nu T^{i\nu} = \nabla_\nu(\rho_r c^2 u^i u^\nu) + \nabla_\nu(q^i u^\nu + q^\nu u^i) + \nabla_\nu T^{i\nu}_{\sigma}. \tag{B.19}$$

If the transmission of heat is not considered $q^\mu = 0$, we have

$$\nabla_\nu T^{i\nu} = \nabla_\nu(\rho_r c^2 u^i u^\nu) + \nabla_\nu T_\sigma^{i\nu}. \tag{B.20}$$

In Newtonian mechanics in Euclidean space-time, we have

$$cu^\mu \approx (v^i, c) \;\; ; \;\; cu^\nu\nabla_\nu = v^i\nabla_i + \frac{\partial}{\partial t} = \frac{d}{dt} \;\; ; \;\; \rho_r c^2 = \gamma\rho c^2 + \gamma\rho e \approx \rho c^2 + \frac{\rho v^2}{2} + \rho e. \tag{B.21}$$

Thus, we have:

$$\begin{aligned}
\nabla_\nu(\rho_r c^2 u^i u^\nu) &\approx \nabla_\nu\left((\rho + \rho\frac{v^2}{2c^2} + \frac{\rho e}{c^2})c^2 u^i u^\nu\right) && \text{(B.22)}\\
&\approx \nabla_\nu\left(\rho v^i c u^\nu\right) && \text{(B.23)}\\
&= \rho c u^\nu\nabla_\nu v^i + v^i\nabla_\nu\left(\rho c u^\nu\right) && \text{(B.24)}\\
&= \rho\frac{dv^i}{dt}, && \text{(B.25)}
\end{aligned}$$

where the conservation of mass has been also applied:

$$\nabla_\nu(\rho c u^\nu) = 0. \tag{B.26}$$

For term $\nabla_\nu T_\sigma^{i\nu}$:

$$\nabla_\nu T_\sigma^{i\nu} = \nabla_j T_\sigma^{ij} + \frac{\partial T_\sigma^{i4}}{c\partial t} \approx \nabla_j\sigma^{ij}. \tag{B.27}$$

Provided that:

$$\frac{T_\sigma^{i4}}{c} \to 0 \;\; \text{when} \;\; \frac{v}{c} \to 0. \tag{B.28}$$

Thus, we have

$$\rho\frac{dv^i}{dt} + \nabla_j\sigma^{ij} = 0. \tag{B.29}$$

Conservation of energy in Newtonian mechanics

Second, let $\mu = 4$ in Eq. B.3, then we have:

$$\nabla_\nu T^{4\nu} = \nabla_\nu(\rho_r c^2 u^4 u^\nu) + \nabla_\nu(q^4 u^\nu + q^\nu u^4) + \nabla_\nu T_\sigma^{4\nu} = 0. \tag{B.30}$$

The transmission of heat is again not considered and the equation above is multiplied by c so that

$$\begin{aligned} c\nabla_\nu T^{4\nu} &\approx \nabla_\nu(\rho_r c^2 v^\nu) + \nabla_\nu(cT_\sigma^{4\nu}) = 0 && \text{(B.31)}\\ &\approx \nabla_\nu\left(\rho(c^2+\frac{v^2}{2}+e)cu^\nu\right) + \nabla_\nu(cT_\sigma^{4\nu}) && \text{(B.32)}\\ &= \rho cu^\nu\nabla_\nu(c^2+\frac{v^2}{2}+e) + (c^2+\frac{v^2}{2}+e)\nabla_\nu(\rho cu^\nu) + \nabla_\nu(cT_\sigma^{4\nu}) && \text{(B.33)}\\ &= \rho\frac{d}{dt}(\frac{v^2}{2}+e) + \nabla_\nu(cT_\sigma^{4\nu}). && \text{(B.34)} \end{aligned}$$

Then the last term can be calculated:

$$\begin{aligned} \nabla_\nu(cT_\sigma^{4\nu}) &= \nabla_\nu\left(c(\sigma^{4\nu} - \sigma^{4\alpha}u_\alpha u^\nu - \sigma^{\nu\beta}u_\beta u^4 + \sigma^{\alpha\beta}u_\alpha u_\beta u^\nu u^4)\right) && \text{(B.35)}\\ &= \nabla_\nu\left(c\sigma^{4\nu} - c\sigma^{4\alpha}u_\alpha u^\nu - c\sigma^{\nu\beta}u_\beta u^4 + c\sigma^{\alpha\beta}u_\alpha u_\beta u^\nu u^4\right) && \text{(B.36)}\\ &\approx \nabla_\nu\left(c\sigma^{4\nu} - \sigma^{44}cu^\nu - \sigma^{\nu\beta}cu_\beta + \sigma^{44}cu^\nu\right) && \text{(B.37)}\\ &= \nabla_\nu\left(c\sigma^{4\nu} - \sigma^{44}cu^\nu - \sigma^{\nu j}v_j - \sigma^{\nu 4}c + \sigma^{44}cu^\nu\right) && \text{(B.38)}\\ &= \nabla_\nu(-\sigma^{\nu j}v_j) && \text{(B.39)}\\ &= -\nabla_i(\sigma^{ij}v_j) - \frac{\partial}{c\partial t}(\sigma^{4j}v_j) && \text{(B.40)}\\ &\approx -\nabla_i(\sigma^{ij}v_j). && \text{(B.41)} \end{aligned}$$

From Eq. B.36 to Eq. B.37, the approximation $u^4 \approx 1$ is used, and the terms $c\sigma^{4\alpha}u_\alpha u^\nu \approx c\sigma^{44}u^\nu$, $c\sigma^{\alpha\beta}u_\alpha u_\beta u^\nu \approx c\sigma^{44}u_4 u_4 u^\nu$ are considered as the other terms are small in Newtonian mechanics. At last we have:

$$\rho\frac{d}{dt}(\frac{v^2}{2}+e) - \nabla_i(\sigma^{ij}v_j) = 0. \qquad \text{(B.42)}$$

B.4 Clausius-Duhem inequality in Newtonian mechanics and 3D projection

B.4.1 Clausius-Duhem inequality in Newtonian mechanics

Of the Clausius-Duhem inequality:

$$\theta\nabla_\mu(\rho_r\eta_r u^\mu) - \frac{q^\mu}{\theta}\nabla_\mu\theta - \nabla_\mu(\rho_r c^2 u^\mu) + q^\mu(u^\nu\nabla_\nu u_\mu)$$
$$+(\sigma^{\mu\nu} - \sigma^{\mu\alpha}u_\alpha u^\nu - \sigma^{\nu\beta}u_\beta u^\mu + \sigma^{\alpha\beta}u_\alpha u_\beta u^\mu u^\nu)d_{\mu\nu} \geq 0, \tag{B.43}$$

Each term will be calculated. The first term is calculated as:

$$\begin{aligned}\theta\nabla_\mu(\rho_r\eta_r u^\mu) &\approx \theta\nabla_\mu(\rho\eta u^\mu) && \text{(B.44)}\\ &= \theta\rho u^\mu\nabla_\mu\eta + \theta\eta\nabla_\mu(\rho u^\mu) && \text{(B.45)}\\ &= \theta\rho u^\mu\nabla_\mu\eta, && \text{(B.46)}\end{aligned}$$

where the conservation of mass is applied. Then the second term remains:

$$\frac{q^\mu}{\theta}\nabla_\mu\theta. \tag{B.47}$$

The third term can be calculated:

$$\begin{aligned}\nabla_\mu(\rho_r c^2 u^\mu) &= \nabla_\mu(\rho_r c u^\mu c u^\nu u_\nu) && \text{(B.48)}\\ \nabla_\mu(\rho_r c^2 u^\mu) &= u_\nu\nabla_\mu(\rho_r c u^\mu c u^\nu) + \rho_r c u^\mu u^\nu\nabla_\mu c u_\nu && \text{(B.49)}\\ &= u_\nu\nabla_\mu(\rho_r c u^\mu c u^\nu) && \text{(B.50)}\\ &\approx u_\nu\nabla_\mu\left((1+\frac{v^2}{2c^2}+\frac{e}{c^2})cu^\nu\rho c u^\mu\right) && \text{(B.51)}\\ &= cu_\nu\rho u^\mu\nabla_\mu\left((1+\frac{v^2}{2c^2}+\frac{e}{c^2})cu^\nu\right) + (1+\frac{v^2}{2c^2}+\frac{e}{c^2})cu_\nu u^\nu\nabla_\mu(\rho c u^\mu) && \text{(B.52)}\\ &= \rho c u_\nu u^\mu\nabla_\mu\left((1+\frac{v^2}{2c^2}+\frac{e}{c^2})cu^\nu\right) && \text{(B.53)}\\ &\approx -\rho v_i u^\mu\nabla_\mu\left((1+\frac{v^2}{2c^2}+\frac{e}{c^2})v^i\right) + \rho c u^\mu\nabla_\mu\left((1+\frac{v^2}{2c^2}+\frac{e}{c^2})c\right) && \text{(B.54)}\\ &\approx -\rho v_i u^\mu\nabla_\mu v^i + \frac{\rho}{2}u^\mu\nabla_\mu v^2 + \rho u^\mu\nabla_\mu e && \text{(B.55)}\\ &= \rho u^\mu\nabla_\mu e. && \text{(B.56)}\end{aligned}$$

Here the minus sign appears, because we have:

$$cu_\mu = cg_{\mu\nu}u^\nu \approx (-v_i, c). \tag{B.57}$$

The fourth term:

$$q^\mu(u^\nu\nabla_\nu u_\mu) = q^i(u^\nu\nabla_\nu u_i) + q^4(u^\nu\nabla_\nu u_4) \approx 0. \tag{B.58}$$

because $u_i \approx 0$ and $q^4 = 0$ The last term:

$$\begin{aligned}
&(\sigma^{\mu\nu} - \sigma^{\mu\alpha}u_\alpha u^\nu - \sigma^{\nu\beta}u_\beta u^\mu + \sigma^{\alpha\beta}u_\alpha u_\beta u^\mu u^\nu)d_{\mu\nu} \\
\approx\ &\sigma^{\mu\nu}d_{\mu\nu} - 2\sigma^{\mu 4}d_{\mu 4} + \sigma^{44}d_{44} &\text{(B.59)}\\
\approx\ &\sigma^{\mu\nu}d_{\mu\nu}, &\text{(B.60)}
\end{aligned}$$

with approximation that

$$d_{i4} \approx d_{4j} \approx d_{44} \approx 0. \tag{B.61}$$

After calculation of the five terms, the Newtonian form of the Clausius-Duhem inequality is obtained:

$$\theta\rho u^\mu\nabla_\mu\eta - \frac{q^\mu}{\theta}\nabla_\mu\theta - \rho u^\mu\nabla_\mu e + \sigma^{\mu\nu}d_{\mu\nu} \geq 0. \tag{B.62}$$

B.4.2 3D projection of Clausius-Duhem inequality

To calculate the 3D version of Clausius-Duhem inequality, it should be first multiplied by c:

$$\begin{aligned}
&c\theta\nabla_\mu(\rho_r\eta_r u^\mu) - \frac{\phi^\mu}{\theta}\nabla_\mu\theta - c\nabla_\mu(\rho_r c^2 u^\mu) + \phi^\mu(u^\nu\nabla_\nu u_\mu) \\
&+(\sigma^{\mu\nu} - \sigma^{\mu\alpha}u_\alpha u^\nu - \sigma^{\nu\beta}u_\beta u^\mu + \sigma^{\alpha\beta}u_\alpha u_\beta u^\mu u^\nu)cd_{\mu\nu} \geq 0, &\text{(B.63)}
\end{aligned}$$

where we define

$$\phi^\mu = cq^\mu. \tag{B.64}$$

Each term of Eq. B.63 will be calculated. With Eq. B.46, the first term is calculated as:

$$c\theta\nabla_\mu(\rho_r\eta_r u^\mu) \approx c\theta\rho u^\mu\nabla_\mu\eta = \theta\rho\frac{d\eta}{dt}. \tag{B.65}$$

The second term is calculated as:

$$\frac{\phi^\mu}{\theta}\nabla_\mu\theta \approx \frac{\phi^i}{\theta}\nabla_i\theta, \tag{B.66}$$

because $\phi^4 = 0$. With Eq. B.56, the third term is calculated as:

$$c\nabla_\mu(\rho_r c^2 u^\mu) \approx c\rho u^\mu \nabla_\mu e = \rho\frac{de}{dt}. \tag{B.67}$$

The fourth term:

$$\phi^\mu(u^\nu\nabla_\nu u_\mu) = \phi^i(u^\nu\nabla_\nu u_i) + \phi^4(u^\nu\nabla_\nu u_4) \approx 0. \tag{B.68}$$

because $u_i \approx 0$ and $\phi^4 = 0$ The last term:

$$\begin{aligned}
&(\sigma^{\mu\nu} - \sigma^{\mu\alpha}u_\alpha u^\nu - \sigma^{\nu\beta}u_\beta u^\mu + \sigma^{\alpha\beta}u_\alpha u_\beta u^\mu u^\nu)cd_{\mu\nu} \\
&= \sigma^{\mu\nu}cd_{\mu\nu} - \sigma^{\mu\alpha}u_\alpha u^\nu cd_{\mu\nu} - \sigma^{\nu\beta}u_\beta u^\mu cd_{\mu\nu} + \sigma^{\alpha\beta}u_\alpha u_\beta u^\mu u^\nu cd_{\mu\nu} && \text{(B.69)} \\
&\approx \sigma^{\mu\nu}cd_{\mu\nu} - \sigma^{\mu 4}cd_{\mu 4} - \sigma^{\nu 4}cd_{4\nu} + \sigma^{44}cd_{44} && \text{(B.70)} \\
&= \sigma^{ij}cd_{ij} + \sigma^{i4}cd_{i4} + \sigma^{j4}cd_{4j} + \sigma^{44}cd_{44} - \sigma^{i4}cd_{i4} - \sigma^{44}cd_{44} - \sigma^{j4}cd_{j4} - \sigma^{44}cd_{44} + \sigma^{44}cd_{44} && \text{(B.71)} \\
&\approx \sigma^{ij}cd_{ij}. && \text{(B.72)}
\end{aligned}$$

In a conclusion, Clausius-Duhem inequality can be approximated in 3D version:

$$\theta\rho\frac{d\eta}{dt} - \frac{\phi^i}{\theta}\nabla_i\theta - \rho\frac{de}{dt} + \sigma^{ij}cd_{ij} \geq 0. \tag{B.73}$$

In 3D context, the rate of deformation $d^{ij} = (\nabla_j v^i)^S = c(\nabla_j u^i)^S$. The 3D version of Clausius-Duhem inequality can be rewritten as:

$$\theta\rho\frac{d\eta}{dt} - \frac{\phi^i}{\theta}\nabla_i\theta - \rho\frac{de}{dt} + \sigma^{ij}d_{ij} \geq 0. \tag{B.74}$$

Appendix C

Generalized isotropic limit for anisotropic elasticity in Chapter 4.

The matrix of coordinate transformations for Eq. 4.48 in Chapter 4 are:

For space reflection to axis-1 corresponds to:

$$\Omega_{\nu}^{\mu} = \begin{pmatrix} -1 & 0 & 0 & 0 \\ 0 & 1 & 0 & 0 \\ 0 & 0 & 1 & 0 \\ 0 & 0 & 0 & 1 \end{pmatrix}. \tag{C.1}$$

The number of independent components is reduced to 34 when this symmetry is valid.

For space, reflection to axis-2 corresponds to:

$$\Omega_{\nu}^{\mu} = \begin{pmatrix} 1 & 0 & 0 & 0 \\ 0 & -1 & 0 & 0 \\ 0 & 0 & 1 & 0 \\ 0 & 0 & 0 & 1 \end{pmatrix}. \tag{C.2}$$

The number of independent components is reduced to 22 when this symmetry is additionally valid, too.

For space reflection to axis-3 corresponds to:

$$\Omega_{\nu}^{\mu} = \begin{pmatrix} 1 & 0 & 0 & 0 \\ 0 & 1 & 0 & 0 \\ 0 & 0 & -1 & 0 \\ 0 & 0 & 0 & 1 \end{pmatrix}. \tag{C.3}$$

The number of independence components is reduced to 16 with when this symmetry is additionally valid, too.

For the time reflection, it corresponds to:

$$\Omega_{\nu}^{\mu} = \begin{pmatrix} 1 & 0 & 0 & 0 \\ 0 & 1 & 0 & 0 \\ 0 & 0 & 1 & 0 \\ 0 & 0 & 0 & -1 \end{pmatrix}. \tag{C.4}$$

The number of independence components remains unchanged.

The material of all these symmetries is orthotropic. It is important to keep in mind that the tensor is a four-dimensional one, which means that the number of independent components is a priori superior from the 3D case.

Rotation symmetries can be also used to reduce the number of independent components. For a material with cubic symmetry, 3 rotations of $\pi/2$ can be applied, with the respective matrix of transformations:

$$\Omega_{\nu}^{\mu} = \begin{pmatrix} 0 & 1 & 0 & 0 \\ -1 & 0 & 0 & 0 \\ 0 & 0 & 1 & 0 \\ 0 & 0 & 0 & 1 \end{pmatrix} \;;\; \Omega_{\nu}^{\mu} = \begin{pmatrix} 0 & 0 & 1 & 0 \\ 0 & 1 & 0 & 0 \\ -1 & 0 & 0 & 0 \\ 0 & 0 & 0 & 1 \end{pmatrix} \;;\; \Omega_{\nu}^{\mu} = \begin{pmatrix} 1 & 0 & 0 & 0 \\ 0 & 0 & 1 & 0 \\ 0 & -1 & 0 & 0 \\ 0 & 0 & 0 & 1 \end{pmatrix}. \tag{C.5}$$

Once the two first symmetries have been applied, the third one is irrelevant since it does not change the number of independent components. It is then possible to prove that a material with cubic symmetry has only a priori 6 independent components, with a stiffness

tensor in Voigt notation (11 $\rightarrow$ 1111, 12 $\rightarrow$ 1122, 14 $\rightarrow$ 1144, 44 $\rightarrow$ 4444, 55 $\rightarrow$ 3434, 88 $\rightarrow$ 1313...) equal to:

$$\mathcal{C}^{\Lambda\Theta} = \begin{pmatrix} \mathcal{C}^{11} & \mathcal{C}^{12} & \mathcal{C}^{12} & \mathcal{C}^{14} & 0 & 0 & 0 & 0 & 0 & 0 \\ \mathcal{C}^{12} & \mathcal{C}^{11} & \mathcal{C}^{12} & \mathcal{C}^{14} & 0 & 0 & 0 & 0 & 0 & 0 \\ \mathcal{C}^{12} & \mathcal{C}^{12} & \mathcal{C}^{11} & \mathcal{C}^{14} & 0 & 0 & 0 & 0 & 0 & 0 \\ \mathcal{C}^{14} & \mathcal{C}^{14} & \mathcal{C}^{14} & \mathcal{C}^{44} & 0 & 0 & 0 & 0 & 0 & 0 \\ 0 & 0 & 0 & 0 & \mathcal{C}^{55} & 0 & 0 & 0 & 0 & 0 \\ 0 & 0 & 0 & 0 & 0 & \mathcal{C}^{55} & 0 & 0 & 0 & 0 \\ 0 & 0 & 0 & 0 & 0 & 0 & \mathcal{C}^{55} & 0 & 0 & 0 \\ 0 & 0 & 0 & 0 & 0 & 0 & 0 & \mathcal{C}^{88} & 0 & 0 \\ 0 & 0 & 0 & 0 & 0 & 0 & 0 & 0 & \mathcal{C}^{88} & 0 \\ 0 & 0 & 0 & 0 & 0 & 0 & 0 & 0 & 0 & \mathcal{C}^{88} \end{pmatrix}. \tag{C.6}$$

If the material would have an isotropic behaviour (in the 3D sense), it should have strictly the same response if the observer rotates by an arbitrary angle ϕ, corresponding to a transformation matrix (for example):

$$\Omega^{\mu}_{\nu} = \begin{pmatrix} cos\phi & sin\phi & 0 & 0 \\ -sin\phi & cos\phi & 0 & 0 \\ 0 & 0 & 1 & 0 \\ 0 & 0 & 0 & 1 \end{pmatrix}. \tag{C.7}$$

To illustrate the method, let us calculate the component $\mathcal{C}^{11}$ by applying Eq. 4.48

$$\mathcal{C}^{1111} = \tilde{\mathcal{C}}^{1111} = 1^{-1}\Omega^1_{\kappa}\Omega^1_{\lambda}\Omega^1_{\mu}\Omega^1_{\nu}\mathcal{C}^{\kappa\lambda\mu\nu} \tag{C.8}$$

$$= \Omega^1_1\Omega^1_1\Omega^1_1\Omega^1_1\mathcal{C}^{1111} + 2\Omega^1_1\Omega^1_1\Omega^1_2\Omega^1_2\mathcal{C}^{1122} + 4\Omega^1_1\Omega^1_2\Omega^1_1\Omega^1_2\mathcal{C}^{1212} + \Omega^1_2\Omega^1_2\Omega^1_2\Omega^1_2\mathcal{C}^{2222} \tag{C.9}$$

$\Longleftrightarrow$

$$\mathcal{C}^{11} = \frac{1}{4}(3 + cos4\phi)\mathcal{C}^{11} + \frac{1}{4}(1 - cos4\phi)\mathcal{C}^{12} + \frac{1}{2}(1 - cos4\phi)\mathcal{C}^{88} \tag{C.10}$$

$$= \frac{1}{4}(3\mathcal{C}^{11} + \mathcal{C}^{12} + 2\mathcal{C}^{88} + (\mathcal{C}^{11} - \mathcal{C}^{12} - 2\mathcal{C}^{88})cos4\phi). \tag{C.11}$$

Eq. C.11 shows that the expression can be independent of ϕ if and only if $\mathcal{C}^{11} - \mathcal{C}^{12} - 2\mathcal{C}^{88} = 0$, which gives the same kind of relation as in 3D. All other relations involving other components lead to the same condition, so that the number of independent components is

reduced to only 5. Thus, the conclusion would be that an isotropic material should have 5 independent components, in contradiction with Eq. 4.47

An extra additional material symmetry has to be taken into account. As for space rotation, space-time rotation can lead to conditions on the stiffness components. In space-time, rotation is equivalent to translation in space in the non-relativistic limit. The corresponding invariance of the material due to a translation seems natural, especially for uniform translation at constant speed v_e. The material is thus supposed to be invariant under the Lorentz transformation, for which the matrix transformation is

$$\Omega^{\mu}_{\nu} = \begin{pmatrix} cosh\psi & 0 & 0 & -sinh\psi \\ 0 & 1 & 0 & 0 \\ 0 & 0 & 1 & 0 \\ -sinh\psi & 0 & 0 & cosh\psi \end{pmatrix}, \tag{C.12}$$

where $\psi = argth(v_e/c)$ is the rapidity. By substituting this matrix in Eq. 4.48, 3 additional relations can be obtained, which are:

$$(\mathcal{C}^{12} + \mathcal{C}^{14})cosh\psi sinh\psi = 0 \implies \mathcal{C}^{12} = -\mathcal{C}^{14} \tag{C.13}$$

$$(\mathcal{C}^{55} + \mathcal{C}^{88})cosh\psi sinh\psi = 0 \implies \mathcal{C}^{55} = -\mathcal{C}^{88} \tag{C.14}$$

$$\left((\mathcal{C}^{12} + \mathcal{C}^{14} + 2\mathcal{C}^{55} + 2\mathcal{C}^{88})cosh^2\psi + (\mathcal{C}^{14} + \mathcal{C}^{44} + 2\mathcal{C}^{55})sinh^2\psi\right) cosh\psi sinh\psi = 0$$

$$\implies \mathcal{C}^{44} = \mathcal{C}^{12} + 2\mathcal{C}^{88}. \tag{C.15}$$

At last the stiffness matrix for isotropic elasticity (model 2) in Voight notation is that:

$$\mathcal{C}^{\Lambda\Theta} = \begin{pmatrix} \mathcal{C}^{**} & \mathcal{C}^{12} & \mathcal{C}^{12} & -\mathcal{C}^{12} & 0 & 0 & 0 & 0 & 0 & 0 \\ \mathcal{C}^{12} & \mathcal{C}^{**} & \mathcal{C}^{12} & -\mathcal{C}^{12} & 0 & 0 & 0 & 0 & 0 & 0 \\ \mathcal{C}^{12} & \mathcal{C}^{12} & \mathcal{C}^{**} & -\mathcal{C}^{12} & 0 & 0 & 0 & 0 & 0 & 0 \\ -\mathcal{C}^{12} & -\mathcal{C}^{12} & -\mathcal{C}^{12} & \mathcal{C}^{**} & 0 & 0 & 0 & 0 & 0 & 0 \\ 0 & 0 & 0 & 0 & -\mathcal{C}^{88} & 0 & 0 & 0 & 0 & 0 \\ 0 & 0 & 0 & 0 & 0 & -\mathcal{C}^{88} & 0 & 0 & 0 & 0 \\ 0 & 0 & 0 & 0 & 0 & 0 & -\mathcal{C}^{88} & 0 & 0 & 0 \\ 0 & 0 & 0 & 0 & 0 & 0 & 0 & \mathcal{C}^{88} & 0 & 0 \\ 0 & 0 & 0 & 0 & 0 & 0 & 0 & 0 & \mathcal{C}^{88} & 0 \\ 0 & 0 & 0 & 0 & 0 & 0 & 0 & 0 & 0 & \mathcal{C}^{88} \end{pmatrix}, \tag{C.16}$$

with $\mathcal{C}^{**} = \mathcal{C}^{12} + 2\mathcal{C}^{88}$. $\mathcal{C}^{12}$ and $\mathcal{C}^{88}$ are two material parameters. As expected, the matrix depends only on these two parameters. It is possible to express the associated components especially those linked to the fourth dimension: $\mathcal{C}^{4444}$, $\mathcal{C}^{1144}$ and $\mathcal{C}^{3434}$. It gives, for inertial coordinates in terms of components:

$$\mathcal{C}^{4444} = \lambda\eta^{44}\eta^{44} + \mu(\eta^{44}\eta^{44} + \eta^{44}\eta^{44}) = \lambda + 2\mu = \mathcal{C}^{44} \tag{C.17}$$

$$\mathcal{C}^{1144} = \lambda\eta^{11}\eta^{44} + \mu(\eta^{14}\eta^{41} + \eta^{41}\eta^{14}) = -\lambda = \mathcal{C}^{14} = -\mathcal{C}^{12} \tag{C.18}$$

$$\mathcal{C}^{3434} = \lambda\eta^{34}\eta^{34} + \mu(\eta^{33}\eta^{44} + \eta^{34}\eta^{43}) = -\mu = \mathcal{C}^{55} = -\mathcal{C}^{88}. \tag{C.19}$$

Appendix D

Details of calculations corresponding to Chapter 5

D.1 Derivation of $\mathscr{L}_{u_p}(\sigma_{eff})$

The effective stress is given by the expression:

$$\sigma_{eff} = \sqrt{S^{\alpha\beta}S_{\alpha\beta}}, \tag{D.1}$$

where the expression of the deviatoric stress $\boldsymbol{S}$ is, by definition:

$$S^{\alpha\beta} = \sigma^{\alpha\beta} - \frac{\sigma^{\gamma\lambda}g_{\gamma\lambda}}{4}g^{\alpha\beta}. \tag{D.2}$$

First note that:

$$\frac{\partial\sigma_{eff}}{\partial S^{\alpha\beta}} = \frac{\partial\sigma_{eff}}{\partial\sigma^{\alpha\beta}} = \frac{S_{\alpha\beta}}{\sigma_{eff}}. \tag{D.3}$$

We wish to derive the expression of $\mathscr{L}_{u_p}(\sigma_{eff})$, the Lie derivative of this effective stress in the plastic velocity field. Using the chain rule, and the fact that σ_{eff} is a scalar density of weight equal to one (Eq. 2.76a), it comes:

$$\mathscr{L}_{u_p}(\sigma_{eff}) = \frac{\partial\sigma_{eff}}{\partial(S^{\alpha\beta}S_{\alpha\beta})}u_p^\lambda\nabla_\lambda(S^{\alpha\beta}S_{\alpha\beta}) + \sigma_{eff}\ d_{p\,\lambda}^{\lambda}. \tag{D.4}$$

Also:

$$S_{\alpha\beta}\ u_p^\lambda\nabla_\lambda(S^{\alpha\beta}) = S_{\alpha\beta}\ u_p^\lambda\nabla_\lambda(\sigma^{\alpha\beta} - \frac{\sigma^{\gamma\lambda}g_{\gamma\lambda}}{4}g^{\alpha\beta}) = S_{\alpha\beta}\ u_p^\lambda\nabla_\lambda(\sigma^{\alpha\beta}) \tag{D.5}$$

because $\boldsymbol{S}$ is deviatoric (and thus $S_{\alpha\beta}g^{\alpha\beta} = 0$) and $\nabla_\lambda(g^{\alpha\beta}) = 0$.

Finally, Eq.D.4 becomes, with the chain rule:

$$\mathscr{L}_{u_p}(\sigma_{eff}) = \frac{S_{\alpha\beta}}{\sigma_{eff}} u_p^\lambda \nabla_\lambda(\sigma^{\alpha\beta}) + \sigma_{eff}\ d_{p\,\lambda}^{\lambda} \tag{D.6}$$

D.2 Derivation of the expression of the plastic rate of deformation

We wish to derive the expression of the plastic rate of deformation for the three elasto-plastic models. It is the necessary to solve a system of equations for $\boldsymbol{d}_p$, constituted with:

- One of the hypoelastic models given by the equations below (corresponding to Eqs. 5.57 to 5.59 in which the transports have been replaced with their respective values):
  - Reversible hypoelastic model:

$$u^\lambda \nabla_\lambda(\sigma^{\mu\nu}) - \sigma^{\lambda\nu} L^\mu_{e_\lambda} - \sigma^{\mu\lambda} L^\nu_{e_\lambda} + \sigma^{\mu\nu} d^\lambda_\lambda = \mathcal{R}^{\mu\nu\alpha\beta} d_{e\alpha\beta}. \tag{D.7}$$

  - Irreversible hypoelastic model constructed with the Lie derivative:

$$u^\lambda \nabla_\lambda(\sigma^{\mu\nu}) - \sigma^{\lambda\nu} L^\mu_{e_\lambda} - \sigma^{\mu\lambda} L^\nu_{e_\lambda} + \sigma^{\mu\nu} d^\lambda_\lambda = \mathcal{H}^{\mu\nu\alpha\beta} d_{e\alpha\beta}. \tag{D.8}$$

  - Irreversible hypoelastic model constructed with Jaumann's transport:

$$u^\lambda \nabla_\lambda(\sigma^{\mu\nu}) - \omega^\mu_\alpha \sigma^{\alpha\nu} + \sigma^{\mu\alpha} \omega_\alpha^{\ \nu} = \mathcal{H}^{\mu\nu\alpha\beta} d_{e\alpha\beta}. \tag{D.9}$$

- The kinematic relations:

$$\begin{aligned} L^\mu_\nu &= d^\mu_\nu + \omega^\mu_\nu \\ d_{\mu\nu} &= d_{e\mu\nu} + d_{p_{\mu\nu}} \\ L^\mu_{e\nu} &= d^\mu_{e\nu} + \omega^\mu_\nu. \end{aligned} \tag{D.10}$$

- The plasticity model:

$$d_{p_{\mu\nu}} = \mathcal{P} S_{\mu\nu} \text{ with } d_{p\,\lambda}^{\lambda} = 0 \text{ and } \mathcal{P} = \frac{S_{\alpha\beta}\, u^{\lambda} \nabla_{\lambda}(\sigma^{\alpha\beta})}{\sigma_{eff}^{2} \frac{\partial \kappa}{\partial r}}. \tag{D.11}$$

Due to the fact that the scalar quantity $S_{\alpha\beta}\, u^{\lambda}\nabla_{\lambda}(\sigma^{\alpha\beta})$ appears in the expression of d_p above, it is possible to contract both sides of the hypoelastic equations D.7 to D.9 with $S_{\mu\nu}$ to solve each of the systems of equations. Further note that:

$$S_{\mu\nu}\sigma^{\mu\lambda}L^{\nu}_{\ \lambda} = S_{\mu\nu}\sigma^{\lambda\nu}L^{\mu}_{\ \lambda} \tag{D.12}$$

$$S_{\mu\nu}\sigma^{\mu\lambda}d^{\nu}_{p_{\lambda}} = S_{\mu\nu}\sigma^{\lambda\nu}d^{\mu}_{p_{\lambda}} \tag{D.13}$$

$$S_{\mu\nu}\sigma^{\mu\lambda}d^{\nu}_{\lambda} = S_{\mu\nu}\sigma^{\lambda\nu}d^{\mu}_{\lambda} \tag{D.14}$$

because $\boldsymbol{S}$ and $\boldsymbol{\sigma}$ are symmetric. Also:

$$S_{\mu\nu}\sigma^{\mu\lambda}L^{\nu}_{\ \lambda} = S_{\mu\nu}\sigma^{\mu\lambda}(d^{\nu}_{\ \lambda} + \omega^{\nu}_{\ \lambda}) = S_{\mu\nu}\sigma^{\mu\lambda}d^{\nu}_{\ \lambda} \tag{D.15}$$

because $S_{\mu\nu}\sigma^{\mu\lambda}\omega^{\nu}_{\ \lambda} = 0$. This corresponds indeed to the contraction of a symmetric with an antisymmetric second-rank tensor, because the product of a symmetric second-rank tensor and its deviator is symmetric.

D.2.1 Derivation of the value of $d^{\mathcal{R}}_{p\mu\nu}$, the plastic rate of deformation for the reversible hypoelastic model

Eq. D.7, corresponding to the reversible hypoelastic model becomes:

$$u^{\lambda}\nabla_{\lambda}(\sigma^{\mu\nu}) - \sigma^{\mu\lambda}(L^{\nu}_{\ \lambda} - d^{\nu}_{p_{\lambda}}) - \sigma^{\lambda\nu}(L^{\mu}_{\ \lambda} - d^{\mu}_{p_{\lambda}}) + \sigma^{\mu\nu}d^{\lambda}_{\ \lambda} = \mathcal{R}^{\mu\nu\alpha\beta}(d_{\alpha\beta} - d_{p_{\alpha\beta}}). \tag{D.16}$$

With the use to the expression of the plastic rate of deformation and of the expressions derived above, it comes:

$$\mathcal{P}^{\mathcal{R}} = \frac{S_{\mu\nu}\left(2\sigma^{\mu\lambda}d^{\nu}_{\ \lambda} + \mathcal{R}^{\mu\nu\alpha\beta}d_{\alpha\beta} - \sigma^{\mu\nu}d^{\lambda}_{\ \lambda}\right)}{\sigma_{eff}^{2}\frac{\partial\kappa}{\partial r} + 2\sigma^{\mu\lambda}S^{\nu}_{\ \lambda}S_{\mu\nu} + \mathcal{R}^{\mu\nu\alpha\beta}S_{\alpha\beta}S_{\mu\nu}} \tag{D.17}$$

where $\mathcal{P}^{\mathcal{R}}$ corresponds to the plastic factor associated to the reversible elastic model. The explicit form of $\mathcal{R}$, given by Eq. 4.53 is now introduced in the expression of $\mathcal{P}^{\mathcal{R}}$; In the end, using the fact that the trace of a deviatoric second-rank tensor vanishes, it comes:

$$\mathcal{P}^{\mathcal{R}} = S^{\alpha\beta}\frac{Ad_{\alpha\beta} - 2d_{\alpha\kappa}\sigma^{\kappa}_{\ \beta}}{\sigma^2_{eff}(\partial\kappa/\partial r + A) - 2S_{\alpha\kappa}\sigma^{\kappa}_{\ \beta}S^{\beta\alpha}}$$

where

$$A = 2\mu + \frac{2\lambda(g_{\gamma\delta}\sigma^{\gamma\delta})}{4\lambda + 2\mu} \tag{D.18}$$

The plastic rate of deformation for the reversible hypoelastic model takes the form:

$$d^{\mathcal{R}}_{p\mu\nu} = \mathcal{P}^{\mathcal{R}}S_{\mu\nu} \tag{D.19}$$

D.2.2 Derivation of the values of the plastic rate of deformation for the irreversible hypoelastic models

The same type of derivation is performed for the irreversible hypoelastic model constructed with the Lie derivative (Eq. D.8), except that $\mathcal{R}$ should be replaced by $\mathcal{H}$ in Eq. D.17 to give:

$$\mathcal{P}^{\mathcal{HL}} = \frac{S_{\mu\nu}\left(2\sigma^{\mu\lambda}d^{\nu}_{\ \lambda} + \mathcal{H}^{\mu\nu\alpha\beta}d_{\alpha\beta} - \sigma^{\mu\nu}d^{\lambda}_{\ \lambda}\right)}{\sigma^2_{eff}\frac{\partial\kappa}{\partial r} + 2\sigma^{\mu\lambda}S^{\nu}_{\ \lambda}S_{\mu\nu} + \mathcal{H}^{\mu\nu\alpha\beta}S_{\alpha\beta}S_{\mu\nu}} \tag{D.20}$$

To obtain the detailed form of this model, the explicit form of $\mathcal{H}$, given by Eq. 4.61, is now introduced in the expression of $\mathcal{P}^{\mathcal{HL}}$ and:

$$\mathcal{P}^{\mathcal{HL}} = \frac{S^{\rho\theta}\left(2\sigma_{\rho}^{\ \lambda}d_{\theta\lambda} + 2\mu\ d_{\rho\theta} - \sigma_{\rho\theta}d^{\lambda}_{\ \lambda}\right)}{\sigma^2_{eff}(\frac{\partial\kappa}{\partial r} + 2\mu) + 2\sigma^{\alpha\lambda}S^{\beta}_{\ \lambda}S_{\alpha\beta}} \tag{D.21}$$

The plastic rate of deformation for this case takes the form:

$$d^{\mathcal{HL}}_{p\mu\nu} = \mathcal{P}^{\mathcal{HL}}S_{\mu\nu}. \tag{D.22}$$

For the hypoelastic model constructed with the Jaumann transport, the plastic factor $\mathcal{P}^{\mathcal{HJ}}$ is obtained with the same methodology but starting with the hypoelastic model given by Eq. D.9. This leads to:

$$\mathcal{P}^{\mathcal{HJ}} = \frac{\mathcal{H}^{\mu\nu\alpha\beta}S_{\mu\nu}d_{\alpha\beta}}{\sigma^2_{eff}\frac{\partial\kappa}{\partial r} + \mathcal{H}^{\mu\nu\alpha\beta}S_{\mu\nu}S_{\alpha\beta}} \tag{D.23}$$

and with the explicit form of $\mathcal{H}$, the plastic rate of deformation for this case takes the form:

$$d_{p\mu\nu}^{\mathcal{HJ}} = \frac{2\mu\ S^{\rho\theta} d_{\rho\theta}}{\sigma_{eff}^2(\frac{\partial\kappa}{\partial r} + 2\mu)} S_{\mu\nu}. \tag{D.24}$$

Appendix E

Algorithm for 3D projected models in finite element analysis

E.1 Algorithm for an elastoplastic model

An example of algorithm of local integration for the constitutive models is given here for the model with a reversible hypoelastic part. For each time increment dt, the values of $\boldsymbol{F}$, $d\boldsymbol{F}$, and $\boldsymbol{\sigma}$ as well as the internal variable r are treated as input data. The value of dr and $d\boldsymbol{\sigma}$ are the output, while E, ν, R_0, Q and b are the known constant parameters of the model.

1. Evaluate the total rate of deformation $\boldsymbol{d}$, the spin $\boldsymbol{\omega}$:

$$\boldsymbol{L} = d\boldsymbol{F}\boldsymbol{F}^{-1}; \quad \boldsymbol{d} = 0.5(\boldsymbol{L} + \boldsymbol{L}^T); \quad \boldsymbol{\omega} = 0.5(\boldsymbol{L} - \boldsymbol{L}^T)$$

2. Evaluate the deviatoric stress $\boldsymbol{S}$, the effective stress σ_{eff} and the radius of the yield surface κ:

$$\boldsymbol{S} = \boldsymbol{\sigma} - 1/3(\boldsymbol{S} : \boldsymbol{I})\boldsymbol{I}; \quad \sigma_{eff} = \sqrt{\boldsymbol{S} : \boldsymbol{S}}; \quad \kappa = R_0 + Q(1 - e^{-br})$$

3. If

$$\sigma_{eff} - \kappa < 0,$$

the material is in the elastic domain and

$$\boldsymbol{d_p} = \mathbf{0}; \quad \boldsymbol{d_e} = \boldsymbol{d}; \quad dr = 0$$

4. Else, the material has reach plasticity and

$$\boldsymbol{d_p} = \frac{A(\boldsymbol{d} : \boldsymbol{S}) - 2(d\boldsymbol{\sigma}) : \boldsymbol{S}}{(\boldsymbol{S} : \boldsymbol{S})(bQe^{-br} + A) - 2(\boldsymbol{S\sigma}) : \boldsymbol{S}}\boldsymbol{S} \tag{E.1}$$

$$\boldsymbol{d_e} = \boldsymbol{d} - \boldsymbol{d_p} \tag{E.2}$$

$$dr = \sqrt{\boldsymbol{d_p} : \boldsymbol{d_p}} \tag{E.3}$$

where

$$A = \frac{2\lambda}{3\lambda + 2\mu}(\boldsymbol{\sigma} : \boldsymbol{I}) + 2\mu \tag{E.4}$$

5. Evaluate the stress increment $d\boldsymbol{\sigma}$:

$$d\boldsymbol{\sigma} = B\boldsymbol{I} + A\boldsymbol{d_e} - \boldsymbol{\sigma}\boldsymbol{d_e} + \boldsymbol{d_e}\boldsymbol{\sigma} - \boldsymbol{\sigma}\boldsymbol{\omega} + \boldsymbol{\omega}\boldsymbol{\sigma} \tag{E.5}$$

where

$$B = \frac{\lambda^2}{\mu(3\lambda + 2\mu)}(\boldsymbol{\sigma} : \boldsymbol{I})(\boldsymbol{d} : \boldsymbol{I}) + \lambda(\boldsymbol{d} : \boldsymbol{I}) - \frac{\lambda}{\mu}(\boldsymbol{\sigma} : \boldsymbol{d_e}) \tag{E.6}$$

6. Integrate $\boldsymbol{\sigma}$ with the Newton-Raphson method.

Appendix F

More figures for the simulations of hypoelasticity and elastoplasticity

In Figures 6.2, 6.3, 6.4, 6.5, 6.6, 6.7 and 6.8, the corresponding models are compared by the stress-time curves. Since the deformation gradient is imposed previously for the loading in one element as the input, the strain calculated with different models for this loading is the same. So the stress-time curves are valid for the result comparing. However, the stress-strain curves are used classically. In this annex, two examples of stress-strain curves are given to supplement the stress-time curves: it is possible to compare the results calculated with the proposed models and those existing in the articles. Figure F.1 is the complementary of Figure 6.5. Figure F.2 is the complementary of Figure 6.8.

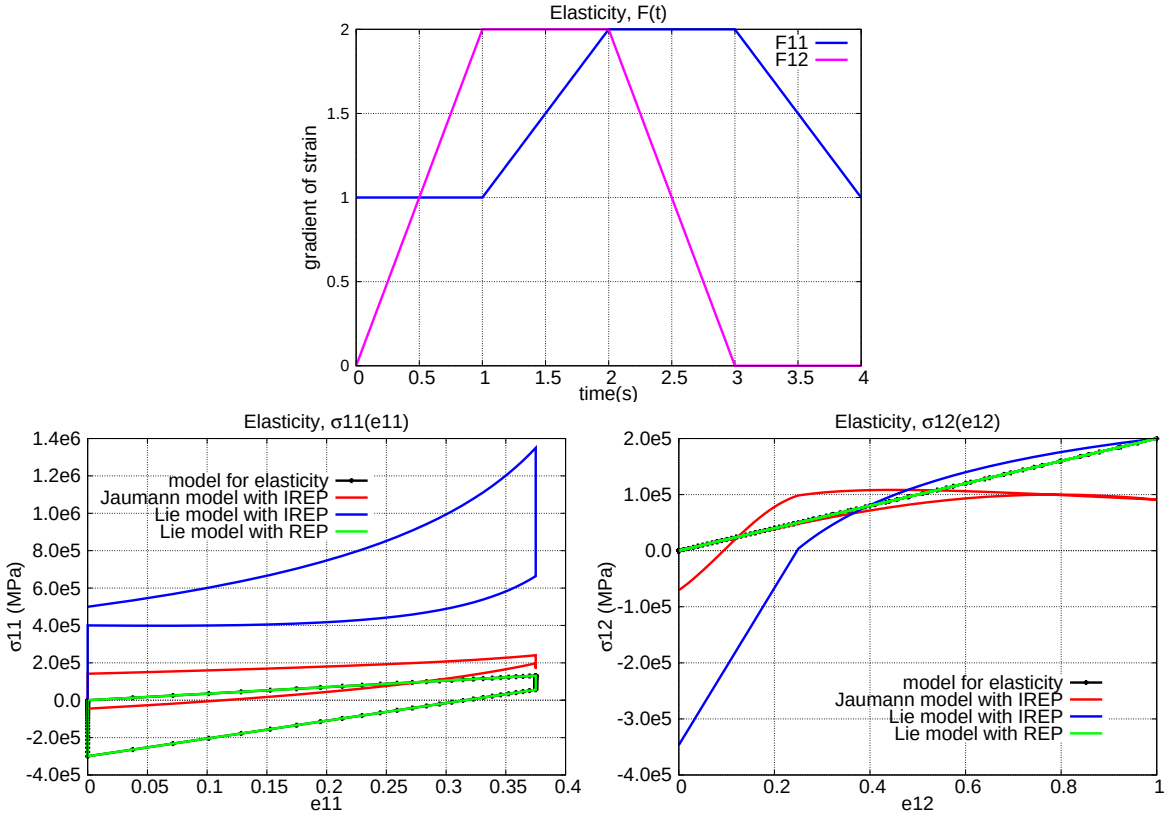

Figure F.1: Stress-strain curve for a cycle in deformation (represented in Figure 6.1) with an important deformation (reaching $b/a = 2$ and $(c-a)/a = 1$) and without plasticity. The varying components of the deformation gradient $\boldsymbol{F}$ is given on the top figures. The components of the Cauchy stress tensor $\boldsymbol{\sigma}$ in function of the components of strain tensor $\boldsymbol{e}$ are given in the bottom figures for the elastic model and the hypoelastic models listed in Section 6.2.2. The hypoelastic models are constructed with the Jaumann transport or the Lie derivative. They are either reversible (REP) or irreversible (IREP).

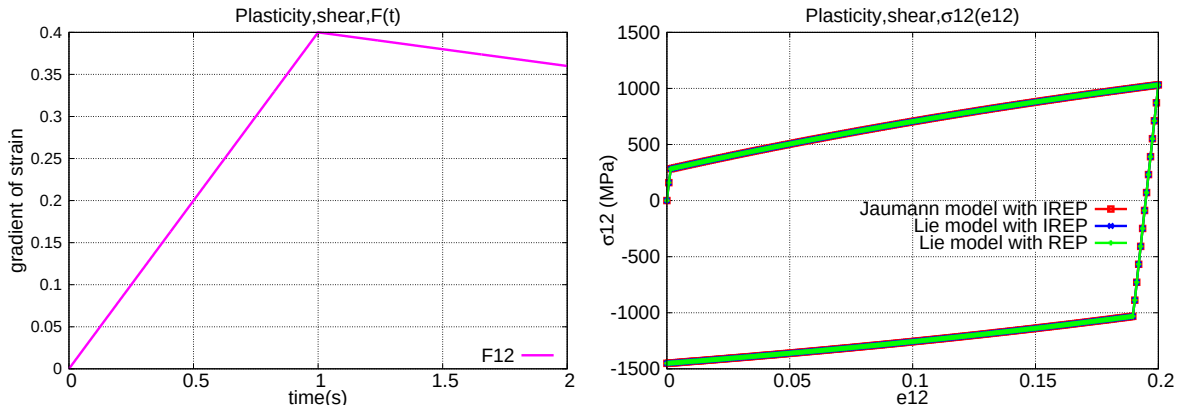

Figure F.2: Stress-strain curve for a loading/unloading cycle considering an important total deformation. The maximal value of b/a reaches 0.4 and is next lowered to 0.36 as defined in Figure 6.1.

Bibliography

[Adélaïde et al., 2003a] Adélaïde, L., Jourdan, F., and Bhatier, C. (2003a). Frictional contact solver and mesh adaptation in space-time finite element method. *European Journal of Mechanics - A/Solids*, 22(4):633–647.

[Adélaïde et al., 2003b] Adélaïde, L., Jourdan, F., and Bhatier, C. (2003b). Méthodes des éléments finis espace-temps et remaillage. *Revue Européenne des Éléments*, 12(4):427–458.

[Anderson and Kimn, 2007] Anderson, M. and Kimn, J. H. (2007). A numerical approach to space-time finite elements for the wave equation. *Journal of Computational Physics*, 226(1):466–476.

[Andersson and Comer, 2007] Andersson, N. and Comer, G. (2007). Relativistic fluid dynamics: Physics for many different scales. *Living Reviews in Relativity*, 10.

[Badreddine, 2006] Badreddine, H. (2006). *Elastoplasticité anisotrope endommageable en grandes déformations : aspects théoriques, numériques et applications*. PhD thesis. Thèse de doctorat dirigée par Dogui, Abdelwaheb et Saanouni, Khémais Systèmes mécaniques et matériaux Troyes 2006.

[Badreddine et al., 2010] Badreddine, H., Saanouni, K., and Dogui, A. (2010). On non-associative anisotropic finite plasticity fully coupled with isotropic ductile damage for metal forming. *International Journal of Plasticity*, 26(11):1541 – 1575.

[Barbera and Müller, 2006] Barbera, E. and Müller, I. (2006). Inherent frame dependence of thermodynamic fields in a gas. acta mechanica. *Acta Mechanica*, 184(1-4):205–216.

[Belytschko et al., 2000] Belytschko, T., Liu, W. K., and Moran, B. (2000). *Nonlinear Finite Elements for Continua and Structures*. Wiley.

[Bertram, 2012] Bertram, A. (2012). *Elasticity and Plasticity of Large Deformations*. Springer, third edition edition.

[Besson et al., 2009] Besson, J., Cailletaud, G., Chaboche, J. L., and Forest, S. (2009). *Non-Linear Mechanics of Materials*. Springer.

[Biscari and Cercignani, 1997] Biscari, P. and Cercignani, C. (1997). Stress and heat flux in non-inertial reference frames. *Continuum Mechanics and Thermodynamics*, 9(1):1–11.

[Biscari et al., 2000] Biscari, P., Cercignani, C., and Slemrod, M. (2000). Time-derivatives and frame-invariance beyond newtonian fluids. *Comptes Rendus de l'Academie des Sciences. Serie IIB-Mechanics*, 328(5):417–422.

[Boehler, 1978] Boehler, J. P. (1978). Anisotropic constitutive equations for continuous media. [lois de comportement anisotrope des milieux continus]. *J Mec*, 17(2):153–190.

[Bonet and Wood, 1997] Bonet, J. and Wood, R. D. (1997). *Nonlinear continuum mechanics for finite element analysis*. Cambridge university press.

[Boratav and Kerner, 1991] Boratav, M. and Kerner, R. (1991). *Relativité*. Ellipses.

[Borja, 2013] Borja, R. I. (2013). *Plasticity*. Springer-Verlag.

[Bressan, 1963] Bressan, A. (1963). Cinematica dei sistemi continui in relatività generale. *Annali di matematica pura ed applicata*, 61(1):99–148.

[Capurro, 1983] Capurro, M. (1983). A general field theory of cauchy continuum: Classical mechanics. *Acta Mechanica*, 49(3-4):169–190.

[Cauchy, 1829] Cauchy, A.-L. (1829). Sur l'équilibre et le mouvement intérieur des corps considérés comme des masses continues. *Ex. de Math*, 4:293–319.

[Chaboche, 2008] Chaboche, J. (2008). A review of some plasticity and viscoplasticity constitutive theories. *International Journal of Plasticity*, 24(10):1642 – 1693. Special Issue in Honor of Jean-Louis Chaboche.

[Choquet-Bruhat, 1968] Choquet-Bruhat, Y. (1968). *Géométrie différentielle et systèmes extérieurs*. Dunod.

[Collino et al., 2006] Collino, F., Fouquet, T., and Joly, P. (2006). Conservative space-time mesh refinement methods for the fdtd solution of maxwell's equations. *Journal of Computational Physics*, 211(1):9–35.

[Crisfield and Jelenić, 1999] Crisfield, M. A. and Jelenić, G. (1999). Objectivity of strain measures in the geometrically exact three-dimensional beam theory and its finite-element implementation. In *Proceedings of the Royal Society of London A: Mathematical, Physical and Engineering Sciences*, volume 455, pages 1125–1147. The Royal Society.

[Dafalias and Younis, 2007] Dafalias, Y. F. and Younis, B. A. (2007). Objective tersorial representation of the pressure-strain correlations of turbulence. *Mechanics Research Communications*, 34:319–324.

[Dafalias and Younis, 2009] Dafalias, Y. F. and Younis, B. A. (2009). Objective model for the fluctuating pressure-strain-rate correlations. *Journal of Engineering Mechanics*, 135:1006–1014.

[De Socio and Marino, 2002] De Socio, L. and Marino, L. (2002). Reference frame influence on transport phenomena in gases. a direct simulations approach. *Computers & Mathematics with Applications*, 44(8):1201–1206.

[De Souza Neto et al., 2011] De Souza Neto, E. A., Peric, D., and Owen, D. R. J. (2011). *Computational methods for plasticity: theory and applications*. John Wiley & Sons.

[Dienes, 1979] Dienes, J. K. (1979). On the analysis of rotation and stress rate in deforming bodies. *Acta mechanica*, 32(4):217–232.

[Dogui, 1989] Dogui, A. (1989). *Plasticité anisotrope en grandes déformations*. PhD thesis, Université Claude Bernard-Lyon I.

[Duszek and Perzyna, 1991] Duszek, M. K. and Perzyna, P. (1991). The localization of plastic deformation in thermoplastic solids. *International Journal of Solids and Structures*, 27(11):1419–1443.

[Eckart, 1940] Eckart, C. (1940). The thermodynamics of irreversible processes. iii. relativistic theory of the simple fluid. *Phys. Rev.*, 58:919–924.

[Edelen, 1967] Edelen, D. G. (1967). Lorentz invariance, momentum-energy tensors and the mhd problem. *International Journal of Engineering Science*, 5(3):235–250.

[Epstein et al., 2006] Epstein, M., Burton, D. A., and Tucker, R. (2006). Relativistic anelasticity. *Classical and quantum gravity*, 23(10):3545.

[Erdmenger and Osborn, 1997] Erdmenger, J. and Osborn, H. (1997). Conserved currents and the energy-momentum tensor in conformally invariant theories for general dimensions. *Nuclear Physics B*, 483(1):431–474.

[Eringen, 1962] Eringen, A. C. (1962). *Nonlinear Theory of Continous Media*. McGraw-Hill.

[Ernst&Young, 2006] Ernst&Young (2006). Etude sur les enjeux et priorités en matière d'innovation dans la filière plasturgie. Online, Ministére de l'Économie des Finances et de l'Industrie, DGE.

[Ferrarese and Bini, 2008] Ferrarese, G. and Bini, D. (2008). Relativistic kinematics for a three-dimensional continuum. In *Introduction to Relativistic Continuum Mechanics*, pages 169–206. Springer.

[Fiala, 2004] Fiala, Z. (2004). Time derivative obtained by applying the riemannian manifold of riemannian metrics to kinematics of continua. *Comptes Rendus Mecanique*, 332(2):97–102.

[Frewer, 2009] Frewer, M. (2009). More clarity on the concept of material frame-indifference in classical continuum mechanics. *Acta Mechanica*, 202(1-4):213–246.

[Fukuma and Sakatani, 2011] Fukuma, M. and Sakatani, Y. (2011). Relativistic viscoelastic fluid mechanics. *Physical Review E - Statistical, Nonlinear, and Soft Matter Physics*, 84(2).

[Garrigues, 2007] Garrigues (2007). *Fondements de la Mécanique des Milieux Continous*. Hermès Science Pulications.

[Gostiaux, 2005] Gostiaux, B. (2005). *Géométrie différentielle: variétés, courbes et surfaces*. Presses Universitaires de France.

[Green and Naghdi, 1965] Green, A. E. and Naghdi, P. M. (1965). A general theory of an elastic-plastic continuum. *Archive for rational mechanics and analysis*, 18(4):251–281.

[Grot and Eringen, 1966] Grot, R. A. and Eringen, A. (1966). Relativistic continuum mechanics part i - mechanics and thermodynamics. *International Journal of Engineering Science*, 4(6):611 – 638.

[Gurtin, 1982] Gurtin, M. E. (1982). *An introduction to continuum mechanics*, volume 158. Academic press.

[Hallquist et al., 2007] Hallquist, J. O. et al. (2007). Ls-dyna keyword user's manual. *Livermore Software Technology Corporation*, 970.

[Havas, 1964] Havas, P. (1964). Four-dimensional formulations of newtonian mechanics and their relation to the special and the general theory of relativity. *Reviews of Modern Physics*, 36(4):938.

[Hibbitt et al., 1997] Hibbitt, Karlsson, and Sorensen (1997). *ABAQUS: Theory Manual*, volume 2. Hibbitt, Karlsson & Sorensen.

[Hill, 1959] Hill, R. (1959). Some basic principles in the mechanics of solids without a natural time. *Journal of the Mechanics and Physics of Solids*, 7(3):209 – 225.

[Hill, 1983] Hill, R. (1983). *The mathematical theory of plasticity*. Clarendon Press.

[Hiscock and Lindblom, 1983] Hiscock, W. A. and Lindblom, L. (1983). Stability and causality in dissipative relativistic fluids. *Annals of Physics*, 151(2):466–496.

[Hiscock and Lindblom, 1985] Hiscock, W. A. and Lindblom, L. (1985). Generic instabilities in first-order dissipative relativistic fluid theories. *Physical Review D*, 31(4):725.

[Hiscock and Lindblom, 1987] Hiscock, W. A. and Lindblom, L. (1987). Linear plane waves in dissipative relativistic fluids. *Physical Review D*, 35(12):3723.

[Israel, 1989] Israel, W. (1989). Covariant fluid mechanics and thermodynamics: An introduction. In Anile, A. and Choquet-Bruhat, Y., editors, *Relativistic Fluid Dynamics*, volume 1385, pages 152–210. Springer Berlin Heidelberg.

[Israel and Stewart, 1979a] Israel, W. and Stewart, J. (1979a). On transient relativistic thermodynamics and kinetic theory. ii. In *Proceedings of the Royal Society of London A: Mathematical, Physical and Engineering Sciences*, volume 365, pages 43–52. The Royal Society.

[Israel and Stewart, 1979b] Israel, W. and Stewart, J. (1979b). Transient relativistic thermodynamics and kinetic theory. *Annals of Physics*, 118(2):341–372.

[Jaumann, 1911] Jaumann, G. (1911). Geschlossenes system physikalischer und chemischer differentialgesetze. *Sitzungsberichte Akad. Wiss. Wien, IIa*, pages 385–530.

[Jou et al., 1988] Jou, D., Casas-Vázquez, J., and Lebon, G. (1988). Extended irreversible thermodynamics. *Reports on Progress in Physics*, 51(8):1105.

[Kerner, 2014] Kerner, R. (2014). Ellipses.

[Khan and Huang, 1995] Khan, A. S. and Huang, S. (1995). *Continuum Theory of Plasticity*. John Wiley & Sons, Inc.

[Kienzler and Herrmann, 2003] Kienzler, R. and Herrmann, G. (2003). On the four-dimensional formalism in continuum mechanics. *Acta Mechanica*, 161:103–125.

[Kijowski and Magli, 1997] Kijowski, J. and Magli, G. (1997). Unconstrained variational principle and canonical structure for relativistic elasticity. *Reports on mathematical physics*, 39(1):99–112.

[Kojić and Bathe, 1987] Kojić, M. and Bathe, K.-J. (1987). Studies of finite element procedures–stress solution of a closed elastic strain path with stretching and shearing using the updated lagrangian jaumann formulation. *Computers & Structures*, 26(1):175–179.

[Labergère et al., 2009] Labergère, C., Saanouni, K., and Lestriez, P. (2009). Numerical design of extrusion process using finite thermo-elastoviscoplasticity with damage. prediction of chevron shaped cracks. In *Key Engineering Materials*, volume 424, pages 265–272. Trans Tech Publ.

[Lamoureux-Brousse, 1989] Lamoureux-Brousse, L. (1989). Infinitesimal deformations of finite conjugacies in non-linear classical or general relativistic therory of elasticity. *Physica D*, 35:203–219.

[Landau and Lifshitz, 1975] Landau, L. D. and Lifshitz, E. M. (1975). *The Classical Theory of Fields*. Elsevier, fourth edition edition.

[Landau and Lifshitz, 1976] Landau, L. D. and Lifshitz, E. M. (1976). *Mechanics*. Pergamon Press.

[Landau and Lifshitz, 1987] Landau, L. D. and Lifshitz, E. M. (1987). *Fluid Mechanics*. Elsevier, second edition edition.

[Lee, 1969] Lee, E. H. (1969). Elastic-plastic deformation at finite strains. *Journal of Applied Mechanics*, 36(1):1–6.

[Lee, 2003] Lee, J. M. (2003). Smooth manifolds. In *Introduction to Smooth Manifolds*, pages 1–29. Springer.

[Lemaitre and Chaboche, 1994] Lemaitre, J. and Chaboche, J.-L. (1994). *Mechanics of solid materials*. Cambridge university press.

[Levi-Civita et al., 2005] Levi-Civita, T., Persico, E., and Long, M. (2005). *The absolute differential calculus*. Dover Phoenix Edition.

[Lichnerowicz, 2013] Lichnerowicz, A. (2013). *Magnetohydrodynamics: waves and shock waves in curved space-time*, volume 14. Springer Science & Business Media.

[Liu, 2004] Liu, I. S. (2004). On euclidean objectivity and the principle of material frame-indifference. *Continuum Mechanics and Thermodynamics*, 16:177–183.

[Liu, 2005] Liu, I. S. (2005). Further remarks on euclidean objectivity and the principle of material frame-indifference. *Continuum Mechanics and Thermodynamics*, 17:125–133.

[Lubarda, 2002] Lubarda, V. A. (2002). *Elastoplasticity Theory*. CRC Press.

[Malvern, 1969] Malvern, L. E. (1969). *Introduction to the Mechanics of a Continuous Medium*. Number Monograph.

[Mandel, 1983] Mandel, J. (1983). Sur la definition de la vitesse de deformation elastique en grande transformation elastoplastique. *International Journal of Solids and Structures*, 19(7):573 – 578.

[Marques and Creus, 2012] Marques, S. P. and Creus, G. J. (2012). *Computational viscoelasticity*. Springer Science & Business Media.

[Marsden and Hughes, 1994] Marsden, J. E. and Hughes, T. J. (1994). *Mathematical foundations of elasticity*. Courier Corporation.

[Matolcsi and Ván, 2006] Matolcsi, T. and Ván, P. (2006). Can material time derivative be objective? *Physics Letters A*, 353(2):109–112.

[Matolcsi and Ván, 2007] Matolcsi, T. and Ván, P. (2007). Absolute time derivatives. *Journal of mathematical physics*, 48(5):053507.

[Maugin, 1971a] Maugin, G. (1971a). Champ des déformations d'un milieu continu dans l'espace-temps de minkowski. *CR Acad. Sci. Paris A*, 273:65–68.

[Maugin, 1971b] Maugin, G. (1971b). Un modèle viscoélastique en relativité générale. *Compt. Rendus Acad. Sci A*, 272:1482–1484.

[Maugin, 1992] Maugin, G. A. (1992). Applications of an energy-momentum tensor in nonlinear elastodynamics: pseudomomentum and eshelby stress in solitonic elastic systems. *Journal of the Mechanics and Physics of Solids*, 40(7):1543–1558.

[Meyers et al., 2000] Meyers, A., Schieße, P., and Bruhns, O. (2000). Some comments on objective rates of symmetric eulerian tensors with application to eulerian strain rates. *Acta mechanica*, 139(1-4):91–103.

[Misner et al., 1973] Misner, C. W., Thorne, K. S., and Wheeler, J. A. (1973). *Gravitation*. W. H. Freeman and Co Ltd.

[Moller, 1972] Moller, C. (1972). The theory of relativity. clarendon.

[Murdoch, 1983] Murdoch, A. I. (1983). On materials frame-indifference, intrinsic spin, and certain constitutive relations motivated by the kinetic theory of gases. *Archive for Rational Mechanics and Analysis*, 83(2):185–194.

[Murdoch, 2003] Murdoch, A. I. (2003). Objectivity in classical continuum physics: a rationale for discarding the 'principle of invariance under superposed rigid body motions' in favour of purely objective considerations. *Continuum Mechanics and Thermodynamics*, 15:309–320.

[Murdoch, 2005] Murdoch, A. I. (2005). On criticism of the nature of objectivity in classical continuum physics. *Continuum Mechanics and Thermodynamics*, 17:135–148.

[Murdoch, 2006] Murdoch, A. I. (2006). Some primitive concepts in continuum mechanics regarded in terms of objective space-time molecular averaging: The key role played by inertial observers. *Journal of Elasticity*, 84:69–97.

[Muschik, 2012] Muschik, W. (2012). Is the heat flux density really non-objective? a glance back, 40 years later. *Continuum Mechanics and Thermodynamics*, 24(4-6):333–337.

[Muschik and Restuccia, 2008] Muschik, W. and Restuccia, L. (2008). Systematic remarks on objectivity and frame-indifference, liquid crystal theory as an example. *Archive of Applied Mechanics*, 78:837–854.

[Muschik and von Borzeszkowski, 2015] Muschik, W. and von Borzeszkowski, H.-H. (2015). Entropy production and equilibrium conditions in general-covariant continuum physics. *Journal of Non-Equilibrium Thermodynamics*, 40(3):131–138.

[Nemat-Nasser, 1972] Nemat-Nasser, S. (1972). On variational methods in finite and incremental elastic deformation problems with discontinuous fields. *Quart. Appl. Math*, 30(2):143–156.

[Nemat-Nasser, 1974] Nemat-Nasser, S. (1974). General variational principles in nonlinear and linear elasticity with applications. *Mechanics today.*, 1:214–261.

[Nemat-Nasser, 1979] Nemat-Nasser, S. (1979). Decomposition of strain measures and their rates in finite deformation elastoplasticity. *International Journal of Solids and Structures*, 15(2):155 – 166.

[Nemat-Nasser, 1982] Nemat-Nasser, S. (1982). On finite deformation elasto-plasticity. *International Journal of Solids and Structures*, 18(10):857 – 872.

[Nemat-Nasser, 2004] Nemat-Nasser, S. (2004). *Plastic: A Treatise on Finite Deformation of Heterogeneous Inelastic Materials*. Cambridge university press.

[Noll, 1955] Noll, W. (1955). On the continuity of the solids and fluids states. *Journal of Rational Mechanics and Analysis*, 4:3–81.

[Oden, 1969a] Oden, J. T. (1969a). A general theory of finite elements. i. topological considerations. *International Journal for Numerical Methods in Engineering*, 1(2):205–221.

[Oden, 1969b] Oden, J. T. (1969b). A general theory of finite elements. ii. applications. *International Journal for Numerical Methods in Engineering*, 1(3):247–259.

[Oldroyd, 1950] Oldroyd, J. G. (1950). On the formulation of rheological equations of state. *Proceedings of the Royal Society of London. Series A. Mathematical and Physical Sciences*, 200(1063):523–541.

[Osakada, 2010] Osakada, K. (2010). History of plasticity and metal forming analysis. *Journal of Materials Processing Technology*, 210(11):1436 – 1454.

[Öttinger, 1998a] Öttinger, H. C. (1998a). On the structural compatibility of a general formalism for nonequilibrium dynamics with special relativity. *Physica A: Statistical Mechanics and its Applications*, 259(1):24–42.

[Öttinger, 1998b] Öttinger, H. C. (1998b). Relativistic and nonrelativistic description of fluids with anisotropic heat conduction. *Physica A: Statistical Mechanics and its Applications*, 254(3):433–450.

[Prost-Domasky et al., 1997] Prost-Domasky, S., Szabo, B., and Zahalak, G. (1997). Large-deformation analysis of nonlinear elastic fluids. *Computers & structures*, 64(5):1281–1290.

[Rougée, 1992] Rougée, P. (1992). Kinematics of finite deformations. *Archives of Mechanics*, 44(1):117–132.

[Rougée, 1997] Rougée, P. (1997). *Mécanique des grandes transformations*. Springer.

[Rouhaud et al., 2013] Rouhaud, E., Panicaud, B., and Kerner, R. (2013). Canonical frame-indifferent transport operators with the four-dimensional formalism of differential geometry. *Computational Materials Science*, 77(0):120 – 130.

[Saanouni and Lestriez, 2009] Saanouni, K. and Lestriez, P. (2009). Modelling and numerical simulation of ductile damage in bulk metal forming. *Steel Research International*, 80(9):645–657.

[SAFRAN, 2009] SAFRAN (2009). Dossier: la recherche au coeur de safran. SAFRAN magazine.

[Salençon, 2012] Salençon, J. (2012). *Handbook of Continuum Mechanics: General Concepts Thermoelasticity*. Springer Science & Business Media.

[Schellstede et al., 2014] Schellstede, G., von Borzeszkowski, H.-H., Chrobok, T., and Muschik, W. (2014). The relation between relativistic and non-relativistic continuum thermodynamics. *General Relativity and Gravitation*, 46(1).

[Schieck and Stumpf, 1993] Schieck, B. and Stumpf, H. (1993). Deformation analysis for finite elastic-plastic strains in a lagrangean-type description. *International journal of solids and structures*, 30(19):2639–2660.

[Schouten, 1954] Schouten, J. A. (1954). *Ricci-Calculus: An Introduction to Tensor Analysis and Its Geometrical Applications*. Springer-Verlag.

[Schuster, 2010] Schuster, F. (2010). Les matériaux au coeur du processus d'innovation, enjeux, avenues de progress et priorités du programme transversal sur les matériaux avancés au cea. Cléf CEA, 59.

[Shutov and Ihlemann, 2014] Shutov, A. and Ihlemann, J. (2014). Analysis of some basic approaches to finite strain elasto-plasticity in view of reference change. *International Journal of Plasticity*, 63(0):183 – 197. Deformation Tensors in Material Modeling in Honor of Prof. Otto T. Bruhns.

[Sidoroff, 1982a] Sidoroff, F. (1982a). Cours sur les grandes déformations. *rapport GRECO*, 51.

[Sidoroff, 1982b] Sidoroff, F. (1982b). Incremental constitutive equation for large strain elasto plasticity. *International Journal of Engineering Science*, 20(1):19–26.

[Sidoroff and Dogui, 2001] Sidoroff, F. and Dogui, A. (2001). Some issues about anisotropic elastic-plastic models at finite strain. *International Journal of Solids and Structures*, 38(52):9569 – 9578.

[Simo and Ortiz, 1985] Simo, J. and Ortiz, M. (1985). A unified approach to finite deformation elastoplastic analysis based on the use of hyperelastic constitutive equations. *Computer methods in applied mechanics and engineering*, 49(2):221–245.

[Speziale, 1987] Speziale, C. G. (1987). Comments on the "material frame-indifference" controversy. *Physical Review A*, 36(9):4522.

[Spivak, 1999] Spivak, M. (1999). A comprehensive introduction to differential geometry.

[Stumpf and Badur, 1990] Stumpf, H. and Badur, J. (1990). On missing links of rate-independent elasto-plasticity at finite strains. *Mechanics Research Communications*, 17:353–364.

[Stumpf and Hoppe, 1997] Stumpf, H. and Hoppe, U. (1997). The application of tensor algebra on manifolds to nonlinear continuum mechanics–invited survey article. *ZAMM-Journal of Applied Mathematics and Mechanics/Zeitschrift für Angewandte Mathematik und Mechanik*, 77(5):327–339.

[Svendsen and Bertram, 1999] Svendsen, B. and Bertram, A. (1999). On frame-indifference and form-invariance in constitutive theory. *Acta Mechanica*, 132(1-4):195–207.

[Synge, 1960] Synge, J. (1960). *Relativity: the general therory.* Elsevier.

[Takahashi, 1986] Takahashi, Y. (1986). Energy-momentum tensors in relativistic and non-relativistic classical field theory. *Fortschritte der Physik*, 34(5):323–344.

[Talpaert, 2000] Talpaert, Y. (2000). *Differential geometry with applications to mechanics and physics.* CRC Press.

[Thiffeault, 2001] Thiffeault, J. L. (2001). Covariant time derivative for dynamics systems. *Journal of Physics A*, 2001:1–16.

[Tolman, 1930] Tolman, R. C. (1930). On the use of the entropy principle in general relativity. *Physical Review*, 35(8):896.

[Tremblay et al., 2003] Tremblay, P., Bourgault, Y., and Tavoularis, S. (2003). Control of discretization error for time-continuous space–time fem through mesh movement. *Computational Fluid and Solid Mechanics*, pages 2156–2159.

[Truesdell, 1955] Truesdell, C. (1955). The simplest rate theory of pure elasticity. *Communications on pure and applied mathematics*, 8(1):123–132.

[Truesdell, 1966] Truesdell, C. (1966). *The elements of continuum mechanics*. Springer-Verlag.

[Truesdell and Noll, 2003] Truesdell, C. and Noll, W. (2003). *The Non-Linear Field Theories of Mechanics*. Springer, third edition.

[Tsallis et al., 1995] Tsallis, C., Levy, S. V., Souza, A. M., and Maynard, R. (1995). Statistical-mechanical foundation of the ubiquity of lévy distributions in nature. *Physical Review Letters*, 75(20):3589.

[Valanis, 2003] Valanis, K. C. (2003). Elasticity of space-time: Basis of newton's 2nd law of motion. *Journal of engineering mechanics*, 129(9):1039–1047.

[Vanderheaegen, 2011] Vanderheaegen, D. (2011). Simulation des matériauxriaux en conditions extremes: l'approche multi-échelles, du microscopique à la simulation des procédés. CEA DIF DPTA.

[Venturi, 2009] Venturi, D. (2009). Convective derivatives and reynolds transport in curvilinear time-dependent coordinates. *Journal of Physics A: Mathematical and Theoretical*, 42(12):125203.

[Volokh, 2013] Volokh, K. (2013). An approach to elastoplasticity at large deformations. *European Journal of Mechanics - A/Solids*, 39(0):153 – 162.

[Voyiadjis and Kattan, 1989] Voyiadjis, G. Z. and Kattan, P. I. (1989). Eulerian constitutive model for finite deformation plasticity with anisotropic hardening. *Mechanics of Materials*, 7(4):279–293.

[Weinberg, 1972] Weinberg, S. (1972). *Gravitation and cosmology: principles and applications of the general theory of relativity*, volume 1. Wiley New York.

[Williams, 1989] Williams, D. N. (1989). The elastic energy momentum tensor in special relativity. *Annals of Physics*, 196(2):345–360.

[Wineman, 2009] Wineman, A. (2009). Nonlinear viscoelastic solids-a review. *Mathematics and Mechanics of Solids*, 14(3):300–366.

[Xiao et al., 2000a] Xiao, H., Bruhns, O., and Meyers, A. (2000a). A consistent finite elastoplasticity theory combining additive and multiplicative decomposition of the stretching and the deformation gradient. *International Journal of Plasticity*, 16(2):143 – 177.

[Xiao et al., 2000b] Xiao, H., Bruhns, O. T., and Meyers, A. (2000b). The choice of objective rates in finite elastoplasticity: general results on the uniqueness of the logarithmic rate. *Proceedings of the Royal Society of London A: Mathematical, Physical and Engineering Sciences*, 456(2000):1865–1882.

[Yavari and Ozakin, 2008] Yavari, A. and Ozakin, A. (2008). Covariance in linearized elasticity. *Zeitschrift für angewandte Mathematik und Physik*, 59(6):1081–1110.

[Zahalak, 1992] Zahalak, G. (1992). Cours de mécanique des milieux continus. Washington University in Saint-Louis.

[Zaremba, 1903] Zaremba, S. (1903). Sur une forme perfectionnée de la théorie de la relaxation. *Bull. Int. Acad. Sci. Cracovie*, 124:594–614.

[Zaremba, 1937] Zaremba, S. (1937). Sur une conception nouvelle des forces intérieures dans un fluide en mouvement. *Mémorial des sciences mathématiques*, 82:1–85.

Résumé extensif en Français

1 Introduction

Pour établir les modèles de comportement mécaniques pour les matériaux en grandes déformations, il faut respecter notamment le principe d'objectivité. C'est un critère classique en mécanique des milieux continus pour s'assurer que le modèle de comportement vérifie les faits physiques suivants.

- Indépendance au changement d'observateurs (ou référentiels): lorsqu'un observateur se déplace autour d'un matériau non déformé, aucune contrainte supplémentaire n'est générée dans le matériau, quel que soit le mouvement de l'observateur.

- Invariance à la superposition de mouvement de corps rigide: quand un matériau non déformé est sollicité par un mouvement de corps rigide, aucune contrainte supplémentaire n'est générée dans le matériau.

Dans le cadre des approches classiques en 3D, les deux notions d'objectivité sont ambigüees et ne peuvent pas être distinguées.

De plus, une formulation en variation est souvent utilisée pour établir les modèles incrémentaux de comportement, tels que l'hypoélasticité, l'élastoplasticité. Dans ce cas, une dérivée objective est nécessaire. En 3D, de nombreuses dérivées objectives ont été proposées, mais la difficulté reste la sélection de ces dérivées objectives pour construire un modèle incrémental cohérent.

Dans le cadre du formalisme quadridimensionnel que nous proposons et issu de la théorie de la Relativité, les deux notions d'objectivité peuvent être clairement distinguées. Par ailleurs, ce formalisme quadridimensionnel issu de la théorie de la Relativité garantit que les tenseurs, les opérations et tous les modèles physiques sont par construction covariants (indépendants du référentiel) en accord avec le principe de covariance. En outre, l'utilisation de ce formalisme permet également de définir une dérivée spécifique, la dérivée de Lie, qui correspond à une variation totale par rapport au temps. Elle est tout à la fois covariante et invariante à la superposition des mouvements de corps rigide.

L'un des objectifs de ce travail est de proposer un cadre thermodynamique en 4D pour développer des modèles de comportement en 4D tels que l'hyperélasticité, l'élasticité anisotrope, l'hypoélasticité et l'élastoplasticité. Ensuite, les projections en 3D sont obtenues à partir des modèles en 4D et étudiées en les testant sur des simulations numériques par éléments finis avec le logiciel Zset©.

2 Formalisme 4D et cinématique 4D

Dans le formalisme 4D, les coordonnées sont représentées par un ensemble de quatre nombres.

$$\xi^\mu = (\xi^1, \xi^2, \xi^3, \xi^4) = (\xi^i, ct). \tag{1}$$

Les trois premières coordonnées correspondent à la position dans l'espace 3D, et la dernière est le temps t multiplié par la vitesse de lumière c. En 4D, le changement d'observateur ou de référentiel est équivalent à un changement de coordonnées. Selon le principe de covariance, un quelconque tenseur 4D $\boldsymbol{\tau}$ vérifient alors les relations suivantes:

$$\widetilde{\tau}^{\mu\nu} = \left|\frac{\partial \xi^\alpha}{\partial \widetilde{\xi}^\beta}\right|^W \frac{\partial \widetilde{\xi}^\mu}{\partial \xi^\lambda}\frac{\partial \widetilde{\xi}^\nu}{\partial \xi^\kappa}\tau^{\lambda\kappa} \tag{2a}$$

$$\widetilde{\tau}_{\mu\nu} = \left|\frac{\partial \xi^\alpha}{\partial \widetilde{\xi}^\beta}\right|^W \frac{\partial \xi^\lambda}{\partial \widetilde{\xi}^\mu}\frac{\partial \xi^\kappa}{\partial \widetilde{\xi}^\nu}\tau_{\lambda\kappa}, \tag{2b}$$

lorsque le système de coordonnées change à partir de ξ^α à $\tilde{\xi}^\alpha$.

Dans un formalisme 4D, les tenseurs de déformation peuvent équalement être définis.

La généralisation 4D de l'inverse du tenseur de déformation de Cauchy-Green gauche est:

$$b_{\mu\nu} = F'^{\alpha}_{\ \mu} F'^{\beta}_{\ \nu} G_{\alpha\beta} \tag{3}$$

Ensuite, le tenseur de déformation de Euler-Almansi peut alors être généralisé en:

$$e_{\mu\nu} = \frac{1}{2}(g_{\mu\nu} - b_{\mu\nu}) \tag{4}$$

Dans les définitions de ces tenseurs de déformation, $F'^{\mu}_{\ \alpha}$ est l'inverse du gradient de déformation $F^{\mu}_{\ \alpha}$, et $g_{\mu\nu}$ et $G_{\mu\nu}$ sont les métriques. Ensuite, les tenseurs du gradient de vitesse $\boldsymbol{L}$, du taux de déformation $\boldsymbol{d}$ et du taux de rotation $\boldsymbol{\omega}$ peuvent être obtenus:

$$L^{\mu}_{\ \nu} = \nabla_\nu u^\mu = \frac{\partial u^\mu}{\partial \xi^\nu} + \Gamma^{\mu}_{\kappa\nu} u^\kappa, \tag{5}$$

$$d^{\mu}_{\ \nu} = \frac{1}{2}(\nabla_\nu u^\mu + \nabla_\mu u^\nu) \tag{6}$$

$$\omega^{\mu}_{\ \nu} = \frac{1}{2}(\nabla_\nu u^\mu - \nabla_\mu u^\nu). \tag{7}$$

où $\nabla_\nu(.)$ est la dérivée covariante. Les composantes de la dérivée covariante 4D d'un tenseur d'ordre deux sont calculées comme:

$$\nabla_\lambda \tau^{\mu\nu} = \frac{\partial \tau^{\mu\nu}}{\partial \xi^\lambda} + \Gamma^{\mu}_{\kappa\lambda}\tau^{\kappa\nu} + \Gamma^{\nu}_{\kappa\lambda}\tau^{\mu\kappa} - W\Gamma^{\kappa}_{\kappa\lambda}\tau^{\mu\nu}, \tag{8}$$

avec $\Gamma^{\alpha}_{\beta\gamma}$ les symboles de Christoffel de seconde espèce.

3 Thermodynamique en 4D

Les transformations thermomécaniques subies par un matériau sont régies par les conservations et l'inégalités de grandeurs qui seront introduites dans cette section. Ce sont les équations des conservations de la masse, de la quantité de mouvement, du moment angulaire et de l'énergie ainsi que l'inégalité de Clausius-Duhem. En 4D, le tenseur moment-énergie $T^{\mu\nu}$, le vecteur de courant de particules n^μ et le vecteur d'entropie $\mathscr{S}^\mu$ sont utilisés pour constituer les équations de conservation et l'inégalité de Clausius-Duhem. Les trois

variables précédentes peuvent être décomposées comme:

$$\begin{cases} T^{\mu\nu} = \rho c^2 u^\mu u^\nu + q^\mu u^\nu + q^\nu u^\mu + T_\sigma^{\mu\nu} \\ n^\mu \quad = n u^\mu \\ \mathscr{S}^\mu = \rho \eta u^\mu + \frac{q^\mu + q^\nu u^\mu u_\nu}{\theta}, \end{cases} \tag{9}$$

où ρ est la densité de masse, c est la vitesse de la lumière, q^μ est le vecteur flux de chaleur, u^μ est la quadri-vitesse, $T_\sigma^{\mu\nu}$ est le tenseur moment-énergie mécanique, n est la densité du nombre de particules, η est la densité d'entropie et θ est la température. En mécanique relativiste des milieux continus, le tenseur moment-énergie mécanique peut être relié au tenseur des contraintes de Cauchy de différentes façons. Nous en proposons une écriture originale dans cette thèse. Ainsi sa quatrième composante est égal à zéro dans un référentiel propre. Il ne convient pas d'appliquer ce choix du tenseur de contrainte dans la modélisation de comportement, car nous voulons une forme projetée en 3D équivalente à celle obtenue habituellement. Donc, on propose d'utiliser un choix du tenseur de contrainte $\sigma^{\mu\nu}$ qui vérifie la relation suivante:

$$T_\sigma^{\mu\nu} = \sigma^{\mu\nu} - \sigma^{\mu\alpha} u_\alpha u^\nu - \sigma^{\nu\alpha} u_\alpha u^\mu + \sigma^{\alpha\beta} u_\alpha u_\beta u^\mu u^\nu, \tag{10}$$

Les conservations peuvent alors être exprimées comme:

$$\begin{cases} \nabla_\mu n^\mu = 0 \\ \nabla_\nu T^{\mu\nu} = 0 \\ T^{\mu\nu} = T^{\nu\mu} \\ \theta \nabla_\mu \mathscr{S}^\mu - u_\mu \nabla_\nu T^{\mu\nu} \geq 0 \end{cases} \tag{11}$$

La conservation $\nabla_\nu T^{\mu\nu} = 0$ représente à la fois la conservation de la quantité de mouvement et de l'énergie. Il contient quatre équations, dont les trois premières sont la conservation de la quantité de mouvement et dont la dernière est la conservation de l'énergie.

Dans l'hypothèse Newtonienne, en supposant la vitesse petite par rapport à celui de la lumière, la conservation $\nabla_\nu T^{\mu\nu} = 0$ conduit alors aux équations suivantes, projetées en 3D puis sur le temps:

$$\rho \frac{dv^i}{dt} + \nabla_j \sigma^{ij} = 0, \tag{12}$$

et

$$\rho\frac{d}{dt}(\frac{v^2}{2}+e)-\nabla_i(\sigma^{ij}v_j)=0, \tag{13}$$

où e est la densité de l'énergie interne.

Dans l'hypothèse Newtonienne, l'inégalité de Clausius-Duhem est calculée comme:

$$-\rho\left(\mathscr{L}_u(\Psi)-\eta\mathscr{L}_u(\theta)\right)-\frac{q^\mu}{\theta}\nabla_\mu\theta+\sigma^{\mu\nu}d_{\mu\nu}\geq 0, \tag{14}$$

qui sert à établir les modèles de comportement en 4D. Dans l'Eq. 14, $d_{\mu\nu}$ est le taux de déformation, Ψ est l'énergie libre spécifique de Helmholtz et $\mathscr{L}_u(.)$ est la dérivée de Lie. La dérivée de Lie d'un scalaire a avec le poids W, et d'un tenseur $\boldsymbol{\tau}$ avec ses composantes covariantes $\tau_{\mu\nu}$ et contravariantes $\tau_{\mu\nu}$ et de poids W, dans le champ de vitesse $\boldsymbol{u}$ exprimée dans un référentiel ξ^μ, est calculée comme:

$$\mathscr{L}_u(a)=u^\lambda\frac{\partial a}{\partial\xi^\lambda}+Wa\frac{\partial u^\lambda}{\partial\xi^\lambda} \tag{15a}$$

$$\mathscr{L}_u(\tau)_{\mu\nu}=u^\lambda\frac{\partial\tau_{\mu\nu}}{\partial\xi^\lambda}+\tau_{\lambda\nu}\frac{\partial u^\lambda}{\partial\xi^\mu}+\tau_{\mu\lambda}\frac{\partial u^\lambda}{\partial\xi^\nu}+W\tau_{\mu\nu}\frac{\partial u^\lambda}{\partial\xi^\lambda} \tag{15b}$$

$$\mathscr{L}_u(\tau)^{\mu\nu}=u^\lambda\frac{\partial\tau^{\mu\nu}}{\partial\xi^\lambda}-\tau^{\lambda\nu}\frac{\partial u^\mu}{\partial\xi^\lambda}-\tau^{\mu\lambda}\frac{\partial u^\nu}{\partial\xi^\lambda}+W\tau^{\mu\nu}\frac{\partial u^\lambda}{\partial\xi^\lambda}. \tag{15c}$$

4 Modèles de comportement en 4D

4.1 Hyperélasticité

À partir de l'inégalité de Clausius-Duhem dans l'Eq. 14, des modèles de comportement pour les matériaux hyperélastiques isotropes peuvent être développés, en supposant que la déformation soit isentropique et isotherme (ou adiabatique), et en choisissant une forme propre de l'énergie libre spécifique de Helmholtz. On choisit par exemple:

$$\Psi=\Psi_{elasticity}(\lambda/\rho,\mu/\rho,e_{\mu\nu},g^{\mu\nu}) \tag{16}$$

$$=\frac{\lambda}{2\rho}(e_{\mu\nu}g^{\mu\nu})^2+\frac{\mu}{\rho}(e_{\mu\nu}e_{\mu\nu}), \tag{17}$$

où λ et μ sont les coefficients de Lamé, $e_{\mu\nu}$ est la déformation et $g^{\mu\nu}$ est la métrique. On peut exprimer la contrainte en fonction de l'énergie libre spécifique de Helmholtz choisie,

comme:

$$\sigma^{\mu\nu} = \lambda g^{\mu\nu}\frac{\partial\Psi}{\partial(\lambda/\rho)} + \mu g^{\mu\nu}\frac{\partial\Psi}{\partial(\mu/\rho)} + \rho\frac{\partial\Psi}{\partial e_{\mu\nu}} - 2\rho\frac{\partial\Psi}{\partial g^{\alpha\beta}}g^{\alpha\mu}g^{\beta\nu}. \tag{18}$$

On peut alors obtenir un modèle de comportement pour l'hyperélasticité:

$$\begin{aligned}\sigma^{\mu\nu} = {} & \lambda(e_{\alpha\beta}g^{\alpha\beta})g^{\mu\nu} + 2\mu e^{\mu\nu} + 0.5\lambda(e_{\alpha\beta}g^{\alpha\beta})^2 g^{\mu\nu} + \mu(e_{\alpha\beta}e^{\alpha\beta})g^{\mu\nu} \\ & - 2\lambda(e_{\alpha\beta}g^{\alpha\beta})e^{\mu\nu} - 4\mu(e^{\mu\delta}e^{\nu}{}_{\delta}).\end{aligned} \tag{19}$$

Lorsque les termes d'ordre 2 de la déformation $e_{\mu\nu}$ de l'Eq. 19 sont négligés, un modèle linéaire peut être obtenu:

$$\sigma^{\mu\nu} = \lambda(e_{\alpha\beta}g^{\alpha\beta})g^{\mu\nu} + 2\mu e^{\mu\nu}, \tag{20}$$

qui est aussi un modèle pour l'hyperélasticité isotrope. Dans le référentiel inertiel ou les composantes du tenseur de métrique $\eta^{\mu\nu}$ sont:

$$\eta_{\mu\nu} = \begin{pmatrix} -1 & 0 & 0 & 0 \\ 0 & -1 & 0 & 0 \\ 0 & 0 & -1 & 0 \\ 0 & 0 & 0 & +1 \end{pmatrix}. \tag{21}$$

Le modèle dans l'Eq. 20 donne une relation linéaire entre les composantes de la contrainte et de la déformation. Il y a deux autres possibilités pour obtenir des relations linéaires entre composantes des contraintes et des déformations, qui conduisent à deux modèles pour l'hyperélasticité isotrope. Ces modèles sont exprimés en termes de composantes:

$$\hat{\sigma}_{\mu\nu} = \lambda(\hat{b}_{\alpha\beta}E^{\alpha\beta})\hat{b}_{\mu\nu} + 2\mu E^{\alpha\beta}\hat{b}_{\mu\alpha}\hat{b}_{\nu\beta} \tag{22}$$

$$\iff \hat{\sigma}^{\mu\nu} = \lambda(\hat{b}^{\alpha\beta}E_{\alpha\beta})\hat{b}^{\mu\nu} + 2\mu E_{\alpha\beta}\hat{b}^{\mu\alpha}\hat{b}^{\nu\beta} \tag{23}$$

$$\iff \sigma_{\mu\nu}J = \lambda(b_{\alpha\beta}e^{\alpha\beta})b_{\mu\nu} + 2\mu e^{\alpha\beta}b_{\mu\alpha}b_{\nu\beta} \tag{24}$$

$$\iff \sigma^{\mu\nu}J = \lambda(b^{\alpha\beta}e_{\alpha\beta})b^{\mu\nu} + 2\mu e_{\alpha\beta}b^{\mu\alpha}b^{\nu\beta}, \tag{25}$$

et

$$\hat{\sigma}^{\mu\nu} = \lambda(\hat{\beta}^{\alpha\beta}E_{\alpha\beta})\hat{\beta}^{\mu\nu} + 2\mu E_{\alpha\beta}\hat{\beta}^{\mu\alpha}\hat{\beta}^{\nu\beta} \tag{26}$$

$$\iff \hat{\sigma}_{\mu\nu} = \lambda(\hat{\beta}_{\alpha\beta}E^{\alpha\beta})\hat{\beta}_{\mu\nu} + 2\mu E^{\alpha\beta}\hat{\beta}^{\mu\alpha}\hat{\beta}^{\nu\beta} \tag{27}$$

$$\iff \sigma_{\mu\nu}J = \lambda(\beta_{\alpha\beta}e^{\alpha\beta})\beta_{\mu\nu} + 2\mu e^{\alpha\beta}\beta_{\mu\alpha}\beta_{\nu\beta} \tag{28}$$

$$\iff \sigma^{\mu\nu}J = \lambda(\beta^{\alpha\beta}e_{\alpha\beta})\beta^{\mu\nu} + 2\mu e_{\alpha\beta}\beta^{\mu\alpha}\beta^{\nu\beta}, \tag{29}$$

où $\boldsymbol{\beta}$ est l'inverse de $\boldsymbol{b}$. Spécialement, on a:

$$\hat{\beta}^{\mu\nu} = \eta^{\mu\nu} \quad ; \quad \hat{b}_{\mu\nu} = \eta_{\mu\nu}, \tag{30}$$

donc l'Eqs. 22 et 26 deviennent:

$$\hat{\sigma}_{\mu\nu} = \lambda(\eta_{\alpha\beta}E^{\alpha\beta})\eta_{\mu\nu} + 2\mu E^{\alpha\beta}\eta_{\mu\alpha}\eta_{\nu\beta} \tag{31}$$

$$\hat{\sigma}^{\mu\nu} = \lambda(\eta^{\alpha\beta}E_{\alpha\beta})\eta^{\mu\nu} + 2\mu E_{\alpha\beta}\eta^{\mu\alpha}\eta^{\nu\beta}. \tag{32}$$

Les composantes du tenseur $\hat{\sigma}^{\mu\nu}$, $\hat{\sigma}_{\mu\nu}$, $E^{\mu\nu}$ et $E_{\mu\nu}$ correspondent à des descriptions dans le référentiel convectif $\hat{\xi}^{\mu}$. Les relations suivantes sont utilisées pour établir les modèles:

$$J = |F| \tag{33}$$

$$E^{\mu\nu} = F'^{\mu}_{\ \alpha}F'^{\nu}_{\ \beta}e^{\alpha\beta} \quad ; \quad E_{\mu\nu} = F^{\alpha}_{\ \mu}F^{\beta}_{\ \nu}e_{\alpha\beta} \tag{34}$$

$$\hat{\sigma}^{\mu\nu} = JF'^{\mu}_{\ \alpha}F'^{\nu}_{\ \beta}\sigma^{\alpha\beta}; \quad \hat{\sigma}_{\mu\nu} = JF^{\alpha}_{\ \mu}F^{\beta}_{\ \nu}\sigma_{\alpha\beta} \tag{35}$$

$$\hat{g}^{\mu\nu} = F'^{\mu}_{\ \alpha}F'^{\nu}_{\ \beta}\eta^{\alpha\beta} \quad ; \quad \hat{g}_{\mu\nu} = F^{\alpha}_{\ \mu}F^{\beta}_{\ \nu}\eta_{\alpha\beta}. \tag{36}$$

4.2 Élasticité anisotrope

La relation entre la contrainte et la déformation peut être exprimée autrement comme:

$$\sigma^{\mu\nu} = \mathcal{C}^{\mu\nu\alpha\beta}e_{\alpha\beta}, \tag{37}$$

en introduisant un tenseur d'ordre quatre $\mathcal{C}^{\mu\nu\alpha\beta}$, qui représente un module sécant d'élasticité ou de rigidité. Dans le formalisme 4D, il a 256 composantes. Le nombre de composantes peut être réduit selon les propriétés de symétrie pour différents types d'anisotropie. Par exemple, le tenseur du module d'élastique du matériau isotrope (correspondant à l'Eq. 20)

est donné ci-dessous, en notation de Voigt, avec 2 éléments indépendants:

$$\mathcal{C}^{\Lambda\Theta} = \begin{pmatrix} \lambda+2\mu & \lambda & \lambda & -\lambda & 0 & 0 & 0 & 0 & 0 & 0 \\ \lambda & \lambda+2\mu & \lambda & -\lambda & 0 & 0 & 0 & 0 & 0 & 0 \\ \lambda & \lambda & \lambda+2\mu & -\lambda & 0 & 0 & 0 & 0 & 0 & 0 \\ -\lambda & -\lambda & -\lambda & \lambda+2\mu & 0 & 0 & 0 & 0 & 0 & 0 \\ 0 & 0 & 0 & 0 & -\mu & 0 & 0 & 0 & 0 & 0 \\ 0 & 0 & 0 & 0 & 0 & -\mu & 0 & 0 & 0 & 0 \\ 0 & 0 & 0 & 0 & 0 & 0 & -\mu & 0 & 0 & 0 \\ 0 & 0 & 0 & 0 & 0 & 0 & 0 & \mu & 0 & 0 \\ 0 & 0 & 0 & 0 & 0 & 0 & 0 & 0 & \mu & 0 \\ 0 & 0 & 0 & 0 & 0 & 0 & 0 & 0 & 0 & \mu \end{pmatrix}. \tag{38}$$

4.3 Hypoélasticité

En 4D, les modèles hypoélastiques sont développés à partir du modèle élastique linéaire via l'Eq. 20. Deux types de modèle hypoélastique sont ensuite développés.

- Un modèle irréversible, obtenu en remplaçant les tenseurs des contraintes et des déformations dans le modèle élastique (l'Eq. 20) par leurs dérivées de Lie respectives:

$$\mathscr{L}_u(\sigma)^{\mu\nu} = 2\mu d^{\mu\nu} + \lambda(d_{\alpha\beta}g^{\alpha\beta})g^{\mu\nu}. \tag{39}$$

  sachant que: $\mathscr{L}_u(e)_{\mu\nu} = d_{\mu\nu}$. Pour le modèle irréversible, la dérivée de Jaumann peut aussi être utilisée:

$$\mathscr{T}^J(\sigma)^{\mu\nu} = 2\mu d^{\mu\nu} + \lambda(d_{\alpha\beta}g^{\alpha\beta})g^{\mu\nu}, \tag{40}$$

  où la dérivée de Jaumann d'un tenseur, usuelle en mécanique des milieux continus 3D est:

$$\mathscr{T}^J(\sigma)^{\mu\nu} = u^\lambda\nabla_\lambda(\sigma^{\mu\nu}) - \omega^\mu_{\ \alpha}\sigma^{\alpha\nu} + \sigma^{\mu\alpha}\omega_\alpha^{\ \nu}. \tag{41}$$

- Un modèle réversible, obtenu en évaluant les dérivées de Lie de chaque côté de modèle élastique (l'Eq. 20):

$$\mathscr{L}_u(\sigma)^{\mu\nu} = \mathscr{L}_u\left(\lambda(e_{\alpha\beta}g^{\alpha\beta})g^{\mu\nu} + 2\mu e_{\alpha\beta}g^{\mu\alpha}g^{\nu\beta}\right). \tag{42}$$

On peut représenter ces modèles sous une forme plus générale en utilisant un tenseur d'ordre quatre, correspondant à l'Eq. 37:

- Pour le modèle irréversible.

$$\begin{aligned} \mathscr{L}_u(\sigma)^{\mu\nu} &= \mathcal{H}^{\mu\nu\alpha\beta} d_{\alpha\beta} && (43) \\ \mathscr{T}^{4D}(\sigma)^{\mu\nu} &= \mathcal{H}^{\mu\nu\alpha\beta} d_{\alpha\beta} && (44) \\ \mathcal{H}^{\mu\nu\alpha\beta} &= \lambda g^{\mu\nu} g^{\alpha\beta} + \mu(g^{\mu\alpha} g^{\nu\beta} + g^{\nu\alpha} g^{\mu\beta}). \end{aligned}$$

- Pour le modèle réversible (R).

$$\begin{aligned} \mathscr{L}_u(\sigma)^{\mu\nu} &= \mathcal{H}_R^{\mu\nu\alpha\beta} d_{\alpha\beta} && (45) \\ \mathcal{H}_R^{\mu\nu\alpha\beta} &= \left(1 + \frac{\lambda(g_{\gamma\delta}\sigma^{\gamma\delta})}{\mu(4\lambda + 2\mu)}\right)\left(\lambda g^{\mu\nu} g^{\alpha\beta} + 2\mu g^{\mu\alpha} g^{\nu\beta}\right) \\ &+ \sigma^{\mu\nu} g^{\alpha\beta} - \frac{\lambda}{\mu} g^{\mu\nu}\sigma^{\alpha\beta} - 2(g^{\mu\alpha}\sigma^{\beta\nu} + g^{\nu\alpha}\sigma^{\beta\mu}). \end{aligned}$$

4.4 Élastoplasticité

Le modèles élastoplastiques dans le cadre d'un formalisme 4D ont été tout d'abord construits à partir de la décomposition addititve du taux de déformation:

$$d_{\mu\nu} = d_{e\mu\nu} + d_{p\mu\nu} \tag{46}$$

Selon cette décomposition, deux comportements sont nécessaires: le modèle hypoélastique pour obtenir $\boldsymbol{d}_e$ et le modèle de plasticité pour obtenir $\boldsymbol{d}_p$. Avec cette décomposition (Eq. 46), et une décomposition de l'énergie libre spécifique de Helmholtz telle que:

$$\Psi = \Psi_{elasticity}(\lambda/\rho, \mu/\rho, e_{e\mu\nu}, g^{\mu\nu}) + \Psi_{plasticity}(r, Q_m), \tag{47}$$

l'inégalité de Clausius-Duhem dans l'Eq. 14 devient ci-dessous:

$$(-\rho u^\mu \nabla_\mu \Psi_{elasticity} + \sigma^{\mu\nu} d_{e\mu\nu}) + (-\rho u^\mu \nabla_\mu \Psi_{plasticity} + \sigma^{\mu\nu} d_{p\mu\nu}) \geq 0. \tag{48}$$

Premièrement, les termes dans la première parenthèse dans l'Eq. 48 sont égaux à zero, car la transformation élastique est réversible:

$$\rho u^\mu \nabla_\mu \Psi_{elasticity} = \sigma^{\mu\nu} d_{e\mu\nu} \quad ; \quad \rho \mathscr{L}_{u_e}(\Psi_{elasticity}) = \sigma^{\mu\nu} d_{e\mu\nu}. \tag{49}$$

Donc le modèle hypoélastique pour obtenir $\boldsymbol{d}_e$ est donné par les même expressions que les Eqs. 43, 44 et 45, sauf que $\boldsymbol{d}$ est remplacé par $\boldsymbol{d}_e$.

Deuxièmement, les termes dans la deuxième parenthèse dans l'Eq. 48 doivent avoir des valeurs maximales, en respectant le critère de plasticité, Von-Mises par exemple:

$$\begin{cases} \mathscr{F} = \sigma_{eff} - \kappa(r) = 0 \\ \sigma_{eff} = \sqrt{S^{\alpha\beta} S_{\alpha\beta}} \end{cases} \tag{50}$$

où κ est une fonction liée à l'écrouissage isotrope, r est la déformation plastique cumulée et $S^{\mu\nu}$ est la contrainte déviatorique. Avec la méthode des multiplicateurs de Lagrange pour obtenir la maximisation sous contraintes, un modèle de plasticité est obtenu:

$$d_{p\mu\nu} = \Lambda \frac{\partial \mathscr{F}}{\partial \sigma^{\mu\nu}}, \tag{51}$$

qui donne finalement:

$$d_{p_{\mu\nu}} = \frac{S_{\alpha\beta}\ u^{\lambda} \nabla_{\lambda}(\sigma^{\alpha\beta})}{\sigma_{eff}^2 \frac{\partial \kappa}{\partial r}} S_{\mu\nu}. \tag{52}$$

Si on combine les parties élastique et plastique par la décomposition additive via l'Eq. 46, des modèles élastoplastiques sont obtenus. En général, le modèle élastoplastique peut être mis sous la forme:

$$\mathscr{L}_{u_e}(\sigma)^{\mu\nu} = \mathcal{H}^{\mu\nu\alpha\beta}(d_{\alpha\beta} - d_{p\alpha\beta}). \tag{53}$$

Après calculs, trois modèles élastoplastiques peuvent être spécifiés:

- Le modèle élastoplastique avec une partie hypoélastique irréversible et la dérivée de Lie,

$$\begin{aligned} \mathscr{L}_{u_e}(\sigma)^{\mu\nu} &= \mathcal{H}^{\mu\nu\alpha\beta}(d_{\alpha\beta} - \dot{d}^{\mathcal{H}}_{p\alpha\beta}) \\ &= 2\mu d^{\mu\nu} + \lambda(d_{\alpha\beta} g^{\alpha\beta}) g^{\mu\nu} \\ &- 2\mu \frac{S^{\rho\theta}\left(2\sigma_{\rho}^{\ \lambda} d_{\theta\lambda} + 2\mu\ d_{\rho\theta} - \sigma_{\rho\theta} d^{\lambda}_{\ \lambda}\right)}{\sigma_{eff}^2(\frac{\partial \kappa}{\partial r} + 2\mu) + 2\sigma^{\alpha\lambda} S^{\beta}_{\ \lambda} S_{\alpha\beta}} S^{\mu\nu}. \end{aligned} \tag{54}$$

- Le modèle élastoplastique avec une partie hypoélastique irréversible et la dérivée de Jaumann,

$$\mathscr{T}^{J}(\sigma)^{\mu\nu} = 2\mu d^{\mu\nu} + \lambda(d_{\alpha\beta} g^{\alpha\beta}) g^{\mu\nu} - \frac{4\mu^2\ S^{\rho\theta} d_{\rho\theta}}{\sigma_{eff}^2(\frac{\partial \kappa}{\partial r} + 2\mu)} S^{\mu\nu}. \tag{55}$$

- Le modèle élastoplastique avec une partie hypoélastique réversible et la dérivée de Lie,

$$\mathscr{L}_{u_e}(\sigma)^{\mu\nu} = \mathcal{H}_R^{\mu\nu\alpha\beta}(d_{\alpha\beta} - d^{\mathcal{R}}_{p\alpha\beta}), \tag{56}$$

où $\mathcal{H}_R$ est donné par l'Eq. 45 et

$$d^{\mathcal{R}}_{p\alpha\beta} = S^{\kappa\lambda}\frac{Ad_{\kappa\lambda} - 2d_{\kappa\theta}\sigma^{\theta}_{\lambda}}{\sigma^2_{eff}(\partial\kappa/\partial r + A) - 2S_{\kappa\theta}\sigma^{\theta}_{\lambda}S^{\lambda\kappa}}S_{\alpha\beta}, \tag{57}$$

avec

$$A = 2\mu + \frac{2\lambda(g_{\gamma\delta}\sigma^{\gamma\delta})}{4\lambda + 2\mu}. \tag{58}$$

5 Application du modèle 4D à la simulation numérique 3D

Il faut utiliser les modèle obtenus dans le cadre du formalisme quadridimensionne et les comparer, pal la méthode des éléments finis. Donc une projection du modèle 4D sur 3D a été faite. Avec les modèles projetés, des simulations numériques sur une structure sont faites, en utilisant un logiciel de calcul (Zset©).

5.1 Modèles projetés sur 3D

Quand on projète le modèle hyperélastique isotrope en 3D (l'Eq. 20), on obtient le modèle de Hooke:

$$\sigma^{ij} = \lambda(I^{ab}e_{ab})I^{ij} + 2\mu e^{ij}. \tag{59}$$

Ensuite, les modèles hypoélastiques sont projetés en 3D comme:

- Un modèle irréversible avec la dérivée de Lie, qui s'appellera "Lie model with IREP" sur la figure,

$$\mathscr{L}_v(\sigma)^{ij} = \mathcal{H}^{ijab}d_{ab}, \tag{60}$$

$$\text{avec} \quad \mathcal{H}^{ijab} = \lambda I^{ij}I^{ab} + \mu(I^{ia}I^{jb} + I^{ja}I^{ib}).$$

- Un modèle irréversible avec la dérivée de Jaumann, qui s'appellera "Jaumann model with IREP" sur la figure,

$$\mathscr{D}^J(\sigma)^{ij} = \mathcal{H}^{ijab} d_{ab}, \tag{61}$$

$$\text{avec} \quad \mathcal{H}^{ijab} = \lambda I^{ij} I^{ab} + \mu(I^{ia} I^{jb} + I^{ja} I^{ib}).$$

- Un modèle réversible avec la dérivée de Lie, qui s'appellera "Lie model with REP" sur la figure,

$$\mathscr{L}_v(\sigma)^{ij} = \mathcal{H}_R^{ijab} d_{eab} \tag{62}$$

$$\begin{aligned} \text{avec} \quad \mathcal{H}_R^{ijab} &= \left(\lambda + \frac{\lambda^2\, tr(\sigma)}{\mu(3\lambda+2\mu)}\right) I^{ij} I^{ab} + \left(2\mu + \frac{2\lambda\, tr(\sigma)}{3\lambda+2\mu}\right) I^{ia} I^{jb} \\ &+ \sigma^{ij} I^{ab} - \frac{\lambda}{\mu} I^{ij} \sigma^{ab} - 2(I^{ia}\sigma^{bj} + I^{ja}\sigma^{bi}). \end{aligned}$$

À la fin, les modèles élastoplastiques sont projetés en 3D comme:

- Un modèle avec la partie élastique irréversible et la dérivée de Lie, qui s'appellera "Lie model with IREP" sur la figure,

$$\begin{aligned} \mathscr{L}_{v_e}(\sigma)^{ij} &= 2\mu d^{ij} + \lambda\, tr(d) I^{ij} \\ &- 2\mu \frac{S^{rt}\left(2\sigma_r{}^l d_{tl} + 2\mu\, d_{rt} - \sigma_{rt}\, tr(d)\right)}{\sigma_{eff}^2(\frac{\partial\kappa}{\partial r} + 2\mu) + 2\sigma^{al} S^b_{\ l} S_{ab}} S^{ij}. \end{aligned} \tag{63}$$

- Un modèle avec la partie élastique irréversible et la dérivée de Jaumann, qui s'appellera "Jaumann model with IREP" sur la figure,

$$\mathscr{D}^J(\sigma)^{ij} = 2\mu d^{ij} + \lambda\, tr(d) I^{ij} - \frac{4\mu^2\, S^{ab} d_{ab}}{\sigma_{eff}^2(\frac{\partial\kappa}{\partial r} + 2\mu)} S^{ij}. \tag{64}$$

- Un modèle avec la partie élastique réversible et la dérivée de Lie, qui s'appellera "Lie model with REP" sur la figure,

$$\begin{aligned} \mathscr{L}_{v_e}(\sigma)^{ij} &= \mathcal{H}_R^{ijab}(d_{ab} - d^{\mathcal{R}}_{pab}) \\ \text{with} \quad \mathcal{H}_R^{ijab} &= \left(\lambda + \frac{\lambda^2\, tr(\sigma)}{\mu(3\lambda+2\mu)}\right) I^{ij} I^{ab} + \left(2\mu + \frac{2\lambda\, tr(\sigma)}{3\lambda+2\mu}\right) I^{ia} I^{jb} \\ &+ \sigma^{ij} I^{ab} - \frac{\lambda}{\mu} I^{ij} \sigma^{ab} - 2(I^{ia}\sigma^{bj} + I^{ja}\sigma^{bi}) \\ d^{\mathcal{R}}_{pab} &= S^{kl} \frac{A d_{kl} - 2 d_{kt} \sigma^t_{\ l}}{\sigma_{eff}^2(\partial\kappa/\partial r + A) - 2 S_{kt} \sigma^t_{\ l} S^{lk}} S_{ab} \\ A &= 2\mu + \frac{2\lambda tr(\sigma)}{3\lambda + 2\mu}. \end{aligned} \tag{65}$$

5.2 Simulations numériques

Différentes simulations numériques sont effectuées avec les modèles projetés en 3D pour l'hypoélasticité et l'élastoplasticité. Sur un seul élément cubique, les modèles hypoélastiques sont appliqués à des calculs combinant du glissement, de la traction et le relâchement. Pour les modèles élastoplastiques, nous avons appliqués du glissement puis un relâchement. Avec une barre maillée à 320 éléments quadrilatérals réduits, les modèles hypoélastiques sont appliqués à des calculs combinant de la torsion, de la traction avec un relâchement. Avec une poutre maillée à 320 éléments quadrilatérals réduits, les modèles élastoplastiques sont appliqués à des calculs de glissement suivi d'un relâchement.

La figure 1 prèsente les différents résultats des calculs effectués avec les trois modèles hypoélastiques. Le modèle irréversible avec la dérivée de Lie donne le même résultat que le modèle élastique de référence, parce qu'il est dérivé du modèle de référence directement, tandis que les deux autres modèles donnent les différences importantes. La déformation est importante, donc la différence est évidente. A la fin du chargement, seul le modèle réversible avec la dérivée de Lie parmi les trois modèles hypoélastiques donne un résultat de la contrainte à zéro, ce qui illustre la réversibilité du modèle réversible avec la dérivée de Lie. La même conclusion peut être tirée du calcul avec la barre maillée à 320 élémants, voir Fig. 3. Cependant, le calcul avec le modèle de Lie va prendre 15% plus de temps qu'avec les autres modèles.

La figure 2 présente les différents résultats des calculs effectués avec les trois modèles élastoplastiques. La différence sur la composante σ^{12} ne peut pas être observée par rapport aux autres modèles. Mais pour les autres composantes, les différences entre les trois modèles sont évidentes. Cependant, cette différence n'est pas évidente pour la simulation de l'écrouissage isotrope, voir Figs. 4 et 5. En comparant les Figs. 4 et 5, la différence de r, déformation plastique cumulée, est plus grande lorsque la déformation élastique devient plus grande. C'est correcte, parce que les parties correspondant à la plasticité des trois modèles sont les mêmes, mais la différence se fait sur les parties correspondant au comportement élastique. On peut en conclure que le modèle élastoplastique avec la partie élastique réversible et la dérivée de Lie donne un résultat plus précis que les

deux autres modèles grâce à sa partie élastique. Le modèle élastoplastique avec la partie élastique réversible et la dérivée de Lie montrera plus d'avantages lors de la simulation de l'élastoplasticité lorsque la déformation élastique est plus grande.

Différentes simulations numériques effectuées avec les modèles projetés sur 3D pour l'hypoélasticité et l'élastoplasticité illustrent qu'un modèle précis et covariant peut être développé avec la dérivée de Lie en formalisme 4D. Le cas le plus approprié où cette approche est recommandée sera quand la déformation élastique est relativement importante, par exemple, pour les élastomères, les biomatériaux, ou encore les métaux avec une grande limite d'élasticité, etc, quand un résultat précis est nécessaire.

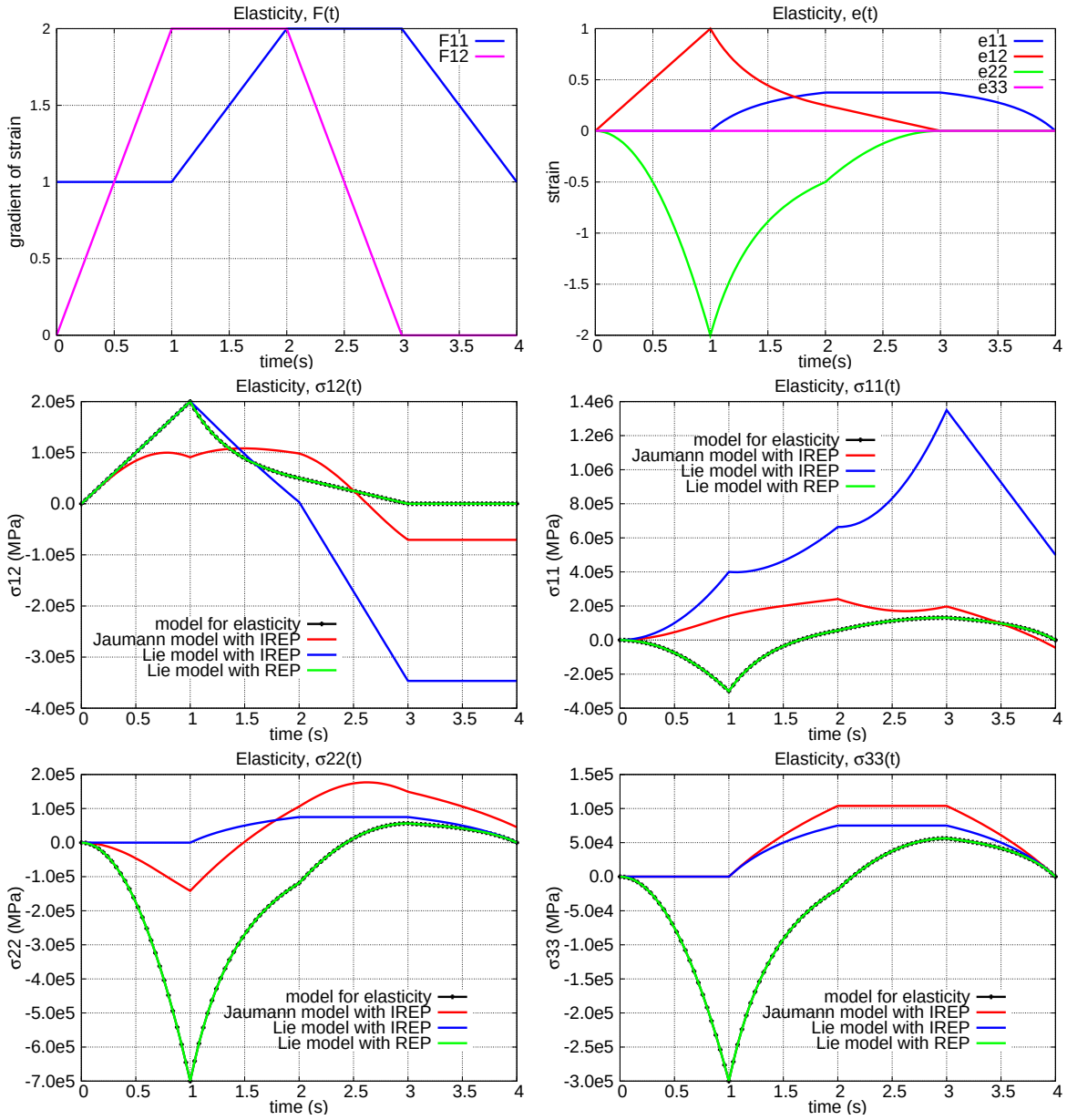

Figure 1: La déformation et la contrainte en fonction du temps pour un cycle de sollicitation, avec une grande déformation et sans plasticité. Les composantes du gradient de déformation $\boldsymbol{F}$ et la déformation $\boldsymbol{e}$ sont données sur les figures en haut. Les composantes de la contrainte $\boldsymbol{\sigma}$ sont données sur les autres figures.

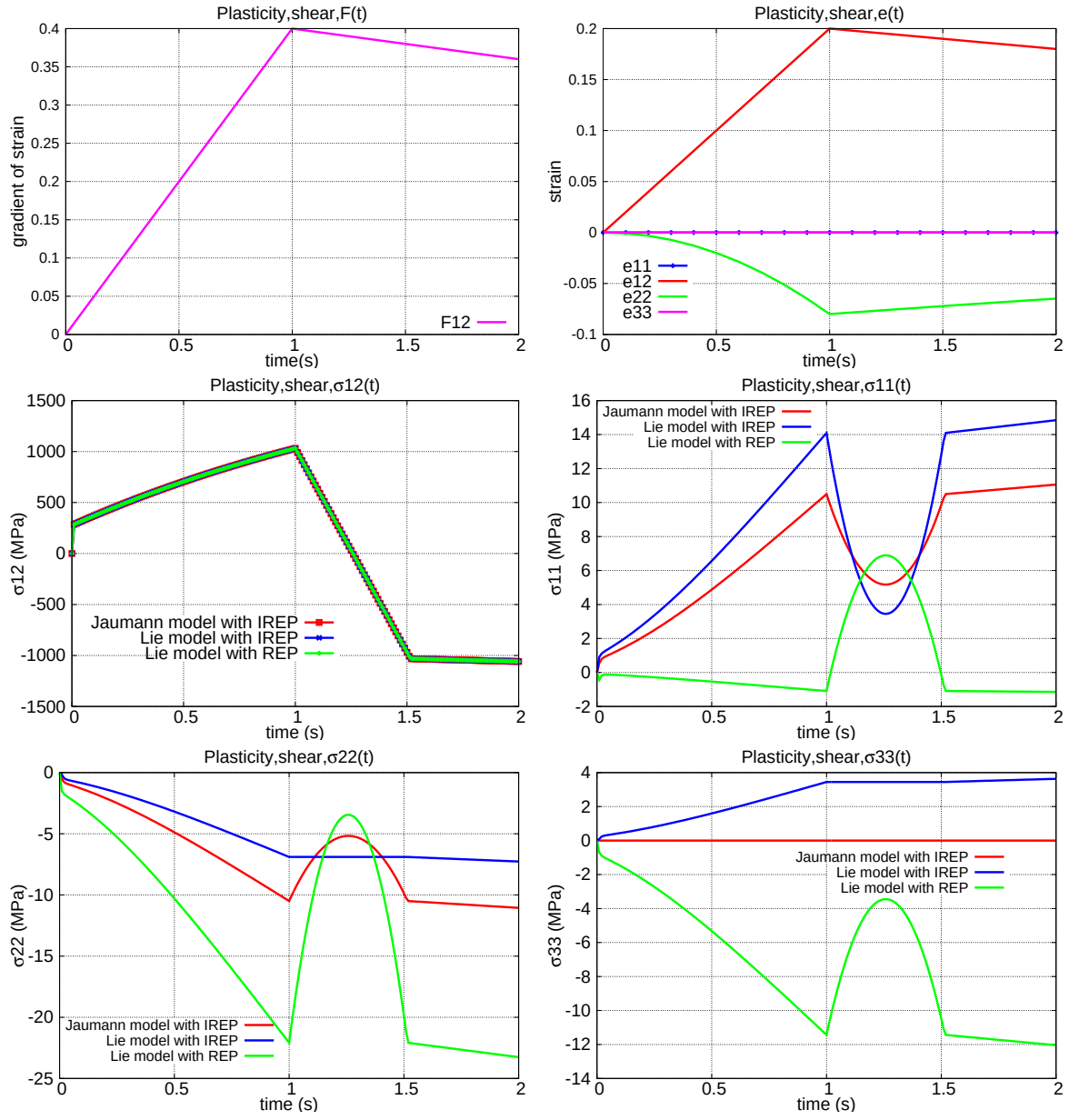

Figure 2: La déformation et la contrainte en fonction du temps pour un cycle de sollicitation, avec une grande déformation et en plasticité. Les composantes du gradient de déformation $\boldsymbol{F}$ et la déformation $\boldsymbol{e}$ sont données sur les figures en haut. Les composantes de la contrainte $\boldsymbol{\sigma}$ sont données sur les autres figures.

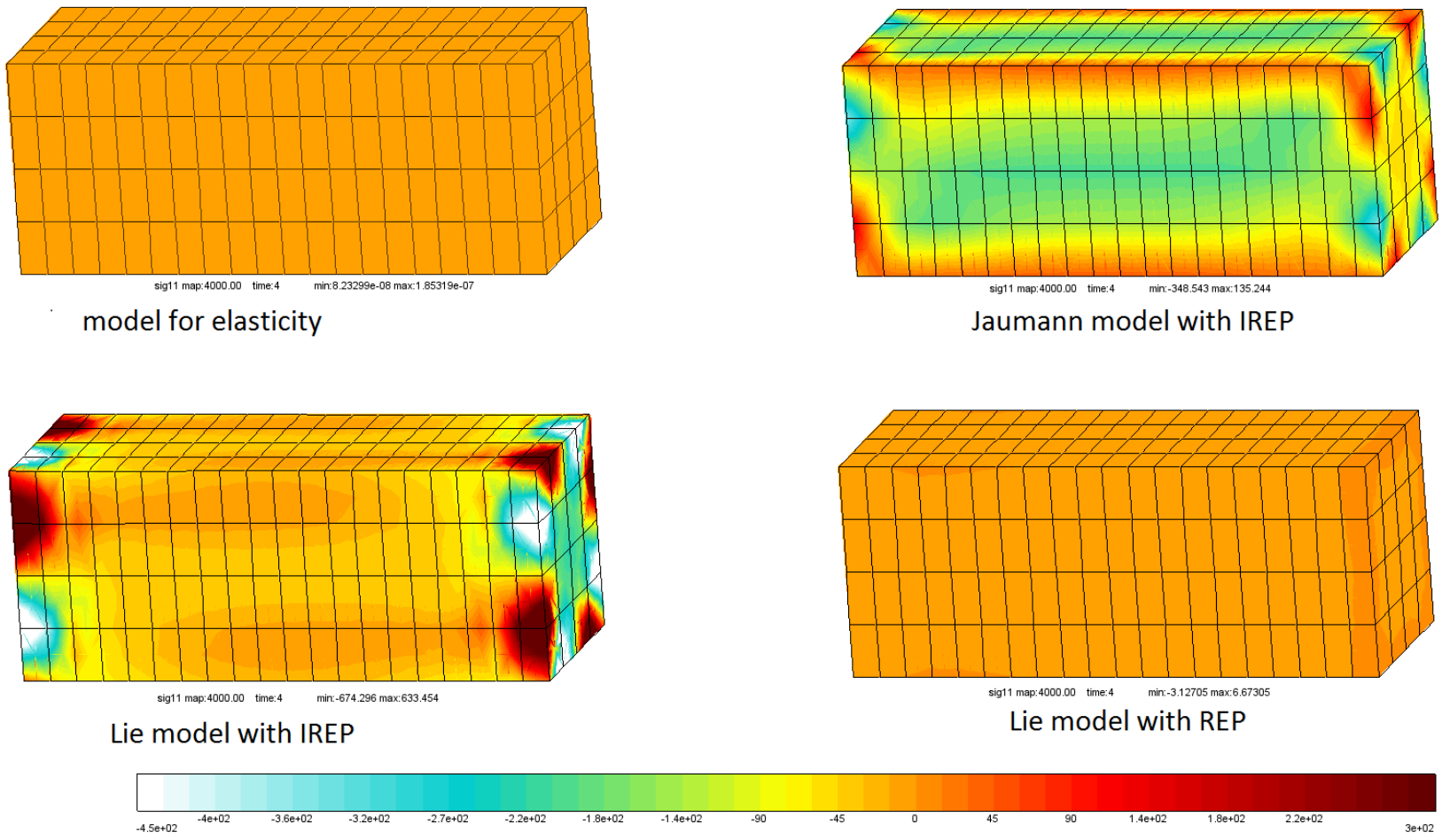

Figure 3: Le calcul est fait dans la domaine de l'élasticité. La figure montre la distribution des valeurs de composantes de la contrainte σ^{11} dans la barre lorsque la sollicitation est déchargée.

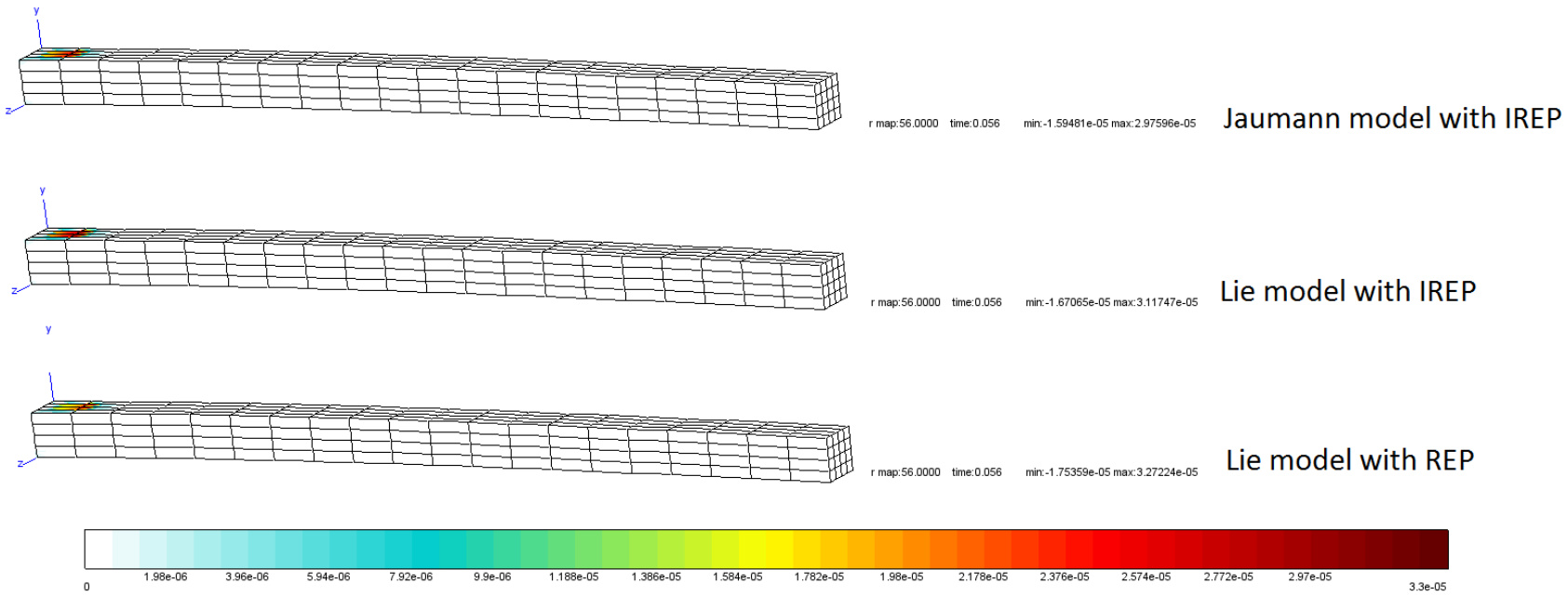

Figure 4: Le calcul est fait dans la domaine de l'élasticité et de la plasticité. La figure montre la distribution des valeurs de la déformation plastique cumulée r au poutre, au moment du commencement de la plasticité pendant la flèxion vers le bas.

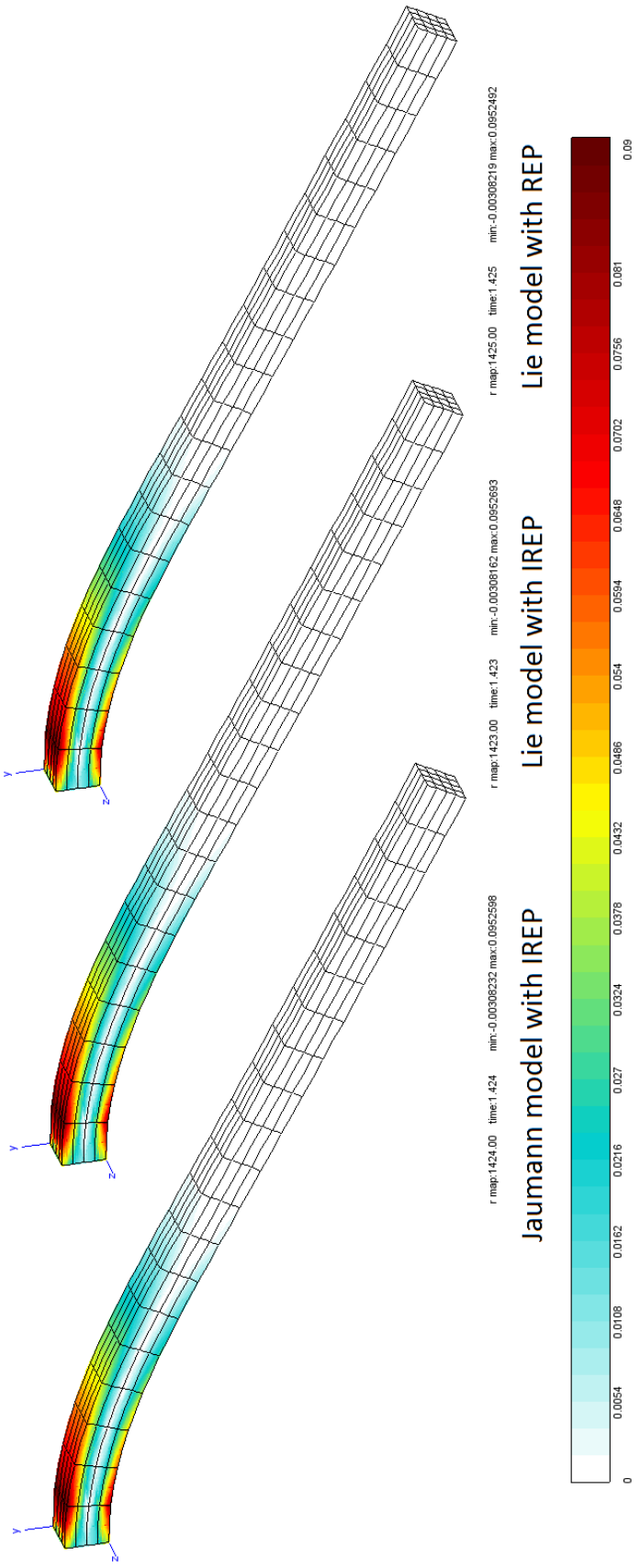

Figure 5: Le calcul est fait dans la domaine de l'élasticité et de la plasticité. La figure montre la distribution des valeurs de la déformation plastique cumulée r dans la poutre, au moment du redémarrage de la plasticité pendant le retour vers le haut.

6 Conclusions et perspectives

Dans cette thèse, une description quadridimensionnelle covariante des grandes déformations d'un matériau est proposée, en tenant compte de l'hypothèse Newtonienne et en utilisant le cadre mathématique de la géométrie différentielle. Une étude de la thermodynamique en 4D est faite. À partir de la thermodynamique en 4D, des modèles de comportement pour l'hyperélasticité, l'élasticité anisotrope, l'hypoélasticité et l'élastoplasticité ont été construits, dans le cadre de formalisme 4D, en utilisant la dérivée de Lie. Le formalisme 4D assure que les tenseurs et les opérations sont nécessairement covariants. La dérivée de Lie est une variation totale par rapport au temps et une dérivée 4D invariante à la superposition du mouvement de corps rigide. Les modèles 4D sont projetés sur la 3D, ce qui démontre que la 3D est un cas particulier. L'approche en 4D permet également de proposer de nouveaux modèles. Enfin, les simulations numériques sur une structure simple illustrent la possibilité d'appliquer des modèles développés avec le formalisme 4D.

La méthode systématique utilisée pour obtenir des modèles de comportement en 4D dans cette thèse n'est pas limitée au développement des modéles indépendants du temps. En utilisant la dérivée de Lie, des modèles dépendants du temps pourraient être développés, tels que les modèles 4D pour la viscoélasticité, la viscoplasticité, etc. Un autre intérêt de la recherche dans le futur est écrire le schéma d'intégration pour les méthodes des éléments finis en utilisant la dérivée de Lie, et développer un solveur covariant pour les méthodes des éléments finis en 4D. En conséquence, des outils numériques innovants pour la simulation numérique des procédés de mise en forme pourraient ainsi être développés.

Mingchuan WANG

Doctorat : Matériaux, Mécanique, Optique et Nanotechnologie

Année 2016

Modèles covariants de comportement issus d'un formalisme 4D : de la thermodynamique aux applications numériques

L'objectif de ce travail est d'établir des modèles de comportement mécaniques pour les matériaux en grandes déformations. Au lieu des approches classiques en 3D dans lesquelles la notion d'objectivité est ambigüe et pour lesquelles différentes dérivées objectives sont utilisées arbitrairement, le formalisme quadridimensionnel dérivé des théories de la Relativité est appliqué. En 4D, les deux aspects de la notion d'objectivité, l'indépendance du référentiel (ou covariance) et l'invariance à la superposition de mouvement de corps rigide, peuvent désormais être distinguées. En outre, l'utilisation du formalisme 4D assure la covariance des modèles. Pour les modèles incrémentaux, la dérivée de Lie est choisie permettant une variation totale par rapport au temps, tout en étant à la fois covariante et invariante à la superposition des mouvements de corps rigide.
Dans ce formalisme 4D, nous proposons également un cadre thermodynamique en 4D pour développer des modèles de comportement en 4D tels que l'hyperélasticité, l'élasticité anisotrope, l'hypoélasticité et l'élastoplasticité. Ensuite, les projections en 3D sont obtenus à partir des modèles en 4D et étudiés en les testant sur des simulations numériques par éléments finis avec le logiciel Zset.

Mots clés : matériaux, propriétés mécaniques - objectivité - thermodynamique - éléments finis, méthode des - modèles mathématiques - variétés topologiques à 4 dimensions - élastoplasticité.

A Covariant 4D Formalism to Establish Constitutive Models: from Thermodynamics to Numerical Applications

The objective of this work is to establish mechanical constitutive models for materials undergoing large deformations. Instead of the classical 3D approaches in which the notion of objectivity is ambiguous and different objective transports may be arbitrarily used, the four-dimensional formalism derived from the theories of Relativity is applied. Within a 4D formalism, the two aspects of notion of objectivity: frame-indifference (or covariance) and invariance to the superposition of rigid body motions can now be distinguished. Besides, the use of this 4D formalism ensures the covariance of the models. For rate-form models, the Lie derivative is chosen as a total time derivative, which is also covariant and invariant to the superposition of rigid body motions.
Within the 4D formalism, we also propose a framework using the 4D thermodynamic to develop 4D constitutive models for hyperelasticity, anisotropic elasticity, hypoelasticity and elastoplasticity. Then, 3D models are derived from 4D models and studied by applying them in numerical simulations with finite element methods using the software Zset.

Keywords: materials, mechanical properties - objectivity - thermodynamics - finite element method - mathematical models - four-manifolds - elastoplasticity.

Thèse réalisée en partenariat entre :

utt
université de technologie
Troyes

Ecole Doctorale "Sciences et Technologies"